STRUCTURAL, ELECTRONIC AND MAGNETIC PROPERTIES OF SPINEL BASED TRANSITION METAL OXIDES

MAHMOOD KHAN

Department of Physics

Hazara University Mansehra

2017

STRUCTURAL, ELECTRONIC AND MAGNETIC PROPERTIES OF SPINEL BASED TRANSITION METAL OXIDES

A dissertation presented

by

Mahmood Khan

in partial Fulfillment of the requirement for the

Degree of Doctor of Philosophy

with Major in Physics

in the

Faculty of Science

Hazara University

Major Professors: Saleh Muhammad, PhD

Bin Amin, PhD

DEPARTMENT OF PHYSICS, HAZARA UNIVERSITY,

MANSEHRA, PAKISTAN

2017

AUTHORIZATION TO SUBMIT DISSERTATION

This dissertation of Mahmood Khan submitted for the degree of Doctor of Philosophy with a major in Physics and titled "STRUCTURAL, ELECTRONIC AND MAGNETIC PROPERTIES OF SPINEL BASED TRANSITION METAL OXIDES" has been reviewed in final form. Permission, as indicated by the signatures given below, is granted to submit the copies to Hazara university for the final evaluation process.

Research Supervisor

Dr. Saleh Muhammad ……

Research Co-Supervisor

Dr. Bin Amin ……

Committee members

1. Dr. Manzoor Hussain ……
2. Dr. Saleh Muhammad ……
3. Dr. Muhammad Farooq ……
4. Dr. Bin Amin ……
5. Dr. Najmul Hassan ……

Chairperson Department of Physics

Dr. Saleh Muhammad ……

Dean Faculty of Science

Dr. Manzoor Hussain ……

DEPARTMENT OF PHYSICS
HAZARA UNIVERSITY, MANSEHRA
Tel #: 0997-414132, Fax:0997-……. URL:http/www.hu.edu.pk

File No. _____/HU/Phy/2012/__ …..…….2018

The Controller of Examinations
Hazara University
Mansehra

Subject: **EVALUATION REPORT OF Mr. MAHMOOD KHAN, PhD STUDENT, DEPARTMENT OF PHYSICS**

The oral examination of Mr Mahmood Khan, regarding his Ph.D. thesis was conducted today, in the …… of Hazara University. He convinced the examiners about the originality of his research work and its scientific significance.

Based on the quality and originality of the research work presented in his thesis and his oral examination, the examiners recommended him for the award of Ph.D. degree in Physics.

External Examiner
……
……
……

External Examiner
……
……
……

Supervisor/Inter Examiner
Dr Saleh Muhammad

Abstract

Theoretical study of Spinel based Transition Metal Oxides is reported. The Density Functional Theory approach is adopted for computational investigation using LAPW code. The structural, elastic properties of (XAl_2O_4 for *X=Mg, Mn, Fe, Co, Ni, Cu, Zn*), (MGa_2O_4 for *M=Mg, Mn, Fe, Co, Ni, Cu, Zn, Cd*), (NIn_2O_4 for *N=Mg, Zn, In*) & (ZnP_2O_4 for P=V, *Cr, Fe, Rh, Sn*) along with electronic & magnetic properties of cubic spinel oxides (XAl_2O_4) and (MGa_2O_4) have calculated. The calculated structural parameters conform to other experimental and theoretical evidences. Fulfillment of elastic stability criteria proves the reliability of the reported data. The calculated elastic constants show that all materials abide its stability opposing elastic deformations and the Cauchy's pressure confirms the dynamical stability of these materials. The high values of bulk moduli show the hardness of these materials while the Young moduli data reveal that $MgAl_2O_4$ is the stiffer material among all. Further, Poisson's ratios testify the compressibility, connote stableness to external deformation of these materials and reveal dominance of central forces being the interatomic forces. Out of 24 materials, only 05 are brittle and the rest are ductile with elastic anisotropy. $MgAl_2O_4$ is the most brittle and $CdGa_2O_4$ is the most ductile material. The electronic structure (Total DOS) show all XAl_2O_4, MGa_2O_4 (M=Fe, Co, Zn, Cd) have antiferromagnetic, $NiGa_2O_4$ & $CuGa_2O_4$ have FM state and the valence near Fermi level due to the transition metal 3d state. The calculation of direct exchange energy $\Delta_x(d)$ shows that the exchange mechanism of electrons is dominant in introducing magnetism and enormous exchange splitting is observed in these materials. The ferromagnetism in the group MGa_2O_4 of spinel oxide compounds is due to hybridization between the electrons in the 3d-states cation and 2p states anion. Appearance of magnetic moments in these materials is due to unpaired electrons in 3d states of Transition metal ions. The negative value of indirect exchange energy confirms the magnetism by spin of electrons.

ACKNOWLEDGEMENT

First, I owe my thanks to Almighty Allah for blessing me with the ability and strength to complete this dissertation. Then I have to mention that actually it is hard to sum up all the people that influenced me during this challenging time of my PhD dissertation, much less who led me till this time and encouraged me to set my goals and to achieve it. This in no manner can literally mention every person that deserves thanks, but is an attempt.

I am honour bound to my supervisor Dr. Saleh Muhammad Associate Professor Hazara University for his keen interest in my project. I have also to praise the HOD Department of IT/Telecom Dr. Noor ul Amin and the then Director IT Hazara University Dr. Arif Iqbal Umar for facilitating the computational work and allowing me to use IT/Telecom laboratory. My obligations are for all those colleagues at Material Modeling Lab, Department of Physics Hazara University, who encouraged me throughout this research work. Manzar Khan and Hayatullah are also thanked for their input at initial stages of the project development. My deepest acknowledgments are due for my co-supervisor, Dr. Bin Amin for introducing me to this project, agreeing to advise on the ins & outs of material modeling, for giving valuable ideas, guidance and directions throughout the research work with professional devotion. Who also checked the entire manuscript with meticulous care, prior handing over it to my Supervisor. Once more express my obligation to him for his kind cooperation and great attitude in the laboratory, which, of course, will remain in my heart for ever. I carried out most of the computational job during nights and on holidays, the only person used to remain available for providing moral support as well a hot cup of water, is the Telecom laboratory Naib Qasid (attendant) Mr Irfan, if I had forgotten writing about him, may have not a justice. My humble thanks to him.

Next comes my office colleagues Amjad Khan, Zubair Alam, Qasim and Aurangzeb who always helped me a lot at every step, specifically Aurangzeb who remained available any time round the clock for a southing and relaxing gossip.

Here I cannot omit mentioning Prof. Dr. Iftikhar Ahmad, who not only inspired me (then my friend, later earned my respect being my teacher during course work) but basically drew me to this PhD and into the material modeling while I had been off from Physics during my professional endeavour. Finally, I would like to give my most heart-felt thanks to my wife Sobia who through-out supported me during the years and my kids Mursaleen, Hassan, Hassam and Zain for their love & immense orison which gave me realms at each and every moment to earn this success. Thanks to them for their patience letting time to me for this dissertation.

Mahmood Khan

T O M Y F A M I L Y

&

To the two affectionate personalities
who invigorated me
to accomplish this project

Prof Dr Muqarrab Shah

Prof Dr Bahadar Shah

List of Publications

1. *Roshan Ali, S. Mohammad, HamidUllah, S. A. Khan, H. Uddin,* ***M. Khan****, N. U. Khan,* "The structural, electronic and optical response of IIA–VIA compounds through the modified Becke–Johnson potential", Physica B 410, 93-98 (2013). DOI: http://doi.org/10.1016/j.physb.2012.09.050 2.

2. *Manzar Ali, Saleh Mohammad, Hayatullah, Muhammad Haneef and* ***Mahmood Khan*** "Opto-electronic Response of Spinel $SiZn_2O_4$ to a Modified Becke-Johnson Potential", Journal of the Korean Physical Society; Vol. 63, No. 5, L961-*L964* (2013).

3. ***Mahmood Khan****, S. Muhammad, B. Amin,* "First principle studies of structural, elastic, electronic and magnetic properties of spinel XAl_2O_4 (X= Mg, Mn, Fe, Co, Cu, Ni, Zn) compounds", Computational Condensed Matter. 13, 72-76 (2017).
   DOI:http://dx.doi.org/10.1016/j.cocom.2017.09.007

DEPARTMENT OF PHYSICS, HAZARA UNIVERSITY

As members of the Dissertation Committee, we certify that we have read the dissertation prepared by Mahmood Khan, entitled "Structural, electronic and magnetic properties of Spinel based Transition Metal Oxides" and recommend that it be accepted as fulfilling the dissertation requirement for the Degree of Doctor of Philosophy.

_____ Date:

_____ Date:

_____ Date:

_____ Date:

_____ Date:

Final approval and acceptance of this dissertation is contingent upon the candidate's submission of the final copies of the dissertation to the Hazara University.

We hereby certify that we have read this dissertation prepared under our direction and recommend that it be accepted as fulfilling the dissertation requirement.

_____ Date:
Dissertation Co-Supervisor, Dr Bin Amin Khan

_____ Date:
Dissertation Supervisor, Dr Saleh Muhammad

STATEMENT BY AUTHOR

This dissertation has been submitted in partial fulfillment of requirements for PhD degree at Hazara University and is deposited in the University Library to be made available to borrowers under rules of the Library.

Brief quotations from this dissertation are allowable without special permission, provided that accurate acknowledgment of source is made. Requests for permission for extended quotation from or reproduction of this manuscript in whole or in part may be granted by the Chairperson of the Department of Physics or the Dean Faculty of Science Hazara University when in his/her judgment the proposed use of the material is in the interests of others. In all other instances, however, permission must be obtained from the author.

Mahmood Khan

Contents

List of Figures

List of Tables

CHAPTER – 1

1.1 Introduction

In the recent past as well today, the need for new and unique materials is the enterprising cause in material science. This forcible factor let the researchers crave to design novel materials that suit particular technological and industrial utilization. To predict new materials, the *First Principle* or *ab initio* calculation is one of the easiest, inexpensive and economical method. Application of basic laws of Physics is the actual idea behind for perceiving and understanding the composition of various materials. A material is composed of atoms, while the atoms it-selves contain electrons, and the calculations of electronic-structure envision the functions and response of the material. This dissertation is an effort via *ab initio* calculations, to have insight understanding of the structure and various properties of a remarkable stacked compounds having an extraordinary account of utility and application. These compounds possess crystal structure related to that of mineral $MgAl_2O_4$, known as Spinel, have general formula AB_2X_4 with Close-Packed-Face-Centered-Cubic structure and belong to space group $Fd\bar{3}m$ (number *227*). They are of tremendous focus due to its use in optoelectronic devices and huge application in technological/industrial fields [1, 2]. Typically, A and B are metal ions of distinct valency while X is Oxygen ion, although a number of sulfides, fluorides and cyanides of similar structure are also known. In this work *Transition Metal Oxide Spinels with mentioned structure* are under consideration for studies. The oxide spinels are dished in earth crust & mantle as a considerable segment and are also known to exist generously in meteorites and celestial rocks. Hence the study concerning to their physical properties is profoundly appreciated and recognized. The oxide spinels constitute a vital class of ceramic compounds, so are outstanding fortuitous ceramics which demonstrate many interesting, unique and fascinating covetable electronic, optical, mechanical, elastic, magnetic, structural and superconducting properties [3-6].

As already stated in the commencing para, the material's research communities are enthusiastically involved in modeling and intellectual investigation of new

materials. For potential applications in everyday life, the knowledge and understanding of physical properties of such materials has always been of top interest. Based on physical features of such materials, they can be conveniently applied in the emergent demand of the hi-tech machines and latest technologies. Even in today's progressed technological time, the material scientists are still searching to find the most reliable, cheap and efficient materials. In the research communities, modeling and searching of cheap and the efficient materials has always been a fascinating field. The compounds in spinel group are varied from insulators to superconductors and from diamagnetic to fantastic magneto-resistive and magneto-capacitive compounds [7-10].

The use and applications of spinels in various ways make its position scientifically glaring, unique and important. The vastness of its use could be imagined from applications in variety of manners, from traditional to scientific, technological, industrial, medical and military fields. Oxide spinels exhibit excellent magnetic, refractory, semiconducting, catalytic and adsorption properties. Spinel structure possesses many enormous properties, which could apply in various industrial fields like pigments [11], magnetic materials [12], electrical materials [13], high frequency devices [14], catalyst for chemical synthesis [15, 16]. Spinels are featured by high melting temperature, high resistance to chemical attack, high strength [17, 18] and lesser electrical loss, hence they are contesting applicant materials for numerous usage in geophysics, catalysis the environment, magnetism [19], super hard materials, elevated temperature ceramics [20], and super capacitor [21, 22].

1.2 Scope of the Proposed Research

In condensed matter, the success of *ab-initio* calculations for predicting new materials and explaining it descriptively is due to thorough and far-reaching research. This success can also be attributed to development in computer technology, which has made the computation faster. Several theories have been exhibited up till now, commencing from Hartree (1930s) to the most popular and modern "Density Functional Theory". To deduce physical properties of a material, many body wave functions are

used. However, even with the fast speed supercomputers, it is highly intricate and perplex to work out the Schrödinger's wave equation. To resolve the problem Hohenberg & Kohn [23] and Kohn & Sham [24] proposed [25] density functional theory (DFT). Walter Kohn and John Pople took up density to solve the problem instead of using electron wave function as a basic variable. In 1998 they were bestowed upon with noble prize in recognition of their work. The DFT reliably serves to give an exact solution to the ground state physical properties of solids for prediction and comprehension of the structural, elastic, electronic, optical, magnetic and distinct physical properties of metals, semi-metals, half metals, semiconductors and insulators [25].

In this thesis we will solve Kohn-Sham equations [24] for investigating the structural, elastic, electronic and magnetic properties of Transition Metal Oxide Cubic Spinel Compounds. This research project will certainly provide theoretical grasp of the structural, elastic, electronic and magnetic properties of these compounds.

1.3 Computational Approach

Over the past few decades, the development of computation based research has established its bearing with firm validity, accuracy and capability in condensed matter physics which can efficiently and trustworthily model every material for study. The scientific method utilized to foresee and anticipate different attributes of such materials, using simply the information and facts of its composition is called *ab-initio* or *First Principle calculations.* In ab initio techniques, the fact that experimental data is not required for preparation/synthesis of materials makes it highly significant [26]. In this process the scientist is free to have full control upon all variable components of the material under investigation with extreme ease; changing the crystal structure, adding or removing atoms, reducing or increasing pressure, developing deformations introducing impurity or spin etc and then estimating the requisite properties as per desire can be plainly done. Hence, such computational results are much authentic than practical experimental work.

The introduction of Density Functional Theory (DFT) and its accession to quantum mechanics has unquestionably done amazing and noteworthy development in condensed matter physics that is able to treat many-body-problem conveniently. This relatively fresh theory concept of DFT, emanated in computational condensed matter physics properly suitable to efficiently portray the physical attributes of solid materials like structural, thermal, electrical, optical and magnetic properties. With emerging of computer technology & on its development and progressive advancement in algorithm, presently simulation of copious systems having 100 or more atoms in unit cell, is entirely conceivable. The aforementioned flourishing technique supply marvelous results in elucidating, transcribing and predicting a huge variety of materials phenomena. In this regard the inspiring examples are the analysis of silicon phase transition under high pressure [27], estimation of stable and meta stable adsorption geometries on surfaces of metal [28], perfect reproduction of structural & elastic parameters of natural spinel $MgAl_2O_4$ [29]. Moreover achieving vast comprehension of the structural, elastic, electronic, optoelectronic, magnetic and optomagnetic characteristics of many diverse materials.

1.4 Aim

The main aim of this work is to apply Density Functional Calculations to gain information about the density of states (DOS) of Spinel based Transition Metal Oxides i.e. to explain the electronic properties in terms of density of states (DOS). To calculate various properties of spinel including; elastic constants (leading to calculation of mechanical properties), electronic structure, and magnetic properties. Simulation Programme WIEN2K (ver.WIEN14) [26, 30] *for Research in Electronic Structure, Simulation, Optimization, calculations of elastic constants etc, and carrying out studies of magnetic properties,* has been used to fulfill the goal.

1.5 Objectives

In this study we will mainly focus on:

(1) To investigate the ground state properties of spinels, like the lattice parameters a_o, the elastic constants (C_{11}, C_{12}, C_{44}) the bulk modulus (B_o), the Reuss and Voigt moduli $(G_R \; and \; G_V)$.

(2) To carry out elastic and mechanical studies.

(3) The electronic structure density of state (DOS) will be studied.

(4) Based on crystalline elastic properties the Shear modulus (G), corresponding Young's modulus (Y), Poisson's ratio (ν), Lamme's coefficients $(\lambda \,\&\, \mu)$ will be determined.

(5) The isotropic/anisotropic behavior will be studied and tetragonal shear moduli $\left(G^{'}, G^{"}\right)$ along-with compressibility (K) will be calculated.

To the best of our knowledge for most of the spinel compounds, either no, or very less earlier studies on the elastic constants exists, as well its related mechanical and magnetic properties either not studied at all, or in some materials a few sequential have been touched only. Hence, we feel that calculations in this work will be used to fulfill the necessity of data for cubic spinels and for further foresight investigation will bear as resource reference.

1.6 Arrangement of the Dissertation

This thesis is arranged in five chapters. In ***chapter 1*** the broad-line introductive background is presented regarding our work. In ***chapter 2***, the literature review regarding spinels is presented, explaining spinel-structure, its types & characterization, applications and description about relevant properties to this dissertation only. In ***chapter 3*** the Density Functional Theory (DFT) is described in detail along with the computational approach which is the pathway for our calculations in this work. ***Chapter 4*** comprises of the results and discussion related to analysis of the structural, elastic, mechanical, electronic and magnetic properties of spinel compounds i.e. XAl$_2$O$_4$ (X = Mg, Mn, Fe, Co, Ni, Cu, Zn), MGa$_2$O$_4$ (M = Mg, Mn, Fe, Co, Ni, Cu, Zn, Cd), NIn$_2$O$_4$ (N=Mg, Cd, Zn) and ZnP_2O$_4$ (P=V, Cr, Fe, Rh, Sn) & VZn$_2$O$_4$. In ***chapter 5***, the work is concluded and future aspect and prospect is presented.

CHAPTER – 2

SPINELS - THEORETICAL FRAMEWORK

The minerals which acquire spinel structure and whose physical characteristics are managed through the general formula AB_2X_4, have obtained enormous consideration due to their workable applications in opto-electronic. Spinel compounds (AB_2X_4) are having densely packed Face-Centered-Cubic structure and belong to space group $Fd\bar{3}m$ (number *227*) [1, 2, 31, 32]. Typically, A and B are metal ions of different valency and X is an Oxygen ion, but a number of sulfides, fluorides and cyanides of similar structure are also known. Spinel-Oxides possess exciting physical and chemical properties due to which they are studied widely [33]. They have workable utility in many technological and industrial applications, including magnetic materials [33-37], super hard materials [20], high-temperature ceramics [38], catalytic materials [39-42], and humidity sensors [42-45,]. Oxide spinels being ionic, contain in its lattice of 'oxygen anions' duly embedded 'properly charged metal cations'. The O^{2-} having closed shell $2p^6$ configuration arranged in 'ABCABC' face-centered cubic (*fcc*) lattice or 'ABABAB' hexagonal-close-packed (*hcp*) lattice, with two forms of interstices in the structure, that may be filled by cations (shown in Figure 2.1). The smaller and larger sites are tetrahedral and octahedral respectively. In present work "Spinel based Transition Metal Oxides" have been studied. It is evident from above passage that the driving factor for studies of the existing Spinel based transition metal oxides, is the glaring and conclusive application and uses of these materials in technological progress.

2.1 Historical Background, Formation and Synthesis of Spinel

Spinels are documented as early as sixteenth century by Eden in 1555 [47], Hakluyt in 1599 [48]. The Spinel, named by Jean Demeste in 1779, that ingeniously designated for red gemstones, same are recognized as $MgAl_2O_4$ crystals. *Spynel*, *spinell*, *spinal*, *espinal* and *spinell*e are the substitute spellings of Spinel [49],

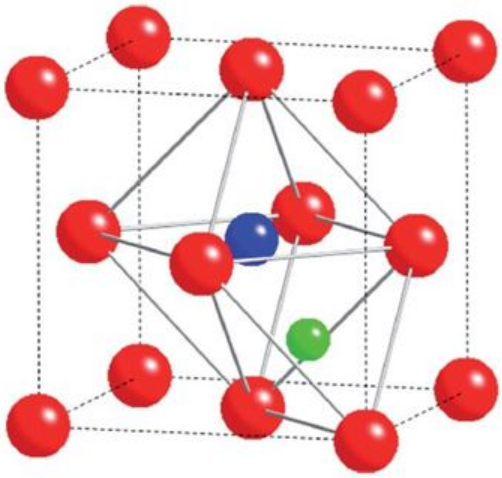

Fig 2.1*: A close-packed, with octahedral and tetrahedral cation sites shown in blue and green respectively* [46].

is derived word from;

(1) "Spina" a Latin word that means 'little thorn" and is attributed to sharp points on some crystals;

(2) or due to spinel's red color, is a pick for spark from Greek language.

Although, confirm derivation of the name 'Spinel' is not sure, but its source may be the Latin "spinella", termed from the bantam 'spina' [50].

The spinels have been incorrectly labeled as rubies. As a result, there are many infamous rubies which are actually red spinels, e.g the Black Prince's ruby that is fixed in England's Imperial State Crown [51-54]. For confirmation of the spinel's splendid and impressive properties, the magnetic characteristics of magnetite (Fe_3O_4) the ancient spinel mineral, is the best consideration. This is arguably the most important mineral, from a historical perspective. In ancient times, magnetite was notorious as *lodestone* (*loadstone,* or *lodysshestone*) that exactly means "way stone," from the use of the magnet in guiding mariners, being used to magnetize the mariner's compass [55]. Several natural compounds were identified in 19th century to have the common structure of spinel. The list of compounds is substantial today that are retaining the spinel structure, refer Table 2.5 procreated from Grimes [56] illustrates the vast variety of spinels.

Roughly every gem spinel is formed by contact metamorphic activity with infringement of molten rock masses into impure lime-stones or dolomites. History conceives that regular mining of spinel for the first time was done in Afghanistan at Badakhsha about 750 AD [17]. In the gem gravels, the spinel is mixed with the rubies. [57]. Presently, Myanmar (Burma) is a source of pink, orange, violet, brilliant red and somber blue spinels. From Ceylon the blue, violet hues, good red and pink spinels have been reported. Non-gem spinels crop up special aluminum-rich volcanic rocks, and also in deposits which originates from the metamorphic alteration of such rocks. Spinels are also recovered in Thailand, Nigeria, Africa, Vietnam [58-64]. Mines of blue spinels exist in Vietnam, Myanmar, Sri Lanka, Tanzania and Pakistan [62, 65, 66]. Different regions producing ruby and red or blue spinel display definite attributes. Red spinel and rubies have a very similar paragenesis but ruby comprising rocks are much different from those carrying blue spinel [64].

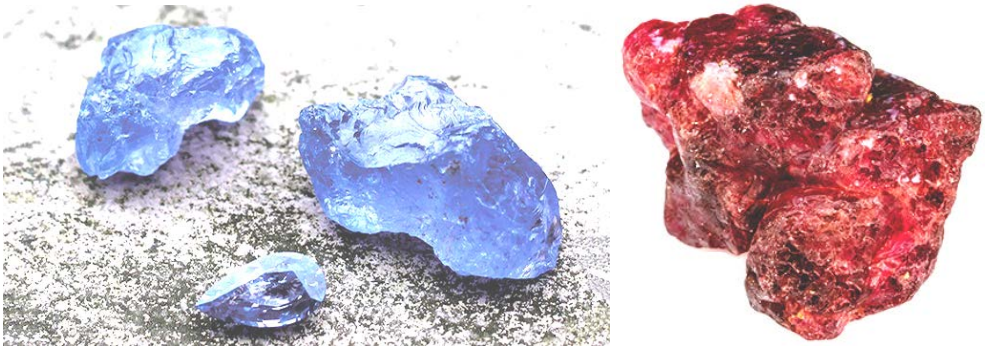

Figure 2.2: (a) Blue Spinel* [64]** ***(b) Red Spinel

Blue spinel is noted in olivine-rich lenses only, associated with dolomite and calcite (Figure 2.3). In absence of olivine blue spinel are not observed. [64]. Blue and Red spinels are always discovered in marble (Figure 2.4) [67-72].

In 1847, a French Chemist named Jacques-Joseph Ebelmen produced the first Synthetic spinel [73]. This fact is also confirmed by Anderson in 1952 [74], who noted that the materials with Spinel structure have been synthesized as early as 1850. In 1916, Rankin and Merwin [75] recount synthesis of $MgAl_2O_4$ solid solution alongwith

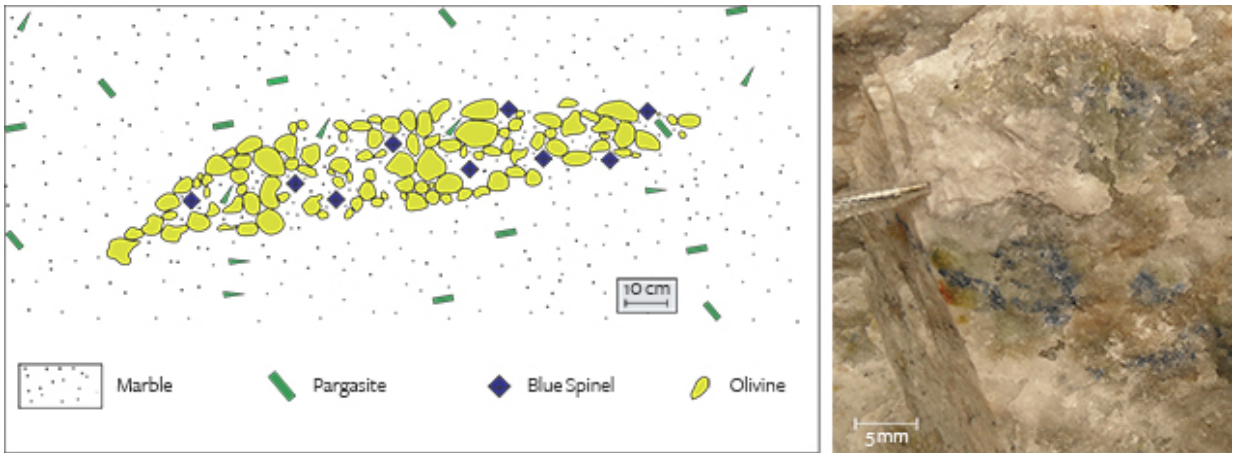

***Figure* 2.3** *Primary blue spinel deposits of lens-shaped bodies rich in olivine, from Vietnam* [64].

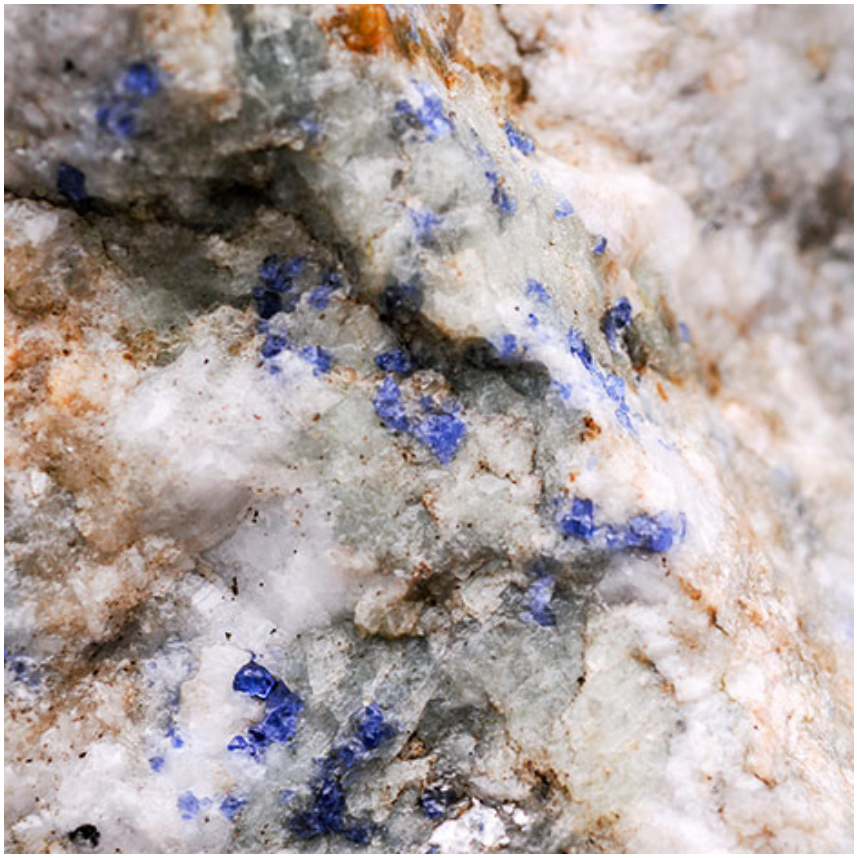

***Figure* 2.4** *Blue spinel from Luc Yen in its marble host* [64].

α-Al_2O_3. Clark in 1924 reported that the magnesium-aluminate spinel, has been synthesized in several ways and by a number of investigators [76]. In 1928, Rinne has carried out an extended study of synthetic spinel [77]. In 1936, Wagner [78] reported

that spinel was initially synthesized over 900°C, in which the reaction occurs at contact surfaces of the two constituent oxides [79];

$$\underset{\text{(rock salt structure)}}{AO} + \underset{\text{(corundum-like structure)}}{B_2O_3} = \underset{\text{(cubic spinel)}}{AB_2O_4} \quad \ldots\ldots\ldots (2.1)$$

Wagner reported that the spinels formation occurs as Cations A^{2+} and B^{3+} diffuse in opposite directions through the previously formed layer of Spinel. During this ionic diffusion, the Oxygen ions remain immobile. Generally the synthesis is done in two stages, the spinelization process is completed first, then in the second stage firing; "crushing, milling, reshaping and sintering the spinel" is done in order to achieve desired properties [80, 81]. High density spinel can be prepared through high sintering temperature and use of oxygen atmosphere or by using costly and specialized techniques such as hot pressing followed by sintering [82-86]. For formation of pure & ultrafine aluminate spinel, the Pechini sol-gel modified method [87] is used. Commonly, the aluminate catalysts and ceramics are synthesized by high-temperature calcination, coprecipitated products [88-90], sol–gel product [89-92], and products of impregnating a porous alumina [88, 93, 94]. During the recent past, the researchers' curiosity in the formation of nanocrstalline metal oxides has been increased [95-99]. For preparation of aluminate spinel, various chemical routes exist ($CoAl_2O_4$, $NiAl_2O_4$, $CuAl_2O_4$, $ZnAl_2O_4$) powders [98-101]. Meyer *et al* [102] created nanosized spinels MAl_2O_4 (M=Co, Ni, Cu) as bivalent cations in different particle sizes. Ordinarily, the transition metal aluminates are prepared using various techniques by implying high-temperature solid state reactions between the constituent oxides [98, 103-121]. Hettig *et al* [122], Zawadzki [111] and Duan *et al* [121, 123], reported the synthesis of $ZnAl_2O_4$. In 1961, Navias [124], Fuerstenau *et al*. [125] and in 1962 Alper *et al*. [126], reported the formation of Spinel $MgAl_2O_4$. In 1993, Kurihara and Steven [107] synthesized several ternary metal oxides $MgAl_2O_4$ "M = Mg, Ni, Co, Cu, Fe, Zn, Mn, Cd, Hg, Sr". Petrova *et al* [127], obtained $MgAl_2O_4$, $ZnAl_2O_4$ and Mg_2TiO_4. Otero *et al* [128] prepared Cobalt aluminate $CoAl_2O_4$, and Al_2O_3–$CoAl_2O_4$ solid solutions. Synthesis of $NiAl_2O_4$, $CoAl_2O_4$, $CuAl_2O_4$ and

$ZnAl_2O_4$ nanocrystal spinel powders have been reported [129-134]. Mimani [115] prepared some transition metal aluminates having notably enhanced properties of the materials. Various techniques have been reported for preparing $MgIn_2O_4$ films [135-140]. Dali *et al* [141] manufactured and marked AIn_2O_4 (A = Mg, Ca, Sr, Ba). Li *et al*. [142] carried experimental study of structural and electrical properties of $CdIn_2O_4$. The results unveil $CdIn_2O_4$ thin films formation with spinel phase, duly supported by increased substrate temperatures [142]. $MgIn_2O_4$ & $Zn_2In_2O_5$ films were prepared by Minami *et al* [143].

2.2 Colour Change in Spinels

In spinels, the dominant origin for colour change is the absorption band varying by several frequencies (nm). Different bands can be allocated due to substitution of various anions in spinel structure at tetrahedral site in lieu of Mg^{2+} [65, 66, 144-152]. There are actually a range of colours that spinel can adopt depending on the foreign element substituted into the basic structure. In fact, blue spinels, which are so coloured due to the presence of iron or cobalt (rarer), are often used as a substitute, and mistaken, for sapphire [65]. The heightened brilliance of spinels is a result of being singularly refractive. This means that the gemstone only has a single refractive index.

In order to copy standard gemstones (like ruby, aquamarine, zircon, tourmaline, emerald and chrysoberyl) the synthetic spinels were contrived in a number of colours in 1930 decade. Various colours are created by fragmenting an amount of metals into the stone. It give blue colour by the addition of cobalt oxide, yellow by manganese, green by chromium oxide and pink colour is produced when iron is added to the stone. The hues of the stone are managed by careful chemical procedures [153].

2.3 Spinel Structure

The physical properties of solid materials are strongly linked to their structural parameters, therefore knowledge of the crystal structure of a studied compound is an essential aspect. Spinel structure is titled in relevance to the mineral spinel ($MgAl_2O_4$),

which is cubic and possesses greatest possible number of symmetries. Sometimes, it is also commissioned as garnet structure and is fundamentally the same as that of the diamond structure [154]. The unit cell of the spinel structure characteristically consist of eight molecules, with the oxygen–O, sulfur–S, selenium–Se or Tellurium–Te anions in almost close packed cubic pattern and the metal ions are arranged among the interstices between the anions, in a fashion to minimize the total energy of the system [155].

Many spinels demonstrate intricate disordering phenomena by implication of two cation sites, which effect significantly, its physical and thermochemical properties [156, 157]. The 'O' ions are placed at (u, u, u) positions, the eight A^{2+} ions at (1/8, 1/8, 1/8) and sixteen B^{3+} ions at (½, ½, ½) [158].

The general chemical formula for spinel family of compounds is $A^{II}B_2^{III}X_4^{VI}$. The roman numerics mark particular columns of elements in the periodic table. In normal circumstances for anion X=O, S, Se or Te, most of these compounds grow in the cubic phase [5]. The cubic spinels with general chemical formula AB_2X_4 having both A and B as the cations and X represents the anion, furnish close packed face centered cubic (fcc) structure. Upon arrangement of cations randomly over each kind of site, gives eight formula units (each $MgAl_2O_4$) making one unit cell ($Mg_8Al_{16}O_{32}$), that is generally designated to the space group $Fd\bar{3}m$ *(#227)* [159-164]. In this study the **A** ion is varied (Mg, Mn, Fe, Co, Ni, Cu, Zn, Cd) and the **B** ion is Aluminum (Al), Gallium (Ga), Indium (In), and the X ion is Oxygen. Further, Zincho spinels with various A & B ions are studied.

For comprehending inside of the structure, the parent spinel $MgAl_2O_4$ is considered as typical material. Each Mg atom is related to four oxygen neighbours tetrahedrally within the eight formula units inside the cubic unit cell, while every Al atom at octahedral site is encircled by six O neighbours. The structure contain eight octants being divided in types I and II as reflected in Fig 2.5. One kind of octant (I) hold Mg ions arranged in tetrahedral balance and the second kind octants (II) hold Al ions in octahedral seat Fig 2.6

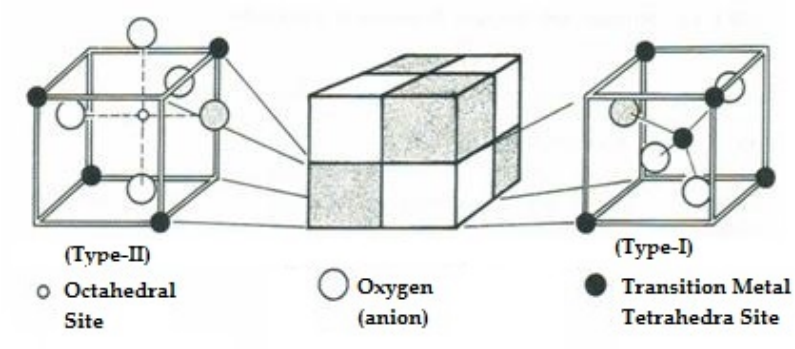

Figure 2.5: Spinel structure showing transition metal sites that are tetrahedrally (Typ-I) and octahedrally coordinated by oxygen anions. The shaded oxygen atom is shown in two subcells; it links A and B sites.

Bragg [154, 165] and Nishikawa [166] individually carried out the determination work of crystal structure of spinel and ascertained it in 1915. The earliest studies of Bragg [154, 165], Nishikawa [166] and Goldschmidt [167] appeared at the dawning era of X-ray structure determination. These authors agree in assigning the diamond type of lattice to the group and the spinel structure which they determined, since become a standard type. The spinel mineral examined by Nishikawa was ruby spinel from Ceylon [168]. Posnjak, worked out the lattice dimensions of spinel via X-ray diffraction patterns describing detailed dimensions [169]. Since then there were numerous reports from various fields of research [170]. In cubic-unit cell of natural $MgAl_2O_4$ (for example a= 8.0898 A^o), 96 interstices exist between the anions; though 24 of them are occupied by cations in compounds of the form AB_2X_4. There are 64 tetrahedral holes amid of anions, of which cation occupy 8. The leftover 16 cations capture half of the 32 octahedral holes. The cations adjust in *tetrahedral* combination, originates a diamond cubic sublattice with a unit repetition equated to the lattice constant. Also, period of the sublattice associated to cations organize in *octahedral* manner is equal to *a* [17].

In the anion's setting, the tetrahedrally pattern interstices are filled by A- type cations as demonstrated by orange colour in the polyhedral crystal structure of Spinel in Fig 2.7 whereas the B cation possess the octahedral holes as displayed by blue colour. The Spinel polyhedral structure holds eight A type tetrahedra and sixteen B octahedra,

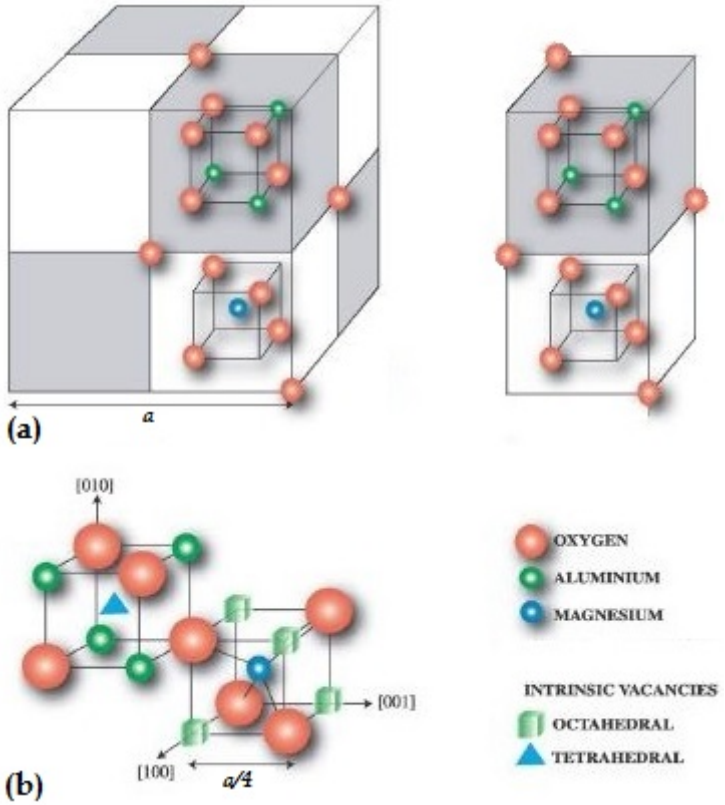

Fig* 2.6: *(a) *Primitive tetragonal & conventional cubic unit cells of spinel adopted from Sickafus* [17]. The unit cell consists of alternate octahedral and tetrahedral structures.
(b) *Mg and Al ions occupy tetrahedral and octahedral sites respectively. Blue triangles depict the unoccupied tetrahedral sites while the green cubes show octahedral sites* [172, 173]**.**

and carries 56 tetrahedral & 16 octahedral vacancies [164] same are not shown in Fig 2.7. Any two neighbouring tetrahedra point towards each other. If perpendicular is drawn from each tetrahedron corner on the opposite face, it will encounter another tetrahedron, passing first through the middle point of a face and then through the opposite corner. A trivalent atom lies on each such connecting line, half-way between the tetrahedra. Four trivalent atoms are associated with each tetrahedron, but each atom is shared by two tetrahedra. The size of the tetrahedron may not be the same in all members of the group of crystals. The divalent atom lies at the centre of a tetrahedron of oxygen atoms, and trivalent occupy the centre of an octahedron [174, 175].

The octahedrally coordinated cations adopt a pyrochlore lattice with a corner shared. Filled octahedral make rows in intersecting lines, with alternating layers of parallel rows offset as shown in Fig 2.8(b). The square rows of octahedral are filled with tetrahedra. The anions order in a pseudo cubic close packed pattern (pccp). The A site tetrahedra in spinels are sufficiently apart from one another, sharing corners with nearest neighbour B-site *octahedra*. But within A site tetrahedra with each-other or with a B site *polyhedra*, edge sharing is not observed. Out of twelve (12) X-X edges the B site octahedra share 6 with other closest B site octahedra, the remaining six (6) edges are shared with those octahedra which are encompassed by vacant sites. The X-X shared edges of B cations outline chains in the lattice along (110) directions. The distances between B-B sites are short, and in some spinels these are responsible for electrical conductivity [176-178].

It is almost impossible to draw the complete unit cell of spinel and its contents, comprehensibly, since it is eight folds (i.e. 2 x 2 x 2) large cube, to the size of a typical face centered cube. However, to illustrate certain features of the cell and to understand how the structure arises, we use the drawing of structural fragments or layers of the cell in Fig. 2.9, which could help in understanding the formation of the cell. To choose or set the origin for spinel in space group Fd $\bar{3}m$, is having an important role in order to describe the atomic positions of the crystal structure, since these atomic positions in the unit cell are dependent on choosing the origin. There are likely two different choice of origin for the unit cell with point symmetries $\bar{4}3m$ and $\bar{3}m$ and therefore origin could be allocated either to a vacant site or to an occupied lattice site**.** Conventional choices are, either $\bar{4}3m$ on an A-site or $\bar{3}m$ on an octahedral vacancy (the latter is an inversion centre) [17]. Four possible origin selections, with order of lattice sites along the unit cell body diagonal are listed in Table 2.1. The structural parameters; atomic placement, point site symmetry and atomic coordinates are presented in Table 2.2. Two numerical restrictions characterizes the crystal structure of spinel, one is the lattice constant *a*, and other is oxygen parameter *u*. Beside *a* and *u* the cation inversion parameter x is taken as third restriction [2]. The anions coordinates at *32e* position rely on distribution,

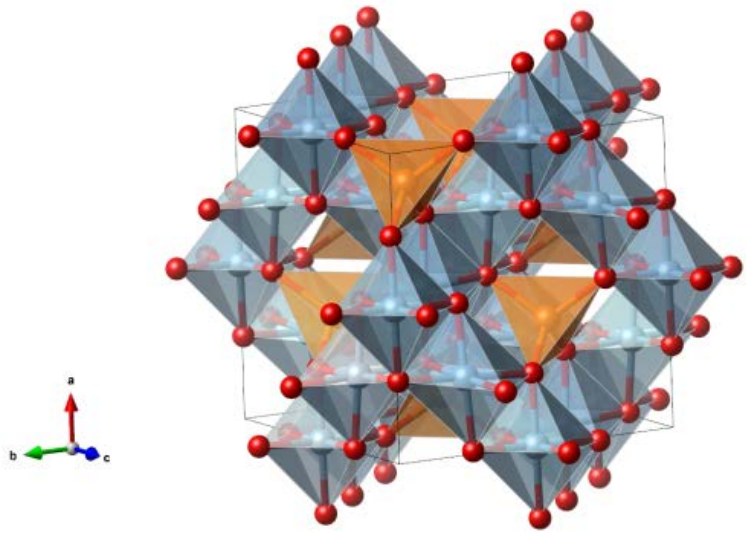

Figure 2.7 A Spinel Unit cell with polyhedra arrangement. [175].

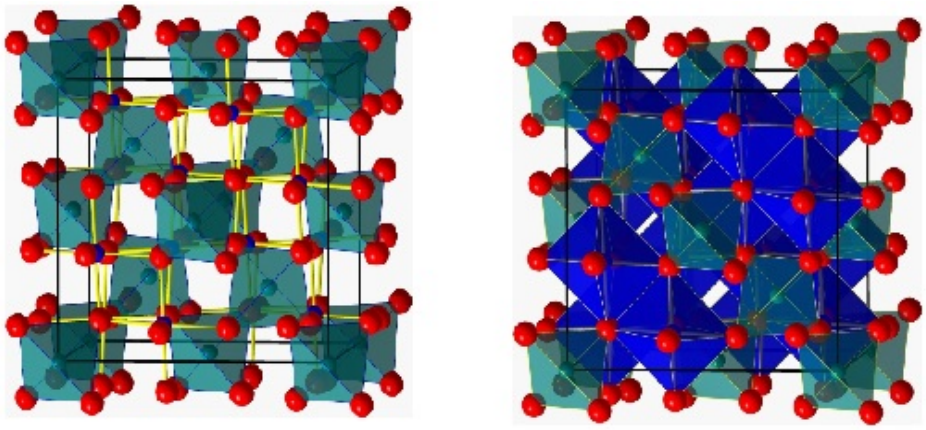

Fig 2.8: (a) A cation is tetrahedrally (Divalent) (b) B cation is octahedrally coordinated (Trivalent) [179]

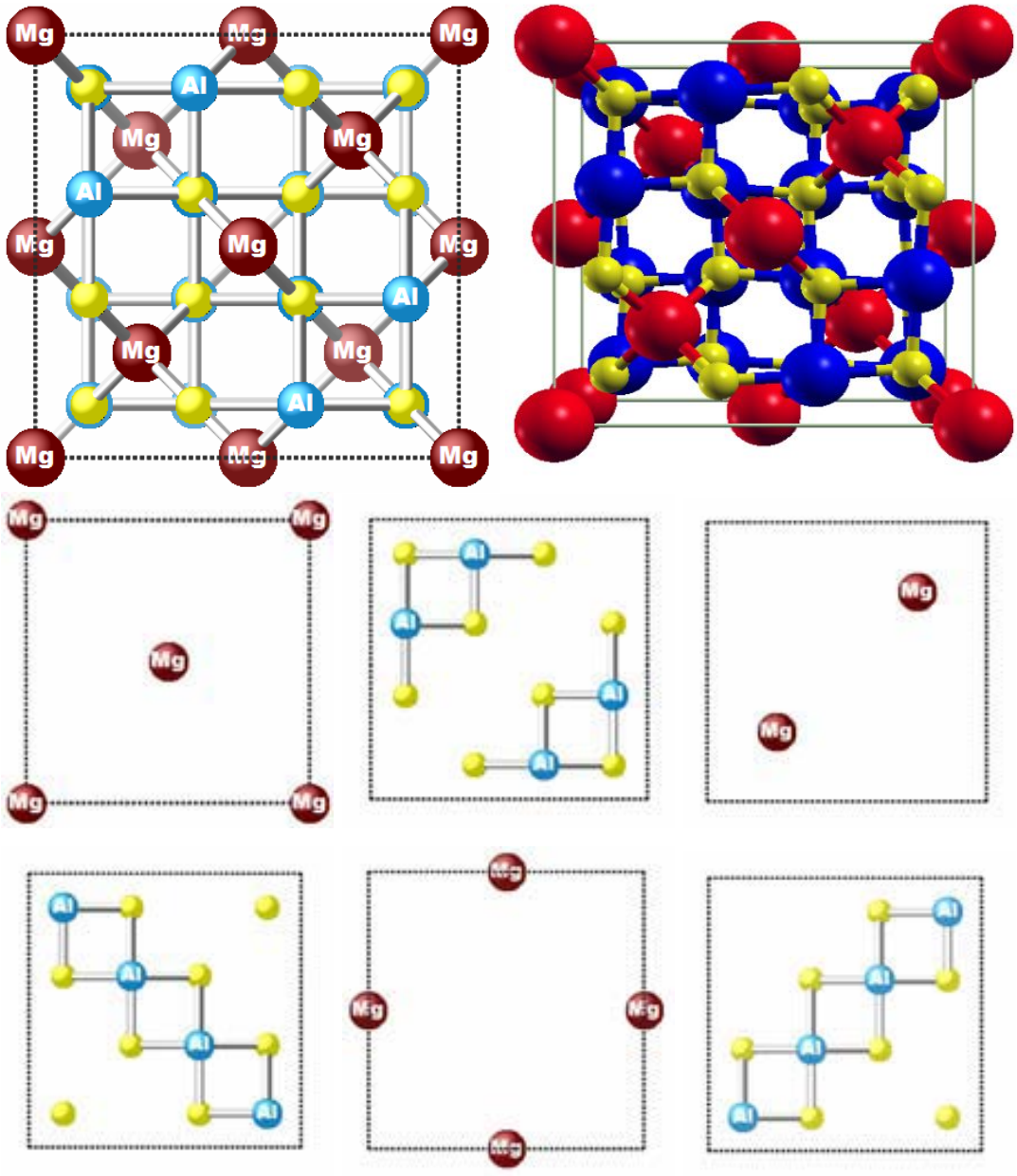

Fig 2.9: Spinel Structure top-view; combined and in split fragments layer by layer [180].

Table 2.1: *Four possible origin choices* [17].

Fractional coordinates along body diagonal of unit cell	Origin at $\bar{4}3m$			Origin at $\bar{3}m$		
	Equipoint	Origin choice		Equipoint	Origin choice	
		A site	Tetrahedral vacancy (**TV**)		B site	Octahedral vacancy (**OV**)
(0,0,0)	8*a*	A site cation	TV	16c	B site cation	OV
$(1/8, 1/8, 1/8)$	16c	OV	B site cation	8*a*	TV	A site cation
$(1/4, 1/4, 1/4)$	8*a*	A site cation	TV	32e	X Anion	X Anion
$(3/8, 3/8, 3/8)$	32e	X Anion	X Anion	8b	A site cation	TV
$(1/2, 1/2, 1/2)$	8b	TV	A site cation	16d	OV	B site cation
$(5/8, 5/8, 5/8)$	16d	B site cation	OV	8b	A site cation	TV
$(3/4, 3/4, 3/4)$	8b	TV	A site cation	32e	X Anion	X Anion
$(7/8, 7/8, 7/8)$	32e	X Anion	X Anion	8*a*	TV	A site cation

Table 2.2 *Spinel structure parameters and fractional coordinates* [17, 182].

Atom lattice site		A site cation	Tetrahedral vacancy	Octahedral vacancy	B site cation	X − Anion
Ion		**8A**	**8A**	**16B**	**16B**	**32X**
Location		8*a*	8*b*	16*c*	16*d*	32*e*
Point Symmetry		$\bar{4}3m$	$\bar{4}3m$	$\bar{3}m$	$\bar{3}m$	$3m$
Fract. Coord. of lattice site	**Origin selection at 43m on A site cation**	*(0, 0, 0); (¼,¼,¼)*	*(½, ½, ½); (¾ , ¾ , ¾)*	*(1/8,1/8,1/8); (1/8,3/8,3/8); (3/8,1/8,3/8); (3/8,3/8,1/8)*	*(5/8,5/8,5/8); (5/8,7/8,7/8); (7/8,5/8,7/8); (7/8,7/8,5/8)*	(u,u,u); $(u,\bar{u},\bar{u})$; $(\bar{u},u,\bar{u})$; $(\bar{u},\bar{u},u)$; $(1/4-u, 1/4-u, 1/4-u)$; $(1/4+u, 1/4+u, 1/4-u)$; $(1/4+u, 1/4-u, 1/4+u)$; $(1/4-u, 1/4+u, 1/4+u)$
	Origin selection at 3m on octahedral vacancy	*(1/8,1/8,1/8); (7/8,7/8,7/8)*	*(3/8,3/8,3/8); (5/8,5/8,5/8)*	*(0,0,0); (0, ¼, ¼); (¼. 0, ¼); (¼,¼,0)*	*(½, ½, ½); (½,¼,¼); (¼, ½, ¼); (¼,¼, ½)*	(u,u,u); $(\bar{u},\bar{u},\bar{u})$; $(u, 1/4-u, 1/4-u)$; $(1/4-u,u, 1/4-u)$; $(1/4-u, 1/4-u,u)$; $(\bar{u}, 3/4+u, 3/4+u)$; $(3/4+u,\bar{u}, 3/4+u)$; $(3/4+u, 3/4+u,\bar{u})$

hence the *u* parameter is introduced in order to locate the anion placement. In a perfect close packed (ccp) anion the parameter *u* equals to 0.375 ($u_{ideal}^{\bar{4}3m}$) and 0.25 ($u_{ideal}^{\bar{3}m}$). Anion dilation occur in true spinel structure from their ideal ccp locations, which is of immense significance and may modify crystal stability as a result of changes to the crystal i.e. effect bond lengths, interstices volume, bond angles and coordination symmetry [17]. Hence, this anion fractional coordinate *u* in the spinel structure strongly depends on the cation inversion parameter [171, 181].

2.4 Space group and Symmetry of Spinel Structure

The spinel unit cell possess 32 anions, is fcc and belongs to $Fd\bar{3}m$ (O_h^7, number *227*) space group, with cations fill the specific positions of 'inversion centers 8a ($\bar{4}3m$) with no free-position parameters' and 'the 16*d* ($\bar{3}m$) positions'. The anions (O^{2-} ions) take up the common place 32*e*, that additionally needs the oxygen parameter *u* for their complete interpretation. Upon taking center of symmetry at the origin of the unit cell, *u* sets in between 0.24 to 0.275 [159]. The anion forms exactly cubic close packing for *u*=0.250, defining polyhedron about the 8a sites point symmetry ($\bar{4}3m$) in regular tetrahedral arrangement and a regular octahedron about the 16d sites (m3m). In this case the bond length distance between octahedral cation-anion becomes larger than the tetrahedral bond length, accordingly the octahedral site becomes smaller.

Nishikawa [166] in 1915, assigned the space group $Fd\bar{3}m$ (O_h^7) to spinel ($MgAl_2O_4$), but in 1958 Jagodzinski and Saafeld [183] suggested for the first time, that a better description might be afforded by the F$\bar{4}$3m space group. Their evidence mainly based on the system $MgCr_xAl_{2-x}O_4$. Same suggestion of F$\bar{4}$3m space group put forth by Grimes in several publications [163, 184-187], referring the crystal structure of cubic spinels to the non-centrosymmetric space group $F\bar{4}3m$ (#216) in lieu of conventional $Fd\bar{3}m$ (#227).

The non-centrosymmetric space group $F\bar{4}3m$ (#216) [188] for a completely normal spinel ($MgAl_2O_4$), having origin at $\bar{4}3m$, the coordinates hold positions 000, $\frac{111}{222}$,

$\frac{1}{2}0\frac{1}{2}$, and $\frac{1}{2}\frac{1}{2}0$. Mg ions take two placement 4*a* and 4*c*, with point symmetry $\bar{4}3m$ and coordinates 000 and $\frac{1}{4}\frac{1}{4}\frac{1}{4}$, both. The Al ions spots 16*e* positions having 3*m* point symmetry, while oxygen ions also pose two 16*e* places, and hence cited as O_1 & O_2 respectively. The Al ions are located at *uuu*, $u\bar{u}\bar{u}$, $\bar{u}u\bar{u}$, and $\bar{u}\bar{u}u$ with $u = \frac{5}{8} + x$; O_1 appear at $u_1u_1u_1$ etc, with $u_1 = \frac{3}{8} + x$. While O_2 fall at $u_2u_2u_2$ etc, with $u_2 = \frac{7}{8} + x$ [189].

Grimes argument [185, 186] was based on the reason that in oxide spinels the octahedrally coordinated metal ions dislocate from the centre of an octahedral interstice along ⟨111⟩ direction [190]. Such off-centre displacements inferred from electron spin resonance [191], optical spectra [192], x-ray Debye-Waller-factor measurements [193] and infrared spectra [163]. Such displacement results two effects [194] i.e (i) weak extra peaks occurs as are done in $F\bar{4}3m$ (but prohibited in $Fd\bar{3}m$), and (ii) an unusual high mean-square deposition (i.e. Debye- Waller factor) of the off-centre ion. The Grimes concluded it on a principal comparison of the Debye temperature acquired from the Debye-Waller factor with the Debye temperature determined from infrared absorption analysis [195]. However, he pointed the problem in proving the presence of an 'off-centre' Al^{3+} ion in $MgAl_2O_4$ and $ZnAl_2O_4$ [190]. Hence, Grimes [185] suggestion of the space group $F\bar{4}3m(T_d^2)$ does not have the inversion centers. Generally, unlike ions (A and B) have dissimilar sizes, as a result the structural parameters *a* and *u* will cause to adjust according to the variation in degree of inversion x. Since in normal spinel, divalent metal ions are big and trivalent cations are small. The big divalent ions reside on smaller tetrahedral sites while the small trivalent metal ions take up the larger octahedral sites. The enlargement of small tetrahedral sites occurs while accommodating the large ions, and displacement of oxygen ions in ⟨111⟩ direction occurs, relative to the placement of the fixed metal ions. As a result the octahedral sites attenuates to small size, degenerating their symmetry from $m3m$ to $\bar{3}m$, however the six octahedral bond distances stay unchanged [156]. In spinel unit cell the placement of oxygen ions are determined in terms of parameter *u*, which carries value 0.250 for an

ideal spinel with fractional coordinates (u, u, u). Hence, this parameter (u) decides the adjustment of the crystal structure for its accommodation of different size cations on tetrahedral and octahedral sites. But, parameter u is the only variable atomic position in the structure and usually deviates from the ideal value (u=0.25).

When origin of the unit cell is at center of symmetry $\bar{3}m$, u equals to 1/4 i.e. 0.25, and oxygen ions form cubic close pack array. With increase (*u>1/4)*, the oxygen ions displaces from nearest placement $\bar{4}3m$ (i.e A-site) in ⟨111⟩ direction and tetrahedral:octahedral radius ratio increases, swelling tetrahedral site on cost of octahedral [156, 196, 197].

More detail of the Grimes' concept given by Smid and Ascher [198], however, Walters and Wirtz [199] reported that electron-diffraction studies show the behaviour of (200) type reflections in $MgFe_2O_4$ but absent for parent spinel $MgAl_2O_4$. While, Hwang *et a1* [190] insist on the space group $F\bar{4}3m$ based on presence of type (200)-electron reflection pattern. In neutron scattering study of magnetite Fe_3O_4, Samuelsen & Ascher [198] did not find (200) pattern. Samuelsen & Steinsvoll [200] describe, that 'adequate comprehension of the dielectric properties and Deby-Waller factors of many spinels, with space group $Fd\bar{3}m$ is difficult', the fact which led Grimes [185, 186] for suggesting a space group that let the B-site ions to budge from their particular positions. The result of Hwang and Heuer [190] electron diffraction study of $MgAl_2O_4$ spinel were consistent with Grime's suggestion of $\bar{4}3m$ space group.

Heuer and Mitchell [189] reviewed $MgAl_2O_4$ space group issue, through electron-diffraction, and re-affirmed the claim in support of the previous work [190] that the space group of $MgAl_2O_4$ is promisingly $F\bar{4}3m$ instead $Fd\bar{3}m$. Thompson and Grimes [201] carried out a detailed neutron diffraction work but gave no conclusion on the space group. Mishra & Thomas [202] proposed, the substitution of space group $Fd\bar{3}m$ by $F\bar{4}3m$. In a Raman spectroscopy work of $MgAl_2O_4$ by Striefler and Barsh [203], supports notion of lower symmetry than $Fd\bar{3}m$. Samuelsen & Steinsvoll [200, 204] by neutron diffraction, [205] a revisit by neutron-diffraction (of larger wavelength 4.17°A), and Tokonami & Horiuchi [206] by electron-diffraction study of $MgAl_2O_4$, rejected the

prospect of the spinel space group as $F\bar{4}3m$.

Rouse *et al* [194] examined $MgAl_2O_4$ carefully by powder neutron diffraction using both $Fd\bar{3}m$ and $F\bar{4}3m$ with supposition of 'no inversion of the two types cation'. They found no evidence of off-centre movement of the octahedrally coordinated cations. Staszak and Poetzinger [195] taking $F\bar{4}3m$ as basis, calculated the positional parameters of the spinel $MgAl_2O_4$. Taking the Mg, Al and O ions locations as described in the international tables 1968, they notioned that $MgAl_2O_4$ structure could be assigned to $Fd\bar{3}m$. The atomic positions of the above mentioned two authors are shown in Table 2.3, comparatively.

As the symmetry of $MgAl_2O_4$ spinel corresponding to space group $Fd\bar{3}m$ is having difficulties for proper and absolute interpretation of several of its physical properties (like dielectric behaviour; magnetism; heat capacity; infrared spectra; electron spin resonance and optical fluorescence spectra etc) and therefore it has become difficult for the spinel materials to reconcile with the experimental observations of physical behaviour with $Fd\bar{3}m$ symmetry. Beside the enormous amount of work by researchers on the issue, the debate has by no means reached a consensus.

Table 2.3 *Atomic sites of $MgAl_2O_4$ in space groups $Fd\bar{3}m$ and $F\bar{4}3m$.*

[194]						[195]		
$Fd\bar{3}m$			$F\bar{4}3m$			$F\bar{4}3m$		
Mg	8(*a*)	0,0,0	Mg	4(*a*)	0,0,0	Mg	4(*a*)	0,0,0 plus FCT
				4(*c*)	¼, ¼ ¼		4(*c*)	¼, ¼ ¼ plus FCT
Al	16(*d*)	$\frac{5}{8},\frac{5}{8},\frac{5}{8}$	Al	1(*e*)	u_2, u_2, u_2, with $u_2 \approx \frac{5}{8}$	Al	1(*e*)	u_3, u_3, u_3; $u_3, \bar{u}_3, \bar{u}_3$; $\bar{u}_3, u_3, \bar{u}_3$; $\bar{u}_3, \bar{u}_3, u_3$; plus FCT u_3=0.625+δ_3
O	32(*e*)	u_1, u_1, u_1, with $u_1 \approx \frac{3}{8}$	O	16(*e*)	u_3, u_3, u_3, with $u_3 \approx \frac{3}{8}$	O	16(*e*)	u_1, u_1, u_1; $u_1, \bar{u}_1, \bar{u}_1$; $\bar{u}_1, u_1, \bar{u}_1$; $\bar{u}_1, \bar{u}_1, u_1$; plus FCT u_1=0.375-δ_1
				16(*e*)	u_4, u_4, u_4, with $u_4 \approx \frac{7}{8}$		16(*e*)	u_2, u_2, u_1; $u_2, \bar{u}_2, \bar{u}_2$; $\bar{u}_2, u_2, \bar{u}_2$; $\bar{u}_2, \bar{u}_2, u_2$; plus FCT u_2=0.875-δ_2

FCT: face centering translations, $\frac{1}{2},0,\frac{1}{2}$; $\frac{1}{2},\frac{1}{2},0$; $0,\frac{1}{2},\frac{1}{2}$.

2.5 Categorization and Classification (Normal, Inverse and Random) of Spinels

The spinels are categorized into two main groups, Oxide spinel and Thio spinel groups. The Thio refers to sulfur at the anion position, or similar anion (selenide or telluride). Hence this group is composed of Sulphides, Selenides and Tellurides. The Nitride spinels is considered as the third group along with the above two mentioned groups. These groups depending on the anion X (i.e, X=O, S, Se, Te) and are further characterized into sub-groups and a series of species. Many oxides, sulphides and halides have the spinel structure with several conceivable charge attribution [11, 181, 197, 207, 208].

For AB_2X_4 spinel, two profound arrangements of cations among the available sites are accepted [209, 210]; the *Normal* $A[B_2]X_4$, and *Inverse* $B[AB]X_4$ distributions. The ions in brackets show occupation of octahedral sites. In fact, almost all spinels are somewhere amid these two terminal limits [211] and are known as *Random* or *Intermediate* spinels. Spinels with intermediate arrangement were outlined by Verwey & Heilmann [176]. For example; $MgAl_2O_4$, $MgTi_2O_4$, $MgCr_2O_4$ and $ZnCr_2Se_4$, crystallize in normal arrangement, while Ferrites and Magnetites take up the inverse structure $NiFe_2O_4$, $CoFe_2O_4$, $MgFe_2O_4$ and Mg_2TiO_4.

The cation distribution may be quantified by fraction of A ions on the octahedral sites and represented by *inversion parameter* x [156, 157, 210]. A general spinel with an intermediate cation arrangement can be written in terms of x as $(A_{1-x}B_x)[A_xB_{2-x}]X_4$, where x is the degree of inversion [79, 159, 210, 212-215]. The intermediate spinels can take a value in between 0 & 1 with description of cation arrangement at tetrahedral and octahedral interstices as below [216];

Normal:	$(A)_{tet}\,[B_2]_{oct}\,O_4$,	$x = 0$
Inverse:	$(A)_{tet}\,[A,B]_{oct}\,O_4$,	$x = 1$
Random:	$(B_xA_{1-x})_{tet}\,[A_xB_{2-x}]_{oct}\,O_4$,	$0 < x < 1$

The degree of inversion x is influenced by several factors such as *ion's site preferences in terms of size, covalent bonding efficacy* and *crystal field stabilization energies*

[217]. The x value in any particular spinel is given by the net effect of these various parameters taken together and is influenced by them such as cationic charge, cationic radii and temperature [218, 219]. Adherence of properties such as color, diffusivity, and magnetic susceptibility can be based upon the measure of x [196].

2.6 Cation Arrangement in Spinels and its significance

The importance of prevalent occurrence of cation arrangement in spinels becomes evident after knowing the types of the spinels. This arrangement of cations is due to different valencies, and accommodating capability of the structure, producing a large number of spinels, and resulting in interesting properties when coordinated on dissimilar tetrahedral & octahedral sites [156, 157, 176, 178, 220]. The physical, thermodynamic & chemical characteristics of spinels, especially their magnetic and electric parameters, perceptibly fluctuate depending on the composition and the arrangement of cations. [11]. A complicating factor in some spinel structures is that the cation distribution may vary, however usually they do not differ greatly in size so the variation will not be wide in range. The variations in arranging cations at A and B positions produce marked changes in some of the physical properties; one of these is the electrical conductivity [176]. The relative ionicity and size of interstices resolves the matter of embracing the tetrahedral or octahedral site symmetry by the cations [221, 222]. Navrotsky and Kleppa [210] reported that, in binary spinels, site preference energies can foresee cation placement, i.e. normal or inverse spinels relate to large difference of the preference energies between the two sites while intermediate spinel relates to small difference. In 1983, Hugh & Navrotsky [156, 223] modified the Navrotsky and Kleppa model according to the necessities and reported that the lattice constant reduces as x increases. Hugh and Navrotsky model was based on cation distributions, electron exchange reactions, and size incompatibility. In 1984 they [157] applied their model, for explaining features of structure and thermodynamic properties of spinels, thereby extending it to a general model.

The above discussion shows that useful properties of spinels not only rely on

cations type, but are also dependent on the cation arrangement through the available crystal sites. It is therefore subjectively very significant to have concept of components that pitch up the total lattice energy in spinels. Some of these factors are Elastic energy, electrostatic (Madelung) energy, Crystal field stabilization energy (CFSE), d-orbital splitting and polarization effects. Taking ions to be spherical in shape, then due to difference in ionic radii leads to the extent of deformity in the crystal structure, termed as elastic energy. Arthur Miller [155] extended the concept of octahedral site preference energy, and included to it, Madelung, short-range as well as crystal field terms thereby formulating a set of site-energies which could put to use for establishing the ionic arrangement in spinels involving the non-transition as well as the transition ions. Madelung potential (constant) handles the calculation of ionic arrangement. In the Madelung potential different comparable energy settlements are function of the ionic order. Verwey *et al*. [176, 224] measured the Madelung constant of the spinel structure for gross Coulomb energy of ionic crystal per molecule AB_2X_4, as function of u and charge distribution among A & B sites, by using the equation:

$$V = -\frac{1}{2}\left(\frac{e^2}{a}\right)(pM_{tet} + 2qM_{oct} + 8M_o) = -M\left(\frac{e^2}{a}\right) \qquad \text{…….. (2.2)}$$

where p and q are ionic charges at tetrahedral & octahedral sites, while M_{tet}, M_{oct} & M_o represent limited Madelung constant that ascertain the electronic potential at A & B sites and at X^{2-} lattice positions respectively. Verwey [176] summarized the general principles, underlying the building up of oxide spinels, as follow:

1. Trivalent and quadrivalent ions, in accordance with electrostatic rules, preferably occupy the octahedral interstices of the 16-fold position.
2. Exceptions are, however, certain trivalent ions: Fe^{3+}, In^{3+}, Ga^{3+} which show a preference for the tetrahedral interstices of the eightfold position.
3. Some divalent ions, Zn^{2+} and Cd^{2+} show a special preference for occupying the tetrahedral position, which can counteract the tendency, mentioned under 2.

Verwey [224] & Navrotsky [79] calculations indicate the difference in lattice

energy between normal and inverse 2-3 spinels, which is fairly small. Hence the individual cations site preference energies, possibly determine large range of cation arrangement. Navarotsky and Klepa [79] reports two steps of the formal spinal-forming reaction as below;

$$AO + B_2O_3 \rightarrow A[B_2]O_4 \quad \ldots\ldots\ldots\ldots\ldots\ldots\ldots\ldots\ldots\ldots\ldots\ldots (2.3a)$$

$$AO + B_2O_3 \rightarrow B[AB]O_4 \quad \ldots\ldots\ldots\ldots\ldots\ldots\ldots\ldots\ldots\ldots\ldots\ldots (2.3b)$$

$$A[B_2]O_4 = A_{1-x}B_x[A_xB_{2-x}]O_4 \quad \ldots\ldots\ldots\ldots\ldots\ldots\ldots\ldots\ldots\ldots\ldots\ldots (2.3a)$$

$$B[AB]O_4 = A_{1-x}B_x[A_xB_{2-x}]O_4 \quad \ldots\ldots\ldots\ldots\ldots\ldots\ldots\ldots\ldots\ldots\ldots\ldots (2.3b)$$

Relation 2.3 show theoretical formation of total normal or total inverse spinel, whichever is stable at low temperature. The cation A^{2+} can be represented by various ions of bivalent metals: Mg, Mn, Fe, Co, Ni, Cu, Zn, Ba, Sr, Cr, Ga, etc. as shown in Table 2.4**.**

Table: 2.4 *Representation of cation A^{2+} by various ions of bivalent metals* [11, 176, 209, 225].

Ions with oxidation degree 3+	**Ions with oxidation degree 2+**							
	Mg	**Mn**	**Fe**	**Co**	**Ni**	**Cu**	**Zn**	**Cd**
Al (aluminates)	N	N	N	N	$0.75I$	I	N	N
V (vandites)	N	N	N	–	I	I	N	N
Cr (chromites)	N	N	N	N	N	N/0.10 *I*	N	N
Mn (manganites)	N	N	N	N	–	N	N	N
Fe (ferrites)	0.90 *I*	N	I	I	I	0.86*I*	N	N
Co (cobaltates)	N	N	N	N	I	N	N	N
Ga (gallites)	I	–	I	I	I	I	N	N
Ti	N	–	–	–	–	–	–	–
In	I	–	–	–	–	–	–	–

N: Normal, I: Inverse, –: No prediction

Hafner and Laves [226] studied the cation distribution through IR spectroscopy in spinel ($MgAl_2O_4$). Via solution calorimetry, Navrotsky and Kleppa [210] quantified deviations in "enthalpy of the cation exchange" in $MgAl_2O_4$ spinel. Hugh [156] emphasize that cation size sets the site preference, and in "oxide 2-3 spinels" the electrostatic energy is inclined to put larger ions on tetrahedral site, however this exercise is opposite in "4-2 spinels" where tetrahedral sites are occupied by smaller ions.

In 1957, Dunitz & Orgel [162] and, independently McClure [225] mentioned that

crystal field theory explains several cation distributions. McClure indicates that in absence of "transition-element-ions" in spinels, the Madelung energy and ion size would have the only factors responsible for relative stability. Hugh reports, that "customarily a transition metal ion in octahedral coordination will carry more crystal field stabilization energy (CFSE) than one in tetrahedral coordination [156]. Thus in the aluminates, only $NiAl_2O_4$ and $CuAl_2O_4$ are inverse [156]." To explore relationship between the structural parameters, *a*, *u* and x, and predicting the anion parameter in spinels, knowledge regarding the cation distribution is imperitive [227]. For spinels $NiA1_2O_4$, $CuA1_2O_4$, and $ZnA1_2O_4$ while using X-ray diffraction analysis, Cooley and Reed [196] determined the parameters *u* and x and anticipated on basis of configuration entropy, that complete normal or complete inverse spinel cannot exist at much larger temperature above 0^oK.

The normal, random or inverse cation arrangement acts substantial effect on the electrical properties of $CdIn_2O_4$ spinel [142]. Wei and Zhang [228] states that in $CdIn_2O_4$ spinel the fundamental band gaps are clinging inversion factor. However, the Brewer *et al* [229] as a result of "atom location by channeling enhanced microanalysis (ALCHEMI) experiments" communicates $CdIn_2O_4$ as normal spinel.

2.7 Physical Properties of Spinel

In nature the spinel structure exist most commonly. There are at least a dozen or more minerals, some of which are commercially important and distinct metalliferous ores. There are more than 200 of them altogether [56]. By virtue of containing of three different chemical elements, spinels conform numerous meaningful physical properties [5]. The enhanced curiosity to investigate and model the physical and chemical properties of spinel compounds is due to their practical application in technology [34, 56]. $MgAl_2O_4$ has been considered in several experimental and theoretical studies focusing on electronic structures [230-232], elastic properties [231, 232] and phonon & Optical spectra [1, 233-236]. These materials have "high melting point, great strength, high chemical stability and low electrical losses", which infer spinels exciting

competitor for many important applications [2].

Table 2.5 *A selection of mineral spinels* [237].

Mineral	***Characteristics***
$MgAl_2O_4$	Parent spinel (parent mineral)
$ZnAl_2O_4$	Gahnite (a transparent diamagnet)
$FeAl_2O_4$	$Hercynite\ (classical\ paramagnet)$
$\gamma - FeO_4$	Maghemite (natural material for magnetic recording)
$FeCr_2O_4$	$Chromite\ (Chrome\ ore\ of\ Rhodesia)$
Mn_3O_4	Hausmannite (natural tetragonal spinel)
Fe_3O_4	Magnetite (used by ancient navigators)
Fe_3S_4	Greigite (ferrimagnetic semimetal)
$NiFe_2O_4$	Tevorite (ferrimagnetic semiconductor)
$ZnFe_2O_4$	Franklinite (paramagnetic ferrite)
$CuCo_2O_4$	Carrollite (natural metallic spinel)
Fe_2TiO_4	Ulvospinel (having giant magnetostrictiveproperties)
Mg_2SiO_4	The high pressure spinel polymorph of forsterite, thought to comprise the inner mantle of the earth

The chemical relationship between the compounds becomes clearer when the valencies absorbed by the atomic sub-division are considered. e.g, in mineral spinel $Mg^{2+}A1_2^{3+}O_4^{2-}$, the Mg^{2+} can be exchanged by vast sort of divalent cations and almost any trivalent cation for Al^{3+}. The former substitution can be used to procure aluminate group. And when the aluminium is supplanted by "Ga^{3+}, In^{3+}, Mg^{3+}, Ti^{3+}, V^{3+}, Cr^{3+}, Mn^{3+}, Fe^{3+}, Co^{3+}, Rh^{3+}, Ir^{3+} & rare earth ions" other series like Gallate, Indate etc are produced.

These spinel compounds together with the associated group or classification which originate by replacement of the anion X by S, Se or Te instead of O, are known as the **II-III** spinels. However, it has been found that charge compensation can be acquired by forming **II-IV** compounds "like $MgGe_2O_4$, Co_2SnO_4, and $ZnTi_2O_4$"; **I-VI** compounds "like Ag_2MoO_4, Na_2MoO_4 and Na_2WO_4", or **I-II** compounds like "$K_2Zn(CN)_4$, $K_2Cd(CN)_4$ and $K_2Hg(CN)_4$". The existence of all these possibilities together with other

strange combinations like γ-Al_2O_3, $LiFe_5O_8$, or $Zn_7Sb_2O_{12}$ gives some idea of the enormous chemical adaptability of the spinel system [56]. When this chemical amiability associates to the physical compliance of the crystal structure of spinel, give possibilities of different kind of physical behavior, resulting in remarkable opportunities for notable practical utilization and usage.

2.8 Elastic Properties of Spinels

The property(ies) of a material(s) when distort upon application of stress, and on its (stress) removal recovers to original form is known as elastic property(ies) [238]. The elastic properties of materials can be bifurcated in two classes, "the bulk modulus" and "the elastic constants or shear moduli". "The bulk modulus is a function of energy and volume [239]", while "the shear moduli need understanding of the acquired energy as a function of a lattice strain [240, 241]". These properties are very important due to their correlation with the basic solid state properties like equation of state and phonon spectra. The ground state total energy calculations give the elastic properties, which thermodynamically, can be connected to specific heat, thermal expansion, Debye temperature, melting points & the Gruneisen parameter [242]. The intimate association of "structural phase transitions" to "the structural stability conditions", as testified by changes of elastic moduli with either "hydrostatic pressure, temperature" or "chemical composition", reflects the previous interest of researchers in the elastic properties of spinels [243-250]. The elastic constants inherit to parameters that pertain to the elastic behaviour of crystals and their significance arise due to its relation with different elementary solid state phenomena, like interatomic bonding, equations of state, and phonon spectra. Elastic constants being indicators of mechanical strength, hence consequential understanding of elastic constants is required for using them practically to determine mechanical traits of solid such as internal strain, load deflection, thermoelastic stress, sound velocities & fracture toughness etc [158, 251]. In present work, Transition metal oxide spinels with cubic structure, are dealt, and it is eminently clear that a cubic crystal is having C_{11}, C_{12} & C_{44} as the only three independent elastic

constants. For calculating these constants, only three equations are sufficient, of which the first equation entail to estimation of bulk modulus *(B)* and that then links to elastic constants [252]. A careful and correct insight of the bulk modulus is essential for the equation of state (EOS) of a material, since this quantity describes the response of the material to applied pressure. Experiment and theory (both) propose bulk modulus being a crucial thermophysical and mechanical trait, especially in high-pressure area and in high-temperature science [253]. Ordinarily the bulk modulus connects to the geometry of solids, like lattice constant and adjacent-neighbour separation. It is asserted that "equilibrium bulk modulus" is converse to the structural parameters described above. Anderson & Nafe [254] suggested a hypothetical connection within bulk modulus and unit-cell volume $B_o \approx \frac{1}{V_o^x}$, here x rely on the bonding type of the solid. The elastic moduli straightly furnish the data about stiffness of the crystal, and ΔE's departure from quadratic behaviour can provide facts regarding the ductility [239]. The elastic moduli C_{ij} for cubic lattice are related to bulk modulus by [238],

$$B = (C_{11} + 2C_{12})/3 \qquad \text{…….(2.4)}$$

For obtaining the elastic constants, a little strain is applied to the structure in order to distort it so that the crystal deforms, in a round off linear elastic manner which transforms the lattice vector *a* according to following relation [253, 255, 256],

$$a' = (I + \varepsilon).a \qquad \text{…….(2.5)}$$

where $a'(a)$ is a matrix comprising of the new lattice vector components, *I* represent *3x3* identity matrix while ε is having strain components.

The second relation covers traditional volume *tetragonal strain* tensor ε [257].

$$\bar{\varepsilon} = \begin{bmatrix} e_1 & 0 & 0 \\ 0 & e_1 & 0 \\ 0 & 0 & \frac{1}{(1+e_1)^2} - 1 \end{bmatrix} \qquad \text{…….(2.6)}$$

By employing this strain, as a result total energy changes from original value;

$$\Delta E(e_1) = 3V(C_{11} - C_{12})e_1^2 + O(e_1^3) \qquad \text{…….(2.7)}$$

In 2.7, *V* is volume of "undistorted lattice" [241] & $O(e_1^3)$ mark "the neglected terms in the polynomial expansion of cubic and higher powers of the e_i" [258]. The symmetry

reduces the 21 independent elastic constants C_{ij} to 03 for cubic lattice. At last, volume conserving *mono-clinic strain* tensor is used for the final type of distortion;

$$\bar{\varepsilon} = \begin{bmatrix} 0 & \frac{1}{2}e_1 & 0 \\ \frac{1}{2}e_1 & 0 & 0 \\ 0 & 0 & \frac{e_1^{\,2}}{(4-e_1^{\,2})} \end{bmatrix} \qquad \text{…….(2.8)}$$

Energy related to this strain is

$$\Delta E(e_1) = \frac{1}{2}VC_{44}e_{1^2} + O(e_{1^4}) \qquad \text{…….(2.9)}$$

These three equations formulate a set required for determining the complete elastic tensor.

Derivation of Shear Modulus (G), Young's Modulus (Y), Poisson's ratio (ν), Lamme's coefficients (μ & λ) can be made from various equations.

The "Reuss modulus (G_R)" is supplied by;

$$G_R = \frac{5(C_{1\ \bar{1}} - C_{1\ 2})C_{4\ 4}}{4(C_{4\ 4} + 3C_{1\ \bar{1}} - C_{1\ 2})} \qquad \text{…….(2.10)}$$

& the "Voigt modulus" is derived from;

$$G_V = \frac{(C_{1\ \bar{1}} - C_{1\ 2} + 3C_{4\ 4})}{5} \qquad \text{…….(2.11)}$$

"Shear modulus" is calculated from (2.10) & (2.11);

$$G = \frac{(G_R + G_V)}{2} \qquad \text{…….(2.12)}$$

The "Young's Modulus (Y), Poisson's ratio (ν), Lamme's coefficients (λ and μ)", are associated to "Bulk Modulus (B) and Shear Modulus (G)" by the succeding relations [259]:

$$Y = \frac{9BG}{(3B+G)} \qquad \text{…….(2.13)}$$

$$\vartheta = \frac{(3B-Y)}{6B} \qquad \text{…….(2.14)}$$

$$\lambda = \frac{\vartheta Y}{((1+\vartheta)(1-2\vartheta))} \quad \text{..... (2.15)}$$

$$\mu = \frac{Y}{2(1+\vartheta)} \quad \text{..... (2.16)}$$

$$\zeta = \frac{C_{11}+8C_{12}}{7C_{11}-2C_{12}} \quad \text{..... (2.17)}$$

Fang *et al*. [260] carried out inelastic neutron scattering and first principle technique studies of phonon spectrum of $ZnAl_2O_4$, and determined mechanical & thermodynamic properties including bulk modulus & elastic constants. Bouhemadou *et al*. [158] while applying "pseudo potential plane wave method within the GGA and LDA" under DFT frame, studied structural & elastic parameters of "Aluminate $MgAl_2O_4$, Gallate $MgGa_2O_4$, and Indate $MgIn_2O_4$ spinels". The combination of mechanical properties makes spinel materials appropriately useful for a series of appliances in defense and aerospace fields [261]. Further, mechanical properties alongwith other properties for some more applications reported by Jonathan [262]. Khasanov *et al* [263] investigated optical and mechanical properties of synthetic "transparent ceramic $MgAl_2O_4$ spinel. Khenata *et al*. [264] studied "structural, electronic & elastic properties of XAl_2O_4 (X=Mg, Zn) "by FP-LAPW method within LDA.

Parallel to experiments, the theoretical method of *First Principles* (*ab initio*) is highly effectual approach for determining and predicting the structural, mechanical and magnetic properties of spinel materials. In this thesis, the elastic and mechanical behaviors of "XAl_2O_4 (X=Mg, Mn, Fe, Co, Ni, Cu, Zn), MGa_2O_4 (M=Mg, Mn, Fe, Co, Ni, Cu, Zn, Cd) and NIn_2O_4 (N=Mg, Zn, Cd) and ZnP_2O_4 (P=V, Cr, Fe, Rh, Sn) & VZn_2O_4." are reported. The elastic constant (C_{11}, C_{12}, C_{44}) are calculated to find various useful mechanical parameters.

2.9 Magnetic Properties of Spinels

In this dissertation, the magnetic properties of "XAl_2O_4 (X=Mn, Fe, Co, Ni, Cu, Zn) and MGa_2O_4 (M=Mg, Mn, Fe, Co, Ni, Cu, Zn, Cd)" form a significant part of the *ab initio* work in chapter 4, therefore, the Magnetic properties fringe topics related to it,

need a description here. The only handy 'permanent magnets', familiar for more than twenty centuries, until about 1740 [264A] were lodestones, which mainly contained impure *magnetite* (i.e, Fe_3O_4) a spinel-structure-oxide [265]. Magnetism has continued its fascination in present living of the advanced civilized community being used in combursome data storage devices and elevated drifting trains [266]. Magnetic oxides are a category of magnetic materials which are of engrossed charm due to spacious electrical, optical and magnetic properties. Shirane *et al* [267] described magnetic structure of $FeCr_2O_4$ & $FeCr_2S_4$ reporting that both are normal spinels. Schmidbauer [268] investigated magnetic properties of Fe_2TiO_4 and $FeCr_2O_4$. Ohgushi *et al* [269] studied magnetic & optical characteristics of "ACr_2X_4 Spinel (A = Mn, Fe, Co, Cu, Zn, Cd and X = O, S, Se)". Keisuke [270] studied $FeCr_2O_4$ and $NiCr_2O_4$ using powder neutron scattering method.

In electrical and magnetic field, the most interesting spinel structured materials normally include iron, manganese and cobalt, at various oxidation states, since these elements can perform many important phenomena like ferrimagnetism, ferro electricity or magneto electric multi ferroic coupling [12, 271-273]. Another reason may be these elements are abundant in Earth surface. Among them, *Spinel ferrites* are the insulating spinel-series being extremely significant, having leading members $ZnFe_2O_4$ with normal cation distribution and $MgFe_2O_4$, $MnFe_2O_4$, $CoFe_2O_4$, $NiFe_2O_4$, & $Li_{0.5}Fe_{2.5}O_4$ having inverse cation distribution with Fe^{3+} on tetrahedral sites. The highest "cubic magneto crystalline anisotropy" with [100] easy axes is related to Cobalt ferrite ($CoFe_2O_4$) while all others have [111] axes. Ferrites have applicability in high frequency inductors as cores.

Oxide spinels, which are having general formula $A^{+2}B_2^{+3}O_4$ and includes a number of compounds in different range like $A^{+2}B_2^{+3}O_4$ (2–3 spinels) and $A^{+4}B_2^{+2}O_4$ (4–2 spinels) [156, 274-276] demonstrates a spacious tier of electric, magnetic, optical & structural properties. These oxide-compounds could be "insulating, semiconducting, metallic, ferroelectric, piezoelectric, ferromagnetic, ferrimagnetic, antiferromagnetic, or superconducting".

In transition metal oxides, antiferromagnetic super-exchange is usually considered the controlling magnetic coupling, which generates antiferromagnetic or ferrimagnetic order [277]. Among transition metal aluminate spinel oxides, galaxite ($MnAl_2O_4$) exhibiting intermediate electrical conductivity ($\sigma \approx 3637$ S/cm) [278] and paramagnetic properties at room temperature [279]. But the magnetic properties of $MnAl_2O_4$ are poor, with low permeability and saturation magnetization, only shows ferrimagnetic properties below Curie temperature of 30K [279]. As Roth predicts [280], that $MnAl_2O_4$ may have only the weak A–A interaction and the partially inversed structure gives an enhancement in magnetic properties. Compositely most spinels contain atleast one, or more than one transition atom(s) that are magnetic in nature, resulting the high temperature bearing of such materials equivalent to paramagnetic material [56]. Hamedoun *et al* [281] studied the ground state of spinel solid solutions and exposed four magnetic structures for AB_2O_4 spinel compounds; "i.e., ferromagnetic (F), helimagnetic (H), modulated structure 1 (M_1), and modulated structure 2 (M_2)". Cobalt and manganese oxide spinels exhibit exciting properties, with possible oxidation numbers, spin states and orbital moments being on A and B Sites occupancy by stocking of each cation, [239]. With the aid of magnetic measurements, the cation arrangement of cobalt and manganese spinels can be described. The magnetically ordered state of these compounds can be characterized at low temperature, due to different scattering factors. Manganese cobaltite $MnCo_2O_4$ exhibits high electrical conductivity and ferri-magnetism property. The electrical conductivity of $MnCo_2O_4$ nanocrystallite is 23570 S/cm [278], much higher than most of ferrite core materials, so it was mainly applied in electrical field, especially in electrode [282, 283] and supercapacitor [284].

Sophie *et al* [285] reported magnetic susceptibility, magnetization & neutron diffraction measurements for Co-Mn spinel, characterizing the magnetic characteristics of $Mn_{3-x}Co_xO_4$ ($0 \leq x \leq 3$) ceramics concluding that these properties depend upon preparation method and thermal treatment and are firmly associated to the cation arrangement of the material, and that the magnetic structure of $Mn_{3-x}Co_xO_4$ is

ferromagnetic. The magnetic order is characterized by a non-collinear arrangement of spins at low temperature.

Meriakri *et al* [286] reported that Co_2FeO_4 posses two coexisting phases while Panner and Bhowmik [287] reported that at high temperatures, irrespective of "structure phase stability" the Co_2FeO_4 is ferromagnetic and confirming active interrelation between cubic spinel structure and magnetism in Co_2FeO_4. They propose the perception of this reciprocity can be exercised on other oxide spinels. $NiCo_2O_4$ is a ferromagnetic spinel with reported Curie temperature ~ 450 K [288-290], though this value may highly depend on the cation valence and occupancy as shown by Silwal *et al* [291]. Bush *et al*. [272] observed ferroelectricity in $Co_{0.8}Ni_{0.2}Cr_2O_4$, describing these compounds show ferroelectric and magnetic properties. The cause of ferroelectricity in RFe_2O_4 (R = rare earth element) in essence is linked with charge ordering transition, arising from strong electron correlation [292-294]. In $LuFe_2O_4$, at normal temperature huge magnetodielectric exhibited which produce chance of its applicability in microelectronics [295-297].

It is probable to conceive new materials by investigation with various procedures in essence, and by experiments in laboratory, having diverge range of structural states. Their design with respect to compositional contents and degree of cation order may be meta-stable. Using thermodynamic models, the inversion parameter x explains process of arrangement of cation's order/disorder [156, 157, 210]. Richard quotes in his work [298], that contemporarily improved study of cation ordering and kinetic processes in metals by use of Landau theory have let on numerous mineralogical procedures to be designed on a plain perceptible grounds [299, 300]. Which has provided new understanding to the association among cation arrangement, magnetic order and subsolvus exsolution [301-304]. The Landau free energy describes the equilibrium & kinetic bearing of the procedure of cation arrangement. [299, 305, 306]. Below the Curie temperature, a spinel take-up a special order of magnetic moments, known as saturated magnetization (M_s) which is function of termperature, composition, cation distribution and magnetic structure [298]. According to Neel's theory, this magnetic structure

adopted by spinels below the Curie temperature, rely on pairing of different inter- & intra- site magnetic interactions [307, 308]. It is worth noting, that "weak octahedral-octaheral and tetrahedral-tetrahedral exchange interactions" control the magnetic arrangement on "octahedral and tetrahedral sub-lattices" which (the interactions) can be either +ve or –ve in sign, showing "lowest enthalpy with magnetic moments parallel (ferromagnetic)" or antiparallel (antiferromagnetic)" respectively [298]. Beside large technological research on composition of ferromagnetic spinels, still trustworthy information regarding their magnetic space groups are insufficient [309]. In ideal cubic spinels with consideration of $F\bar{4}3m$ space group (refer *Section 2.4*), the metal ion displaces off the center of octahedral site, however long-range ordering of such ionic shifts are not proved. Nonetheless, for ionic displacements leading to antiferroelectricity such ordering will be vital. This property is attributed to class $\bar{4}3m$ [198], having space group $F\bar{4}3m$ [186].

Positive susceptibility ($\chi > 0$) at all temperatures, is a trait of antiferromagnetic crystals. They comply "Curie Weiss Law" above Neel (Curie) temperature and beneath this temperature the mobility of the ions is not loose, so they do not obey the field. Therefore the susceptibility (though +ve) does not adhere to "Curie Weiss Law" however susceptibility is zero at absolute zero due to the spins [310]. The Chromium spinels (ACr_2X_4) have tremendous order of magnetic exchange strengths and peculiar magnetic ground states [311] and are distinguished through Curie Weiss temperatures, which at low temperatures, reveals to be antiferromagnetism or ferromagnetism [312]. The studies of magnetic properties of $ZnCr_2O_4$ & $CoCr_2O_4$ by Brent *et al* [313] shows that at low concentrations of magnetic cations in tetrahedral sites, their behaviour is of ferromagnetic order. When lattice geometry in spinels is ruled by magnetic ordering, then an emergent behaviour called "geometric frustration" occurs [314-316]. Magnetic frustration results from competition between constraints on magnetic interactions in a lattice such that all constraints cannot be satisfied simultaneously [317]. In systems with frustrated spin, new states like zero-energy excitations [36], complex spin & structural configurations [36, 318] occur. In spinels, the structure-property reliance is very

important in regulating the structure evolution and prediction of novel properties, leading to understanding the ground state of frustrated substances. Since magnetic behaviour of materials is based on interatomic separation therefore at high pressure and low temperature the geometrical inconsistency may occur and hence the structural deformation results magnetic transitions [319].

Geometrically-frustrated spin systems reveal exciting fundamental physics, due to which they have been broadly studied [320] and have enticed recent importance because of their usually owning ground states spiral magnetic structures [321]. Frustrated antiferromagnetic spinels, expressing different magnetic ordering like antiferromagnetic, ferromagnetic, semi-spin glass, cluster spin glass property, are of special attention now adays [322]. AB_2O_4 cubic spinel compounds are the prime examples of frustrated magnets [323]. Frustration in the magnetic spin system puts down long-range magnetic order and improves spin fluctuations. Kalvius and Krimmel [323] studied "MAl_2O_4 (M=Mn, Fe, Co)", reporting that A-site sublattice is subjected to powerful frustration, inclining these materials being on brink amid long-range and short-range magnetic order. The frustration is normally visualized with triangle-based moment geometry and is evident that frustration is ordered by the crystal structure [324]. The A-sublattice in spinel crystal contrives "a diamond lattice", and the B-sublattice constitutes "a pyrochlore lattice". The pyrochlore lattice referes to pyrochlore structure, $A_2B_2O_7$, is created by the network of edge-shared octahedral enclosures. Upon stripping the anions, as a result the cations of B-sublattice builds a network of corner-sharing tetrahedron (see **Fig 2.10(b)**). When the union within the magnetic moments on the pyrochlore lattice is antiferromagnetic, then due to triangle-based geometry strong frustration is anticipated [266].

The first nearest neigbours in spinels are oxygen anions and the second nearest neighbours are the magnetic cations. When tetrahedral interstice is occupied by non-magnetic cation (e.g. Mg, Zn, Cd), the Trivalent^{3+} ion having no orbital degrees of freedom, develops tough geometric frustration. However, if the tetrahedral interstice is taken by magnetic cation (e.g. Mn, Fe, Co, Ni, Cu) then frustration is decreased by

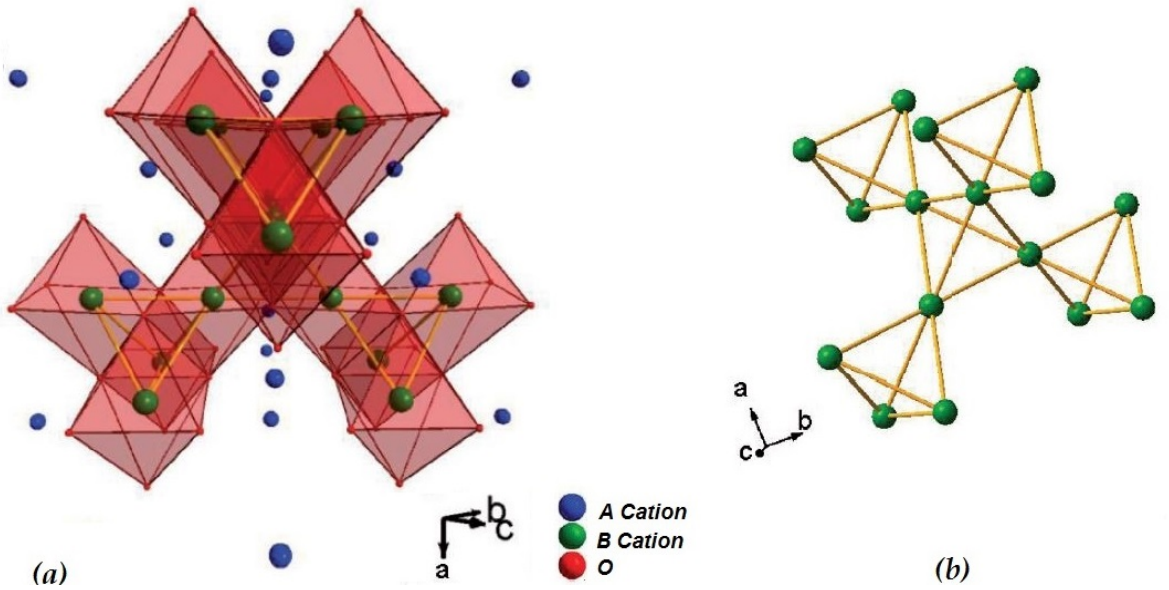

Fig: 2.10 *(a) Crystal Structure of AB_2O_4, and (b) The octahedrally-coordinated cations form a network of corner sharing tetrahedra illustrating its three-dimensional triangle-based geometry (Yellow connector lines used to distinguish the tetrahedron, and do not represent bonds).* [266, 325]

several folds producing noteworthy non-collinear ordered spin configurations. Theoretical investigation had focused on the spin ordering stability [210] while experiments have scrutinized spin-lattice coupling [326], multiferroicity [327-329] and anisotropic lattice dynamics [316]. Chromite ACr_2O_4, and vandate AV_2O_4 spinels are well known for demonstrating different levels of frustrated magnetism [330]. Noriaki & Masashige [331] with X-ray diffraction using nuclear and magnetic resonance (NMR), investigated the structural and magnetic properties of geometrically frustrated CdV_2O_4.

Besides the magnetic materials (ferromagnets, antiferromagnets and ferrimagnets), there are many which exhibit contrast 'structural-dimensions', signs & range of interactions with holding anisotropy of magnetic spin, hence are termed as 'magnetic compounds' including various spinel compounds. The frustrated magnet carries two types, the geometrical frustrated and bond frustrated magnets. In the chromium spinels ACr_2X_4, the nonmagnetic cations (A = Zn^{2+}, Cd^{2+} or Hg^{2+}) possess tetrahedral holes while the magnetic cation (Cr^{3+}) takes the octahedral interstice which

are in octahedral coordination with X = O, S and Se from group VI. The Chromium sublattice form pyrochlore structure where spins are localized and builts a very strong frustration [332]. The geometrical frustration and bond frustration coexists forming different complex ground states depending on distances of chromium cations from each other. In $CdCr_2O_4$ at 7.8K the antiferromagnetic order is exhibited [333, 334]. Several oxide spinels carry negative Curie-Weiss temperature demonstrating antiferromagnetic insulating behavior, duly influenced by "strong direct Cr-Cr exchange" [332]. Most of chalcogenide Chromium are plainly merely ferromagnets [335] so cannot be frustrated geometrically. In $ZnCr_2Se_4$ the direct exchange reduces because of increase of Cr-Cr space [336, 337].

2.10 Opto-electronic Properties of Spinels

For transparent ceramic materials, the optical properties are extremely significant [261]. Study of optical attributes of materials is a very vast field, having the basic essential as reflection, refraction, scattering, dispersion, absorption and transmittance. A material can be used in optoelectronic or/and photonic devices based on its electronic and optical behaviour. Generally the optical properties of materials are calculated by gleaming monochromatic light on suitable specimen and then measuring the reflectance or transmittance of the sample as a function of photon energy [338]. The photoelectric emission and characteristic energy loss leads to its usefulness in studying electronic band structure. The electrons' transition from valence to conduction band results due to energetic photons absorption by a sample. Majority of spinels have wide and direct band gaps with high thermal stability and the combination of mechanical properties makes them uniquely suitable [361] for a series of utility in optoelectronics. These properties make spinel as candidate materials for studies of their optoelectronic properties. The optical data is generally debated in terms of "frequency or wavelength" and the band structure is deliberated in terms of energy (eV). For wavelength to Energy, Frequency and color relationship Table 2.6 is utmost important during studies of optoelectronic properties.

Table 2.6: *Relationship of Wavelength to Energy, Frequency, and Colour* [338].

12, 400A^{o}	↔ 1 eV ↔	ω=1.5x10^{15} sec^{-1}
6,200A^{o}	↔ 2eV ↔	Red
5,800A^{o}	↔ 2.14eV ↔	Yellow
5,200A^{o}	↔ 2.38eV ↔	Green
4,700A^{o}	↔ 2.64 eV↔	Blue

The optical properties of materials are usually expressed according to the physical parameters like "refractive index, reflectivity, absorption coefficient, optical conductivity etc". Ceramics spinel compounds exhibit desirable optical properties [3, 5, 6, 339] and are promising applicants in optoelectronic devices as transparent conducting oxides (TCO's) [340]. Spinel compounds are used as windshield defrosters, ultra-violet photo detectors, optimizers of solar cells, liquid crystal flat panel displays (LCD) [340-342] and in leading retail business of military sector, aerospace and lasers [261].

The optical properties of spinel oxides are well investigated for measuring reflectivity and estimating the refractive indices of these materials. For efficiency of a material exhibiting complex refractive index with "high real part (relative to refraction) and low imaginary part (relative to absorption)" is required [343]. The "real part of the refractive indices" of about 509 oxides (including spinels) and 55 Fluorides indicated and analysed by Shannon [344]. Excellent optical transmission, refractive index & low scatter are required for infrared sensors, which are eventually needed for missiles, aerial vehicles & surveillance systems and it has revitalized the demand for transparent affordable magnesium aluminate ($MgAl_2O_4$) spinel to replace expensive sapphire [345]. Several spinels having isotropic mechanical properties so can be optically fabricated with ease at lower cost [345]. Chasserio *et al* [343] studied optical properties of magnetite family of spinels (i.e. manganese mixed oxides, $M_xMn_{3-x}O_4$ (M = Ni, Cu, Ni + Co or Ni + Cu)) in the infrared range, measuring the reflectivity, refractive index and

correlating the optical characteristics. Wood *et al*. [346] investigated optical spectrum of Cr^{3+} in the Spinel $MgAl_2O_4$ and $ZnAl_2O_4$. Optical properties of the spinel crystal $MgAl_2O_4$ have been studied by Wickersheim & Lefever [347], Wang & Zanzucchi [348], Eiichi *et al* [346], Arcan *et al* [349]. While Hosseini [2] using DFT, has reported the studies of the band structure, dielectric function along with reflectivity, refractive index etc. of $MgAl_2O_4$. Nin Mironova *et al* [350] investigated the absorption and luminescence of $MgAl_2O_4$ while its electronic and optical properties were measured using *first-principal* by Shengli *et al* [351]. Vitaly *et al* [352] correlatively carried out the investigation of "optical & magneto-optical properties" of normal, disordered, and inverse oxide-spinels. Structural, optical & photocatalytic properties of $ZnAl_2O_4$ have studied by Rahman *et al* [353]. Arbi *et al* [354] have presented *ab initio* determination of structural, electronic and optical properties of $ZnAl_2O_4$ through FP-LAPW, while its phonon spectrum is also examined by Fang [355]. Fabian *et* al [356] have reported the Infrared optical properties of various mixed spinels. Amin *et al* [1] studied opto-electronic response of $MgAl_2O_4$ and $MgGa_2O_4$ through mBJ exchange potential. M. G. Brik [357] estimated elastic, electronic and optical properties of $ZnAl_2O_4$ and $ZnGa_2O_4$ via *ab initio* method. "Optical spectra & electronic structure" of ZnX_2O_4 (X=Al, Ga, In) were investigated using DFT calculations by Smagul and Ravindran [358]. Krishna *et al*. [359] reported electrical & optical properties of $ZnGa_2O_4$. $MgIn_2O_4$ has been validated as transparent material for making of optoelectronic devices due to its high optical transparency and electrical conductivity. Moses [140] prepared $MgIn_2O_4$ thin films by pyrolysis, having deposition of optical band gap 3.82 eV at 450^oC, hence these $MgIn_2O_4$ thin films under appropriate optimized condition is candidate material for optoelectronic applications. Esther [360] reports by measurements of diffuse reflectance spectra, the optical band gap of $MgIn_2O_4$ (~3.3 eV). Bouhemadou *et al* [361] studied structural, electronic and optical properties of cadmium Gallate & Cadmium Indate implying FP-APW.

2.11 Importance, Applications and Uses of Spinels

The importance of spinels is evident from its use in various fields of life, and in a variety of manners, from traditional ornamental and jewelry to scientific, technological and industrial fields as well as medical and military. The importance of nano-materials of spinels in the medical field is now not a nav-culture but has achieved a great attention for several years. Verwey [224] highlighted the importance of spinels in 1948, mentioning that spinels are not just aesthetically pleasing; they are of considerable attraction from technical perspective. They could be easily synthesized so that their properties, which are composition-sensitive, may be controlled within varying limits. Oxide spinels are indispensable to the military and armor technology being used in it extensively. The singularly refractive nature of spinel in combination with the relative ease of producing synthetic spinel has led to its use as high strength window material in military applications. Spinel's performance as outstanding magnetic, refractory, semiconducting, catalytic and adsorption material remained evident throughout. They are also utilized in high temperature arc-enclosing enfolds, humidity sensors, infrared sensors, transparent pans & domes [362]. Spinel being one of the largest groups of inorganic compounds existing in nature, has drawn great attentions as its close-packed structure possesses many enormous properties, which could apply in various industrial fields like pigments [11], magnetic materials [12], electrical materials [13], high frequency devices [14], catalyst for chemical synthesis [15, 16]. Theoretically as well as experimentally spinel compounds are much studied being described by large melting point, strong resistance to chemical transformations, large strength and minimal electrical loss which provides a proof, that they are contestants for several application in geophysics, catalysis, magnetism [19], super hard materials, high temperature ceramics [20], and super capacitor [21, 22]. In addition, the relative ease and low cost associated with manufacture of oxide spinel, has come to replace the previous state-of-the-art material, sapphire [345]. The oxide spinels are inexpensive, having cubic structure (i.e. uniform thermal expansion), and high melting points therefore has achieved and

maintained commercial importance since almost hundred years, especially in electronic and refractory industries.

In ancient periods, the loadstone or magnetite, was the first (spinel) whose recognition for navigational purposes was done. Other spinels were used for decoration and ornamental purposes followed by its use in jewelry. Several oxide spinels are natural gem stones and are used as such, especially $MgAl_2O_4$ and $ZnAl_2O_4$. They are naturally crop-up transparent materials, having prominent refractive index (≈ 1.7) and their hardness is surpassed by diamond & corundum only [56], While $CdCr_2S_4$ and $CdCr_2Se_4$ posses transparency in the infrared range and are beneficial magneto-optical candidates [363]. Presently, in jewelry trade water clear crystals of aluminate spinels are grown in a variety of colours. In liquid silicates the chromite spinels have low solubility, therefore this prized equity cause these spinels high resistive materials to wear at high temperatures. Due to this property, the Chrome-magnesite bricks are used as main lining material for the structures in industrial furnaces. Spinel is used for ceramic composite because $MgO\text{-}Al_2O_3$ is very much stable compound, being chemically consistent to alumina, zirconia & mullite [364]. Superior strength of $MgAl_2O_4$ spinel at atmospheric & high temperatures, exceptional defiance to corrosion, erosion, abrasion and admirable thermal stalling are some properties that raises it to extra-ordinary refractory material, hence making bulkheads, laid as bottom of steel filling ladles and used in burning areas in cement kilns. [365-369]. The spinel oxide ceramic compounds possess attractive electrical, magnetic and optical properties. These distinct properties make magnesium spinel substantial user in several specific applications. Oxide-spinels being naturally occurring minerals are very important in solid state sciences. In order to search for catalytic materials with upgraded better properties, the compounds with spinel-like structures have got enough attention. Among them, Aluminates are favourible choice to be fascinating catalyst, due to their high thermal, high mechanical resistance, hydrophobicity, and low surface acidity [370]. These characteristics also adjust them to replace traditional systems as carriers for strong metals. Moreover, because of their powerful metal-support interaction, some of

them (including $ZnAl_2O_4$, $CoAl_2O_4$) favour impeding sintering of noble metals [111, 371]. Nickel aluminates have been reported to be applicatory in magnetic materials, pigments, catalysts and refractories [131]. The transition metal aluminates have been brought to lime light by their catalytic employment and made them enormously appealing as ceramic pigments, coatings, catalysts, etc. [34, 372, 373]. In the production of town gas $NiAl_2O_4$ was used as beneficial catalyst [56], while $CoAl_2O_4$, $NiAl_2O_4$, $CuAl_2O_4$, $ZnAl_2O_4$ are used as ceramic materials beside its catalytic bearing for dehydrogenation of n-hexanol and cyclohexanol [56, 133, 227, 374-376]. They are also used as dehydrates of saturated alcohols to olefins, in hydrogenation, in preparation of polymethylbenzenes, the double-bond isomerization process of alkenes, for steam methane-reforming reactions, for methanol, for higher alcohol & styrenes synthesis, for synthesis of fine chemicals optical coating or host matrix as support for alkane dehydrogenation catalyst and as catalytic material for decomposition of methane [88-90, 110, 114, 377-386]. The $FeAl_2O_4$ is widely used in cell separation, contrast agent in magnetic resonance imaging (MRI), consigning spot fix medicines, treatment of cancer cells & nanobiosensors, and magnetite is used as magnetic fluids hyperthermia (MFH) in hyperthermia treatment for cancer [387-389].

The incredible development and growth of the spinel materials, commercially (specifically in electronics) increased in rapid manner since the World War – II. Grime [56] highlighted the fact that the emerging new phenomena "the importance of eddy current, being lost in the load coils of telecommunication equipment and transformer", had necessitated for such materials in the field of electronics which at the same time, are ferromagnetic as well as electrically insulator. Kingon *et al* [390] predicted the future of spinels, that the integrated circuit technology is very bright for spinel compounds. $MgAl_2O_4$ is transparent over complete visible spectrum, possess cubic symmetry, is optically isotropic & chemically inert, hence is extremely good substrate. $MgAl_2O_4$ crystals are used in microwaves, bulk acoustic & fast IC epitaxial substrates [368, 391, 392]. $CdCr_2S_4$, $CdCr_2Se_4$ & $HgCr_2Se_4$ are of practical use [393] in monolithic microwave integrated circuits. Initially, the quality of such type of materials was not good, as due

to suffering awkwardly by magnetic after effects like degradation in permeability and dielectric losses. But gradual improvements resulted latterly in large use of ferrites in radio/television, and magnetite & γ-Fe_2O_3 turned compulsory materials for manufacturing of magnetic recording tape [56]. Ferrites are having excellent electrical and magnetic properties so are contending materials for a range of applications in technology. The Spinel ferrites are semiconducting ferrimagnetic materials, therefore are vital materials for technological uses [394]. Co-existing, advanced materials for microwave frequencies were formed that steered into a chain of practical circuit components e.g, gyrator, frequency mixers and frequency doublers etc [395].

In 1975, the prevailing trend in electronics towards increasing miniaturization commenced, which is in vogue and seems likely to continue in future as well. The ferrite-spinels have performed efficiently their effectiveness for localize magnetic flux which has added a juncture to trim and diminish a proportion from dimensions of inductive loads and filters, thereby decreasing the size. Brown and Albert [396] states regarding the revelation that "some polycrystalline ferrites exhibit a rectangular hysteresis loop" leaded to its use as memory elements which created the importance of spinels, and its application in computer-industry. Subsequent decrease in proportion of size leaded to large commercial applications in both computers and telecommunications by venturing perfection at hand in single crystal technology, resulting fabrication of complete circuits "within thin films grown on insulating substrates" or "within a monolithic single crystal chip" [56]. Spinel-ferrites do not require protective coating and therefore also proved its usefulness in magnetic recording materials for high density recording, with obtaining high storage capacity by reducing the particle size of the magnetic (bits) [397]. These magnetic nano-ferrite-materials are used in magnetic toners in the Direct Image Printing (DIP) [398].

The mixed metal ferrite spinel materials, Fe_3O_4, CFe_2O_4 and $NiFe_2O_4$, are abundant and relatively inexpensive, having a wide variety of applications like: electronics, they make up the magnetic layers of hard drives; catalysis [399-401], batteries [402] and oxygen carriers in chemical looping and solar thermal water spitting

processes [403-409]. The moderate saturation magnetization and very high coercive field of the nano sized $CoFe_2O_4$ with combination of physical & chemical properties adjust it as candidate material for magnetic recording in audio, video & high density disks [410].

Each Transition metal oxide comply to some special properties in one way or the other way as they are having chemically inert crystals and lie in good transparent range of several optical frequencies hence they are good substrate materials and are applied in optical switches/photoconductive effects [56]. Transition metal oxide spinels are significant for a wide use in semiconductor and sensor technology and also as catalysts [128, 411-418]. $MgAl_2O_4$ is transparent through the complete visible spectrum, being cubic and also optically isotropic, hence is the lucrative substrate material of all the spinels [56]. The spinel aluminates "MAl_2O_4; M= Mn, Cu and Zn" intrigued as catalysts [34], pigment ($CoAl_2O_4$) [419] and high alumina cement ($CaAl_2O_4$) [420]. $MgAl_2O_4$ spinel possess very high tolerance to radiation damage and therefore is good candidate for application in hostile radiation environments (high neutron or energetic particle flux fields). This resistive property to radiations, and its high stability also makes it an attractive host material for the disposal of surplus actinides and high level radioactive wastes [227].

The spinels are used as "transparent conducting oxides (TCOs)" in optoelectronic gadgets and their utilization in flat display-screen, windshield's defrosters & solar cells is now reality [421]. Owing to intense nonlinear susceptibility, luminescence & photo/optical-sensitivity they are in frequent functionality in optoelectronics as ultraviolet photodetectors and optimizers in solar cells [342]. More uses of spinels include; high density storage devices, ferro-fluids, microwave absorption, humidity sensor, drug consignment, DNA separation, hypothermia and MRI (magnetic resonance imaging technique) [208], hydrogenation, cracking, catalytic reactions, dehydration [422].

CHAPTER – 3

COMPUTATIONAL APPROACH AND THEORY OF CALCUALTION

This chapter of the thesis focuses on introducing the 'theoretical methods based on computational approach' used in this dissertation, including the derivation/formalism of "Density-Functional Theory (DFT)", which is ultimately pre-owned as electronic-structure technique for solving the many-body problem of quantum mechanics [423]. The background of traits of DFT are furnished along with the challenges of growing approximate exchange-correlation functionals. The DFT addresses various predicaments in computational materials science to foresee its place and type, so is common path now for such work prediction [424]. In *ab initio* process for simulations through DFT, the feeding data demanded are simply the atomic numbers & positions of the implicating elements, and they furnish exact and authentic information of properties so concluded from the electronic structure, including description of the atomic bonds. However, in terms of computational resources these methods are quite exigent and are moderately restricted to small number of atoms within the order of hundreds, but as a result leading to get parameters needed for a large scale modeling of properties related to the material.

We start with Mehl and Osburn statement [239], that "a role of computational physics is, to help determine materials worthy of experimental attention, and to indicate possible candidates for substitutional alloying".

Upon increase in the computing speed of computational machines and improved algorithms, the Materials modeling/simulations have attracted an unusual focus in the last several years. DFT predictions are widely adopted with remarkable credibility for investigation of various physical & chemical properties of materials. The experimental data can be reproduced with the help of Quantum mechanical calculations and various properties can be satisfactorily calculated that are partially or completely not available in experimental data. All types of materials could be effortlessly and correctly modeled

and deliberated by employing these techniques. The approach adopted for the forecasting of different characteristics of various materials on the basis of data related to its composition is termed as *ab-initio* or *First Principle* method, whose significance is non-requirement of experimental facts & figures for synthesis of the materials. [26]. Since the inception of fast speed computers, this technique is in vogue for determining the electronic structure and total energy of solids [425] and have demonstrated the reliability of the technique for predicting ground state properties of solids [256].

In our work, we have attempted all calculations for structural parameters and elastic moduli prediction using *ab initio (first principal)* method, in which the only inputs needed are the position of atoms in the crystal structure and the atomic numbers of the relevant elements [239].

With onset of quantum mechanics the "Density Functional Theory (DFT)" has become in fact a special development in the rink of condensed matter physics, having efficiency of controlling the many-body-problem. In computational physics, it is able to authentic investigation of physical aspects of materials. Due to possession of great capabilities, the "*ab-initio DFT methods*" are widely applied since more than last twenty to thirty years. Its significance is evident from the Nobel Prize in the year 1998 awarded to W. Kohn & J. Pople [424].

In condensed matter physics, the *ab-intio* calculations with DFT setting have been accepted as dependable, steady, explicit and computationally economical. The aforementioned flourishing technique supply marvelous results in elucidating, transcribing and predicting a huge variety of materials phenomena. In this regard the inspiring examples are the analysis of silicon phase transition under high pressure [27], determination of stable/meta stable adsorption geometries on metal surfaces [28], accurate reproduction of structural and elastic properties of $MgAl_2O_4$ [29]. Further to it great success in investigating the structural, elastic, optoelectronic, magnetic and optomagnetic properties of various materials.

In this thesis we investigate structural, electronic, elastic and magnetic response of twenty-four (24) compounds of *Transition Metal Oxide Spinels* using the DFT.

3.1 Density Functional Theory – Background

We are aware that all material systems are essentially composed of electrons & nuclear charge, and various properties of the materials (like mechanical, electronic, magnetic etc) are the results of interactions of electrons. The best tool for defining electrons and their interactions, is the Schrödinger equation. If it is solved accurately and efficiently for many electron problem, then property(ies) of materials can be determined accurately, however it is not as easy to have such solution. To workout the problem approximately, for its solution several techniques such as "complex system methods *as free electron process*" and "Tight binding methods" were introduced, which proved slack and unreliable. The first reputed & duly acknowledge mechanism for solving this problem was Wigner-Seitz method. Later on, many more procedures were evolved including "*Hartree-Fock (HF), Quantum Monte Carlo, Perturbation theory, Density Functional theory (DFT))*", and brought-in for computation of numerous properties.

For quantum mechanical approaches, there are commonly two descriptive techniques; "Hartree Fock (HF) method [426, 427]" and "Density Functional Theory (DFT) [23, 24]". Hartree Fock is governed by wave function in which exchange is dealt but correlation is disregarded, while Density Functional is founded on the electron density instead of wave function, and though approximately but entertains exchange & correlation both [427A].

The main concept, that electron density $n(r)$ devises the ground-state properties of an atomic or molecular system at each point r, precedes back to the original work on the free-electron-gas in 1920s-30s [428] by Thomas [429], Fermi [430], Dirac [431] and Von Weiszacker [432]. In 1950s, Slater in his XR method, carried out the study of molecules & solid state by DFT [433-435], plainly considering only one-parameter approximate exchange correlation functional, in shape of "an exchange-only functional". In 1964 upon development of Hohenberg & Kohn theorems, DFT turned into a complete theory, insinuating the procedure (as happened in Kohn-sham formalism) [24, 436] making way to a computational innovation [428]. In mid 1990s, the debut of DFT through the Kohn-Sham formalism in Pople's GAUSSIAN software

package [437], popularized it as alternative computational choice to wave function techniques such as Hartree Fock [438], Moller-Plesset [439], configuration interaction [440], coupled cluster theory [441] and many others [428, 442-445]. Founded on the prominent Hohenberg & Kohn theorems [23], DFT serves as remarkable footing for progress of computational schemes, to accomplish knowledge regarding the structure, properties and energetics of atoms & molecules at considerable depreciated expenses than conventional *ab initio* wave function approaches [428]. DFT rendered imperative act in the development of quantum chemistry [428].

Density Functional Theory [23, 24] is the default computational method for problems involving atoms and electrons. The basic concept of DFT is to interpret & present an interacting system of particles via its density in lieu of its many-body wave function [446]. DFT is among the extensively adopted electronic-structure methods and successful approach for the description of ground-state properties (particularly lattice constants, bulk modulus, crystal structure, electronic, optical and magnetic properties etc) of bulk materials (i.e. metals, semiconductors, insulators and superconductors) and complex materials like molecules, non structures, proteins, and carbon nanotubes. It has also been used with great success in nuclear physics [447-450]. In DFT, estimation of the ground state properties, for instance "band structure, optical properties, lattice parameter, equilibrium volume, phonon frequencies, elastic constants etc", depend on the calculation of the total energy and are determined utmost precisely and hence, its popularity results primarily good accuracy at reasonable computational expense for a broad order of useful & implicit practicable applications. Hence, in principle, DFT provides good values for ground state properties. The practical applications of DFT are formed on the basis of approximations for "exchange correlation potential", which states the outcome of Pauli principle & Coulomb potential past the absolute electrostatic interaction of the electrons. Leading to exact exchange correlation potential anticipates that many-body problem is solved exactly, however in solids it is not achievable distinctly. Local Density Approximation (LDA) is one of the familiar and commonly used approximation, that replaces exchange-correlation energy density of an

inhomogeneous system by that of an electron gas evaluated at the local density. In the last few decades, DFT has been proved as a very powerful technique for solving problems in "condensed matter physics and quantum chemistry", specifically for large systems. In chemistry it is used for calculating "the binding energy, bond length, bond angle & the nature of bond" and in physics this theoretical tool is applied to determine "elastic constants, density of state, the band structure and magnetic properties of materials etc".

3.1.1 The Many-Body Problem

Upon disregarding the relativistic effects, the whole matter is basically described by quantum theory, whose pivotal component is the many-body-wave- function which specify the evolution of probabilities, and is outcome of the product of N single-particle functions for N-electrons system,

$$\psi(\mathbf{r}_1, \mathbf{r}_2, \ldots \mathbf{r}_N) = \psi_{\mathbf{1}}(\mathbf{r_1}) \ldots \psi_{\boldsymbol{N}}(\mathbf{r_N}) \qquad \ldots\ldots\ldots\ldots\ldots\ldots (3.1)$$

where every individual $\psi_i(\mathbf{r}_i)$ fulfill one-electron Schrödinger equation with a potential term originating from the average field of the other electrons.

In theoretical solid state physics, the main issue is, "to determine ground state properties of N-interacting-electrons exposed to external local potential given by the nuclei". Quantum mechanics show that all possible data related to a system is embodied in the wave function $|\psi(\mathbf{r}_1, \ldots . \mathbf{r}_N)\rangle$ of that system and non-relativistically this ψ is determined by Schrödinger's equation [451]. For a single electron moving in a potential $V(\mathbf{r})$, the Schrödinger equation is;

$$\left[-\frac{\hbar^2 \nabla^2}{2m} + V(\mathbf{r})\right] \psi(\mathbf{r}) = E\psi(\mathbf{r}) \qquad \ldots\ldots\ldots\ldots\ldots\ldots\ldots\ldots (3.2a)$$

Generally the left side is an operator known as Hamiltonian $\hat{H}$, such that

$$\hat{H} \left| \psi \right\rangle = E|\psi\rangle \qquad \ldots\ldots\ldots\ldots\ldots\ldots\ldots\ldots (3.2b)$$

while, E denotes the total energy of the system, duly equal to the expectation value of $\hat{H}$ i.e.

$$E = \left\langle \psi \right| \hat{H} \left| \psi \right\rangle \qquad \ldots\ldots\ldots\ldots\ldots\ldots\ldots\ldots (3.3)$$

The Eq. (3.2) with Eq. (3.3) is differential equation of second order having 3N independent coordinates. Its solving analytically for N>1, is highly intricate job. So, alternative methods are needed to be used to solve this equation. In N-body system, the DFT reduces the 3N degrees of freedom to only three spatial coordinates via its particle density, which is its significant benefit.

A solid is composed of positive charged nuclei which are surrounded by negative electrons. For N nuclei, a problem of $N + ZN$ electromagnetically interacting particles arises (i.e. a many body problem), for which the many body Hamiltonian is;

$$\hat{H} = -\frac{h^2}{2}\sum_i \frac{\nabla^2_{\boldsymbol{R_i}}}{M_i} - \frac{h^2}{2}\sum_i \frac{\nabla^2_{\boldsymbol{r_i}}}{m_e} - \frac{1}{4\pi\varepsilon_o}\sum_{i,j}\frac{e^2 Z_i}{|\boldsymbol{R}_i - \boldsymbol{R}_j|} + \frac{1}{8\pi\varepsilon_o}\sum_{i\neq j}\frac{e^2}{|\boldsymbol{r_i} - \boldsymbol{r_j}|} + \frac{1}{8\pi\varepsilon_o}\sum_{i\neq j}\frac{e^2 Z_i Z_j}{|\boldsymbol{R}_i - \boldsymbol{R_j}|} \quad \ldots\ldots\ldots\ldots\ldots\ldots\ldots\ldots (3.4)$$

3.1.2 Born-Oppenheimer approximation

The "electronic structure" is a formal name for the wave function of all electrons (expressly interacting with the fixed-nuclei in space) in the system, for settled set of nuclear coordinates. For estimating the electronic structure of inconsistent atoms and molecules, the Schrödinger equation is used. The electronic structure serves to affiliate the energies with the "electron-electron and electron-proton interactions", and these electrons remain in any stimulated states, which correspond to distant peculiar eignefunctions of the wavefunction, however, our interest in particular is in the lowest energy of the system, commonly named "ground state of the system".

Perceptibly, a complete wave function describes a molecule that holds both electron and nuclei. According to Born-Oppenheimer approximation [452], nuclei are more massive, so are substantially slower than the electrons, therefore are considered freezed at permanent positions and conceivably taken in instantaneous equilibrium with electrons. Means, the electrons are the key actors in the many body problem, and the nuclei just positive charges and become external to electrons cloud.

$$\psi_{tot}(nuclei, electrons) = \psi(nuclei)\psi(electrons)$$

Consequently,

$$E_{tot} = E_{nuc}\,(nuclei - nuclei) + E(electons - nuclei\ and\ electrons - electrons)$$

This *E* means to the description of the electronic structure.

After Born Oppenheimer approximation is adapted, we have left with negative interacting particles *NZ*, floating in the potential of the nuclei, which now is external or given potential. The effects of this approximation on Eq. (3.4) prompts, that forth with the nuclei do not maneuver, their kinetic energy gets to zero, the first term vanishes, and the last term trims to a constant. Therefore, only the kinetic energy of the electron gas remains, and the potential energy of the electrons is in the external potential (which is potential of the nuclei). Hence according to Born-oppenheimer approximation, the Hamiltonian becomes;

$$\begin{aligned}\hat{H} &= \hat{T} + \hat{V}_{ee} + \hat{V}_{ext} \\ &= \sum_{i=1}^{N} -\frac{1}{2}\nabla_i^2 + \sum_{i<j}\frac{1}{|r_i - r_j|} + \sum_{i=1}^{N} V(r_i) \qquad \text{..... (3.5)}\end{aligned}$$

In the above equation operator $\hat{T}$ shows K.E of the electrons, $\hat{V}_{ee}$ represents Coulomb interaction among the electrons, and $\hat{V}_{ext}$ is external potential which arises as a result of interaction between the electrons and the nuclei. Hence, the system depends on the potential $V(r_i)$ irrespective of being an atom, a molecule or a solid. Therefore, the general quantum-mechanical access to Schrodinger equation, shall be summed as [453];

$$V(\mathbf{r}) \xrightarrow{SE} \psi(\mathbf{r}_1, \mathbf{r}_2, \mathbf{r}_3 \ldots\ldots \mathbf{r}_N) \xrightarrow{\langle\psi|\ldots|\psi\rangle} Observables \qquad \text{..... (3.6)}$$

i.e. the system is defined by picking $V(r)$, fitting it in Schrödinger's equation, to solve it for the wave function ψ, and then compute observables by taking expectation values of the operator with this wave function.

3.1.3 Variational Principal

We know that the many-body Hamiltonian cannot be solved for the wave function exactly, however a phenomenal postulate, called Ritz variational principle [454] stand for locating approximations for it. Ritz variational principle is one of the key methods unfolding solution of ground state wave function $|\psi\rangle$, such that the wave

function is acquired by minimizing the ground state energy of N particles i.e.

$$E_o = Min_{\psi \to N} \left\langle \psi \middle| \hat{H} \middle| \psi \right\rangle \qquad \text{..... (3.7)}$$

The notation "$\psi \longrightarrow N$" indicates all allowed, normalizable and asymmetric electron wave functions. Albeit the proposition facilitates to deal with the many body problem though it implicitly does not shorten the problem due to $3N$ independent coordinates.

The Hartree-Fock approach is a test process casting the *N*-electron wavefunction and implying variational theorem to get an approximate solution. *Fock* [455] and *Slater* [456] admit that the produced wave function (Eq. (3.1)) "(which is often termed Hartree-approximation)" together with the variational principle ushered to a generalization of the method that may apply to systems more complicated than atoms. They also demonstrated, that replacing Eq. (3.1) with a determinant of such functions, prevailed equations which were sparely more difficult while fulfilling the Pauli exclusion principle. Such elemental functions, that had been used in examination of atoms and ferromagnetism [457, 458] are now known as *Slater determinants,*' which are ensuing the formation of 'Hartree-Fock equations' as the basis for analysis of atomic and molecular structure since then.

3.1.4 Density as a Basic Variable

Here it is needed to remind that, one observable among that of Eq. (3.6) is the particle density. The notion of calculating the energies of electronic systems with "the density as basic variable" dates back to the advent of quantum mechanics and the inadequacy of achieving complete solution of Schrödinger equation. In this regard, initial attempts were the statistical atom of Gombas [459], while the approximations by Thomas [429] & Fermi [430] identified the basic description of the electron density and are considered as the first "density functional theory" for electronic systems [460]. Followed by the Hohenberg & Kohn theorems [23] in 1964, and meanwhile the work of Kohn & Sham [24] in 1965. They explained, that from simple one-electron theory, the electron density of a thoroughly interacting system could be actually obtained [461].

The ground state density of electrons is adopted as a basic variable, for simplifying the many body problem, as;

$$n(\mathbf{r}) = N \int d\sigma dX_2 \dots dX_N \langle \psi(\mathbf{r}, \sigma, X_2, \dots, X_N) \big| \psi(\mathbf{r}, \sigma, X_2, \dots, X_N) \rangle \qquad \dots\dots\dots (3.8)$$

Where $X_i = (\mathbf{r}_i, \boldsymbol{\sigma}_i)$ are having additional spin variable σ. On taking density into account as basic variable, the wave function of the N-particle system (containing $3N$ variables) is blown out and the basis that "n($\mathbf{r}$) depends only on the three spatial variables $\mathbf{r} = (x, y, z)$" utilized, which obviously is vital simplification of the problem.

On this point, the DFT arranges a suitable alternative, perhaps imperfect but very much flexible. DFT precisely conceives that non-relativistic Coulomb systems diverge only due to their potential v($\mathbf{r}$), and provides remedy to treat the universal operators $\hat{T}$ and $\hat{V}_{ee}$ promptly. Moreover, the DFT in a very systematic manner map the many body problem with V($\mathbf{r}$), over a single-body problem, excluding $\hat{V}_{ee}$. This all happens just by upholding the particle density n($\mathbf{r}$) from amongst several observables to the position of leading variable, upon which the measuring of all other observables may be established. This approach pursue in physics & chemistry, to constitute foundation for majority of calculations of electronic-structure, such as electrical, magnetic and structural properties of materials are resulted by application of DFT [453].

A precise approach of DFT is reflected by the following sequence;

$$n(\boldsymbol{r}) \implies \psi(\mathbf{r}_1, \mathbf{r}_2, \mathbf{r}_3 \dots \dots \mathbf{r}_N) \implies v(\boldsymbol{r}) \qquad \dots\dots\dots\dots\dots (3.9)$$

It means understanding of n($\mathbf{r}$) entail information regarding the wave function, the potential and all other observables. whereas, this arrangement delineates the conceptual structure of DFT, but in fact does not show "what happens in actual applications of it?" [453].

3.1.5 Thomas-Fermi Theory

Thomas and Fermi [429, 462] applied the density as "a basic variable" and presented a theory for "multi-particles system", called Thomas-Fermi (TF) theory. This theory was the first density based approach. This theory alongwith its extended

previews, approximately express "the charge-density, electrostatic-potential & the variation of total energy", and its mathematical properties have achieved a lot of concentration [463-466]. According to this theory, for a system of uniform N independent fermions the kinetic energy is approximated, given by

$$T_{TF}[n] = \frac{3}{10}(3\pi^2)^{2/3} \int n^{\frac{5}{3}}(\mathbf{r}) d^3\mathbf{r} \qquad \text{..... (3.10)}$$

In this expression $n(\mathbf{r})$ denotes "electron density" of uniform composition. Even, if the particles system is moving under influence of a potential having transmutation in space, yet above relation is used to acquire the kinetic energy of the system. Henceforth density of such particles does not remain homogenous, but the kinetic energy with density at point **r** is determined by Eq. (3.10). In it, the total energy functional is given by

$$E[n] \approx T_{TF}[n] + \frac{1}{2}\iint \frac{n(\mathbf{r})\boldsymbol{n}(\acute{\mathbf{r}})}{\boldsymbol{r}-\acute{\boldsymbol{r}}} d^3\mathbf{r} d^3\mathbf{r}' + \int V(\mathbf{r}) n(\mathbf{r}) d^3\mathbf{r} \qquad \text{.....(3.11)}$$

On R.H.S. the second term represent "electrostatic energy" while third term show "interaction energy due to the external potential". The total energy accomplished from above expression overrates its value. Minimization of the TF-energy in Eq. (3.11) give an expression for "Thomas-Fermi-density" with restraint that density furnishes appropriate number of particle, leading to;

$$\frac{1}{2}[3\pi^2 n(\mathbf{r})]^{2/3} + V_{ext}(\mathbf{r}) + \int \frac{n(\mathbf{r})}{\mathbf{r}-\acute{\mathbf{r}}} d(\mathbf{r}) = \mu \qquad \text{..... (3.12)}$$

Here μ is "Lagrange multiplier" that safeguard settlement of the constraint $\int n(\mathbf{r}) d\mathbf{r} = N$. The density $n(\mathbf{r})$ from Eq. (3.12) is given in terms of the potential as

$$\begin{aligned} n(\mathbf{r}) &= \frac{\mathbf{2}^{\frac{\mathbf{2}}{\mathbf{3}}}}{\mathbf{3\pi^2}}[\mu - V(\mathbf{r})]^{\frac{\mathbf{2}}{\mathbf{3}}} \qquad \text{for } \mu \geq V(\mathbf{r}) \\ &= 0 \qquad\qquad\qquad\quad \text{otherwise} \qquad \text{..... (3.13)} \end{aligned}$$

where, $V(\mathbf{r}) = V_{ext}(\mathbf{r}) + \int \frac{\mathbf{n}(\mathbf{r})}{\mathbf{r}-\acute{\mathbf{r}}} d\mathbf{r}$ represent the total potential experienced by the electrons. The TF theory is accurate inside the limit of nuclear charge only, but is having resolutely unsatisfactory description of outer regions of an atom. It give poor predictions for realistic systems, even failing to represent some general features of the density like "shell structures in atoms and friedel oscillations in solids" [23]. TF model

does not bind neutral atoms or (with some restrictions) ions to constitute molecules or solids. This notion does not support its use in material science & chemistry at normal temperatures and pressures [460].

3.1.6 Functional and Functional Derivatives

Functional: Now we know, that wavefunction $\psi = \psi[n](\mathbf{r}_1, \mathbf{r}_2, \ldots \mathbf{r}_N)$ is concluded by the density, which proclaim ψ as a function of its N spatial variables, but a "*functional* of $n(\mathbf{r})$". However, Functional can be simply defined as a function of another function and usually written with square brackets.

Commonly, *Functional* $F[n]$ is interpreted as an action progressing from a function to a number, just like $y = f(x)$ is an action (f) for proceeding from a number (x) to another number (y). The simple example of a functional is the particle number, which is a principle for getting the number N, disposed by the function $n(\mathbf{r})$;

$$N = \int d^3 r n(\mathbf{r}) = N[n] \qquad \ldots\ldots\ldots\ldots\ldots\ldots\ldots\ldots \quad (3.14)$$

A function relies on the function itself and not on its variable. In other case, a functional may depend on a parameter, as in following relation;

$$v_H[n](\mathbf{r}) = q^2 \int d^3 \acute{r} \frac{n(\acute{\mathbf{r}})}{|\mathbf{r} - \acute{\mathbf{r}}|} \qquad \ldots\ldots\ldots\ldots\ldots\ldots\ldots\ldots\ldots\ldots \quad (3.15)$$

i.e. as a rule for any value of the parameter **r** associates a value $v_H[n](\mathbf{r})$ with the function $n(\mathbf{r'})$. This term is nominally called Hartree potential.

Functional Derivatives: Functionals also carry derivatives just like traditional derivatives for functions. Such derivatives in terms of differential *df/dx*, calculates the first-order change of *y=f(x)* upon changes of x (i.e., slope of f(x) at x);

$$f(x + dx) = f(x) + \frac{df}{dx} dx + O(dx^2) \qquad \ldots\ldots\ldots\ldots\ldots\ldots\ldots\ldots\ldots\ldots \quad (3.16)$$

The differential of the functional is defined as:

$$\delta F[F] = F[f + \delta f] - F[f] = \int \frac{\delta F}{\delta f(x)} \delta f(x) dx \qquad \ldots\ldots\ldots\ldots\ldots\ldots\ldots\ldots \quad (3.17)$$

The functional derivatives have properties similar to traditional function derivatives and permit learn "how a functional changes upon changes in the form of the function it

depends on" [453].

3.1.7 Hohenberg-Kohn Theorems

We have discussed the Thomas Fermi model in Sect. 3.1.5 above, which was not founded on exact physical base and then the defining energy as a functional of electron density was formally disproportionate. The TF model, superseded by "Density Functional Theory (DFT)" for which the basis are the Hohenberg & Kohn (HK) theorem's two fundamental statements [23], that founds DFT as an exact theory. The significant recognition of Hohenberg-Kohn theory was the perception that "density of electron alone, can determine all properties of a physical system." The conventional formation of HK two statements are given in ensuing paragraphs.

First Theorem: *The ground state density* $n(\boldsymbol{r})$ *of electrons sort out the external potential* $V_{ext}(\boldsymbol{r})$ *and thus the density acknowledges the analogous Hamiltonian operator, the ground state stationary wave function* $|\psi[n]\rangle$ *alongwith complete electronic properties of the prime system.*

As a conclusion, the kinetic energy & electron-electron interaction energy may be determined by the density. Therefore, the total energy functional for a system of electrons in an external potential V(**r**) becomes;

$$E_{Vext}[n] = \left\langle \psi \middle| \hat{T} + \hat{V} \middle| \psi \right\rangle + \left\langle \psi \middle| \hat{V}_{ext} \middle| \psi \right\rangle$$

$$= F_{HK}[n] + \int n(\mathbf{r})\, V_{ext}\, d\mathbf{r}$$

$$E[n] = T[n] + V_{ee}[n] + \int V(\mathbf{r}) n(\boldsymbol{r}) d\boldsymbol{r} = F[n] + \int V(\mathbf{r}) n(\boldsymbol{r}) d\boldsymbol{r} \qquad \ldots\ldots(3.18)$$

Where $F[n] = T[n] + V_{ee}[n] = \left\langle \psi[n] \middle| \hat{T} + \hat{V}_{ee} \middle| \psi[n] \right\rangle$ is the HK-functional.

Cardinally the interpretation of electron-electron interaction splits its relevant term into two;

$$V_{ee} \equiv U[n] + E_{xc}[n] \qquad \ldots\ldots\ldots\ldots\ldots\ldots\ldots\ldots (3.19)$$

where U[n] denote classical Coulomb energy, given by

$$U[n] = \frac{1}{2}\iint \frac{n(\mathbf{r})n(\acute{\mathbf{r}})}{\mathbf{r}-\acute{\mathbf{r}}} d^3\mathbf{r} d^3\mathbf{r}' \qquad \text{..... (3.20)}$$

and $E_{xc}[n]$ is indicating the non-classical input to the electron-electron interaction, containing a correction for self-interaction beside quantum mechanical exchange. It is compelling to comprehend that all inherent properties of the electronic system are fully assimilated in the HK-functional $F[n]$, whose understanding is therefore commensurate to the exact solution of the Schrödinger Eq. (3.2). The one-to-one conformity amid "ground state density" and "external potential" is exciting, as all observables can be obtained uniquely from the density.

Second Theorem: *Total energy functional $E[n]$ fulfills a variational principle with regard to density, i.e. the energy $E[n]$ attain the least value E_o for the appropriate ground state density n_o:*

$$E_0 = min_{n\rightarrow N} E[n] = E[n_0] \qquad \text{..... (3.21)}$$

The notation "$n \longrightarrow N$" represent variation over entire ground state densities of arbitrary entity of N-electron.

The first Hohenberg-Kohn Theorem entails that there subsists an external potential $V(\mathbf{r})$ (called *v-representable*) for any changeable density $n(\mathbf{r})$, however upon this happening weaving of densities which are not *v*-representable are expedient. This connotation evidently leads to formal problems which can be prevented by the more general formulation of Hohenberg-Kohn Theorem, known as "*constrained search formulation*" [467]. The second theorem provides the opportunity of using the Rayleigh-Ritz's variational principle to determine the ground state density [468].

3.1.8 Constrained-Search Formulation

Levy [467] and Lieb [464] separately presented the "*constrained search proof*" (Eq. 3.22 to 3.24) of HK- theorem. The substantiated argument of Hohenberg-Kohn [23] advanced with assumption that ψ_0 was established uniquely by n_o and showed that this creates dissent to the variational principle. In agreement to outline of *v*-representability, a density $n(\mathbf{r})$ is known as "B-representable" if it can be conceived from wave function of N-antisymmetic-partiles through Eq. (3.8). For single particle

density, the matter of N-representability has been worked out, and with the help of antisymmetric $\psi(\mathbf{r}_1, \mathbf{r}_2, \ldots \mathbf{r}_N)$ any non-negative function can be written in shape of Eq. (3.8) [469, 470]. On the basis of "N-representable densities" for an adjusted generalized system for the total energy functional $E[n]$ minimization reveals no definite connection to an external potential $V(\mathbf{r})$, such that the total energy functional is;

$$E[n] = min_{\psi \to n(\mathbf{r})} \left\langle \psi[n] \middle| \hat{T} + \hat{V}_{ee} \middle| \psi[n] \right\rangle + \int V(\mathbf{r}) n(\mathbf{r}) d\mathbf{r}$$
$$= F[n] + \int V(\mathbf{r}) \mathbf{n}(r) d\mathbf{r} \qquad \ldots\ldots\ldots\ldots\ldots\ldots\ldots\ldots (3.22)$$

"$\psi \longrightarrow n(\mathbf{r})$" now symbolize a minimization over all the wave functions $|\psi\rangle$ leading to density n($\mathbf{r}$) through Eq. (3.8). The HK-functional F[n] is now defined over the constrained search

$$F[n] = min_{\psi[n] \to n(\mathbf{r})} \left\langle \psi \middle| \hat{T} + \hat{V}_{ee} \middle| \psi \right\rangle \qquad \ldots\ldots\ldots\ldots\ldots\ldots\ldots\ldots (3.23)$$

Since in Eq. (3.7) the Ritz variational principle holds all yielded wave functions in reach of its search, whereas the variation principle in Eq. (3.22) is being bounded to wave functions that muster the density $n(\mathbf{r})$. So, forthwith the minimization continues without requirement of v-representability through all wave functions. A connection between the Ritz variational principle in Eq. (3.7) and the variation principle of 2nd HK theorem in Eq. (3.21) could be fixed plainly by individualizing the search over all wave functions "$\psi \longrightarrow N$" as it is carried-out in the Ritz variation, into two separate searches that lead to a variation achieved by using the second HK-Theorem

$$E_0 = min_{\psi \to N} \left\langle \psi \middle| \hat{T} + \hat{V}_{ee} + \hat{V} \middle| \psi \right\rangle$$
$$= min_{\psi \to N} [min_{\psi \to n(\mathbf{r})} \left\langle \psi \middle| \hat{T} + \hat{V}_{ee} + \hat{V} \middle| \psi \right\rangle$$
$$= min_{\psi \to N} [min_{\psi \to n(\mathbf{r})} \left\langle \psi[n] \middle| \hat{T} + \hat{V}_{ee} + \hat{V} \middle| \psi[n] \right\rangle + \int V(\mathbf{r}) n(\mathbf{r}) d\boldsymbol{r}$$
$$= min_{\psi \to N} E[n] \qquad \ldots\ldots\ldots\ldots\ldots\ldots\ldots\ldots (3.24)$$

The minimum search in Eq. (3.22) extends over the whole range of wave functions originating the density "$n(\mathbf{r})$". While the second search upon revoking the constraint to a distinct density and get through the new search "$n(\mathbf{r}) \longrightarrow N$" over all densities. Though the HK-Theorems and the constrained-search creation devise rigorous mathematical

environment such that the presence of the total energy functional is established, but still practically attainable scheme for dealing accessible interacting electrons, is not available, which resolved by Kohn and Sham [24].

3.1.9 Kohn-Sham scheme and Exchange Correlation Energy

The Schrödinger equation for an imaginary simulated scheme "known as the 'Kohn-Sham-Scheme" of non-interacting particles, which create the same density as any given system of interacting particles, is called *the Kohn-Sham equation* [24, 471].

It means, the central concept of the Kohn-Sham scheme is to project the actual interacting particles (commonly electrons) system to a mythical system of non interacting particles that conceive just the same ground state density and ground state energy as the interacting system do. Therefore, this scheme reflects mean-field theory, as in this scheme the particles acts like chargeless bodies that do not interact with one another but everyone sense the field generated by all other particles of the system. Hence, the definition of Kohn-Sham equation is attributable to an effective external potential (represented by $V_s(\mathbf{r})$ or $V_{eff}(\mathbf{r})$ in which the non-interacting particles occur, and is known as the *Kohn-Sham potential*. A precise scheme to tackle the "kinetic energy functional of interacting particles "$T[n]$" builds on fragmenting it in two parts, one part depict the kinetic energy $T_s[n]$ of noninteracting particles having density n and the other part portray the remnant marked by $T_c[n]$. The subscript s and c imply to "single-particle" & "correlation" respectively, given as $T[n] = T_s[n] + T_c[n]$ [453].

The wave function that reduces the constrained search minimization, is known as the wave function of Kohn-Sham schem i.e. $\phi[n]$;

$$T_s[n] = \left\langle \phi[n] \middle| \hat{T} \middle| \phi[n] \right\rangle = min_{\psi \to n(\mathbf{r})} \left\langle \psi \middle| \hat{T} \middle| \psi \right\rangle \qquad \text{…….(3.25)}$$

where $T_s[n]$ is "the kinetic energy functional of the KS system".

Then total energy can be written as

$$E[n] = T[n] + V_{ee} + \int V(\mathbf{r})\, n(\mathbf{r}) d\mathbf{r}$$
$$\equiv T_s[n] + U[n] + E_{xc}[n] + \int V(\mathbf{r}) n(\mathbf{r}) d\mathbf{r} \qquad \text{…….. (3.26)}$$

Eq. (3.26) is customarily perfect, but needlessly E_{xc} is unknown (i.e. the problems in re-expressing in a pattern, that main part of the energy is dealt in precise manner while the whole unknown contributions are consumed in the exchange-correlation functional E_{xc} despite the HK theorem promises of being density functional. This aspect can be comprehended as one of the great benefits of the KS-DFT. This functional $E_{xc}[n]$ is known as exchange-correlation (xc) energy and in Eq. (3.26) it is,

$$E_{xc}[n] = E_x[n] + E_c[n] \qquad \ldots\ldots\ldots\ldots\ldots\ldots\ldots\ldots \quad (3.27)$$

By definition E_{xc} is summing the "difference of the kinetic energies, $T - T_s$ $(\mathrm{i.e.\,T_c})$" with "the expectation values of the electron-electron interaction of the two systems"

$$E_{xc}[n] = T[n] - T_s[n] + V_{ee}[n] - U[n] \qquad \ldots\ldots\ldots\ldots\ldots\ldots\ldots\ldots \quad (3.28)$$

E_{xc} is some times breakdown as E_{xc}=E_x+E_c, where E_x is exchange energy (resulted by Pauli principle) and E_c due to correlations (note that T_c is then a part of E_c). By definition the "exchange energy" is

$$E_x[n] = \left\langle \phi[n] \middle| \hat{V}_{ee} \middle| \phi[n] \right\rangle - U[n_o] \qquad \ldots\ldots\ldots\ldots\ldots\ldots\ldots\ldots \quad (3.29)$$

and the "correlation energy" is

$$E_c[n] = \left\langle \psi[n] \middle| \hat{T} + \hat{V}_{ee} \middle| \psi[n] \right\rangle - \left\langle \psi[n] \middle| \hat{T} + \hat{V}_{ee} \middle| \psi[n] \right\rangle \qquad \ldots\ldots\ldots\ldots \quad (3.30)$$

3.1.10 Derivation of Kohn-Sham Equation

Until now, the primitive problem of Eq. (3.2) the solution of Schrödinger's equation has only ceded over to the matter of extracting required methodical argument for the functional $E_{xc}[n]$ of exchange-correlation, which is unknown yet. As T_s is reported to be an orbital functional, Eq. (3.26) cannot be minimized straightly w.r.t $[n]$, rather ordinarily Kohn-Sham scheme is selected for carrying-out minimization. In variational problem presented in the second HK-theorem, the ground state energy for a many-particles system can be acquired by minimizing the energy functional, subject constraining conservation of the number of electrons, which gives

$$\delta[E[n] - \mu(\int n(\mathbf{r})d\mathbf{r} - N)] = 0 \qquad \ldots\ldots\ldots\ldots\ldots\ldots\ldots\ldots \quad (3.31)$$

By conversion of Eq. (3.28) w.r.t density yields the Euler-Lagrange equation of the

Kohn-Sham theory

$$\mu = \frac{\delta E[n]}{\delta n[\mathbf{r}]} = \frac{\delta T_s[n]}{\delta n(\mathbf{r})} + \frac{\delta U[n]}{\delta n(\mathbf{r})} + \frac{\delta E_{xc}[n]}{\delta n(\mathbf{r})} + V(\mathbf{r}) \quad \ldots\ldots\ldots\ldots\ldots\ldots\ldots\ldots \text{(3.32)}$$

Now, explicating the potential of KS in Eq. (3.32) as

$$\begin{aligned} V_s(\mathbf{r}) &= V(\mathbf{r}) + \frac{\delta U[n]}{\delta n(\mathbf{r})} + \frac{\delta E_{xc}[n]}{\delta n(\mathbf{r})} \\ &= V(\mathbf{r}) + V_H(\mathbf{r}) + V_{xc}(\mathbf{r}) \quad \ldots\ldots\ldots\ldots\ldots\ldots\ldots\ldots \text{(3.33)} \end{aligned}$$

And the Lagrange multiplier in Eq. (3.24) becomes

$$\mu = \frac{\delta T_s[n]}{\delta n(\mathbf{r})} + V_s[n] \quad \ldots\ldots\ldots\ldots\ldots\ldots\ldots\ldots \text{(3.34)}$$

With the Hartree potential

$$V_H(\mathbf{r}) = \int \frac{n(\acute{\mathbf{r}})}{\mathbf{r}-\acute{\mathbf{r}}} d\acute{\mathbf{r}} \quad \ldots\ldots\ldots\ldots\ldots\ldots\ldots\ldots \text{(3.35)}$$

$$V_{xc}(\mathbf{r}) = \frac{\delta E_{xc}[n]}{\delta n(\mathbf{r})} \quad \ldots\ldots\ldots\ldots\ldots\ldots\ldots\ldots \text{(3.36)}$$

As functional $T_s[n]$ is not known clearly, straight solution of Euler-Lagrange equation is used. KS Pioneered to imply the orbitals for the solution of this problem, the corresponding variation leaded to;

$$\frac{\delta}{\delta \phi_i}\left[E(n) - \sum_{j,k=1}^{N} \epsilon_{jk} \int \phi_j^{\dagger}(\acute{\mathbf{r}})\phi_k(\acute{\mathbf{r}})d\acute{\mathbf{r}}\right] = 0 \quad \ldots\ldots\ldots\ldots\ldots\ldots\ldots\ldots \text{(3.37)}$$

Lagrange multipliers ϵ_{jk} preserve ortho-normality constraint of the orbitals ϕ_i for individual electrons, with its use the variation finally results

$$H_s(\mathbf{r})\phi_i(\mathbf{r}) = \left[-\frac{1}{2}\nabla^2 + V_s(\mathbf{r})\right]\phi_i(\mathbf{r}) = \epsilon_{ij}\,\phi_j(\mathbf{r}) \quad \ldots\ldots\ldots\ldots\ldots\ldots\ldots\ldots \text{(3.38)}$$

Where V_s represents potential of single particle. The Hamiltonian H_s is indeed hermitian & holding the matrix ϵ_{ij}. Hence, with unitary transformation it can be diagonalized, leaving the relevant physical observables unvarying and so results the canonical form of Kohn-Sham equations;

$$\begin{aligned} H_s(\mathbf{r})\phi_i(\mathbf{r}) &= \left[-\frac{1}{2}\nabla^2 + V_s(\mathbf{r}) + V_H(\mathbf{r}) + V_{xc}(\mathbf{r})\right]\phi_i(\mathbf{r}) \\ &= \epsilon_i\phi_i(\mathbf{r}) \quad \ldots\ldots\ldots\ldots\ldots\ldots\ldots\ldots \text{(3.39)} \end{aligned}$$

Applying the Hamiltonian on Kohn Sham orbitals $\phi_i(\mathbf{r})$ in Eq. (3.39) makes a pack of uncoupled equations with the Hamiltonian symbolize a non-interacting (non-degenerate) system of particles for which the ground state is depicted by a Slater's

determinant duly formed from KS orbitals ϕ_i settled by the single particle Eq. (3.39);

$$|\phi\rangle = \frac{1}{N!} det[\phi_1(\mathbf{r}), \phi_2(\mathbf{r}), \ldots \phi_n(\mathbf{r})] \qquad \ldots\ldots\ldots\ldots\ldots\ldots\ldots\ldots \quad (3.40)$$

While, the density $n(\mathbf{r})$ of the original system is simply built out of KS orbitals using

$$n(\mathbf{r}) = \sum_{i=1}^{N} f_i |\phi_i(\mathbf{r})|^2 \,, where\ f_i\ is\ the\ occupation\ of\ the\ ith\ orbital$$

$$\ldots\ldots\ldots\ldots\ldots\ldots\ldots\ldots \quad (3.41)$$

It is equivalent to the density of the degenerate system n_o. Hence the electron density (i.e the most significant property) can be examined from electron structure. This density promulgates notable properties of a molecule and is the commencing point for producing simpler, fixed-charge models of molecules. Eqs. (3.39) and (3.41) are the Kohn-Sham equations, replacing the problem of minimizing $E[n]$ by that of solving a non-interacting Schrödinger equation. With use of variational principal scheme, the Kohn-Sham function of Eq. (3.40) can be analogously explained as the minimizing wave function in the constrained search minimization giving the kinetic energy functional of non-interacting system having the real ground state density n_o.

$$T_s[n_o] = \min_{\psi \to n(\mathbf{r})} \langle \psi | T | \psi \rangle \qquad \ldots\ldots\ldots\ldots\ldots\ldots\ldots\ldots \quad (3.42)$$

Solving Kohn-Sham equations is nonlinear due to the reason that both V_H and V_{xc} depend on n, which is dependent upon ϕ_i, and $\phi_i$in turn depend on V_s. Commonly such problems are solved by commencing with an initial guess for $n(\mathbf{r})$, in parallel calculate the relevant $V_s(r)$ and accordingly solve the differential Eq. (3.39) for the ϕ_i. New density can be calculated from this, using Eq. (3.41) & starts again. The procedure is reiterated until convergence is acquired, technically known as '*self-consistency cycle*'. Where convergence cannot be attained, will mean self consistent solution of Kohn-Sham equations cannot be obtained [453].

Various convergence criteria (like the energy, density or some observable) and many convergence accelerating algorithms are in ordinary use (like mixing of previous & fresh iterations). In rare cases over few dozen iterations are needed for achieving convergence, and in scarce cases convergence could not be achieved [453]. As soon converged solution n_o is acquired, accordingly the total energy can be calculated, and

from Eq. (3.26), the total energy functional with orbitals depending on the electronic density, can be clearly written as

$$E[n] = -\int dr \sum_{i=1}^{N} \phi_i^{\dagger}(\mathbf{r}) + \frac{1}{2}\nabla^2\phi_i(\mathbf{r}) + \frac{1}{2}\iint \frac{n(\mathbf{r})n(\acute{\mathbf{r}})}{\mathbf{r}-\acute{\mathbf{r}}} d\mathbf{r}d\acute{\mathbf{r}} + E_{xc}(\mathbf{r}) + \int V(\mathbf{r})n(\mathbf{r})d\mathbf{r}$$

…….. (3.43)

From Eq. (3.43), E_o is not simply the sum of all ϵ_i, actually from Eq. (3.39) it is clear that ϵ_i are unnatural factitious entity being the eigen values of a contributory single body equation whose eignefunctions (i.e. orbitals) describe the correct density [453] which is having firm physical value in the Kohn-Sham equations. Hence Eq. (3.43) affirms that the total energy within Kohn-Sham formalism rely on "electron density and orbitals" both, whereas the Hamiltonian operator within it is judged on the basis of density, that in turn originates from orbitals.

Therefore, the Kohn-Sham scheme in Eq. (3.39) necessitates for solving self consistently and the orbitals accumulated by this scheme shall provide physical meanings. Further, as the Slater's determinant made out of Kohn-Sham orbitals does not give the correct many-body wavefunction. The affiliated Kohn-Sham eigenvalues were genuinely considered to have no (or almost no) physical implication. But, the several works [472-477] argued and revealed that Kohn-Sham eigenvalues are defined distinctly to the zeroth order approximations for ionization and also for excitation energies and consequently are meaningful physical quantities. However the highest occupied Kohn-Sham eigenvalues are an exclusion to this prescription. The Nth eigenvalues for 'M electrons' system is denoted by $\in_N (M)$, which by deliberations give the negative of the first ionization energy of the N-body system $\epsilon_N(N) = -I$, and show the negative of the electron affinity of N-Body system $\epsilon_{N+1}(N+1) = -A$ [472, 473, 478].

The essential band gap allied to the quasi-particles in the form of Kohn-Sham eigenvalues can be written as

$$E_{gap} = \epsilon_{N+1}(N+1) - \epsilon_N(N) \qquad \text{…….. (3.44)}$$

Here $\epsilon_{N+1}(N+1)$ are eigenvalues of $(N+1)$ orbitals for N-particles system. Realistic calculations solve the Kohn-Sham equations for N particles system, giving the

associated eigenvalues $[\epsilon_i(N)]$. Contrary to Eq. (3.44), the bandgap within the Kohn-Sham scheme is

$$E_{gap}^{s} = \epsilon_{N+1}(N+1) - \epsilon_{N+1}(N) \qquad \ldots\ldots\ldots\ldots\ldots\ldots\ldots\ldots \quad (3.45)$$

Certainly this band-gap vary from that of the quasipartiles band-gap and is called as the "discontinuity term" [479, 480] given by

$$\Delta_{xc} = \epsilon_{N+1}(N+1) - \epsilon_{N+1}(N) \qquad \ldots\ldots\ldots\ldots\ldots\ldots\ldots\ldots \quad (3.46)$$

Upon neglecting this term, may result in underestimating of bandgap. If exchange correlation functional $E_{xc}[n]$ of the particles system is accurately known, which is equivalent to solve the many-particles Schrödinger's equation precisely. Therefore intricacy of the basic problem has been assimilated in general by the complex dependence of the Kohn-Sham potential on density and so the exchange-correlation functional is always approximated in practical calculations.

The simple construction of such energy functional is not possible easily, but it is rigorously built by separating the exchange and correlation parts of the energy. Similar action is applicable to the exchange and correlation potentials as well, so that the functional derivative of the energy functionals w.r.t density is

$$V_x(\mathbf{r}) = \frac{\delta E_x[n]}{\delta[n(\mathbf{r})]}; \qquad V_c(\mathbf{r}) = \frac{\delta E_c[n]}{\delta[n(\mathbf{r})]} \qquad \ldots\ldots\ldots\ldots\ldots\ldots\ldots\ldots \quad (3.47)$$

In DFT, "the exchange energy functional" is given by the expression [481];

$$V_x^{DFT}[n] \equiv E_x[n] \equiv \left\langle \psi[n] \middle| \hat{V}_{ee} \middle| \psi[n] \right\rangle - U(n)$$
$$-\frac{1}{2}\sum_{i,j}^{N} \iint \frac{\phi_i^{\dagger}(\mathbf{r})\phi_j^{\dagger}(\acute{\mathbf{r}})\phi_j(\mathbf{r})\phi_i(\acute{\mathbf{r}})}{|\mathbf{r}-\acute{\mathbf{r}}|} d\mathbf{r}d\acute{\mathbf{r}} \qquad \ldots\ldots\ldots\ldots\ldots\ldots\ldots\ldots \quad (3.48)$$

The term $\left(\left\langle \phi[n] \middle| \hat{V}_{ee} \middle| \phi[n] \right\rangle\right)$ is not the true "electron-electron interaction energy" but it refers to the "expectation value of electron-electron interaction of Kohn-Sham state". The comparison of Eq. (3.48) and Eq. (3.28) reveals the distinction of "true electron-electron interaction energy" and "expectation value $\left(\left\langle \phi[n] \middle| \hat{V}_{ee} \middle| \phi[n] \right\rangle\right)$" which is being preoccupied in correlation energy and also hold kinetic energy differences of real & Kohn-Sham non-degenerate system of electrons. This correlation energy is

$$E_c[n] = T[n] - T[n]_s + V_{ee}[n] - \left\langle \phi[n] \middle| \hat{V}_{ee} \middle| \phi[n] \right\rangle \quad \ldots\ldots\ldots\ldots (3.49)$$

Beside the analysis of the ground state physical properties of electronic system, the insight perception upon application of external perturbations are also required. The infinitesimal change at point $\mathbf{r}$ of total potential $\delta V_{tot}(\mathbf{r})$ associated to an infinitesimal change at point $\mathbf{r}'$ of the external potential $\delta V(\mathbf{r})$ is explained by the dielectric function $\epsilon^{-1}(\mathbf{r}, \acute{\mathbf{r}})$ of the system,

$$\epsilon^{-1}(\mathbf{r}, \acute{\mathbf{r}}) = \frac{\delta V_{tot}(\mathbf{r})}{\delta V(\mathbf{r})} \quad \ldots\ldots\ldots\ldots\ldots\ldots\ldots\ldots (3.50)$$

In Kohn-Sham DFT, $\delta V_{tot} = \delta V_s$ can be recognized and corresponding change in density is characterized by the response function of individual particle

$$\chi_o(\mathbf{r}, \acute{\mathbf{r}}) = \frac{\delta n(\mathbf{r})}{\delta V_s(\acute{\mathbf{r}})} \quad \ldots\ldots\ldots\ldots\ldots\ldots\ldots\ldots (3.51)$$

First order perturbation [482] applied to KS Eq. (3.39) results in

$$\chi_o(\mathbf{r}, \acute{\mathbf{r}}) = \sum_i^N \sum_{j=1+N}^{\infty} \frac{\phi_i^\dagger(\mathbf{r})\phi_j^\dagger(\acute{\mathbf{r}})\phi_j(\mathbf{r})\phi_i(\acute{\mathbf{r}})}{\epsilon_i - \epsilon_j} + c.c \quad \ldots\ldots\ldots\ldots\ldots (3.52)$$

where *i* refers to all occupied and *j* unoccupied orbitals. The variation in density due to the variation in external potential is

$$\chi_o(\mathbf{r}, \acute{\mathbf{r}}) = \frac{\delta n(\mathbf{r})}{\delta V(\acute{\mathbf{r}})} \quad \ldots\ldots\ldots\ldots\ldots\ldots\ldots\ldots (3.53)$$

Here $\chi(\mathbf{r}, \acute{\mathbf{r}})$ represent response function of the real system. Now w.r.t. density the change of the Kohn-Sham potential is

$$\begin{aligned} \delta V_s(\mathbf{r}) &= \delta V(\mathbf{r}) + \frac{\delta V_H(\acute{\mathbf{r}})}{\delta n(\mathbf{r})}\delta n(\mathbf{r}) + \frac{\delta V_{xc}(\acute{\mathbf{r}})}{\delta n(\mathbf{r})}\delta n(\mathbf{r}) \\ &= \delta V(\mathbf{r}) + K_h(\mathbf{r}, \acute{\mathbf{r}})\delta n(\mathbf{r}) + K_{xc}(\mathbf{r}, \acute{\mathbf{r}})\delta n(\mathbf{r}) \quad \ldots\ldots (3.54) \end{aligned}$$

where $K_h(\mathbf{r}, \acute{\mathbf{r}})$ is "Hartree kernel" and $K_{xc}(\mathbf{r}, \acute{\mathbf{r}})$ is "exchange correlation kernel". The "exchange correlation kernel" can be separated into "exchange" and "correlation part"

$$K_{xc}(\mathbf{r}, \acute{\mathbf{r}}) = K_x(\mathbf{r}, \acute{\mathbf{r}}) + K_c(\mathbf{r}, \acute{\mathbf{r}}) \quad \ldots\ldots\ldots\ldots\ldots\ldots\ldots\ldots (3.55)$$

Combining Eqs. (3.51), (3.53) and (3.54), we get

$$\chi = (1 - \chi_o K_h - \chi_o K_{xc})^{-1}\chi_o \quad \ldots\ldots\ldots\ldots\ldots\ldots\ldots\ldots (3.56)$$

Ultimately with dielectric function Eq. (3.50) for the response function we get

$$\epsilon = 1 - (K_h - K_{xc})\chi_o = [1 + (K_h - K_{xc})]^{-1} \quad \ldots\ldots\ldots\ldots\ldots (3.57)$$

Finding proper approximations for exchange-correlation kernel K_{xc} is clearly a dreadful challenge.

3.2 "Exchange-Correlation Energy" Functionals

In DFT, the "exchange correlation energy (E_{xc})" is the crucial main quantity [481, 483-485], already explained in section 3.1.9 above, given by Eq. (3.27) and is described as the difference between the "exact total energy" of a system and "other augmentations that may be evaluated numerically exactly" [486]. Since the closeness of the approximate exchange and the correlation, to exact value, determines the quality of DFT calculation, therefore, making approximation for this term in practice is necessary. Accurate values of the exchange energy E_x and correlation energy E_c energies are essential for analysis of the effect of electron correlation within KS theory in order to calibrate various DFT approximations [484]. The Kohn-Sham scheme alone does not affirm the exchange correlation functional, but approximating it is demanded in order to obtain benefit of the simplified framework of the Kohn Sham Scheme. In DFT calculations are fundamentally elaborated by three types of approximations;

(1). Conceptual: which refers to the understanding of Kohn-Sham "eigenvalues & orbitals" as physical energies and wave functions.

(2). Numerical: it actually concerns the process for unraveling the differential equation i.e. Eq. (3.39).

(3). The third brand of approximation associates to devising a relation for the unexplored function xc in $E_{xc}[n]$ (refer Eq. 3.26), which accommodate all many-body aspects of the problem and leads to computational procedures. We have to deal with this type of approximation in our work.

3.2.1 "Local Density" Approximation (LDA)

This approximation is used widely, proposed by Kohn & Sham, and it glue to the DFT and Kohn-Sham formalism. It is the most important approximation historically and practically (in several applications). For LDA, the rudimentary physical system is

homogeneous electron gas, which is electrically neutral as a whole so that the electrons N and the volume of the gas V approach infinity, whereas the electron density $n = {}^{N}/_{V}$ grasp a constant value, that stay compatible for each dimensional point **r**. The electons' nonuniform system like an atom, a molecule or solid are considered as homogeneous with associating exchange & correlation energy $\epsilon_{xc}^{LDA}\big(n(\mathbf{r})\big)$ per electron at point **r** by comparable homogenous electron gas with density at each point **r**. By construction, LDA is suitable for systems with slowly varying density and astonishingly appears more accurate for many other realistic cases [487]. It is the most engaged technique in solid state physics.

In homogeneous system it is known that, per volume

$$t_s^{hom}(n) = \frac{3\hbar^2}{10m}(3\pi^2)^{2/3}n^{5/3} \qquad \text{…….. (3.58)}$$

Where $n = \text{constant}$.

In nonhomogeneous system, with $n = n(\mathbf{r})$, one approximates locally

$$t_s(\mathbf{r}) \approx t_s^{hom}\big(n(\mathbf{r})\big) = \frac{3\hbar^2}{10m}(3\pi^2)^{2/3}n(\mathbf{r})^{5/3} \qquad \text{…….. (3.59)}$$

which by integration over whole space gives the total kinetic energy

$$T_s^{LDA}[n] = \int d^3r\, t_s^{hom}\big(n(\mathbf{r})\big) = \frac{3\hbar^2}{10m}(3\pi^2)^{2/3}\int d^3r\, n(\mathbf{r})^{5/3} \qquad \text{…... (3.60)}$$

The approximation for kinetic energy $T_s[n] \approx T_s^{LDA}[n]$, is much lower to the explicit appraisal of T_s in relevancy of orbitals, presented by the Kohn-Sham equations. However, the LDA perception proved to be profoundly convenient and handy for another component "exchange-correlation energy $E_{xc}[n]$" of the total energy (Eq. (3.26)). For $E_{xc}[n]$ the process is commonly simplistic due to the exactly known "per volume exchange energy" of the homogeneous electron system [481, 483]

$$e_x^{hom}(n) = -\frac{3q^2}{4}\left(\frac{3}{\pi}\right)^{1/3} n^{4/3} \qquad \text{…….. (3.61)}$$

so that

$$E_x^{LDA}[n] = -\frac{3q^2}{4}\left(\frac{3}{\pi}\right)^{1/3}\int d^3r\, n(\mathbf{r})^{4/3} \qquad \text{…….. (3.62)}$$

Eq. (3.62) gives the LDA for exchange energy E_x. But as $e_c^{hom}(n)$ is unknown precisely, therefore the case for the correlation energy $E_c[n]$ is excessively difficult. Upon

appearance of quite accurate "Quantum Monte Carlo (QMC) calculations" for the electron system, the LDA approximations turned obsolete passé [488]. Beside it the exact density dependence of correlation energy is unexplored yet, however proper values for $\epsilon_{xc}^{LDA}\big(n(\mathrm{r})\big)$ exists; more oftenly applied are Vosko, Wilk, and Nusair (VWN) [489]. Other modern expression for $e_c^{hom}(n)$ [490, 491] are framework guidelines of these data which fulfill general DFT packages and in usual appliance produce almost identical results. Contrarily, the former developed parameterization of LDA which was based on perturbation theory [492, 493], which can seldomly vary from the QMC.

Formally, for exchange-correlation energy, the LDA is composed of;

$$E_{xc}[n] \approx E_{xc}^{LDA}[n] = \int d^3r e_{xc}^{hom}(n)|_{n\to n(\mathbf{r})} = \int d^3r e_{xc}^{hom}\big(n(\mathbf{r})\big) \qquad \ldots\ldots\ldots\ldots\ldots\ldots \text{(3.63)}$$

where $e_{xc}^{hom} = e_x^{hom} + e_c^{hom}$.

Accordingly, the interrelated exchange-correlation potential is;

$$v_{xc}^{LDA}[n(\mathbf{r})] = \frac{\partial e_{xc}^{hom}(n)}{\partial n}\Big|_{n\to n(\mathbf{r})} \qquad \ldots\ldots\ldots\ldots\ldots\ldots\ldots\ldots \text{(3.64)}$$

This approximation for $E_{xc}[n]$ has been demonstrated remarkably fortuitous and since many decades the LDA is in use for determination of band structures and total energies in solid-state physics. The concept of LDA inculcating into the DFT is, that the DFT with LDA handles the non-homogeneous many-particles problem by breaking it in two individual non-trivial problems. In one, the solving of spatially homogeneous interacting electron gives uniform exchange-correlation energy $e_{xc}^{hom}(n)$, and in other the inhomogeneous non-interacting electrons system is determined by Kohn-Sham equations. The local-density-potential Eq. (3.64) connects these two problems, which yields the inclusion of exchange-correlation (*xc)* energy of uniform interacting system to the equations of inhomogeneous non-interacting system. The main cause behind the accomplishments of DFT in quantum mechanics is due to the peculiar manner in which the inhomogeneous many-body problem is disintegrated and as well different improvements on LDA [453].

3.2.2 Generalized Gradient Approximation (GGA)

LDA can get advanced further, if the exchange-correlation subsidy for energy diminutive (infinitesimal) volume is considered to rely on the local density within that volume, and also on the density in the neighbouring volumes too. Means, the *gradient* comes into effect to perform a role. Since, the basis for LDA is the homogeneous non-interacting electron system, therefore incorporating the remedy of gradient was the natural mode to progress beyond the LDA [461]. For dealing "inhomogeneous system with fast varying electron density" in more accurate manner, is to include the "gradient of the density" in the exchange-correlation functional. In LDA, insight of the density at point $\mathbf{r}$ (with spatially inhomogeneous system, having spatially varying density $n(\mathbf{r})$) is exploited, in a way that inclusion of information regarding such change in the functional will be useful. In this regard the "gradient-expansion approximation (GEA)" was the first effort, where systematic gradient-corrections of the form $|\nabla n(\mathbf{r})|, |\nabla n(\mathbf{r})|^2, \nabla^2 n(\mathbf{r})$etc. to the LDA were tried.

In early eighties, upon comprehension that experiment can be performed with more general functions of the form $n(\mathbf{r})$ and $\nabla n(\mathbf{r})$ which can be introduced in lieu of power-series-like systematic gradient expansions. The processing of these functions is not needed to be done order by order. With its inclusion, the electron density is described by;

$$E_{xc}^{GGA}[n] = \int f_{xc}^{GGA}\big(n(\mathbf{r}), \nabla n(\mathbf{r})\big)d\mathbf{r} \qquad \text{…….. (3.65)}$$

This new method is familiarized with the name "Generalized Gradient approximations (GGAs)" [494] and commonly is elaborated by a functional that clearly carry "density gradient $\nabla n(\mathbf{r})$". Here too, the exchange & correlation terms are dealt separately.

$$E_{xc}^{GGA}[n] = E_{x}^{GGA}[n] + E_{c}^{GGA}[n] \qquad \text{…….. (3.66)}$$

Nearly in all cases GGA-functional for the exchange term with dimensionless parameters, is given by

$$E_{x}^{GGA}[n] = \int n(\mathbf{r})\epsilon_{x}^{LDA}\big(n(\mathbf{r})\big)F(s)d\mathbf{r} \qquad \text{…….. (3.67)}$$

where $$s = \frac{|\nabla n(\mathbf{r})|}{2k_f((\mathbf{r}))n(\mathbf{r})} \qquad \text{…….. (3.68)}$$

F(s), a scaling function with somewhat difficult form, and $k_f(\mathbf{r})$ stands for "Fermi wave vector" defined by $k_f(\mathbf{r}) = \left(3\pi^2 n(\mathbf{r})\right)^{1/3}$.

The GGA-functionals are often optimized for obtaining elevated reliable energy values and better satisfactory results for corresponding potentials. Various GGAs differ whilst choice of function $f(n, \nabla n)$, ultimately building every GGA enough different from each other as compared to difference of parameterizations in LDA: implicitly carrying single correct expression of $e_{xc}^{hom}(n)$, and the miscellaneous parameterizations of LDA [489-493] are simply different ways of writing it. Based on application of the process used for obtaining $f(n, \nabla n)$, different GGAs could be acquired. The GGAs practiced in physics stress on correctly definite constraints. Presently, prominent and most dependable GGA is PBE, denoting the functional suggest by Perdew-Bruke-Ernzerhof in 1996 [495-497]), and BLYP is used in chemistry, representing the coalition of "Becke's 1988 exchange-functional" [498] with the 1988 "correlation-functional of Lee, Yang & Parr" [499]). The broad applicability of GGAs has led to important advancements both in physics and chemistry, as compared to LDA.

The functional derivative of exchange correlation functional of general GGA is given by [500]

$$V_{xc}^{GGA} = \left[\frac{\delta f_{xc}}{\delta n} - \nabla\left(\frac{\delta f_{xc}}{\delta \nabla n}\right)\right]_{n(\mathbf{r}),\nabla\mathbf{r}}$$

$$= -\frac{3}{4}\left(\frac{3}{\pi}n\right)^{1/3}\left[\frac{3}{4}F - ts^{-1}\frac{dF}{ds} - \left(u - \frac{4}{3}s^3\right)\frac{d}{ds}\left(s^{-1}\frac{dF}{ds}\right)\right] \quad \text{.....(3.69)}$$

with two dimensionless parameters

$$t = t(\mathbf{r}) = \frac{\nabla^2 n(\mathbf{r})}{4k_f(\mathbf{r})^2 n(\mathbf{r})} \quad \text{..... (3.70)}$$

$$u = u(\mathbf{r}) = \frac{\nabla n(\mathbf{r})\nabla|\nabla n(\mathbf{r})|}{4k_f(\mathbf{r})^3 n(\mathbf{r})^2} \quad \text{..... (3.71)}$$

These expressions clearly show that GGA potentials are having even higher density derivatives than the corresponding energy functionals, and analytically the equations for potentials may turn extremely difficult.

3.3 "Full Potential Linearized Augmented Plane Wave (FP-LAPW)" Procedure

In existing thesis, the reckoning computation, estimations, judgments and predications have been done with use of "Full potential Linearized Augmented Plane Wave (FP-LAPW)" method as executed in the WIEN2K [30]. Primarily this technique is evolved from the augmented-plane-wave (APW) method. In it a special basis set is taken-up for solving the problem. The size of basis set is very large for LAPW as equated to APW (augmented plane wave method), neverthless it fully depends on the approach of "augmented plane wave method". The LAPW technique is highly effective and precise for the calculations of electronic structure [501-503]. APW was introduced by Slater in 1937 [504], based on the existence that the potential & wave functions about the nucleus are matching to those of an atom, generally spherical and strongly varying. While in between, both potential & wavefunction were invariably plane. As a result, the space of the unit cell is cleaved in two zones; one is the non overlapping atomic spheres and other is interstitial region. The solution of Schrödinger's equation for the spherical zone (radial part) and interstitial region (plane-wave) is given by

$$\varphi(\mathbf{r}) = \begin{cases} \sum_{lm} A_{lm}\, u_l(\mathbf{r}) Y_{lm}(\mathbf{r}) & \dots \mathbf{r} \in S_\alpha \ (spherical\ region) \\ \frac{1}{\Omega^{1/2}} \sum_G C_G e^{i(G+k)\mathbf{r}} & \dots \mathbf{r} \in I \ (interstitial\ region) \end{cases} \quad \text{…....(3.72)}$$

where φ represent "wave function of the system", Ω denotes "volume of unit cell" and u_l is "usual solution" of equations (3.72). The A_{lm} & C_G are "expansion coefficients", when E_l is a parameter equal to the band energy and V is a spherical component of the potential inside the sphere:

$$\left[-\frac{d^2}{dr^2} + \frac{l(l+1)}{r^2} + V(\mathbf{r})E_l\right] r u_l = 0 \qquad \text{…….. (3.73)}$$

The meticulously careful choice of the functions persuaded Slater to perceive that plane waves are solutions of the Schrödinger equation for "constant potential", whereas radial functions are solutions for "spherical potential", for E_l equal to eigenvalues. This approximation is notorious as *muffin-tin approximation*, and is highly effective for close-packed materials. The dual illustration in Eq. (3.73) is unsure to be steady on sphere boundaries, whereas is assumed exact for kinetic energy. Hence, a bound on APW method is laid by delineating A_{lm} in shape of C_G by spherical harmonic expansion of

plane waves. While coefficient of every lm component is equated at the sphere boundary;

$$A_{lm} = \frac{4\phi_i^l}{\sqrt{\Omega}u_l(R)} \sum_G C_G(|\mathbf{k}+\mathbf{G}|) R Y_{lm}^*(\mathbf{k}+\mathbf{G}) \qquad \text{…….…..} \quad (3.74)$$

Where R is radius of the sphere, whose origin is chosen at the center. Therefore, A_{lm} are prescribed fully by plane-wave coefficients C_G and energy parameters E_l.

In LAPW method, the "basis functions" are the linear combinations of a "radial function $u_l(\mathbf{r})Y_{lm}(\mathbf{r})$" as well as their "energy derivatives $\dot{u}_l Y_{lm}(\mathbf{r})$" inside the spheres E_l are set for the u_l, which satisfy Eq. (3.75) in non-relativistic predicament.

$$\left[-\frac{d^2}{dr^2} + \frac{l(l+1)}{r^2} + V(\mathbf{r})E_l\right] r\dot{u}_l = ru_l \qquad \text{……..} \quad (3.75)$$

Aforementioned functions are on the sphere boundaries are associated to values and derivatives of plane waves. The "Plane-waves" builtup in such manner are known as the "LAPW basis functions". The wave functions for this basis are given by;

$$\varphi(\mathbf{r}) = \begin{cases} \sum_{lm}[A_{lm}u_l(\mathbf{r}) + B_{lm}\dot{u}_l]Y_{lm}(\mathbf{r}) \ldots\ldots \mathbf{r} \in spherical\ region \\ \frac{1}{\Omega^{1/2}} \sum_G C_G e^{i(G+k)\mathbf{r}} \qquad \ldots\ldots \mathbf{r} \in interstitial\ region \end{cases} \quad \ldots. \quad (3.76)$$

where B_{lm} are the coefficients for energy derivatives like A_{lm}. Shape approximations are not made in this scheme, and consequently such a method is titled "*Full Potential Linearized Augmented Plane Wave* (FP-LAPW)". LAPW being evolved out of APW, is surely better than APW. In APW the diagonalization for each band is needed, whereas in LAPW energy bands are obtained at a given k-point with single diagonalization. Furthermore, LAPW basis contain two radial functions instead one, hence is more manageable inside the spheres. However, hindrance is, that this manageability or flexibility necessitate that the basis functions must have continuous derivatives. For accomplishing given level of convergence, high value of plane-wave cut-off is required. The Weinert scheme is used in the WIEN2K code for total energy calculations [505]. The cutoff parameter $R_{mt}K_{max}$ governs the convergence of the basis set and ordinarily grip value of 6 to 9. The R_{mt} is called the muffin tin radii and is the smallest of all of the atomic sphere radii in the unit cell and K_{max} is magnitude of the largest K vector. Higher angular momenta (mostly $l_{max} \approx 8$ to 12 for precise computation) in the wavefunctions

are demanded to satisfy the continuity conditions meticulously.

3.4 The WIEN2K Software

In our work we have used the WIEN2K software [504]. It was developed initially in 1990 [26]. The WIEN2K software has been written in Fortran 90 and the Linux operating system support this software. Presently many variants i.e. WIEN95, WIEN97 and WIEN2K of this software are reuputably in practically applicaiton. The current version is WIEN-14.2, which is a minor update but offering refinely superior footing for various options in w2web. Hence, the WIEN2K software has proven its trustworthiness and significance in calculating most of the ground state physical properties of many families of compounds. The programme WIEN2K performs electronic structure calculations of solids by application of density functional theory (DFT). It rests on the full-potential (linearized) augmented plane wave. The ***Cubic-elastic*** package provides a set of programs and scripts that allows elastic tensor calculations for cubic phases by using WIEN [506]. *Cubic-elastic* package is used for calculating elastic constants of cubic symmetries with WIEN2K by second-order derivative of Polynomial fit of Energy [531, 532], called as energy approach [533].

3.5 Computational Details

In this study, calculations have been carried out through DFT executed in WIEN2K code [504] and using FP-LAPW method [530, 530A]. To aquire convergence, the basis set expands in term of plane waves up to $R_{MT}K_{max}= 7$, where R_{MT} is the smallest atomic radius (muffin-tin radius) in a unit cell and K_{max} is the magnitude of the maximum amount of k-vector in the plane waves expansion cut-off. For the valence wave function inside muffin-tin spheres, the maximum value of angular momentum taken were $l_{max}= 12$. In the interstitial region, the charge density was Fourier expanded up to $G_{max}=24$. High precision is demanded for calculation of elastic properties, hence a dense k mesh compose of 132 k-points are occupied in the irreducible wedge of the Brillouin zone with griding 12 12 12 applying the Monkhorst and Pack mesh. In this work, we use Cubic-elastic software available at WIEN2k website 29 within GGA [496]

with spin polarization to calculate the elastic properties. The calculations for elastic constants C_{11}, C_{12} and C_{44} are also performed without spin polarization and the results are compared with the spin polarized results. The specification about Cubic-elastic software are accessible in Ref. [531, 532]. We use energy approach [533] implemented in WIEN2K code. Using Voigt notations by replacing and taking into account the additional symmetry imposed by the crystal symmetry, the number of elastic constants reduces. Particlarly for cubic lattice, only three independent elastic constants C_{11}, C_{12} and C_{44} remain.

CHAPTER – 4
RESULTS AND DISCUSSIONS

Various physical properties such as lattice constant, bandgap, density of states, electron density, dielectric function, etc) of solids can be predicted easily by *ab initio (First Principles)* calculation-method. Density functional theory, which requires atomic constant as the input parameter, has made this quest easy to explore ground state physical aspects of material traits (like structural, electronic, elastic, magnetic and optical properties). Full Potential Linearized Augmented Plane Wave method has been implemented in present thesis to reckon the electronic structure, elastic and magnetic attributes of different groups of spinels i.e. Aluminate $\boldsymbol{X}Al_2O_4$ (X = Mg, Mn, Fe, Co, Ni, Cu, Zn), Gallate $\boldsymbol{M}Ga_2O_4$ (M = Mg, Mn, Fe, Co, Ni, Cu, Zn, Cd) and Indate $N In_2O_4$ (N = Mg, Zn, Cd), while the elastic properties of $Zn\boldsymbol{P}_2O_4$ (P=V, Cr, Fe, Rh, Sn) & VZn_2O_4 are also manifested in this work.

4.1 Elastic Constants and elastic properties of Aluminate $\boldsymbol{X}Al_2O_4$ (X = Mg, Mn, Fe, Co, Ni, Cu, Zn), Gallate $\boldsymbol{M}Ga_2O_4$ (M = Mg, Mn, Fe, Co, Ni, Cu, Zn, Cd) and Indate $\boldsymbol{N}In_2O_4$ (N = Mg, Zn, Cd) Spinels

The Spinels constitute expressive blend of ceramic compounds that compose of variety of interesting physical properties. The parent spinel $MgAl_2O_4$ is having unification of several covetable properties such as high melting point, high strength, resistance to chemical changes and less electrical losses [369]. Its thin films demonstrate exciting peculiarity in use of humidity measurement devices [507, 508]. These distinct properties of magnesium spinel realizes its use in many important applications. A number of inorganic compounds [171] having AB_2X_4 as generic representation (with A, B metal cations and X anions) and carry similar crystal structure as that of mineral spinel (magnesium aluminate, $MgAl_2O_4$). Spinels are open substances to multiform experimental and theoretical investigations with special focus on structural [509], electronic [230, 231, 510], mechanical [511-515] and optical properties [235, 516-519].

$X Al_2O_4$ (X = Mg, Mn, Fe, Co, Ni, Cu, Zn), $M Ga_2O_4$ (M = Mg, Mn, Fe, Co, Ni, Cu, Zn, Cd) and $N In_2O_4$ (N = Mg, Zn, Cd) are spinel compounds, having the desirable characteristics as described above i.e. high melting point, high reflectivity, high strength, chemical resistivity at high temperatures and low electrical loss [520, 521] which conceive them as aspirant contenders for diverse applications [508, 522-525].

The cubic spinel posses space group $Fd\bar{3}m$ (#227) [159, 160, 227] while lattice parameter a and the anions' parameter u ordain its crystal structure. "32 Oxygen atoms" settle in a fcc-lattice to arrange a *unit cell* of spinel, furnishing '64 tetrahedral' and '32 octahedral' interstices. The Magnesium cations fill eight *tetrahedral* interstices and Aluminum cations take up 16 *octahedral* interstices. Though, specific outlay of magnesium and aluminum cations swaps interstices, devising an inverse disorder of spinel [227]. Spinel has beneficial properties and applications as an important ceramic material support for catalysts [522], gas-sensory materials [507, 508, 526], ultrafiltration membranes [527], etc. Profound analysis have been carried out by various researchers regarding spinels, related to their crystal structure [165, 166], defects [227, 528, 230], phase relationship [355, 525] and physical properties [171, 230, 529].

With augmentation in the computational speed of computers and improved alogorithms, the Materials modeling/simulations have attracted an unusual focus in the last decade. Predictions based on Density functional theory are widely used in the study of different physical and chemical properties of materials with remarkable precision. The experimental data can be reproduced with the help of Quantum mechanical calculations and the cases of various properties, where experimental predicaments are fully not available, can be calculated satisfactorily. Among these properties, *elastic constants* depict a good inquest for determining the standard of a theoretical approach [19]. According to our information (to the best knowing), experimental or theoretical calculations in relation to elastic constants of XAl_2O_4 (X = Mg, Mn, Fe, Co, Ni, Cu, Zn), MGa_2O_4 (M = Mg, Mn, Fe, Co, Ni, Cu, Zn, Cd) and NIn_2O_4 (N = Mg, Zn, Cd) compounds scarecly exist. Even, it appears to have no former calculations known of the strain effect on elastic properties of XAl_2O_4 (X = Mg, Mn, Fe, Co, Ni, Cu, Zn), MGa_2O_4

(M = Mg, Mn, Fe, Co, Ni, Cu, Zn, Cd) and NIn_2O_4 (N = Mg, Zn, Cd) compounds. Hence reposefully to aid in understanding, the above materials with their properties under stress, in this thesis *ab initio* investigation is presented, based on a theoretical study of the pressure dependence of structural and elastic properties of XAl_2O_4 (X = Mg, Mn, Fe, Co, Ni, Cu, Zn), MGa_2O_4 (M = Mg, Mn, Fe, Co, Ni, Cu, Zn, Cd) and NIn_2O_4 (N = Mg, Zn, Cd) compounds.

For all calculations in this study, FP-LAPWlo method [530] is used within the frame work of DFT accomplished in the WIEN2K code [504].

4.1.1 Description of Various conditions Related to explain the Results

The elastic constants of solids are of consequential interest and have great importance in material properties. They define the response of the material to an applied stress i.e. a retort function to the external forces [242, 534-536] and so relates stress tensor to strain tensor [537, 538]. The elastic constants are being a resourceful means to retrieve properties of materials related to technological and mechanical importance such as "strength, hardness, wear, Voigt's modulus, Reuss's modulus, Hill's modulus, shear modulus, Young's modulus, bulk modulus, elastic stiffness coefficients, Poisson's ratio, and melting temperature" [539]. The "elastic anisotropy ratio" is a meaningful physical measure for the structural phase stability of crystal structure and one can also define it on the basis of estimated elastic constants [540]. Also in materials, the sound velocities can be measured with the help of elastic constants, further leading to obtaining the Debye temperature [541, 542]. Moreover, Phonon density of states, phonon dispersion spectrum, and thereby phonon heat capacity, entropy, thermal expansion coefficient, and other thermodynamic properties are linked to the elastic constants [543-545].

Elastic constants are among the properties that provide a great deal of information regarding stability and are utilized to identify elastic region from plastic region through the elastic stability criteria [546]. The Elastic constants are also associated with the dynamical matrix within the theory of elasticity [538, 547] based on

macroscopic nature of materials. For cubic system, the crystal has only three independent elastic constants C_{11}, C_{12} and C_{44} which are required to describe elastic properties (in particular, for a body or face-centered cubic crystal $C_{11} = C_{22} = C_{33}, C_{12} = C_{23} = C_{31}, C_{44} = C_{55} = C_{66}$). Hence, a set of three equations are sufficient to establish all the constants.

The Born stability criteria describe a state of requirements on the elastic constants (C_{ij}) duly associated to the second-order change in the internal energy of a crystal under deformation criteria [548, 549]. In order to be mechanically stable, the elastic stiffness constants of a crystal should satisfy the generic elastic stability criteria [548, 550] which, at ambient conditions, for a cubic crystal [256, 550, 551] are;

$$(C_{11} + 2C_{12}) > 0, C_{44} > 0, C_{11} - C_{12} > 0, \text{and } C_{11} > 0 \quad \ldots\ldots\ldots\ldots\ldots (4.1)$$

The criteria in Equation (4.1) coincide with the bulk moduli ($B_o = (C_{11} + 2C_{12})/3$), shear ($C_{44}$), and tetragonal strain ($G' = (C_{11} - C_{12})/2$) moduli, which are positive and referred to as *spinodal, shear and Born criteria*, respectively [549].

The first two criterion in equation (4.1) are plainly significant, since presence of bulk modulus B_o and shear $G = C_{44}$ are certainly imperative for stability. The third criterion i.e. presence of the modulus against tetragonal shear $G' = (C_{11} - C_{12})/2$, is anticipated to play a profound act that can be dominated since generally $G' < G < B_o$ [550]. In number of long-standing problems such as melting [552], polymorphism [553], and pressure-induced amorphization [554], the criterion which is violated first is regarded as the mechanism causing the onset of the structural transformation [550]. Further, the first criterion in equation (4.1) involves calculating the bulk modulus (B_o), which is associated to elastic constants [252]. The elastic moduli provide candid information regarding the stiffness of the crystal, and ΔE's departure from quadratic behavior can remit information concerned with ductility [239].

The Bulk Modulus (B_o) is known through a theoretical calculation, and can be obtained from the *relation (2.4) of chapter 2*, as performed in references [555, 556].

Reuss Modulus (G_R), Viogot Modulus (G_V), Fracture Energy (R), Fracture toughness (K) could also be easily calculated using equations *(2.10)*, *(2.11)*, *(4.5)*, *(4.6)*.

These all are important elastic parameters, and are essential to delineate the mechanical response of a material. Derivation of Shear Modulus (G) *(i.e relation (2.12))*, Young's Modulus (Y) *(relation (2.13))*, Poisson's ratio (ν) *(relation (2.14))*, Lamme's coefficients (λ & μ) *(relations (2.15) & (2.16))* can be made from different equations, using the Voigt-Reuss-Hill approximations [259, 557].

The Young's modulus (Y) governs the degree of stiffness and stability of the solids and is measured using relation (*2.13*). It is the firmness of material to the linear strain along edges, defining the ratio between stress and strain. The compound is stiffer for the larger value of Y.

Another interesting elastic property for any application, particularly for the anisotropy, is the Zener factor (anisotropic ratio) A, introduced by C. Zener [558]. Zener factor, determines the elastic properties in different directions and is unity for fully isotropic materials and the shift from unity rates the amount of elastic anisotropy [251]. Value of A less or more than 1 shows the degree of elastic anisotropy (anisotropic $A < 1$ or >1, and isotropic $A = 1$). As A approaches 1, the gap between the bounds vanishes and the crystal becomes isotropic [256]. Anisotropic ratio A is closely related with the possibility of inducing microcracks [557]. The width of the lower and upper bounds upon shear modulus in terms of the calculated C_{ij}, is affiliated to the anisotropy constant [256, 559, 560] using the relation;

$$A = \frac{2C_{44}}{C_{11}-C_{12}} = \frac{C_{44}}{G'} \qquad \text{…….……..……. (4.2)}$$

For a cubic material with its two shear constants, C_{44} and G', the value of G_V should be between these two constants. Therefore, G_V has a unique value if $C_{44} = G'$. This happens only if the material is isotropic (i.e. when A=1). By assuming a homogeneous strain on the compound, Voight [560] established the upper limit of G_V as given by relation (2.11).

On the other hand, assuming a homogeneous stress, as the lower bound Reuss [559] proposed G_R as given by relation (*2.10*). The average shear modulus G is a standard check to plastic deformations upon shear stress [560]. In this work, the

arithmetic average as proposed by Hill [557] vide relation (*2.12*) is used to calculate the values of *G*. The shear modulus, would obey $G^{'} = C_{44} = (C_{11} - C_{12})/2$ [259] in an isotropic material duly bounded by [256];

$$G_R < G^{'} < G_V \qquad \text{……..……..} \quad (4.3)$$

Almost all materials in this study obey relation (4.3).

Commonly hard compounds are related to high bulk modulus and shear modulus values [561]. However, bulk modulus is not the lone mechanical quantity that regulates the ductility of a material for hard coatings. Another important material property to be also considered is toughness, which is dominated by the degree of plastic deformation (ductility) of the material under mechanical load [562]. Cauchy's pressure $G^{"}$ is the difference between two specific elastic constants C_{12} and C_{44}. To analyze the ductility of the compounds, we use the Pettifor's criterion [563, 564], which states that, for metallic non-directional bonding compounds, the value of Cauchy pressure $\left(G^{"} = C_{11} - C_{44}\right)$ is positive. This region corresponds to a ductile behavior of a material. In fact, a widely used empirical gauge for differentiating ductile behaviour of a material from its brittle behaviour is the Pugh's ratio B_o/G [565]. The value of B_o/G could be obtained directly if B_o and *G* are known or could be calculated with the help of Poisson's ratio as the ratio of the shear to the bulk modulus is [566]

$$\frac{G}{B_o} = \frac{3(1-2\nu)}{2(1+\nu)} \qquad \text{…….……..……} \quad (4.4)$$

In conformity to Pugh's empirical criteria, if the value of B_o/G is surpassing 1.75 (i.e, if $G/B_o < 0.57$) the material will anticipate ductile response, otherwise it obeys brittle manner [251, 565]. Pettiffor and Chen *et al*. [563, 567] have demonstrated the brittle versus ductile shift in intermetallic compounds from first principle calculations, that larger the value of B_o/G, the more would be the extent of ductility of the material.

The Poisson's ratio ν scales the compressibility calculated by relation (*2.14*). It is defined as the ratio of the corresponding contraction to the elongation and is of especial interest, since ν may demonstrate a time or frequency relationship. The ν provides more information about the characteristics of the bonding forces. For central forces in solids,

the lower and upper limits of Poisson's ratio ν are given as 0.25 and 0.5, respectively [568]. For ν = 0 stretching a specimen cause no lateral contraction and at ν=0.5 the materials are incompressible. If Poisson's ratio approaches 0.5, then materials have a tendency to be incompressible [569]. Mathematically, when $\nu = 1/2$ the ratio of the bulk to shear modulus B_o/G is infinite and the system is described as incompressible. This deduce the anticipation, that the bulk modulus becomes anomalously large as a material approaches ''incompressibility.'' But, experimentally, all materials are compressible (i.e., B_o is finite), means that the Poisson's ratio can approach $1/2$ but it never actually equals ½ . As ν approaches ½, B_o decreases, and hence mathematically for ν close to $1/2$, changes in the bulk modulus are small [569], duly in agreement with the observations of real materials.

Lamme's Coefficients (λ & μ) are calculated from young modulus and Poisson's ratio by using relations (*2.15*) and (*2.16*), and are acknowledged as Lame's First and second constants respectively. They create a framework of the elastic moduli for homogeneous isotropic media [570]. For isotropic materials, $\lambda = C_{12}$ and $\mu = G^{'}$ (Where $G^{'} = (C_{11} - C_{12})/2$) [251, 532].

Kleinman introduced a parameter ζ called internal strain parameter [571] which depict comparative disposition of bond bending versus the bond stretching. The lower limit (ζ =0) relates to the "minimizing *bond bending* term" and the upper limit (ζ =1) confirms "minimizing *bond stretching* term". Harrison [572] associated the Kleinman parameter in an approximated fashion to the elastic constants by using equation (*2.17*).

The surface energy is a quantity, which cannot be calculated freely, but is proportional to the fracture energy. Stewart and Bradt [573, 574] assessed the fracture energy *R* of spinel from the fracture toughness and elastic constants according to the relation;

$$R = \frac{K^2(1-\nu^2)}{2Y} \qquad \text{..... (4.5)}$$

Where *K* is the fracture toughness, *Y* the Young's modulus and ν the Poisson's ratio. *K* is given by

$K=1/B_o$ ……..……..…… (4.6)

4.1.2 Results and Discussions

As the elastic constants are very closely related to the ground state properties of materials, therefore in order to obtain accurate and reliable results, we first optimized the lattice constants for the chosen transition metal cubic spinel compounds XAl_2O_4 (X = Mg, Mn, Fe, Co, Ni, Cu, Zn), MGa_2O_4 (M = Mg, Mn, Fe, Co, Ni, Cu, Zn, Cd) and NIn_2O_4 (N = Mg, Zn, Cd). The calculated results of lattice constants a_o are presented in Table 4.1 column II. For comparison, experimental and other calculated values of lattice constants for these compounds are also listed in columns IV and VI. It is clear from the table that our calculated values show convenient resemblance with experimental results. These values of the optimized PBE-GGA lattice constants a_o were then used for performing the computation of the Elastic Constants.

The results of the elastic constants C_{11}, C_{12} & C_{44} for eighten compounds under consideration, seven from the Aluminate group XAl_2O_4 (X=Mg, Mn, Fe, Co, Ni, Cu, Zn); eight from Gallate group MGa_2O_4 (M=Mg, Mn, Fe, Co, Ni, Cu, Zn, Cd) and three from Indate group NIn_2O_4 (N=Mg, Zn, Cd) are presented in Table 4.1 column III alongwith the previous experimental & other theoretical data column V and VII . To our utmost knowledge, experimental data are not available for most of the compounds except for $MgAl_2O_4$ and other theoretical values for $ZnAl_2O_4$, $MgGa_2O_4$, $ZnGa_2O_4$, $CdGa_2O_4$, $MgIn_2O_4$, $ZnIn_2O_4$, $CdIn_2O_4$. Our computed elastic constants reveals that they are in sound agreement with experimental and other theoretical data, and for the compounds for which the experimental and theoretical values of lattice constants available, matches our calculated results in close proximity as shown in Table 4.1, which verify the accuracy of the work presented in this thesis. The Table 4.1 also reveals that these compounds fulfill the stability criterion for cubic structures, i.e., equation 4.1 hence we find that all spinel compounds XAl_2O_4 (X=Mg, Mn, Fe, Co, Ni, Cu Zn); MGa_2O_4 (M=Mg, Mn, Fe, Co, Ni, Cu, Zn, Cd) and NIn_2O_4 (N=Mg, Zn, Cd) are stable against elastic deformation. Results in Table 4.1 also show that C_{11} is substantially greater than C_{12}

which is in conformity with the available experimental and other theoretical results, hence, ensuring the reliability of our results.

The computed Bulk moduli B_o for XAl_2O_4 (X=Mg, Mn, Fe, Co, Ni, Cu, Zn); MGa_2O_4 (M=Mg, Mn, Fe, Co, Ni, Cu, Zn, Cd) and NIn_2O_4 (N=Mg, Zn, Cd) are listed in Table 4.2. Our results are in good agreement with the previous experimental & theoretical calculations available for $MgAl_2O_4$, $CoAl_2O_4$, $ZnAl_2O_4$, $MgGa_2O_4$, $ZnGa_2O_4$, $CdGa_2O_4$, $MgIn_2O_4$, $ZnIn_2O_4$ & $CdIn_2O_4$. The bulk moduli B_o for the other compounds under studies are not available and surely have not been calculated. So we use the available experimental & theoretical data on above mentioned compounds (i.e. $MgAl_2O_4$, $ZnAl_2O_4$, $MgGa_2O_4$, $MgIn_2O_4$, $ZnIn_2O_4$ & $CdIn_2O_4$ to believe the authenticity and accuracy of our estimated results for the remaining spinel compounds. The close agreement of the calculated values for $MgAl_2O_4$, $ZnAl_2O_4$, $MgGa_2O_4$, $MgIn_2O_4$, $ZnIn_2O_4$ & $CdIn_2O_4$ compounds confirms that our predicted values of bulk moduli for the remaining compounds will be consistent with the associated experimental results. The higher values of the bulk moduli show the hardness of these compounds. Further, from Table 4.2 one can notice that the calculated values of the bulk moduli B_o decreases from XAl_2O_4 to NIn_2O_4. The MGa_2O_4 avails values in between of the above two mentioned groups of compounds. Hence suggesting that NIn_2O_4 compounds are more compressible than the MGa_2O_4, and the MGa_2O_4 are more compressible than the XAl_2O_4. In our results we also deduce that for all compounds (under studies) the bulk moduli are greater than tetragonal shears i.e. $B_o > G^{'}$.

The other mechanical parameters i.e. Reuss Modulus G_R, Viogot Modulus G_V, shear modulus G, Young's modulus Y, Poisson's ratio ν, Anisotropic parameter A, Lame's coefficients (λ & μ), shear constant G', Pugh's ratio B_o/G, Cauchy's pressure $G^{"}$, compressibility/fracture toughness K and fracture energy R are calculated and for the spinel groups of compounds XAl_2O_4 (X=Mg, Mn, Fe, Co, Ni, Cu, Zn); MGa_2O_4 (M=Mg, Mn, Fe, Co, Ni, Cu, Zn, Cd), and NIn_2O_4 (N=Mg, Zn, Cd) are presented in Table 4.3, 4.4, & 4.5 respectively.

For a cubic material with its two shear constants, C_{44} and G', the value of G_V falls

between them. We observe from Table 4.1, 4.3, 4.4, & 4.5 that our calculated values comply this rule. If the material is isotropic, the Zener anisotropy factor is equal to 1 and $C_{44} = G'$. From Table 4.3 we see that the values of Zener factor A for $CoAl_2O_4$ is 0.947 & the C_{44}=114.321 while G'=120.775, having the most closer values among all the compounds (this study) to the above mentioned conditions, followed by $MnAl_2O_4$ (A=0.919, C_{44}=127.809 & G'=139.0135). Table 4.5 shows that $ZnIn_2O_4$ carries the farthest values off this condition (i.e. A=0.399, C_{44}=38.494 & G'=96.439). For isotropic material Lame's coefficients $\lambda = C_{12}$ & $\mu = G'$. Since these are anisotropic compounds, hence condition for isotropic compounds is not satisfied. From the calculated values in Table 4.1 and Table 4.3, we observe that for $CoAl_2O_4$ (λ=134.020, C_{12}=130.252 & μ=116.871, G'=120.775) and $MnAl_2O_4$ (λ=114.532, C_{12}=110.757 & μ=132.304, G'=139.0135) are nearest to this condition, while Table 4.1 & Table 4.5 together, reveals that the values of $ZnIn_2O_4$ (λ=95.65, C_{12}=72.428 & μ=61.67, G'=96.439) is having the largest difference. Hence, the $CoAl_2O_4$ and $MnAl_2O_4$ are although anisotropic but nearer to isotropic conditions.

The calculated values of shear modulus G, for all the three groups of spinel compounds are given in Table 4.3, 4.4, & 4.5, which indicates that from among Aluminate group XAl_2O_4 (X=Mg, Mn, Fe, Co, Ni, Cu, Zn); the $MgAl_2O_4$ is having the highest value of shear modulus G=150.225 GPa (Table 4.3), while from the Gallate group MGa_2O_4 (M=Mg, Mn, Fe, Cu, Ni, Zn, Cd); $CdGa_2O_4$ is having the lowest value for G=49.275 GPa (Table 4.4). From Indate group NIn_2O_4 (N=Mg, Zn, Cd); $CdIn_2O_4$ the value of G is 58.927 GPa (Table 4.5). For $MgAl_2O_4$, similar is the case for value of Young's Modulus, it carries the largest value of Young's modulus while $CdIn_2O_4$ is having the smallest value of Y. The largest value of Y indicates the stiffness of a material. Hence, we conclude that $MgAl_2O_4$ is the most stiffer of all the compounds while $CdGa_2O_4$ & $CdIn_2O_4$ are the least stiffer. The remaining compounds rest amidst these two values. From Table 4.3 & 4.5, it is evident that values of Young's moduli for all the materials are large than the shear moduli. Further, comparing the values of Young's moduli from these Tables with values of bulk moduli in Table 4.2 we find that

the Young's modulus values are higher than the bulk moduli as well.

The ductile/brittle character of a material can be determined through the ratio of bulk modulus to shear modulus (B_0/G) [565]. We have calculated this value for verifying the ductility and brittleness of the compounds of our studies and the results are presented in Table 4.3, 4.4 & 4.5. The B_0/G ratio's critical value is 1.754 separating ductile and brittleness, the high B_0/G associate to ductile nature and the lowest value indicate the brittleness of a material. It can be concluded from Table 4.3, 4.4 & 4.5, that the $CdGa_2O_4$ is having 3.164 value for B_0/G and $MgAl_2O_4$ carries the lowest value 1.156 for B_o/G. Overall, $CdIn_2O_4$ (3.164), $MnGa_2O_4$ (2.687), $CoGa_2O_4$ (2.591), $ZnIn_2O_4$ (2.413), $MgGa_2O_4$ (2.397), $NiGa_2O_4$ (2.370), $FeGa_2O_4$ (2.014), $CuGa_2O_4$ (2.004), $MnIn_2O_4$ (1.989), $CdIn_2O_4$ (1.960), $CoAl_2O_4$ (1.810), $ZnGa_2O_4$(1.805), $CuAl_2O_4$ (1.789) are having B_0/G ratio larger than the critical value and are ductile in the sequence as noted above, the high ductile first leading in reducing order. While $MgAl_2O_4$ (1.156), $ZnAl_2O_4$ (1.497), $MnAl_2O_4$ (1.534), $FeAl_2O_4$ (1.683), $NiAl_2O_4$ (1.696) are in brittle range. Our studies indicate that all Aluminate spinels have the lesser B_0/G ratio's values as compared to Gallate and Indate spinels. Among the seven studied aluminate compounds five show brittle character while the remaining two i.e $CuAl_2O_4$ & $CoAl_2O_4$ are just ductile.

In order to exemplify the angular characteristic of atomic bonding in a compound, the Cauchy pressure $G^{"}$ is an important elastic parameter [563]. Its positive value relates to "ionic bonding", while negative value of Cauchy pressure is responsible for "angular or directional character in bonding (covalent bonding)". The growth in the negative value of Cauchy pressure influence more directional bonding, i.e. lower mobility characteristic of a material. A compound with more negative Cauchy pressure will possess more brittle nature [570]. The Cauchy pressure calculated with equation $G^{"} = C_{12} - C_{44}$ are given in Tables 4.3, 4.4 & 4.5 for XAl_2O_4 (X=Mg, Mn, Fe, Co, Ni, Cu, Zn); MGa_2O_4 (M=Mg, Mn, Fe, Co, Cu, Ni, Zn, Cd), and NIn_2O_4 (N=Mg, Zn, Cd) respectively, which are all positive showing that the Spinel compounds are having ionic bonding. For $CdIn_2O_4$ a lesser value of $G^{"}$, however as already we have observed from B_0/G analysis it is the most ductile material among the studied compounds.

The Poisson's ratio ν is a measure of compressibility as described above. At ν=0.5, the material is incompressible. Typically Poisson's ratio ranges from 0.2 to 0.49 and is around 0.3 for most of the materials. Interestingly, as $\nu \rightarrow 0.5$, material tends to be incompressible [569] and volume of the material remains constant, no matter how it is deformed. If ν=0, then stretching a specimen causes no lateral contraction. Some extraordinary materials have $\nu < 0$, if you stretch a round bar of such material, the bar increases in diameter [570]. The calculated results of Poisson's ratio can be checked out from Table 4.3, 4.4, & 4.5. It is clear that for our materials under studies, the values lie from 0.155 upto 0.327 indicating that all our materials are less compressible and stable against elastic deformation. $MgAl_2O_4$ carry the lowest value, while $CdGa_2O_4$ & $ZnGa_2O_4$ the highest value. The remaining compounds are having variants in between these two. The Aluminate Spinels on lower side, the Gallate spinels on higher side. The two Indate spinels $CdIn_2O_4$ & $MgIn_2O_4$ are exactly in the middle position, however, the $ZnIn_2O_4$ goes up along with the Gallate spinels. Among the studied materials, $CdGa_2O_4$ is having the highest incompressibility. Furthermore, Poisson's ratio also contributes knowledge regarding the characteristics of the bonding forces. For central forces in solids, the lower limit of Poisson's ratio ν is 0.25 and upper limit of ν is 0.5 [568]. The values of Poisson's ratio for our compounds fall in this limit except for $MgAl_2O_4$, $ZnAl_2O_4$, $MnAl_2O_4$ and $ZnGa_2O_4$ which carries the values for ν as 0.155, 0.226, 0.232 & 0.2342 respectively, which are below the lower limit range but approach the lower limit. Hence our studies demonstrate that for our all materials, the dominant interatomic forces are central forces.

The Ziner factor *A* is a measure of the degree of elastic anisotropy of a material and is unity for ideal isotropic system. Deviation from unity measures the amount of elastic anisotropy. From Table 4.3, 4.4, & 4.5 we can see that the calculated anisotropic ratio for the materials (except $CoAl_2O_4$) under studies degress from 1, which designate these compounds elastically anisotropic and that their properties vary in different directions. However, the anisotropic ratio for $CoAl_2O_4$ slightly deviates from unity, which shows the anisotropic behavior of $CoAl_2O_4$. This result match the earlier

discussed data in Lame's coefficient para, above. Whereby we have derived that $CoAl_2O_4$ and $MnAl_2O_4$ are although anisotropic but nearer to isotropic conditions.

The Kleinman parameter ζ , which quantify the internal strain of a material, is measured using relation (2.17) and for the three groups of our spinel compounds the results are presented in Table 4.3, 4.4, & 4.5. It describes the relative ease of bond bending versus the bond stretching. Minimizing bond bending leads to ζ=0 and minimizing bond stretching leads to ζ=1. Our calculated values of Kleinman parameter ζ forecast that in $CuGa_2O_4$, $ZnIn_2O_4$ & $MnAl_2O_4$ compounds, bond bending is dominated (ζ falls between 0 & 0.5). In $NiAl_2O_4$, $MgAl_2O_4$, $ZnAl_2O_4$, $CoAl_2O_4$ the value of ζ is just above 0.5, that of $ZnGa_2O_4$, $CuAl_2O_4$, $FeAl_2O_4$, $NiGa_2O_4$, $CdIn_2O_4$, $MgIn_2O_4$, $FeGa_2O_4$, $CoGa_2O_4$ sequentially increases from over 0.6212 to 0.842, while in $MgGa_2O_4$ (0.944), $MnGa_2O_4$ (0.959) & $CdGa_2O_4$ (1.164) the value of ζ is close to unity and hence, the bond stretching is dominated.

The important parameter shear constant G' defines the dynamical stability of the compounds. Shear constant show stability to the tetragonal distortion. Their values for XAl_2O_4 (X=Mg, Mn, Fe, Co, Ni, Cu, Zn) compounds are given in the Table 4.3 and for MGa_2O_4 (M = Mg, Mn, Fe, Co, Ni, Cu, Zn, Cd) and NIn_2O_4 (N = Mg, Zn, Cd) are presented in Tables 4.4 and 4.5, respectively. The positive value of shear constant ($G' > 0$) fulfill the desired norm of dynamical stability. From calculated value of G' it is anticipated that these compounds are dynamically stable materials.

All materials (solids, liquids or gases) are more or less compressible i.e. everyone is having a resistance to change in its volume when subjected to applied stress. A measure of the relative volume change of a solid as a response of mean stress or pressure change, is known as compressibility denoted by *K*. It is the capability of a material to reduce in volume with applied pressure only. The inverse of the compressibility gives a substance's bulk modulus (B_o). Hence, the compressibility relates to the compactness of molecules in a material to clarify the density of the material. Generally, an incompressible material is having constant density and cannot be compressed i.e. higher the density, lower is the compressibility. Commonly the

molecules in solids are dense, so most of the solid materials have low compressibility or, are incompressible at all, since the strong forces of attraction exists between the molecules and leaving no space between these molecules. In a completely non-compressible material, upon application of pressure instead compressing, the material gets deformed. The values of *K* for our compounds are presented in Tables 4.3, 4.4 and 4.5.

We have also calculated the fracture energy R_C using the relation (4.5), listed in Table 4.3, 4.4, & 4.5 respectively for each group of spinel compounds. The fracture toughness is also included in the same tables along with it. The study of propagation of cracks in a material is known as *Fracture Mechanics*, which is considered an important tool in material science in order to improve the mechanical performance of mechanical components. It (FM) applies the physics of stress-strain, particularly the elasticity and plasticity theories to microscopic crystallographic defects in materials for predicting the macroscopic mechanical failure. The energy release rate of failure criterion states that a crack grows when the available energy release rate R is greater than or equal to a critical value R_c (i.e. $R \geq R_c$). Where the R_c is called the fracture energy. This quantity is considered the property of a material which is independent of the applied loads and the geometry of the body.

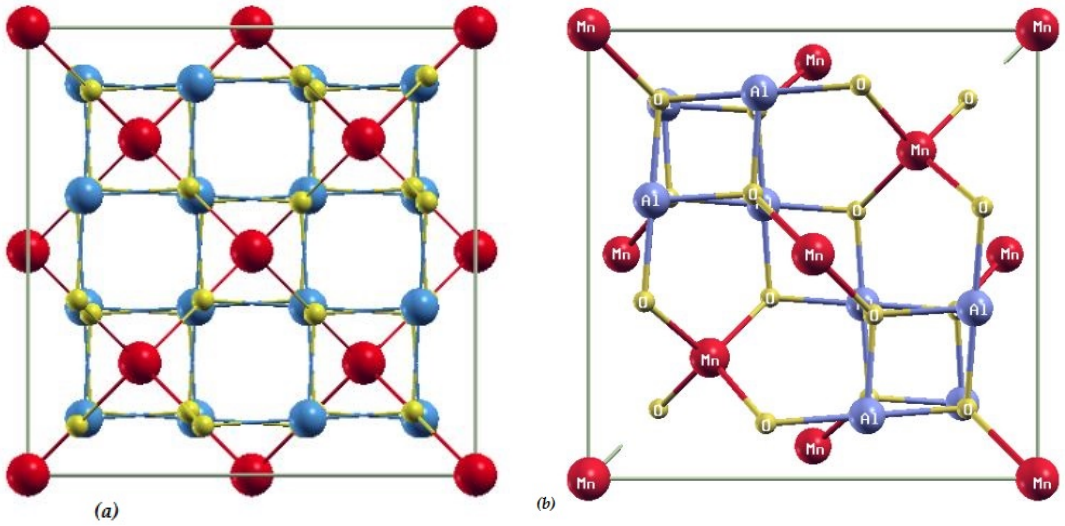

Fig 4.1: *(a) Spinel Structure and (b) showing Octahedral & tetrahedral sites in* $MnAl_2O_4$

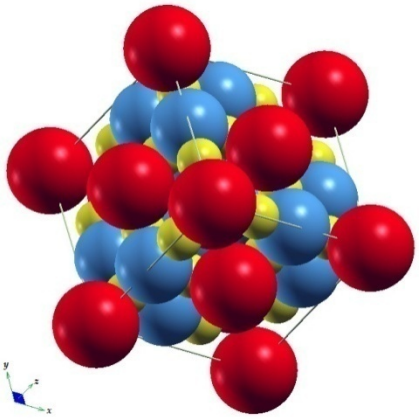

Fig 4.2: *A close packed array of Spinel structure* $MnAl_2O_4$

Table 4.1 : *DFT Optimized lattice constant a_o (in A°), Elastic Constants C_{ij} (in GPa) for Spinel compounds XAl_2O_4 (X = Mg, Mn, Fe, Co, Ni, Cu, Zn), MGa_2O_4 (M = Mg, Mn, Fe, Co, Ni, Cu, Zn, Cd,) and NIn_2O_4 (N=Mg, Cd, Zn) within PBE-GGA in comparison with the experiment (Exp.) and other values.*

	Calculated				Exp.				Others			
I	II	III			IV	V			VI	VII		
Spinel Comp.	a_o	C_{11}	C_{12}	C_{44}	a	C_{11}	C_{12}	C_{44}	a(A°)	C_{11}	C_{12}	C_{44}
$MgAl_2O_4$	**8.160**	**319.996**	**101.399**	**187.970**	8.0832[a] 8.06[c] 8.027[e] 8.086[h]	282[i] 283.6[k] 282.9[l] 286.33[p]	154[i] 156.9[k] 155.4[l] 157.23[p]	154[i] 154.6[k] 154.8[l] 153.45[p]	7.886[b] 8.0747[m] 8.166[h] 8.1074[n]	378[e] 332[j] 262[m] 293.32[o] 279.90[ag] 301[ak]	140[e] 174[j] 140[m] 157.09[o] 153[ag] 162[ak]	124[e] 153[j] 154[m] 150.26[o] - 148[ak]
$MnAl_2O_4$	**8.150**	**388.784**	**110.757**	**127.809**	8.2410[a]	-	-	-	-	-	-	-
$FeAl_2O_4$	**8.150**	**322.757**	**138.077**	**139.764**	8.1490[a]	-	-	-	-	266[ah]	182.5[ah]	133.5[ah]
$CoAl_2O_4$	**8.100**	**371.800**	**130.252**	**114.321**	8.0950[a]	-	-	-	8.098[q]	-	-	-
$NiAl_2O_4$	**8.150**	**347.970**	**120.545**	**131.142**	8.0430[a]	-	-	-	-	-	-	-
$CuAl_2O_4$	**8.150**	**321.385**	**135.038**	**123.790**	8.0860[a]	-	-	-	-	-	-	-
$ZnAl_2O_4$	**8.150**	**363.739**	**123.104**	**148.012**	8.0860[a] 8.0911[r] 8.02[s] 8.00[t]	-	-	-	8.0505[g] 8.073[d] 7.995[e] 8.087[v] 8.174[w] 8.0215[af] 8.020[ai] 8.034[aj]	280[g] 436[e] 316[u] 450.08[v] 341.8[x]	134[g] 171[e] 169[u] 136.83[v] 246.8[x]	152[g] 139[e] 148[u] 158.36[v] 150.4[x]
$MgGa_2O_4$	**8.460**	**222.262**	**139.314**	**98.122**	8.2800[a] 8.602[y]	-	-	-	8.460[m] 8.081[b] 8.341[d] 8.759[z]	233[m]	129[m]	112[m]
$MnGa_2O_4$	**8.450**	**224.130**	**142.867**	**85.019**	8.4350[a]	-	-	-	-	-	-	-
$FeGa_2O_4$	**8.390**	**270.346**	**142.132**	**117.340**	8.3600[a]	-	-	-	-	-	-	-
$CoGa_2O_4$	**8.410**	**253.725**	**140.517**	**78.327**	8.3070[a]	-	-	-	-	-	-	-
$NiGa_2O_4$	**8.510**	**243.271**	**120.859**	**72.051**	8.2580[a]	-	-	-	-	-	-	-
$CuGa_2O_4$	**8.390**	**372.472**	**105.618**	**79.531**	8.3900[a]	-	-	-	-	-	-	-
$Zn\ Ga_2O_4$	**8.500**	**304.187**	**118.069**	**105.167**	8.330[a] 8.41[g] 8.341[r]	-	-	-	8.319[v] 8.311[d] 8.4063[g] 8.4412[ae] 8.0657[af] 8.289[ai]	390.41[v] 228[g] 287.7[x] 249.45a[e]	142.77[v] 120[g] 218.3[g] 121.81[ae]	113.77[v] 107[g] 124.9[g] 115.50[ae]

									8.212j[aj]			
$CdGa_2O_4$	**8.750**	**182.996**	**142.741**	**88.330**	8.5700[a] 8.062[ab, ac]	-	-	-	8.7327[aa]	203[aa]	130[aa]	91[aa]
$MgIn_2O_4$	**9.000**	**223.064**	**112.199**	**92.193**	8.884[d] 8.8100[a]	-	-	-	9.1022[m] 8.884[d]	182[m]	96[m]	68[m]
$ZnIn_2O_4$	**9.250**	**265.306**	**72.428**	**38.494**	-	-	-	-	9.076[g] 8.869[v] 8.868[d] 8.8424[af]	180[g] 331.95[v]	85[g] 107.66[v]	68[g] 112.93[v]
$CdIn_2O_4$	**9.400**	**173.583**	**88.153**	**73.100**	9.1150[a] 9.1651[y,ac] 9.1673[ad]	-	-	-	9.3631[aa] 9.13[d] 9.330[z]	159[aa]	102[aa]	57[aa]

a [159] b [576] c [577] d [509] e [231] f [578] g [4] h [524] i [579]
j [29] k [580] l [581] m [158] n [2] o [582] p [583] q [584] r [585]
s [586] t [587] u [355] v [588] w [589] x [590] y [591] z [361] aa [232]
ab [592] ac [421] ad [593] ae [357] af [358] ag [594] ah [243] *ai* [595] *aj*[596]
ak [236]

Table 4.2: *Calculated values of Bulk Moduli B_o together with experimental and other theoretical values.*

Spinel Comp.	Bulk Modulus B_o		
	This work	**Exp.**	**Other/Theoretical**
$MgAl_2O_4$	**174.862**	196[a,b,c,f] 220[d] 227[e] 198.93[al]	220[d] 226[e] 190[f] 202[g] 180[h] 205.01[i,b] 215.2[j] 213[k] 188.4[l] 208[ak]
$MnAl_2O_4$	**202.828**	-	-
$FeAl_2O_4$	**199.248**	-	-
$CoAl_2O_4$	**211.517**	-	218.8[m]
$NiAl_2O_4$	**196.219**	-	-
$CuAl_2O_4$	**197.367**	-	-
$ZnAl_2O_4$	**204.004**	202[n] 201.7[o] 219.65[p] 218[q]	206.91[i] 183[r] 229.17[s] 219[aa]
$MgGa_2O_4$	**166.527**	-	163[h] 206.91[i]
$MnGa_2O_4$	**169.840**	-	-
$FeGa_2O_4$	**185.391**	-	-
$CoGa_2O_4$	**178.175**	-	-
$NiGa_2O_4$	**160.639**	-	-
$CuGa_2O_4$	**196.371**	-	-
$Zn\ Ga_2O_4$	**180.755**	233[o]	156[r] 164[v] 237[w] 243[y] 192.87[z] 205[aa]
$CdGa_2O_4$	**155.914**	-	166.68[t] 154[u]
$MgIn_2O_4$	**149.505**	-	125[h]
$ZnIn_2O_4$	**136.734**	-	123[r] 182.43[s] 163[aa]
$CdIn_2O_4$	**115.493**	-	135.05[t] 121[u]

a [578] b [514] c [246] d [231] e [29]
f [524] g [582] h [158] i [576] j [512]
k [230] l [2] m [584] n [597] o [585]
p [586] q [587] r [4] s [588] t [361]
u [232)] v [357] w [590] y [389] z [6]
aa [358] *ak* [236] *al* [583]

Table 4.3: *Reuss Modulus G_R (GPa), Viogot Modulus G_V, Shear Modulus G (GPa), Young's Modulus Y (GPa) , Lame's Coefficients λ & μ (GPa), Poisson's ratio ν, Zener Anisotropy parameter A, Kleinman parameter ζ, Tetragonal Shear Moduli G', Cauchy's pressure G'', Compressibility K and Fracture Energy R_C of Spinels XAl_2O_4 (X = Mg, Mn, Fe, Co, Ni, Cu, Zn).*

Comp.	–	G_R	G_V	G	Y	λ	μ	A	ν	G'	G''	ζ	B_o/G	K	R_C
$MgAl_2O_4$	**Present**	**145.949**	**156.501**	**150.225**	**361.621**	**70.528**	**156.501**	**1.720**	**0.155**	**109.299**	**145.134**	**0.529**	**1.156**	**0.00572**	**4.463x10^{-8}**
	Expt.	-	108.1[a]	199.1[a]	274.6[a]	-	-	-	0.270[a]	-	-	-	-	-	-
	theo/others	-	-	109[b] 68.12[c] 79[d]	187[b] 183.74[c] 212[d] 153[e]	-	-	2.13[b] 2.20[c]	0.3499[b] 0.344[c] 0.3439[d] 0.3558[e]	-	-	-	-	0.0048[b] 0.00494[c] 0.00441[d]	-
$MnAl_2O_4$	Present	**132.067**	**132.291**	**132.179**	**325.998**	**114.532**	**132.304**	**0.919**	**0.232**	**139.014**	**260.975**	**0.4883**	**1.534**	**0.00493**	**3.527x10^{-8}**
	Expt.	-	-	-	-	-	-	-	-	-	-	-	-	-	-
	theo/others	-	-	-	-	-	-	-	-	-	-	-	-	-	-
$FeAl_2O_4$	**Present**	**115.945**	**120.794**	**118.370**	**291.326**	**121.663**	**115.974**	**1.514**	**0.256**	**92.340**	**182.993**	**0.673**	**1.683**	**0.005**	**4.025x10^{-8}**
	Expt.	-	-	-	-	-	-	-	-	-	-	-	-	-	-
	theo/others	-	-	-	-	-	-	-	-	-	-	-	-	-	-
$CoAl_2O_4$	**Present**	**116.818**	**116.903**	**116.861**	**296.150**	**134.020**	**116.871**	**0.947**	**0.267**	**120.775**	**257.479**	**0.572**	**1.810**	**0.00473**	**1.085x10^{-8}**
	Expt.	-	-	-	-	-	-	-	-	-	-	-	-	-	-
	theo/others	-	-	-	-	-	-	-	-	-	-	-	-	-	-
$NiAl_2O_4$	**Present**	**115.009**	**115.330**	**115.170**	**289.100**	**118.162**	**115.363**	**0.898**	**0.253**	**122.867**	**249.044**	**0.527**	**1.696**	**0.00512**	**4.241x10^{-8}**
	Expt.	-	-	-	-	-	-	-	-	-	-	-	-	-	-
	theo/others	-	-	-	-	-	-	-	-	-	-	-	-	-	-
$CuAl_2O_4$	**Present**	**109.202**	**111.393**	**110.298**	**281.261**	**122.613**	**111.435**	**1.334**	**0.262**	**92.796**	**197.595**	**0.663**	**1.789**	**0.0051**	**4.30x10^{-8}**
	Expt.	-	-	-	-	-	-	-	-	-	-	-	-	-	-
	theo/others	-	-	-	-	-	-	-	-	-	-	-	-	-	-
$ZnAl_2O_4$	**Present**	**135.632**	**136.934**	**136.283**	**335.693**	**112.897**	**136.906**	**1.230**	**0.226**	**120.318**	**215.727**	**0.557**	**1.497**	**0.0049**	**3.39x10^{-8}**
	Expt.	-	-	-	-	-	-	-	-	-	-	-	-	-	-
	theo/others	-	-	157.66[f]	388.38[f] 193[g]	136.14[f]	157.66[f]	1.01[f]	0.232[f] 0.3241[g]	-	-	-	1.53[f]	-	-

a [580] b [236] c [582] d [29] e [158] f [588] g [4]

Table 4.4: *Reuss Modulus G_R (GPa), Viogot Modulus G_V, Shear Modulus G (GPa), Young's Modulus Y (GPa) , Lame's Coefficients λ & μ (GPa), Poisson's ratio ν, Zener Anisotropy parameter A, Kleinman parameter ζ, Tetragonal Shear Moduli $G^{'}$, Cauchy's pressure $G^{"}$, Compressibility K and Fracture Energy R_C of Spinels MGa_2O_4 (M = Mg, Mn, Fe, Co, Ni, Cu, Zn, Cd) .*

Comp.	–	G_R	G_V	G	Y	λ	μ	A	ν	$G^{'}$	$G^{"}$	ζ	B_o/G	K	R_C
$MgGa_2O_4$	**Present**	**63.454**	**75.463**	**69.459**	**196.680**	**116.158**	**75.472**	**2.366**	**0.303**	**41.474**	**124.140**	**0.944**	**2.397**	**0.006**	**$8.311x10^{-8}$**
	Expt.	-	-	-	-	-	-	-	-	-	-	-	-	-	-
	theo/others	-	-	-	140[a]	-	-	-	0.3566[a]	-	-	-	-	-	-
$MnGa_2O_4$	**Present**	**59.165**	**67.264**	**63.215**	**178.259**	**124.858**	**67.268**	**2.092**	**0.325**	**40.632**	**139.111**	**0.959**	**2.687**	**0.0059**	**$8.696x10^{-8}$**
	Expt.	-	-	-	-	-	-	-	-	-	-	-	-	-	-
	theo/others	-	-	-	-	-	-	-	-	-	-	-	-	-	-
$FeGa_2O_4$	**Present**	**88.117**	**95.973**	**92.045**	**245.087**	**121.847**	**95.737**	**1.830**	**0.280**	**64.108**	**153.006**	**0.804**	**2.014**	**0.0054**	**$5.4x10^{-8}$**
	Expt.	-	-	-	-	-	-	-	-	-	-	-	-	-	-
	theo/others	-	-	-	-	-	-	-	-	-	-	-	-	-	-
$CoGa_2O_4$	**Present**	**67.903**	**69.638**	**68.770**	**184.834**	**131.692**	**69.644**	**1.383**	**0.327**	**56.604**	**175.398**	**0.842**	**2.591**	**0.00561**	**$7.6x10^{-8}$**
	Expt.	-	-	-	-	-	-	-	-	-	-	-	-	-	-
	theo/others	-	-	-	-	-	-	-	-	-	-	-	-	-	-
$NiGa_2O_4$	**Present**	**67.823**	**67.713**	**67.868**	**178.113**	**115.207**	**67.722**	**1.177**	**0.315**	**61.206**	**171.220**	**0.765**	**2.370**	**0.00623**	**$9.799x10^{-8}$**
	Expt.	-	-	-	-	-	-	-	-	-	-	-	-	-	-
	theo/others	-	-	-	-	-	-	-	-	-	-	-	-	-	-
$CuGa_2O_4$	**Present**	**94.858**	**101.089**	**97.974**	**258.850**	**129.004**	**101.113**	**0.5961**	**0.2803**	**133.43**	**292.941**	**0.468**	**2.004**	**0.0051**	**$9.261x10^{-6}$**
	Expt.	-	-	-	-	-	-	-	-	-	-	-	-	-	-
	theo/others	-	-	-	-	-	-	-	-	-	-	-	-	-	-
$Zn\ Ga_2O_4$	**Present**	**99.964**	**100.324**	**100.144**	**253.983**	**90.661**	**102.894**	**1.130**	**0.2342**	**93.059**	**193.02**	**0.6212**	**1.805**	**0.0055**	**$5.695x10^{-8}$**
	Expt.	-	-	-	-	-	-	-	-	-	-	-	-	-	-
	theo/others	87.24[b]	94.83[b]	91.04[b] 117.71[c]	169.52[b] 300.73[c] 145[d]	146.78[c]	117.71[c]	0.92[c]	0.328[b] 0.277[c] 0.345[d]	-	-	-	1.91[c]	-	-
$CdGa_2O_4$	**Present**	**37.501**	**61.049**	**49.275**	**162.003**	**115.378**	**61.041**	**4.389**	**0.327**	**20.128**	**94.666**	**1.164**	**3.164**	**0.00641**	**$1.134x10^{-7}$**
	Expt.	-	-	-	-	-	-	-	-	-	-	-	-	-	-
	theo/others	-	-	-	102[e]	20.22[e]	91.64[e]	-	0.3898[e]	-	-	-	-	-	-

a [158] b [357] c [588] d [4] e [232]

Table 4.5: *Reuss Modulus G_R (GPa), Viogot Modulus G_V, Shear Modulus G (GPa), Young's Modulus Y (GPa) , Lame's Coefficients λ & μ (GPa), Poisson's ratio ν, Zener Anisotropy parameter A, Kleinman parameter ζ, Tetragonal Shear Moduli G', Cauchy's pressure G'', Compressibility K and Fracture Energy R_C of Spinels NIn_2O_4 (N=Mg, Zn, Cd).*

Comp.	–	G_R	G_V	G	Y	λ	μ	A	ν	G'	G''	ζ	B_o/G	K	R_C
$MgIn_2O_4$	**Present**	**72.865**	**77.489**	**75.177**	**198.221**	**97.851**	**77.491**	**1.663**	**0.279**	**55.433**	**130.199**	**0.773**	**1.989**	**0.0067**	**$1.04x10^{-8}$**
	Expt.	-	-	-	-	-	-	-	-	-	-	-	-	-	-
	theo/others	-	-	-	115[a]	-	-	-	0.3471[a]	-	-	-	-	-	-
$ZnIn_2O_4$	**Present**	**51.260**	**61.672**	**56.66**	**160.835**	**95.65**	**61.67**	**0.399**	**0.304**	**96.439**	**226.812**	**0.473**	**2.413**	**0.0073**	**$1.509x10^{-7}$**
	Expt.	-	-	-	-	-	-	-	-	-	-	-	-	-	-
	theo/others	-	-	112.61[a]	280.18[b] 146[c]	107.35[b]	112.61[b]	1.01[b]	0.244[b] 0.3019[c]	-	-	-	1.62[b]	-	-
$CdIn_2O_4$	**Present**	**56.908**	**60.946**	**58.927**	**155.488**	**75.072**	**60.928**	**1.711**	**0.276**	**42.715**	**100.483**	**0.770**	**1.960**	**0.0087**	**$2.238x10^{-7}$**
	Expt.	-	-	-	-	-	-	-	-	-	-	-	-	-	-
	theo/others	-	-	-	79[d]	43.55[d]	57.96[d]	-	0.391[d]	-	-	-	-	-	-

a [158] b [588] c [4] d [232]

4.2 Electronic and Magnetic Properties of XAl_2O_4 (X=Mg, Mn, Fe, Co, Ni, Cu, Zn) and MGa_2O_4 (M=Mg, Mn, Fe, Co, Ni, Cu, Zn, Cd)

In 2007, Bouhemadou *et al* [158)] analyzed the structural and elastic specifications of MgX_2O_4 (X= Al, Ga, In) by "pseudo potential plane wave (PP-PW) method" using GGA and LDA within framework of DFT. Further, different reporters [361, 410, 598] carried out research on $CdIn_2O_4$, $CdGa_2O_4$ and $CdAl_2O_4$ regarding its structural, electronic, optical and elastic formats while exercising "full potential augmented plane-wave plus local orbital method" and application of generalized gradient approximation (GGA), as well employing Eugel-vassko GGA (EV-GGA). Hosseini [2] determined the electronic properties of $MgAl_2O_4$ alongwith structural & optical properties, and anticipated the underestimation by 20% in the band gap in comparison to the experimental value. Mo & Ching [230] investigated the electronic structure of normal, inverse and intermediate Spinel in the $MgAl_2O_4$ by implementing *ab initio* calculation. Sawada [170] reported the electron density residual study of magnesium aluminium oxide spinel.

Amin *et al*. [1] adopting "the modified Becke-Johnson exchange potential approximation (mBJ)", while investigating the optoelectronic response of $MgAl_2O_4$ and $MgGa_2O_4$, has described in parallel its electronic and optical properties. Employing the "full potential linearized augmented plane wave (FP-LAPW) method" within the LDA, the structural, electronic & elastic properties of $MgAl_2O_4$ and $ZnAl_2O_4$ have been investigated separately by Khenata *et al* [231] and M. Hachemaoui *et al* [599]. Zerarga *et al* [600] investigated the Structural, electronic and optical properties of $ZnAl_2O_4$, $ZnGa_2O_4$ and $ZnIn_2O_4$ spinel oxides. By first principle method Liang *et al* [6] studied the structural, mechanical and electronic properties of ZnX_2O_4 (X=Al, Cr and Ga). Brik [357] reported first principle calculations of electronic, optical and elastic properties of $ZnAl_2O_4$ and $ZnGa_2O_4$ while Arbi *et al* [354] carried out First principles studies of structural, electronic and optical properties of $ZnAl_2O_4$.

Tielens *et al* [584] carried periodic DFT study of the structural and electronic properties of bulk $CoAl_2O_4$ Spinel. It has been reported by Ueda *et* al [601] that spinel

oxide $MgIn_2O_4$ is having high electrical conductivity and is capable of transmitting ultraviolet radiation. Li *et al*. [142] experimentally found the structural and electrical properties of $CdIn_2O_4$. Utilizing mBJ potential, Manzar *et al* [602, 603], investigated Electronic band profile and optical properties of spinel $MgIn_2O_4$, and of CdX_2O_4 (X=In, Ga, Al).

The cadmium gallate ($CdGa_2O_4$) and cadmium indate ($CdIn_2O_4$) oxides are wide band gap semiconductors [159] and have vast utilization in electronic devices [604-606]. Due to vast energy separation between first & second conduction bands, they have meaningful transmissibility and ameliorated electrical properties [361, 598, 602, 607, 608].

For adjustment of band gap materials, several theoretical methods are being in use with comparison to the experimental testimony. Among them, the "Optimized Effective Potential (OEP)" [609, 610] and "Many Body Perturbation (MBPT)" produce admiring results as compared to the experimental data [598, 611, 612] but these techniques are computational exorbitant. A finest superlative preference for the band gap refitting is the LDA+U method [611, 613], which is economical [612] and also computationally reasonable. The limitation is that it could be merely applied to correlated and localized 3d or 4f electrons, i.e., in the case of transition and rare-earth oxides. The modified Becke–Johnson (mBJ) approximation [614] is another fresh technique, more reliable and has turned to be the dominant mechanism to apprehend the underestimation of band gap in materials. With mBJ the calculated band gap values are significantly rectified becoming closer to the experimental findings [360, 612, 615-619] as compared to LDA, GGA and EV-GGA.

With *ab intio* investigation Wei *et al.,* [509] explored the total energies, structural properties and band gap of normal & inverse spinels. Koller [612] revealed that a great anomaly between experimental and theoretical calculations of the mentioned spinel compounds exist, associated with electronic band structure and its ancillary optical properties. Arguing that common LDA and GGA underestimates the energy band gap and optical properties, creating this anomaly. Hence, it is confirmed that common LDA,

GGA and EV-GGA strikingly depreciate the energy band gap of materials and resultantly their optical parameters [361, 608, 620].

In this study, we report the electronic and magnetic behaviors in XAl_2O_4 (X=Mg, Mn, Fe, Co, Ni, Cu, Zn) and MGa_2O_4 (M=Mg, Mn, Fe, Co, Ni, Cu, Zn, Cd) which are determined by employing LAPW code.

4.2.1 Results and Discussion: Electronic & Magnetic Properties of XAl_2O_4 (*X* = Mg, Mn, Fe, Co, Ni, Cu, Zn)

To investigate electronic structure & magnetic behaviour, we estimated the ground state energy, total and partial density of states of transition metal cubic spinel compounds XAl_2O_4 (X= Mg, Mn, Fe, Co, Ni, Cu, Zn). As a means to calculate the ground state energy we relaxed the non-magnetic, ferromagnetic and anti-ferromagnetic ground states of these materials. The relax ground state energy of these materials show that the anti-ferromagnetic state of these materials are stable, presented in table 4.6. Total density of states (TDOS) presented in Fig. 4.3 show anti-ferromagnetic states of these materials. Partial density of states (PDOS) clearly reveals that valence band near the fermi level is due to the transition metal 3d-state with small contribution of the O p-state. These states are pinned at the Fermi level for all compounds Fig. 4.5.

The considered compounds XAl_2O_4 (X=Mn, Fe, Co, Ni, Cu) have sturdy pd exchange interaction that can be revealed by computed total and partial density of states. The increase in the number of d-electrons (Mn-$3d^5$, Fe-$3d^6$, Co-$3d^7$, Ni-$3d^8$, Cu-$3d^{10}$) produce an enormous exchange splitting arising from Mn to Cu. Also, the tetrahedral environs designed by the O anions generate a crystal field that is liable for splitting 3d-states of the X ions (X=Mn, Fe, Co, Ni, Cu, Zn) into two and three states of $e_g(d_{z2}; d_{x2y2})$ and $t_{2g}(d_{xy}; d_{yz}; d_{zx})$ respectively as displayed in Fig. 4.4. Only dt_{2g} states contribute in hybridization, while e_g states do not participate. Further, Jahn-Teller distortion breaks the degeneracy of doublet and triplet states by raising the state dxy at high energy relative to d_{yz}, d_{zx} and at high energy relative to d_{x2-y2}. The John Teller distortion energy is calculated by taking into account the crystal field effect in both up

spin channel and down spin channel as shown in Table 4.8. The direct exchange energies $\Delta_x(d)$ involved in the structures (see Table 4.8) have greater values than the John Teller distortion ($\Delta_x(d) > \Delta_{JT}$). Therefore, the exchange mechanism of electrons is dominant to introduce magnetism than any other effect. It is also noted from Table 4.8, that values of both John Teller energy and direct exchange energy decreases from Mn to Cu because of unavailability of free electrons increase. For $ZnAl_2O_4$ the exchange splitting is zero because of filled 3d-states.

The indirect exchange energy $\Delta_x(pd)$ shows the splitting of states at valence band edge is calculated from the maximum position of anion (oxygen) in the down spin channel. Its negative value ensures the hybridization exchange of the electrons between 2p-states of oxygen and 3d-states of X ions (X=Mn, Fe, Co, Ni and Cu). Therefore, the energy $\Delta_x(pd)$ confirms the magnetism by spin of electrons. The X impurity atom of total number of unpaired electrons in the 3d-states prescribe the magnitude of the magnetic moment revealed per atom. Hence, Mn, Fe, Co, Ni and Cu have five, four, three, two and one unpaired electrons, correspondingly, in their particular 3d-states, which signs to their free magnetic moment, as conferred in Table 4.7. Therefore, the highest value of magnetic moment is five for Mn and the lowest value is one for Cu in XAl_2O_4 (X=Mn, Fe, Co, Ni, Cu). As the strong interaction between the d-state of X impurities and s, p states of host semiconductors, touches of magnetic moments are convinced at Al and O sites. The free-space values of the magnetic moments of X atoms are approximately alike to the total magnetic moments that are calculated.

Table 4.6: *Ground State Energies of XAl_2O_4 (X=Mg, Mn, Fe, Co, Ni, Cu, Zn).*

Material	**FM**	**AFM**	**NM**
$MgAl_2O_4$	-3949.86868321	-3949.88953260	**-3949.88953303**
$MnAl_2O_4$	-7782.74533530	**-7782.75029655**	-7782.31040401
$FeAl_2O_4$	-8239.16336473	**-8239.17803843**	-8238.87639952
$CoAl_2O_4$	-8721.82864401	**-8721.83360088**	-8721.58747477
$NiAl_2O_4$	-9231.16315865	**-9231.16585188**	-9231.8211901
$CuAl_2O_4$	-9767.93852399	**-9767.93399591**	-9767.92677468
$ZnAl_2O_4$	-10332.68447142	**-10332.68447238**	-10332.68447186

Table 4.7: *Magnetic Moments of Aluminate group of spinels.*

Material	**Interstitial**	**Atoms**			**Spin of the Cell**
	$\boldsymbol{m^{int}}$	$\boldsymbol{m^{TM}}$	$\boldsymbol{m^{Al}}$	$\boldsymbol{m^{O}}$	$\boldsymbol{m^{total}}$
$MgAl_2O_4$	0.00000	0.00000	0.00000	0.00000	0.00000
$MnAl_2O_4$	0.00000	4.128844	0.00000	0.05552	0.00000
$FeAl_2O_4$	-0.00047	3.33982	-0.00004	0.06590	-0.01130
$CoAl_2O_4$	0.00000	2.46281	0.00000	0.06839	0.00000
$NiAl_2O_4$	0.00034	1.52415	0.00002	0.08490	0.00361
$CuAl_2O_4$	0.00000	0.57429	0.00000	0.07541	0.00000
$ZnAl_2O_4$	0.00000	-0.00000	0.00000	-0.00000	0.00000

Table 4.8: *Calculated values of John Teller energy (Δ_{JT}), direct exchange energy $(\Delta_x(d))$, and indirect exchange energy $(\Delta_x(pd))$ of cubic spinels XAl_2O_4 (X=Mg, Mn, Fe, Co, Ni, Cu, Zn).*

Monolayer	$\boldsymbol{\Delta_{JT}}$	$\boldsymbol{\Delta_x(d)}$	$\boldsymbol{\Delta_x(pd)}$
$MnAl_2O_4$	0.348	3.04	-2.95
$FeAl_2O_4$	0.381	1.61	-1.76
$CoAl_2O_4$	0.310	1.93	-1.28
$NiAl_2O_4$	0.227	1. 47	-1.02
$CuAl_2O_4$	0.210	0.83	-0.45
$ZnAl_2O_4$	0.00	0.00	0.00

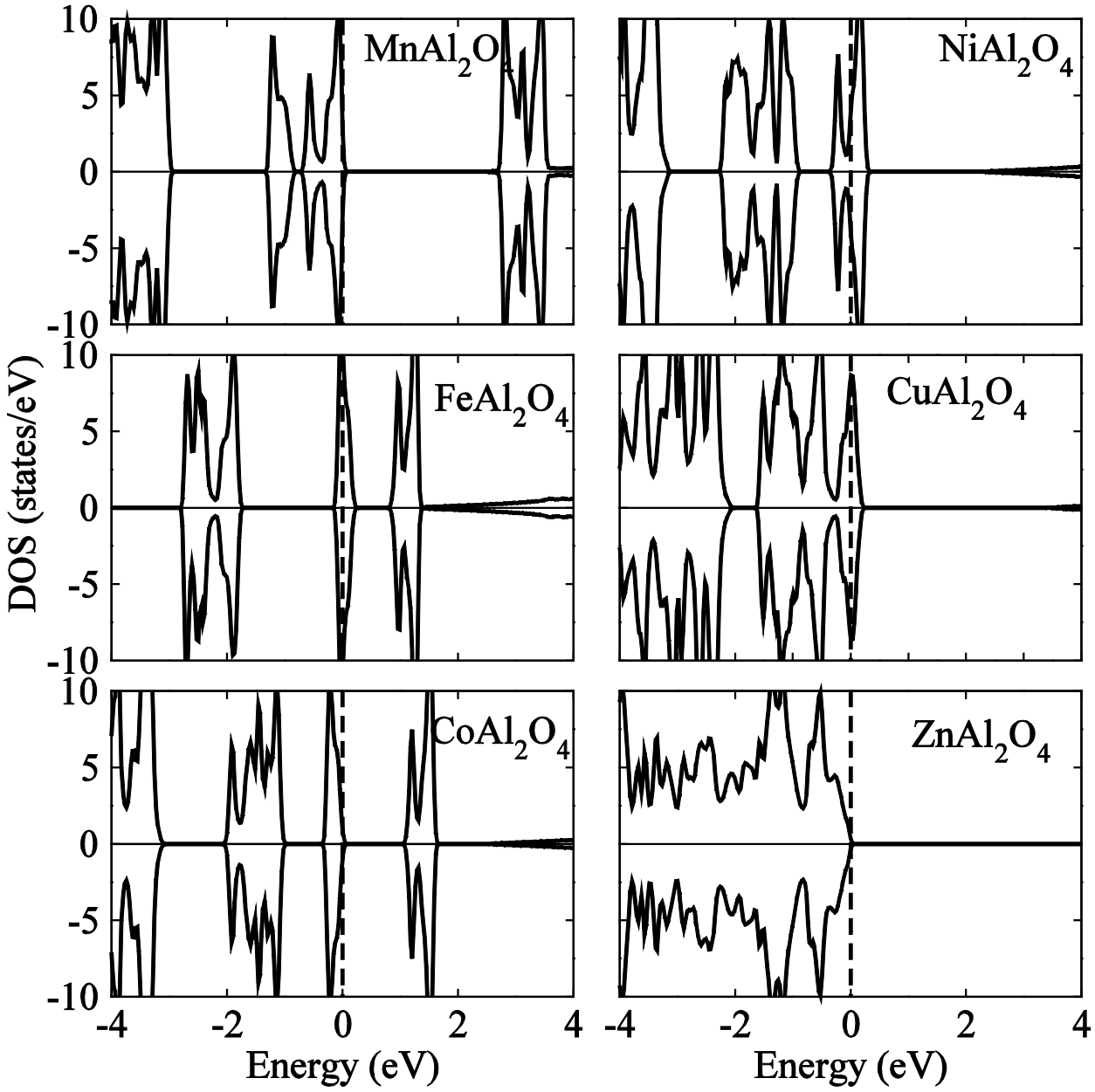

Fig. 4.3: *Total density of states XAl_2O_4*

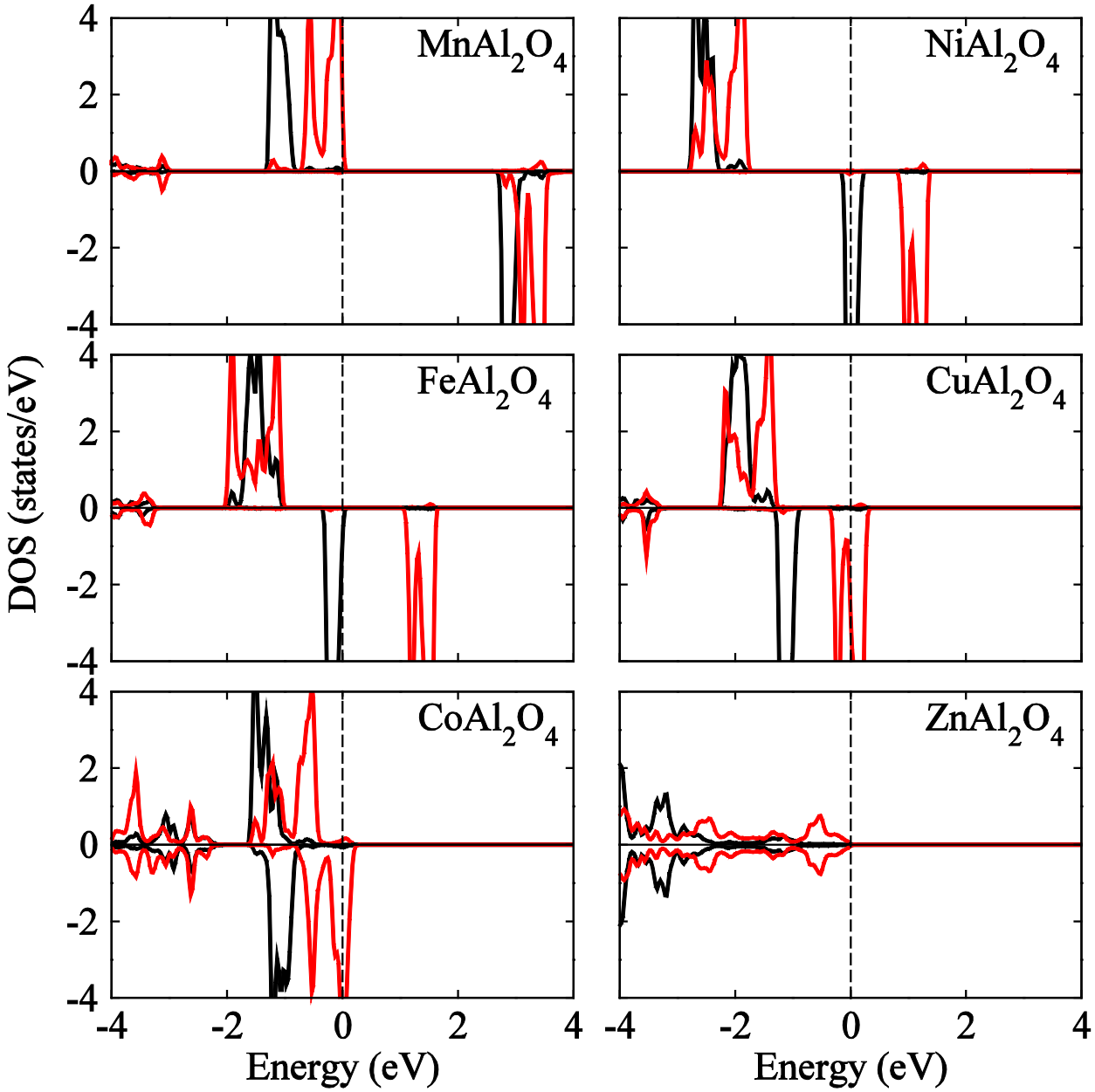

Fig 4.4: *Partial density of states e_g (black), t_{2g} (red) XAl_2O_4*

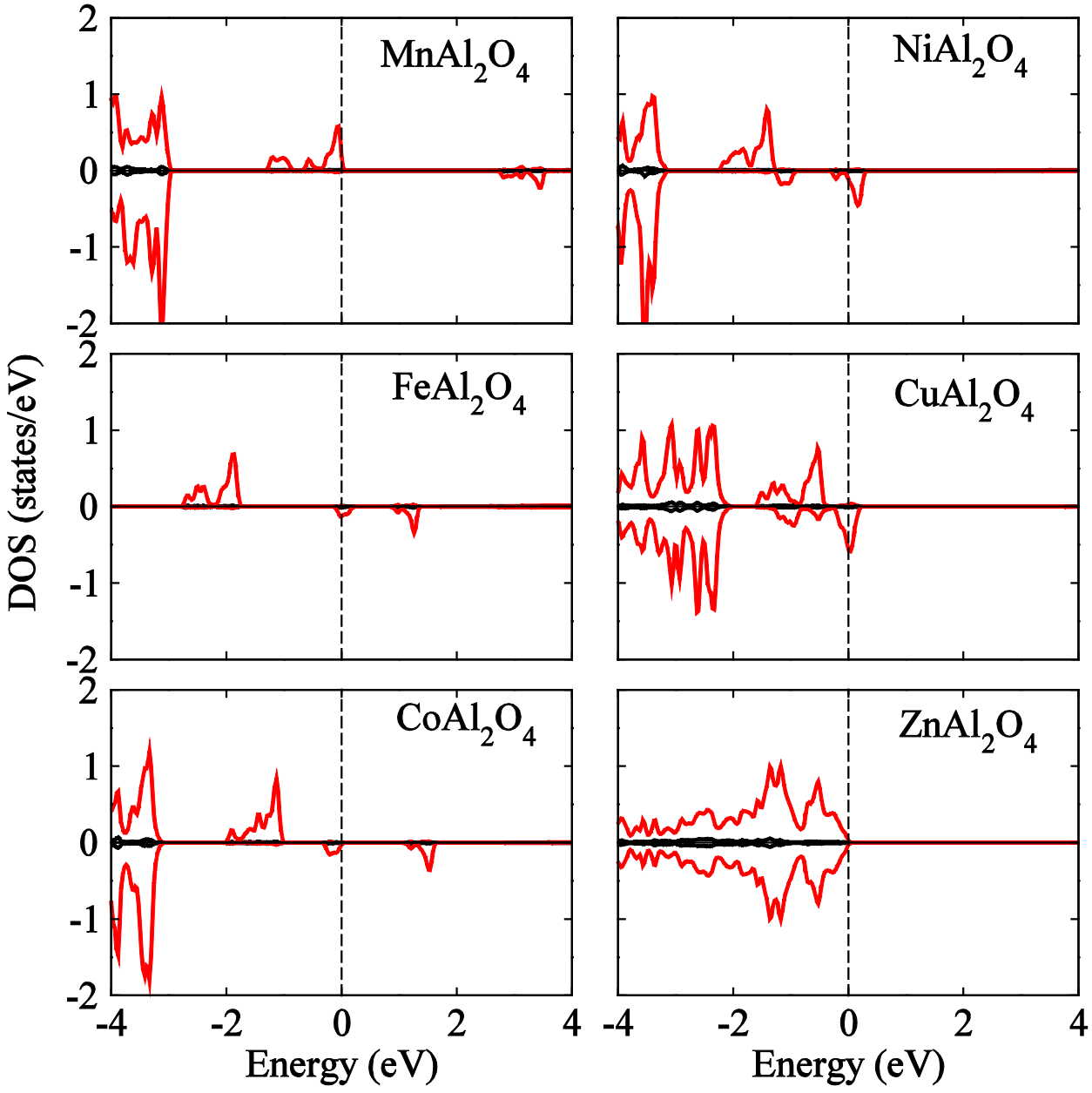

Fig 4.5: *Partial density of states Al-p (black), O-p (red) XAl_2O_4*

4.2.2 Results and Discussion: Electronic and Magnetic Properties of MGa_2O_4 (M = Mg, Mn, Fe, Co, Ni, Cu, Zn, Cd)

To explain the nature of magnetism, the Total Density of States (TDOS) and Partial Density of States (PDOS) of MGa_2O_4 (M= Mg, Mn, Fe, Co, Ni, Cu, Zn and Cd) are shown in Figure 4.6 and 4.7 respectively and calculated values of John Teller, crystal field and exchange energies are explained in Table 4.11. The ferromagnetism in the spinel oxides arise as a result of hybridization between the electrons in the 3d-states of a cation and 2p-states of anions. Among MGa_2O_4 (M= Mg, Mn, Fe, Co, Ni, Cu, Zn and Cd) oxides, MGa_2O_4 (M= Fe, Co, Ni and Cu) oxides having +2 valency are trapped in the tetrahedral environment of oxygen and Ga with +3 valency trapped in the octahedral environment of oxygen. Therefore, the octahedral and tetrahedral states electrons are exchanged to induce strong magnetic effect. The electrons in 3d-states of M present at the edges of tetrahedron bears unfavorable coulomb repulsion that has strong influence near the tetrahedron and becomes weaker for those electrons which are at larger distance from the oxygen atoms. This electrostatic environment provided by the tetrahedron and octahedron of oxygen electrons in both spin up and spin down channels induced crystal field energy calculated through the relations for up spin $\Delta_{CF}^{\uparrow} = t_{2g}^{\uparrow} - e_g^{\uparrow}$ and $\Delta_{CF}^{\downarrow} = t_{2g}^{\downarrow} - e_g^{\downarrow}$ in the crystal lattice [621, 622]. This crystal strain shifts the $d_{x^2-y^2}$ and d_{z^2} at high energy than d_{xy}, d_{yz} and d_{zx} by removing the degeneracy as shown in Figure. This shifting of states induce crystal field energy in both up spin and down spin channels that is calculated in terms of John-Teller energy $\Delta_{JT} = \Delta_{CF}^{\uparrow} - \Delta_{CF}^{\downarrow}$ try to reduce the exchange energy $\Delta_x(d) = \Delta_d^{\uparrow} - \Delta_d^{\downarrow}$ as presented in Table 4.11. This type distortion elongates the tetrahedron by lowering the overall energy of the system. As a whole, the comparison of exchange energy $\Delta_x(d)$ and John-Teller energy shows the MGa_2O_4 (M= Fe, Co, Ni and Cu) oxides have dominant exchange energy as compared to Jahn-Teller energies $\left(\Delta_x(d) > \Delta_{JT}\right)$. This shows the ferromagnetism is dominated by the spin of electrons. On the other hand, MGa_2O_4 (M= Mg, Mn, Zn and Cd) have all the 3d-states filled and do not contribute to the hybridization process and having zero exchange energy that leads its diamagnetic behavior.

For magnetic MGa_2O_4 (M= Fe, Co, Ni and Cu) oxides, the total and local magnetic moments (μ_B) are calculated (see Table 4.10) in terms of atoms inside the muffin-tin spheres and interstitial sites. The data represents that magnetic moments appear, due to total number of unpaired electrons in the 3d states (M= Fe, Co, Ni and Cu). The M atoms have four, three, two and one unpaired electrons, respectively, which show major contributions of magnetic moments in these oxides with small contributions from non-magnetic (Ga, O) atoms. Hence, Fe atoms have highest value of magnetic moment is 3.36 and the lowest value is 0.62 for Cu in MGa_2O_4 (M= Fe, Co, Ni and Cu) *refer Table 4.10*. From TDOS plot in Fig 4.7, we found that net magnetic moments are reduced due to strong interaction between unpaired electrons in the 3d states and p states of anions and induced small magnetic moments at nonmagnetic sites (Ga, O). Therefore, our calculated values of M atoms magnetic moments represent the total magnetic moments (see Table 4.11).

Table 4.9: *Ground State Energies of MGa_2O_4 (M=Mg, Mn, Fe, Co, Ni, Cu, Zn, Cd).*

Material	**FM**	**AFM**	**NM**
$MgGa_2O_4$	-17559.40673086	-17559.40673014	**-17559.40673092**
$MnGa_2O_4$	-21392.31212489	-21392.32005385	**-21392.87648646**
$FeGa_2O_4$	-21848.72294020	**-21848.72619325**	-21848.42369481
$CoGa_2O_4$	-22331.37337488	**-22331.37631694**	-22331.13587326
$NiGa_2O_4$	**-22840.68460315**	-22840.67636835	-22840.05243579
$CuGa_2O_4$	**-23377.45939879**	-23377.45343284	-23377.44555831
$ZnGa_2O_4$	-23942.19866445	**-23942.21341427**	-23942.19866554
$CdGa_2O_4$	-39141.65301983	**-39141.65302108**	-39141.65302035

Table 4.10: *Magnetic Moments of Gallate group of spinels.*

Material	Interstitial	Atoms			Spin of the Cell
	m^{int}	m^{TM}	m^{Ga}	m^{O}	m^{total}
$MgGa_2O_4$	-0.00000	0.00000	-0.00000	0.00000	-0.00000
$MnGa_2O_4$	-0.00000	0.00000	-0.00000	0.00000	-0.00000
$FeGa_2O_4$	0.000002	**3.35827**	-0.0002	0.06871	0.00147
$CoGa_2O_4$	0.00000	2.48419	0.00000	0.06832	0.00000
$NiGa_2O_4$	0.15110	1.56339	0.09036	0.00000	4.00037
$CuGa_2O_4$	0.07411	**0.62195**	0.08523	0.00000	2.00000
$ZnGa_2O_4$	-0.00000	-0.00000	0.00000	0.00000	-0.00000
$CdGa_2O_4$	-0.00001	-0.00000	0.00000	0.00000	0.00000

Table 4.11: *Exchange splitting energy $\Delta_x(d)$, Crystal Field energy for up spin$\uparrow\Delta_{CF}$, Crystal Field energy for down spin $\downarrow\Delta_{CF}$ and John-Teller energy $\Delta_x(JT)$ calculated for MGa_2O_4 (M = Fe, Co, Ni, Cu, Zn, Cd).*

Composition	$\Delta_x(\boldsymbol{d})$	$\uparrow \Delta_{\boldsymbol{CF}}$	$\downarrow \Delta_{\boldsymbol{CF}}$	$\Delta_x(\boldsymbol{JT})$
$Mg\ Ga_2O_4$	0.00	0.00	0.00	0.00
$Mn\ Ga_2O_4$	0.00	0.00	0.00	0.00
$Fe\ Ga_2O_4$	1.90	0.60	1.88	0.588
$Co\ Ga_2O_4$	1.55	0.29	1.59	1.301
$Ni\ Ga_2O_4$	1.40	0.30	1.07	0.774
$Cu\ Ga_2O_4$	1.38	0.55	0.66	0.116
$Zn\ Ga_2O_4$	0.00	0.00	0.00	0.00
$CdGa_2\ O_4$	0.00	0.00	0.00	0.00

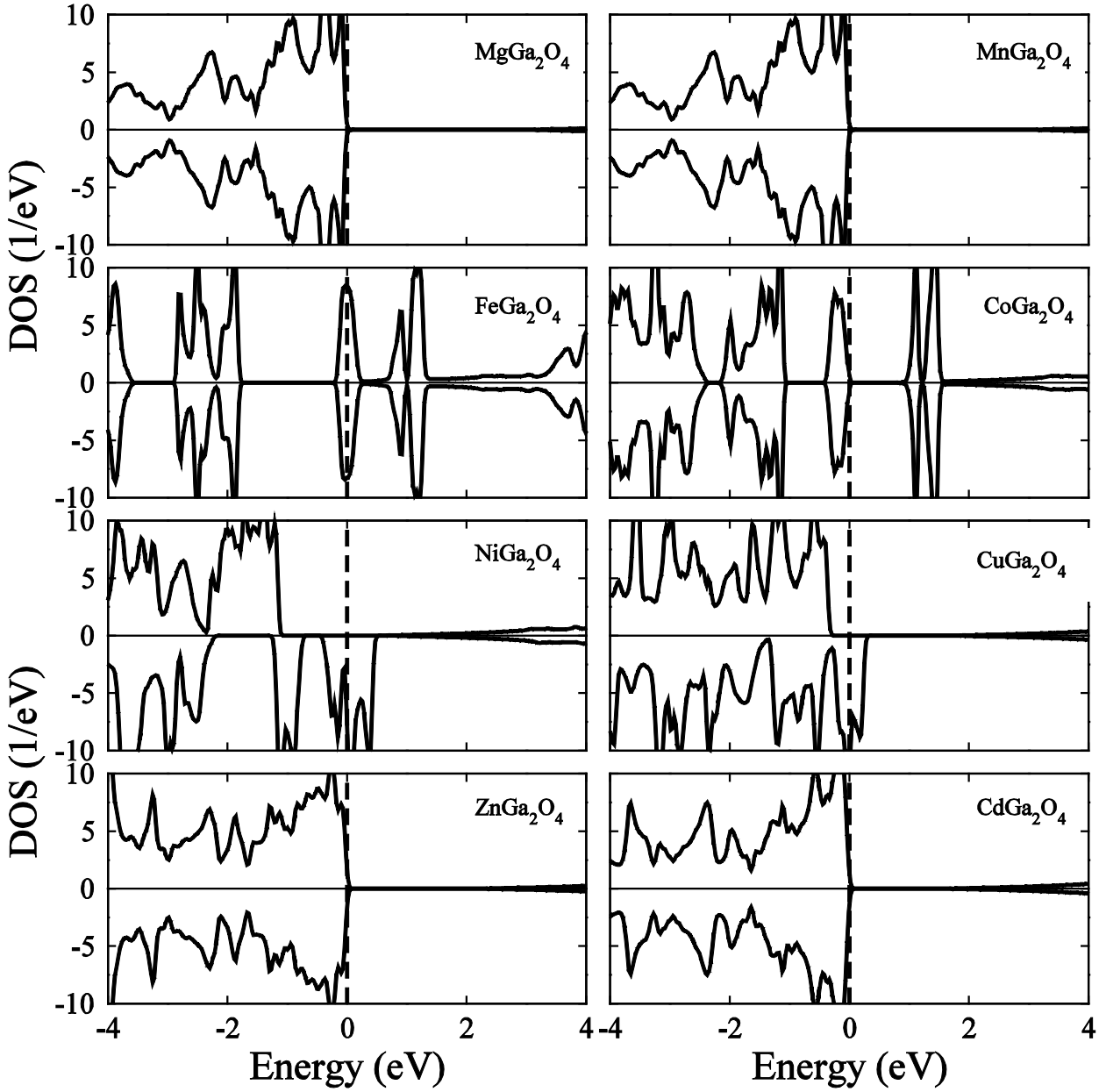

Fig. 4.6: *Total density of states (TDOS) MGa_2O_4*

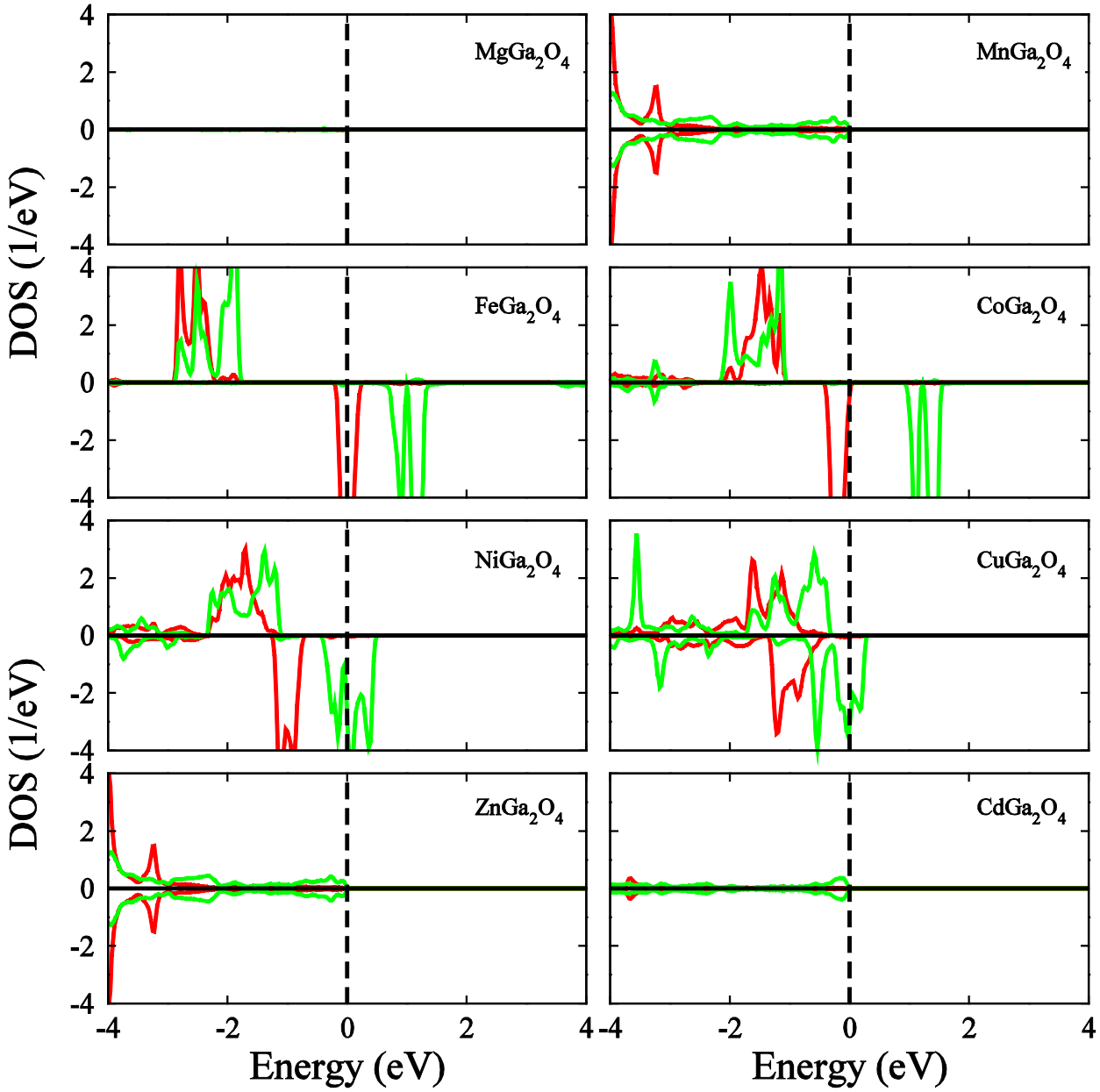

Fig 4.7: *Partial density of states (PDOS) e_g (red), t_{2g} (green) MGa_2O_4*

4.3 Elastic Constants and elastic properties of ZnP_2O_4 (P= V, Cr, Fe, Rh, Sn) & VZn_2O_4

Optimized lattice parameter of cubic spinel ZnP_2O_4 (P=V, Cr, Fe, Rh, Sn) & VZn_2O_4 are presented in Table 4.12 and values of Bulk modlus B_o in Table 4.13. Using the optimized lattice parameter, the elastic constant C_{11}, C_{12} and C_{44} of these compounds ZnP_2O_4 (P=Cr, Fe, Rh, Sn) & VZn_2O_4 are calculated and produced in table 4.12. It is evident from our computed elastic constant, that all compounds are stable against elastic deformation given by $C_{11} - C_{12} > 0;\ C_{44} > 0; C_{11} + 2C_{12} > 0$ [548, 550]. Higher values of the bulk moduli show hardness of these materials. Table 4.13 reveals that ZnV_2O_4 has the highest value while $ZnSn_2O_4$ carries the lowest value for B_o. Based upon the optimized lattice parameter, elastic constants and bulk moduli, more mechanical parameters such as Reuss Modulus G_R, Viogot Modulus G_V, shear modulus G, Youngs modulus Y, Poissons ratio ν, Anisotropic parameter A, Lames coefficients (λ and μ), Kleinman parameter ζ, shear constant $G^{'}$, Pughs ratio (B_o/G), Cauchy's pressure $G^{"}$, compressibility K and fracture energy R of spinel compounds ZnP_2O_4 (P = V, Cr, Fe, Rh, Sn) & VZn_2O_4 are calculated and presented in Table 4.14.

Calculated values of shear modulus G, for these compounds in Table 4.14, indicates that $ZnRh_2O_4$ (98.359 GPA) is having the highest value *preceded by $ZnAl_2O_4$ (136.283 GPA) from Table 4.3 which is maximum*, while $ZnSn_2O_4$ has lowest value.

The stability of a solid material against the linear strain along edges i.e. Young's modulus Y, is the ratio stress over strain and computed from the values of Voigt shear modulus G_V and bulk modulus B_o [251] by *relation (2.13)*. Calculated values of Young's modulus are presented in Table 4.14. The compound is stiffer for the larger value of Y. For $ZnRh_2O_4$ the value of Y is the largest i.e 274.372 GPa (*preceded by $ZnAl_2O_4$ (335.693 GPa) from Table 4.3*) showing that it is more rigid and more inflexible as compared to $ZnSn_2O_4$ which is carrying the smallest value 132.805. The remaining compounds lie amidst these two ranges. From Table 4.14 it is obvious that Young's moduli for all the materials are large than the shear moduli. The larger values of Young's moduli indicate the stiffness of these materials.

As already stated, the ductile or brittle behaviour of materials can be judged by ratio of bulk modulus to shear modulus (B_o/G) [565] and which takes cutting value of 1.754 for separating the ductile from brittle character. High B_o/G ratio is associated with ductility while a low value corresponds to brittle nature of materials. It is clear from the Table 4.14 that $ZnCr_2O_4$ is having highest ductility, the others are less than it, *while from Table 4.3 $ZnAl_2O_4$ can be seen as brittle material*.

The Poissons ratio ν is calculated by the relation (2.14). At $\nu = 0.5$, the volume of a material remains constant and is incompressible, however when $\nu \to 0.5$ then the material meant to have tendency heading to be incompressible [569]. However if $\nu = 0$, then stretching a specimen cause no lateral contraction. Our calculated values for ν rest amid 0.249 and 0.347, hence indicating their stability against elastic deformation and shows that these materials are less compressible.

Lame's constants (λ and μ) constitute a parameterization of the elastic moduli for homogeneous isotropic media. These parameters are calculated by using relations (2.15) & (2.16) [251]. Our calculations show that Lames second modulus is equal to Voigts shear modulus ($\mu = G_V$). For isotropic materials, $\lambda = C_{12}$ and $\mu = G'$. Since compounds under consideration are fully anisotropic compounds hence do not satisfy the condition for isotropic compounds.

Anisotropic ratio A can be calculated with the help of elastic constants [557] through relation (4.2)**.** Its value is used to show whether the elastic properties remain constant in different directions. Magnitude of A is unity for completely isotropic materials and the deviation from unity measures the amount of elastic anisotropy [251]. The calculated values of A are presented in Table 4.14 clearly indicate that these compounds are anisotropic.

Shear constant or tetragonal shear modulus is another important parameter, calculated by $G' = \frac{1}{2}(C_{11} + C_{12})$ [256, 550, 551]. $G' > 0$, is the obligation for dynamical stability. The calculated G' values are given in Table 4.14 all being positive, confirming the mechanical stability of these materials. The bigger shear modulus corresponding 'more rigidity of the material' to 'the tetragonal distortions'.

Cauchy's pressure $\left(G^{"} = C_{12} - C_{44}\right)$ is exercised to outline the bonding make-up of the compounds under investigation [563]. The positive value of Cauchys pressure relates to metallic bonding while negative Cauchy's pressure is indication of angular or directional bonding (covalent bonding) of materials. Our calculated Cauchy's pressure values for all compounds are positive and have metallic character in their bonds.

The internal strain parameter or Kleinman parameter ζ [571)] is an information regarding the relative tendency of bond bending versus the bond stretching. The lower limit (ζ = 0) corresponds to the minimizing bond bending term, and minimizing bond stretching term leads to upper limit (ζ = 1). Later, Harrison [572)] linked the Kleinman parameter in an approximated way to the elastic constants by relation (2.17). Our calculated results of ζ in Table 4.14 show that Bond bending is dominant in these materials.

Table 4.12 : *DFT Optimized lattice constant a_o (in A^o), Elastic Constants C_{ij} (in GPa) for Zincian Spinel compounds within PBE-GGA in comparison with the experiment (Exp.) and other values for ZnP_2O_4 (P=V, Cr, Fe, Rh, Sn) & VZn_2O_4.*

Spinel Comp.	**Calculated**				**Exp.**				**Others**			
	a_o	**C_{11}**	**C_{12}**	**C_{44}**	**a**	**C_{11}**	**C_{12}**	**C_{44}**	**a(A^o)**	**C_{11}**	**C_{12}**	**C_{44}**
ZnV_2O_4	**8.392**	**423.78**	**110.112**	**58.598**	-	-	-	-	-	-	-	-
$ZnCr_2O_4$	**8.400**	**344.127**	**109.566**	**27.620**	-	-	-	-	8.39[a]	-	-	-
$ZnFe_2O_4$	**8.260**	**377.980**	**108.007**	**74.620**	-	265[b]	157[b]	135[b]	8.549[c]	-	-	-
$ZnRh_2O_4$	**8.730**	**419.731**	**65.039**	**64.833**	-	-	-	-	-	-	-	-
$ZnSn_2O_4$	**9.350**	**205.932**	**80.247**	**42.024**	-	-	-	-	-	-	-	-
VZn_2O_4	**8.510**	**308.301**	**102.788**	**70.581**	8.41[d]	-	-	-	-	-	-	-

a [587] b [249] c [595] d [625]

Table 4.13 : *Calculated values of Bulk Moduli B_o together with experimental and other theoretical values for ZnP_2O_4 (P=V, Cr, Fe, Rh, Sn) & VZn_2O_4.*

	Bulk Modulus B_o		
Spinel Comp.	**This work**	**Exp.**	**Other/Theoretical**
ZnV_2O_4	215.648	-	-
$ZnCr_2O_4$	185.851	-	183[a]
$ZnFe_2O_4$	196.760	-	-
$ZnRh_2O_4$	182.175	-	-
$ZnSn_2O_4$	122.143	-	-
VZn_2O_4	170.931	-	-

a [587]

Table 4.14 : *Reuss Modulus G_R (GPa), Viogot Modulus G_V, Shear Modulus G (GPa), Young's Modulus Y (GPa) , Lame's Coefficients λ & μ (GPa), Poisson's ratio ν, Zener Anisotropy parameter A, Kleinman parameter ζ, Tetragonal Shear Moduli $G^{'}$, Cauchy's pressure $G^{"}$, Compressibility K and Fracture Energy R_C of Spinels ZnP_2O_4 (P=V, Cr, Fe, Rh, Sn) & VZn_2O_4.*

Property	ZnV_2O_4	$ZnCr_2O_4$	$ZnFe_2O_4$	$ZnRh_2O_4$	$ZnSn_2O_4$	VZn_2O_4	Exp/ Others
	Present Values						
G_R	78.188	39.787	90.876	86.881	48.443	80.687	-
G_V	97.892	63.484	98.767	109.838	50.351	83.451	-
G	88.040	51.635	94.821	98.359	49.397	82.069	-
Y	255.080	170.984	253.829	274.372	132.805	215.314	-
ν	0.303	0.347	0.285	0.249	0.319	0.290	-
λ	150.386	143.528	130.916	108.950	88.575	115.297	-
μ	97.892	63.484	98.767	109.838	50.351	83.451	-
A	0.374	0.236	0.553	0.366	0.669	0.687	-
ζ	0.4568	0.2309	0.4894	0.3272	0.6229	0.5501	-
$G^{'}$	2.449	117.281	134.987	177.346	62.843	102.757	-
$G^{"}$	208.132	158.276	181.220	237.556	83.789	137.37	-
B_o/G	2.449	3.599	2.075	1.852	2.473	2.083	-
K	0.00464	0.0058	0.00508	0.00549	0.00819	0.00585	-
R	3.828×10^{-8}	7.449×10^{-8}	4.675×10^{-8}	5.151×10^{-8}	2.267×10^{-8}	7.279×10^{-8}	-

CHAPTER – 5
CONCLUSIONS

By employing density functional theory in generalized gradient approximation and full potential linearized augmented plane wave (FP-LAPW+lo) plus local orbital method we have investigated the structural, elastic, electronic and magnetic properties of transition metal cubic spinels compounds, XAl_2O_4 (X = Mg, Mn, Fe, Co, Ni, Cu, Zn), MGa_2O_4 (M = Mg, Mn, Fe, Co, Ni, Cu, Zn, Cd), NIn_2O_4 (N=Mg, Cd, Zn) and ZnP_2O_4 (P=V, Cr, Fe, Rh, Sn) & VZn_2O_4.

The calculated lattice constants *a*, elastic constants (C_{11}, C_{12}, C_{44}) and bulk moduli (B_o) are consistent with the available experimental & other theoretical data. Calculated Elastic constants show that these compounds are mechanically stable against elastic deformation. Higher values of the bulk moduli and Young's moduli of XAl_2O_4 (X = Mg, Mn, Fe, Co, Ni, Cu, Zn) indicate more hardness and stiffness of these materials as compared to the Gallate and Indate groups. $MgAl_2O_4$ is found to be the most stiffer material while $CdIn_2O_4$ the lesser. The Pugh's ratio (B_o/G) show that $CdGa_2O_4$ is the most ductile, while $MgAl_2O_4$ is most brittle. Calculated values of poisson's ratio ν scales that these materials are less compressible and stable against elastic deformation. Hence the results are duly in agreement with the observations of real materials, with $MgAl_2O_4$ *(ν =0.218)* having highest compressibility while $CdGa_2O_4$ *(ν=0.327)* is the lesser compressible material. Further, the values of ν also demonstrate that the dominant interatomic forces are central forces. Mechanical properties indicate that $MgAl_2O_4$ carries the highest values for shear modulus G (150.225 GPa) and Young's modulus Y (361.621 GPa), hence further confirm that it is the stiffer among all the compounds. The study of Lamme's coefficients λ & μ unveil that all of our materials are anisotropic. This fact is also confirmed by test of Zener factor A and the condition C_{44}=G' values. Though $MnAl_2O_4$, $CoAl_2O_4$ and $NiAl_2O_4$ are anisotropic but having values nearest to isotropic conditions.

The total density of state show the anti-ferromagnetic state of XAl_2O_4 (Mn, Fe,

Co, Ni, Cu, Zn) materials, while for MGa_2O_4 (M = Mg, Mn, Fe, Co, Ni, Cu, Zn, Cd) group the relax ground state energy reveal anti-ferromagnetic state of $FeGa_2O_4$, $CoGa_2O_4$, $ZnGa_2O_4$, $CdGa_2O_4$ and Ferromagnetic state of $NiGa_2O_4$, $CuGa_2O_4$. The $MgAl_2O_4$, $MgGa_2O_4$ & $MnGa_2O_4$ have non magnetic state. From Mn to Cu the increase in the number of d-electrons produce an enormous exchange splitting. These compounds have strong exchange interaction. For both Aluminate and Gallate groups exchange mechanism of electrons is dominant to introduce magnetism than any other effect as $\Delta_x(d) > \Delta_{JT}$. Due to unavailability of free electron increase, the values of $\Delta_x(d)$ and Δ_{JT} decrease from Mn to Cu. The negative values of indirect exchange energy $\Delta_x(pd)$ for XAl_2O_4 means the hybridization exchange of electrons between 2p states of Oxygen and 3d states of Transition metal ions. Increase in number of d electrons from Mn to Cu produce enormous exchange splitting. In these compounds, oxides having +2 valency are trapped in the tetrahedral environment of oxygen and Al/Ga with +3 valency trapped in the octahedral environment of oxygen. Therefore, the octahedral and tetrahedral states electrons are exchanged to induce strong magnetic effect. The dominant exchange energy $\Delta_x(d)$ shows the ferromagnetism is dominated by the spin of electrons and hence the ferromagnetism in these spinel oxides arise as a result of hybridization between the electrons in the 3d-states of a cation and 2p-states of anions. The total and local magnetic moments data represents that magnetic moments appear, due to total number of unpaired electrons in the 3d states since Mn, Fe, Co, Ni, Cu have 5, 4, 3, 2, 1 unpaired electrons in their particular 3d states which prescribe their free magnetic moment per atom. For Aluminate group the highest magnetic moment is 5 for $MnAl_2O_4$ and lowest value is 1 for $CuAl_2O_4$. While in MGa_2O_4, the M atoms have four, three, two and one unpaired electrons respectively, which show major contributions of magnetic moments in these oxides with small contributions from non-magnetic (Ga, O) atoms. In XAl_2O_4 the tetrahedral environ created by O anions generate crystal field (CF) which is liable for splitting 3d state of Transition metals. Jahn Teller distortion breaks the degeneracy of doublet and triplet states raising the state d_{xy} at high energy relative to d_{yz} & d_{zx} and at high energy relative to d_{x2-y2} , hence only dt_{2g} states participate in

hybridization and e_g do not. On the other hand, MGa_2O_4 (M= Mg, Mn, Zn and Cd) have all the 3*d*-states filled and do not contribute to the hybridization process and having zero exchange energy that leads its diamagnetic behavior.

Hence, it is clear from the above decrypted composition of spinel based transition metal oxides are of great importance from scientific and technological point of view. The hardness of the Aluminate group in general and in specific the strength of these materials make them valuable for the armor shield applicability as well in transparent canopies and flat glass shield. These materials can also be used as refractory materials. These materials can be easily used as magnetic materials for storage devices, can also be applied as electrical materials and can be candidate applicant in multifunctional devices, microwave electronics and frequency sensor.

In this thesis the ground state properties have been portrayed, simply concentrating on crystal structure in relation to the structural energies which are described with in *ab initio* approach. In future, further work by entailing some excited state properties beyond the density functional theory (DFT) are proposed, which may comprise of optical properties, thermal properties, calculations of sound velocities, Debye temperature, phonon heat capacity, entropy, thermal expansion coefficients etc. The field still offers vide interest. It is worth noting, that discrete data & knowledge regarding exchange interactions and their dependence on structure is very important complement for the type of compounds considered in this thesis, but DFT is having limitations. As magnetism in transition metal spinel oxides involves considerable electron correlations and many body effects which cannot be governed well in DFT. Hence DFT+U approach or work with any other approach will be carried out in future not only on our existing materials but also for more spinel compounds.

REFERENCES

1. B. Amin, R. Khenata, A. Bouhemadou, I. Ahmad, M. Maqbool, "Opto-electronic response of spinels $MgAl_2O_4$ and $MgGa_2O_4$through modified Becke-Johnson exchange potential"; Physica B 407, 2588–2592 (2012).
2. S. M. Hosseini, "Structural, electronic and optical properties of spinel $MgAl_2O_4$ oxide"; Phys Stat. Sol. (b) 245, 2800-2807 (2008).
3. T. Hagino, Y. Seki, N. Wada, S. Tsuji, T. Shirane, K. –I. Kumagai, S. Nagata, "Superconductivity in Spinel-type compounds CuRh2S4 and RuRh2Se4"; Phys. Rev. B 51, 12673 (1995).
4. A. Bouhemeadou, R. Khenata, "Pseudo-potential calculations of structural and elastic properties of spinel oxides ZnX_2O_4 (X=Al, Ga, In) under pressure effect"; Physics Letters A 360, 339-343 (2006).
5. F. Semari, R. Khenata, M. Rabah, A. Bouhemadou, S. Bin Omran, Ali H. Reshak and D. Rached, "Full potential study of the elastic, electronic, and optical properties of spinels $MgIn_2S_4$ and $CdIn_2S_4$ under pressure effect"; Solid State Chemistry, 183, 2818-2825 (2010).
6. Z. Liang, J. Guang-fu, Z. Feng and G. Zi-Zheng, "First Principles study of the structural, mechanical and electronic properties of ZnX_2O_4 (X=Al, Cr and Ga)", Chin. Phys B Vol 20, 047102 (2011).
7. M. Boujnah, O. Dakir, H. Zaari, A. Benyouseef, A. El Kenz, "Optoelectronic response of spinels CdX_2O_4 with X=(Al, Ga, In) thorugh the modified Becke-johnson functional"; J. App. Phys. 116, 123703-7 (2014).
8. J. van den Brink, G. Khaliullin, D. Khomskii, "Orbital effects in manganites"; Colossal Magnetoresistive Manganites, Chapter-6, 263-301 (2004).
9. S. Krohns, F. Schrettle, P. lunkenheimer, V. Tsurkan, A. Loidl, "Colossal magnetocapacitive effect in differently sysnthesized and doped $CdCr_2S_2$"; Physica B 403, 4224-4227 (2008).
10. H. J. Reichmann, S. D. Jacobsen, T. B. Ballaran, "Elasticity of franklinite and

trends for transition-metal oxide spinels"; Am. Min. 98, 601-608 (2013).

11. G. N. Maslennikova, "Pigments of the spinel type"; *Glass and Ceramics*, 58, 6, 23-27 (2001).
12. A. Goldman, *Modern Ferrite Technology,* 2nd edition, Springer, 2006.
13. P. F. Ndione, Y. Shi, V. Stevanovic, S. Lany, A. Zakutayev, P. A. Parilla, J. D. Perkins, J. J. Berry, D. S. Ginley, M. F. Toney, "Control of the electrical properties in Spinel Oxides by manipulating cation disorder"; *Advanced Functional Materials*, 24, 1, 1-170 (2014).
14. A. K. Subramani, K. Kondo, M. Tada, M. Abe, M. Yoshimura, N. Matsushita, "Spinel ferrite films by a novel solution process for high frequency applications"; *Materials Chemistry and Physics,* 123, 1, 16-19 (2010).
15. F. Conrad, M. Bauer, D. Sheptyakov, S. Weyeneth, D. Jaeger, K. Hametner, P. E. Car, J. Patscheider, D. Gunther, G. R. Patzke, "New spinel oxide catalysts for visible-light-driven water oxidation"; RSC Advances, 2, 7, 3076-3082 (2012).
16. J. Lee, Y-Ki Hong, W. Lee, G. S. Abo, J. Park, R. Syslo, W-Mo Seong, S-H Park, W-Ki Ahn, "High ferromagnetic resonance and thermal stability spinel $Ni_{0.7}Mn0_{.3-x}Co_xFe_2O_4$ ferrite for ultra high frequency devices"; Journal of Applied Physics, 111, 7, A516-1-3 (2012).
17. K. E. Sickafus, R. Hughes, "Spinel Compounds: Structure and Property Relations", J. Am. Ceram. Soc., 82, 3277-78 (1999).
18. S. Samanta "Study of systematic trends in electronic and optical properties within ZnM2O4 (M=Co, Rh,Ir) family by FPLAPW method with PBE and TB-mBJ potentials"; Optical Mat. 45, 141-147 (2015).
19. A. Bouhemadou, "Theoretical study of the structural, elastic and electronic properties of the GeX_2O_4 (X = Mg, Zn, Cd) compounds under pressure"; Model. Simul. Mater. Sci. Eng. 16, 055007 (2008).
20. A. Zerr, G. Miehe, G. Serghiou, M. Schwarz, E. Kroke and R. Riedel, "Synthesis of cubic silicon nitride"; Nature 400, 340 (1999).

21. T. Y. Wei, C. Chen, S. Y. Lu, C. C. Hu, "A cost-effective supercapacitor material of ultrahigh specific capacitances: spinel nickel cobaltite aerogels from an epoxide-driven sol-gel process"; Adv Mater, 22(3), 347-351 (2010).

22. X. Wang, X. Hang, M. Lim, N. Singh, C. L. Gan, M. Jan, P. S. Lee, "Nickel Cobalt Oxide-Single Wall Carbon nanotube Composite Material for Superior Cycling Stability and High-Performance Supercapacitor Application"; J. Phys. Chem. C, 116(23), pp 12448-12454 (2012).

23. P. Hohenberg, W. Kohn, "Inhomogeneous Electron Gas"; Phys. Rev. B 136, B864-B871 (1964).

24. W. Kohn, L. J. Sham, "Self-Consistent Equations Including Exchange and Correlation Effects"; Phys. Rev. A 140, A1133-A1138 (1965).

25. S. Arif, I. Ahmad, B. Amin, "Theoretical investigation of half-metallicity in Co/Ni substituted AlN"; Quant. Chem. 112 (3), 882-888 (2012).

26. K. Schwarz, P. Blaha, "Solid state calculations using WIEN2K"; Comput. Mater. Sci. 28, 259 (2003).

27. M. T. Yin, M. L. Cohen, "Theory of lattice-dynamical properties of solids: Application to Si and Ge", Phys. Rev. B 26, 3259 (1982).

28. J. Neugebauer, M. Scheffler, "Adsorbate-substrate and adsorbate-adsorbate interactions of Na and K adlayers on al(111)"; Phys. Rev. B46, 16067 (1992).

29. M. Catti, G Valerio, R. Doversi, M. Causa, "Quantum-mechanical calculation of the solid-state equilibrium $MgO+\alpha\text{-}Al_2O_3 \rightleftarrows MgAl_2O_4$ (spinel) versus pressure"; Phys. Rev. B 49, 14179 (1994).

30. P. Blaha, K. Schwarz, J. Luitz, "A Full Potential Linearized Augmented Planewave Package for Calcualting Crystal Properties"; (Technical university Wien, Vienna, ISBN 3-9501031-0-4, (2001).

31. X. Ying, Z. Zhi, "Ground state property of LiV_2O_4"; Chin. Phys. Lett. 24, 184 (2007).

32. E. Nazarenko, J. E. Lorenzo, Y. Joly, J. L. Hodeau, D. Mannix, C. Marin,

"Resonant X-ray Diffraction Studies on the Charge Ordering in Magnetite"; Phys. Rev. Lett. 97, 056403-4 (2006). DOI: 10.1103/PhysRevLett.97.056403

33. Z. Mousavi, M. E. Zare, M. S. Niasari, "Magnetic and optical properties of zinc chromite nanostructures prepared by microwave method"; Trans. Nonferrous Met. Soc. China 25, 3980-3986 (2015).

34. T. Ohgushi, S. Umeno, "Low Temperature Synthesis of Dispersed Fine Particle of Cobalt Aluminate—A New Application of Zeolite"; Bull. Chem. Soc. Jpn., 60, 4457-4458 (1987). doi.org/10.1246/bcsj.60.4457

35. H. Martinho, N. O. Moreno, J. A. Sanjurjo, C. Rettori, A. J. Garcia-Adeva, D. L. Huber, S. B. Oseroff, W. Ratcliff, II, S.-W. Cheong, P. G. Pagliuso, J. L. Sarrao, and G. B. Martins, "Magnetic properties of the frustrated antiferromagnetic spinel $ZnCr_2O_4$ and the spin-glass $Zn_{1-x}Cd_xCr_2O_4$ (x=0.05,0.10) "; Phys. Rev. B 64, 024408 (2001).

36. S. H. Lee, C. Broholm, W. Ratcliff, G. Gasparovic, Q. Huang, T. H. Kim, S. W. Cheong, "Emergent excitations in a geometrically frustrated magnet"; Nature 418, 856-858 (2002).

37. B. S. Son, S. J. Kim, C. S. Kim, M. H. Chung and Y. Jo, "The Site Dependence on Exchange Interaction of the Fe Spinel"; J. Korean Phys. Soc. 52, 1077-1080 (2008).

38. B. N. Kim, K. Hiraga, K. Morita and Y. Sakka, "A high-strain-rate superplastic ceramic"; Nature 413(6853):288-91 (2001).

39. R. M. Gabr, M. M. Girgis and A. M. El-Awad, "Formation, conductivity and activity of zinc chromite catalyst"; Mater. Chem. Phys. 30, 169-177 (1992).

40. E. A. El-Sharkawy, "Textural, Structural and Catalytic Properties of $ZnCr_2O_4$-Al_2O_3Ternary Solid Catalysts"; Adsorpt. Sci. Technol. 16, 193-216 (1998).

41. W. S. Epling, G. B. Hoflund, D. M. Minahan, "Reaction and surface characterization study of higher alcohol synthesis catalysts-VII-CS-Promoted and PD-Promoted 1 1 Zn/Cr Spinel"; J. Catal. 175(2), pp.175-184 (1998).

42. P. Parhi, V. Manivannan, "Microwave metathetic approach for the synthesis and characterization of $ZnCr_2O_4$"; J. of Eur. Cer. Soc. 28, 1665-1670 (2008).

43. M. Bayhan, T. Hashemi and A. W. Brinkman, "Sintering and humidity-sensitive

behaviour of the $ZnCr_2O_4$–K_2CrO_4 ceramic system"; J. Mater. Sci. 32(24), 6619-6623 (1997).

44. S. Pokhrel, B. Jeyaraj and K. S. Nagaraja, "Humidity-sensing properties of $ZnCr_2O_4$ – ZnO"; Mater, Lett. 57, 3543-3548 (2003).
45. L. J. Golonka, B. W. Licznerski, K. Nitsch and H. Teterycz, "Thick-film humidity sensors"; Meas. Sci. Technol. 8, 92 (1997).
46. *Functional Metal Oxides: New Science and Novel Applications,* First Edition. Edited by Satishchandra B. Ogale, Thirumalai V. Venkatesan, and Mark G. Blamire. © 2013 Wiley-VCH Verlag GmbH & Co. KGaA. Published 2013 by Wiley-VCH Verlag GmbH & Co. KGaA.
47. R. Eden, *The decades of the newe worlde or west India;* p. 264. 1555 (reprinted 1885).
48. R. Hakluyt, *The principall navigations, voiages and discoueries of the English nation;* p. 264. 1589 (reprinted 1598–1600).
49. The Philological Society, Ed. *The Compact Edition of the Oxford English Dictionary.* Oxford University Press, Oxford, 1971.
50. C. Hall, *Gem Stones.* Dorling Kindersley, Inc., New York, 1994.
51. R. W. Hughes, *Ruby & Sapphire.* RWH Publishing, Boulder, Colorado, 1997.
52. G. Orpen, *Stories About Famous Precious Stones.* Lothrop, Boston, 1890.
53. G. Younghusband and C. Davenport, *The Crown Jewels of England.* Cassell and Co., Ltd., London, 1919.
54. H. D. W. Sitwell, *The Crown Jewels and Other Regalia in the Tower of London.* Dropmore Press, London, 1953.
55. P. Holland, *Pliny's Historie of the World, commonly called the Natural History.* Vol. II; p. 515. 1601 (reprinted 1634).
56. N. W. Grimes, "The Spinels: versatile materials"; Physics in Technology, 6, 22-27 (1975). DOI: doi.org/10.1088/0305-4624/6/1/I02
57. http://www.gemstones-guide.com/Spinel.html
58. J. B. Senoble, "Beauty and rarity – A quest for Vietnamese blue spinels" *InColor*,

Summer, pp.2–7 (2010).

59. R. Webster, *Gems: Their Sources, Descriptions and Identification*, 5th ed. Butterworth-Heinemann, Oxford, edited by P.G. Read, pp.1026 (1994).

60. C. A. Hauzenberger, T. Häger, W. Hofmeister, V. X. Quang, G. W. A. R. Fernando, "Origin and formation of gem quality corundum from Vietnam"; *Geo- and Materials-Science on Gem-Minerals of Vietnam, Proceedings of the International Workshop*, Hanoi, October, p. 1–8 (2003).

61. P. V. Long, G. Giuliani, V. Garnier, D. Ohnenstetter, "Gemstones in Vietnam"; *The Australian Mineralogist.* 22, 4, 162–168 (2004).

62 V. Pardieu, R. W. Hughes, "Spinel: The resurrection of a classic"; *InColor*, Summer, pp. 10–12 (2008) (also on www.ruby-sapphire.com and www.fieldgemology.org).

63. L. T. –T. Huong, T. Häger, W. Hofmeister, C. Hauzenberger, D. Schwarz, P. V. Long, U. Wehmeister, N. N. Khoi, N. T. Nhung, "Gemstones from Vietnam: An update"; *G&G*, 48, 3, 158–176 (2012).

64. B. Chauvire, B. Rondeau, E. Fritsch, P Ressigeac, J. Luc Devidal, "Blue Spinel from the Luc Yen District of Vietnam"; Gems & Gemology, 51, 1 (2015).

65. J. E. Shigley, C. M. Stockton, ""Cobalt-blue" gem spinels"; *Gems and Gemology,* 20, 1, 34–41 (1984).

66. A. Delaunay, "Les spinelles bleus", (2008). http://www.geminterest. com/. (26:09:2016, 19:57PM)

67. G. Giuliani, J. Dubessy, D. Banks, V. H. Quang, T. Lhomme, J. Pironon, V. Garnier, T. P. Trong, L. P. Van, D. Ohnenstetter, D. Schwarz, "CO_2-H_2S-COS-S_8-AlO(OH)-bearing fluid inclusions in ruby from marble-hosted deposits in Luc Yen area, North Vietnam"; *Chemical Geology*, 194, 167–185 (2003).

68. V. Garnier, G. Giuliani, D. Ohnenstetter, A. E. Fallick, J. Dubessy, D. Banks, H. Q. Vinh, T. Lhomme, H. Maluski, A. Pêcher, K. A. Bakhsh, P. V. Long, P. T. Trinh, D. Schwarz , "Marble-hosted ruby deposits from Central and South-East Asia:

Toward a new genetic model"; *Ore Geology Reviews*, 34, 169–191 (2008).

69. K. Bucher, M. Frey, "*Petrogenesis of Metamorphic Rocks"*; 6th ed. Springer-Verlag, 308 pp. (1994).

70. A. S. Janardhan, K. Sriramguru, S. Basava, M. A. Shankara, "Geikielite-Mg.Al.Spinel-titanoclinohumite association from a marble quarry near Rajapalaiyam area, part of the 550 Ma of southern granulite terrain, southern India"; *Gondwana Research*, 4, 3, 359–366 (2001).

71. A. Proyer, E. Mposkos, I. Baziotis, G. Hoinkes, "Tracing high-pressure metamorphism in marbles: Phase relations in high-grade aluminous calcite-dolomite marbles from the Greek Rhodope massif in the system CaO-MgO-Al_2O_3-SiO_2-CO_2 and indications of prior aragonite"; *Lithos*, 104 (1–4), 119–130 (2008).

72. J. M. Ferry, T. Ushikubo, J. W. Valley, "Formation of forsterite by silicification of dolomite during contact metamorphism"; *Journal of Petrology*, 52, 9, 1619–1640 (2011).

73. Restoring the Luster to a Once-Loved Gem, article by Victoria Gomelsky on *The New York Times* website, May 12, 2011.

74. H. H. Anderson, "Magnesium aluminate spinel as a refractory material"; Unpublished Ph. D. Thesis, M. I. T., Cambridge. (Microfilm Service, M. I. T) (1952).

75. G. A. Rankin, and H. E. Merwin, "The ternary system CaO-Al_2O_3-MgO"; Am. Ceram. Soc. 38, 571 (1916).

76. F. W. Clarke, "Data of Geochemistry", 5th ed., Bull. 770, U. U. Geol. Surv., 1924.

77. F. Rinne, "Morphologische und physikalisch-chemische Untersuchungen an synthetischen Spinellen als Beispiel unstochiometrisch zusammengesetzter Stoffe"; N. Jb Min. Beil.-Bd. A 58, 43-108 (1928).

78. C. Wagner, "The mechanism of formation of ionic compounds of higher order (double salt, spinels, silicates)"; Phys. Chem. 34 B, 309 (1936).

79. A. Navrotsky, O. J. Kleppa, "Thermodynamics of formation of simple spinels," Ino. Nucl. Chem. 30, 479-498 (1968).

80. E. Ryshkewitch, Oxide Ceramics, Academic Press, New York, 1960, pp. 257-274.

81. J. T. Bailey, R. Russel, "Sintered spinel ceramics"; Am. Ceram. Soc. Bulletin 47 (11), 1025-1029 (1968).

82. C. J. Ting, H. -Y. Lu, "Deterioration in the Final-Stage Sintering of Magnesium Aluminate Spinel"; J. Am. Ceram. Soc. 83, 1592-1598 (2000).

83. R. J. Bratton, "Coprecipitates yielding $MgAl_2O_4$ spinelpowders"; Am. Ceram. Soc. Bull. 48, 759-762 (1969).

84. C. J. Ting, H. -Y. Lu, "Hot-pressing of magnesium aluminate spinel – I. Kinetics and densification mechanism"; Acta Mater. 47(3), 817-830 (1999).

85. S. K. Behera, P. Barpanda, S. K. Pratihar, S. Bhattacharyya, "Synthesis of magnesium-aluminium spinel from autoignition of citrate-nitrate gel"; Mat. Letters 58(9), 1451-1455 (2004).

86. K. C. Stella, A. S. Nesaraj,"Effect of fuels on the combustion synthesis of $NiAl_2O_4$ spinel particles"; *Iranian Journal of Materials Science & Engineering, 7 (2),* 36-44 *(2010*).

87. M. P. Pechini, Method of preparing lead and alkaline earth titanates and niobates and coating method using the same to form a capacitor; US Patent. 3330697, (1967).

88. G. Aguilar-Rios, M. Valenzuela, P. Salas, H. Armendariz, P. Bosch, G. D. Toro, R. Silva, V. Bertin, S. Castillo, A. Ramirez-Solis, I. Schifter, "Hydrogen interactions and catalytic properties of platinum-tin supported on zinc aluminate"; Appl. Catal. A: Gen. 127, 65-75 (1995). DOI:10.1016/0926-860X(95)00269-3

89. V. N. Stathopoulos, P. J. Pomonis, "Low-Temperature Synthesis of Spinels M Al_2O_4 (M=Mg, Co, Ni, Cu, Zn) Prepared by a Sol–Gel Method"; Prog. Colloid Polym. Sci., 118, 17–21 (2001).

90. D. Dhak, P. Pramanik, "Particle Size Comparison of Soft-Chemically Prepared

Transition metal (Co, Ni, Cu, Zn) Aluminate Spinels"; J. Am. Ceram. Soc. 89(3), 1014-1021 (2006).

91. S. Daniele, D. Tcheboukov, L. G. Hubert Pfalzgraf, "Characterization of Transparent ZnM_2O_4 Coatings (M=Al, Ga) Obtained by Sol-Gel Routes with Heterometallic Alkoxides as Precursors"; International Conference on Thin Film Deposition of Oxide Multilayers Hybrid Structures, 283–287 (2001).
92. S. Mathur, M. Veith, M. Haas, H. Shen, N. Lecerf, V. Huch, S. Hü fner, R. Haberkorn, H. P. Beck, M. Jilavi, "Single-Source Sol–Gel Synthesis of Nanocrystalline $ZnAl_2O_4$: Structural and Optical Properties"; J. Am. Ceram. Soc., 84, 1921–8 (2001).
93. D. W. Walker, "Zinc Aluminate Prepared Using an Alumina Hydrate"; U.S. Patent 4, 370, 310, 1983.
94. G. B. Carrier, "Process for Producing Porous Spinel Materials"; U.S. Patent 4, 256, 722, 1981.
95. K. Suresh, K. C. Patil, ''Preparation and Properties of Fine Particle of Ni–Zn Ferrite, A Comparative Study of Combustion and PrecursorMethod''; J. Solid State Chem., 99, 12–7 (1992).
96. P. Pramanik, "Synthesis of Nano Particles of Inorganic Oxides by Polymer Matrix"; Bull. Mater. Sci., 18, 819–29 (1995).
97. P. Pramanik, "Chemical Synthesis of Nanosized Oxides"; Bull. Mater. Sci., 19, 957–61 (1996).
98. A. K. Adak, A. Pathak, P. Pramanik, "Characterization of $ZnAl_2O_4$ Nanocrystals Prepared by the Polyvinyl Alcohol Evaporation Route"; J. Mater. Sci. Lett., 17 (7), 559–61 (1998).
99. R. N. Das, A. Pathak, P. Pramanik, "Low Temperature Preparation of Nanocrystalline Lead Zirconate Titanate and Lead Lanthanum Zirconate Titanate Powders Using Triethanolamine"; J. Am. Ceram. Soc., 81, 3357–60 (1998).

100. M. Barj, J. F. Bocquet, K. Chhor, and C. Pommier, "Submicron Magnesium Aluminum Oxide ($MgAl_2O_4$) Powder Synthesis in Supercritical Ethanol"; J. Mater.Sci., 27, 2187–92 (1992).

101. R. E. Rocheleau, Z. Zhang, J. W. Gilje, J. A. Meese-MarktscheVel, "MOCVD Deposition of $MgAl_2O_4$ Films Using Metal Alkoxide Precursors"; Chem. Mater., 6, 1615 (1994).

102. F. Meyer, R. Hempelmann, S. Mathurb, M. Veith, "Microemulsion mediated sol–gel synthesis of nano-scaled MAl_2O_4 (M=Co, Ni, Cu) spinels from single-source heterobimetallic alkoxide precursors"; J. Mater. Chem. 9, 1755-1763 (1999).

103. J. A. Hedvall, J. Heuberger, "A Hitherto Unknown Copper Aluminate of the Spinel"; Z. Anorg. Allg. Chem., 116, 137 (1921).

104. J. W. Mellor, "Cobalt and Nickel Colors"; Trans. Ceram. Soc., 36, 1-9 (1937).

105. A. Yamakawa, , M. Hashiba, Y. Nurishi, "Growth of zinc aluminate on the surfaces normal to the various crystal axes of an alumina single crystal"; *J. Mater. Sci.* 24, 1491-1495 (1989).

106. J. E. Baker, R. Burch, N. Yugin, "Investigation of $CoAl_2O_4$, $Cu/CoAl_2O_4$ and $Co/CoAl_2O_4$ Catalysts for the Formation of Oxygenates From a Carbon Monoxide–Carbon Dioxide–Hydrogen Mixture"; Appl. Catal., 73, 135–52 (1991).

107. L. K. Kurihara, S. L. Suib, "Sol-Gel Synthesis of Ternary Metal Oxides. 1. Synthesis and Characterization of $MA1_2O_4$ (M = Mg, Ni, Co, Cu, Fe, Zn, Mn, Cd, Ca, Hg, Sr, and Ba) and $Pb_2A1_2O_5$"; Chem. Mater. 5, 609-613 (1993).

108. N. Guilhaume, M. Primet, "Catalytic Combustion of Methane : Copper Oxide supported on High-specific-area Spinels synthesized by a Sol-Gel Process"; J. Chem. Soc. Faraday Trans 90, 1541-1545 (1994).

109. W. S. Hong, L. C. D. Jonghe, X. Yang, M. N. Rahaman, "Reaction Sintering of $ZnO\text{-}Al_2O_3$"; J. Am. Ceram. Soc. 78, 3217-24 (1995).

110. M. A. Valenzuela, J. P. Jacobs, P. Bosch, S. Reijne, B. Zapata, H. H. Brongersma, "The Influence of the Preparation Method on the Surface Structure of $ZnAl_2O_4$";

Appl. Catal. A: Gen., 148, 315–24 (1997).

111. M. Zawadzki, J. Wrzyszcz, "Hydrothermal synthesis of nanoporous zinc aluminate with high surface area"; Mat. Res. Bulletin 35 (11), 109–114 (2000).

112. M. Zayat, D. Levy, "Blue $CoAl_2O_4$ Particles Prepared by the Sol-Gel and Citrate-Gel Methods"; Chem. Mater. 12, 2763–2769 (2000).

113. S. Chemlal, A. Larbot, M. Persin, J. Sarrazin, M. Sghyar, M. Rafiq, "Cobalt spinel $CoAl_2O_4$ via sol-gel process: elaboration and surface properties"; Mater. Res. Bull. 35, 2515 (2000).

114. A. R. Phani, M. Passacantando, S. Santucci, "Synthesis and characterization of zinc aluminum oxide thin films by sol–gel technique"; Mater. Chem. Phys. 68, 66 (2001).

115. T. Mimani, "Instant Synthesis of Nanoscale Spinel Aluminates"; J. Alloys Compd., 315, 123–8 (2001).

116. Z. Chen, E. Shi, Y. Zheng, W. Li, N. Wu,W. Zhong, "Synthesis of mono-dispersed $ZnAl_2O_4$ powders under hydrothermal conditions"; Mater. Lett. 56, 601 (2002).

117. Z. Chen, E. Shi, W. Li, Y. Zheng, N. Wu, W. Zhong, "Particle Size Comparison of Hydrothermally Synthesized Cobalt and Zinc Aluminate Spinels"; J. Am. Ceram. Soc., 85, 2949–2955 (2002). DOI: 10.1111/j.1151-2916.2002.tb00561.x

118. N. J. Van der Laag, M. D. Snel, P. C. M. M. Magusin, G. de With, "Structural, elastic, thermophysical and dielectric properties of zinc aluminate ($ZnAl_2O_4$)"; J. Eur Ceram Soc. 24, 2417 (2004).

119. X. L. Duan, Yuan, Z. H. Sun, C. N. Luan, D. Y. Pan, D. Xu, M. K. Lv, "Preparation of Co^{2+}-doped $ZnAl_2O_4$ nanoparticles by citrate sol–gel method"; J. Alloy Comp. 386, 311-314 (2005).

120. X. L. Duan, D. R. Yuan, X. Q. Wang, H. Y. Xu, "Synthesis and Characterization of Nanocrystalline Zinc Aluminum Spinel by a New Sol-Gel Method"; J. Sol–Gel Sci. Technol. 35, 221 (2005).

121. X. Wei, D. Chen, "Synthesis and characterization of nanosized zinc aluminate spinelby sol–gel technique"; Materials Letters 60, 823–827 (2006).

122. G. F. Hettig, H. Worl, H. H. Z. Weiter, "Uber die Bildung von Zinkaluminat aus Zinkoxyd und Aluminiumoxyd und die Bildung von Kupfer/Nickellegierungen aus Gemischen von Kupfer- und Nickelpulvern"; Anorg. Allg. Chem. 283, 207 (1956).

123. X. Duan, D. Yuan, X. WANG, H. XU, "Synthesis and Characterization of Nanocrystalline Zinc Aluminum Spinel by a New Sol-Gel Method"; Journal of Sol-Gel Science and Technology 35, 221–224, (2005).

124. L. Navias, "Preparation and properties of spinel made by vapor transport and diffusion in the system MgO-Al_2O_3"; Am. Ceram. Soc. 44, 434-146 (1961).

125. D. W. Fuerstenau, R. M. Fulrath, and J. A. Pesk , "A fundamental study of the variables associated with the mixing of ceramic raw materials"; Quarterly Progress Reports, Nos. 2, 49, and 5. Contract *No. AF* 33(613)-7763. Wright Air Development Division. lnst. Engr. Research, University of California, Berkeley, Calif, (1961).

126. A. M. Alper, R. N. McNally, P. H. Ribbe and R. C. Doman, "The system MgO-$MgAl_2O_4$"; Am. Ceram. Soc. 45, 263-268 (1962).

127. M. A. Petrova, G. A. Mikirticheva, A. S. Novikova, and V. F. Popova, "Spinel solid solutions in the systems $MgAl_2O_4$–$ZnAl_2O_4$ and $MgAl_2O_4$–Mg_2TiO_4"; J. Mater. Res. 12, 10, 2584-2588 (1997).

128. C. O. Arean, M. P. Mentruit, E. E. Platero, F. X. L. Xamena, J. N. Parra, "So-gel method for preparing high surface area $CoAl_2O_4$, and Al_2O_3–$CoAl_2O_4$ spinels"; Mater. Lett. 39, 22-27 (1999).

129. M. M. Amini, L. Torkian," Preparation of nickel aluminate spinel by microwave heating"; *Matter. Lett.*, 57(3), 639-642 (2002).

130. D. Khak, P. Pramanik, "Particle size comparison of soft-chemically prepared Transition Metal (Co, Ni, Cu, Zn) Aluminate Spinels"; J. Am. Ceram. Soc. 89(3),

1014-1021 (2006).

131. J. W. Kim, P. W. Shin, M. J. Lee, S. J. Lee, 'Effect of particle size on the strength of a porous nickel aluminate fabricated by a polymer solution route"; *J. Ceramic Processing and Research*, 7 (2), 117-121 (2006).

132. J. Yanyan, L. Jinggang, S. Xiaotao, N. Guiling, W. Chengyu, G. Xiumei, "$CuAl_2O_4$ powder synthesis by sol-gel method and its photodegradation property under visible light irradiation"; J. Sol-Gel. Sci. Technol. 42, 41-45 (2007).

133. L. Gama, M. A. Ribeiro, B. S. Barros, R. H. A. Kimnami, I. T. Weber, A. C. F. M. Costa, "Synthesis and characterization of the $NiAl_2O_4$, Co Al_2O_4 and Zn Al_2O_4 spinels y the polymeric precursors method"; J. Alloys and comp. 483, 453-455 (2009).

134. M. S. Niasi, F. Davar, M. Farhadi, "Synthesis and characterization of spinel-type CuAl2O4 nanocrystalline by modified so-gel method"; J. Sol-Gel Sci Technol 51, 48-52 (2009).

135. H. J. J. Van Boon, R. Groth, "Low-pressure Sodium Lamps with Indium Oxide Filter"; Philos. Tech. Rev. 29, 17 (1968).

136. J. C. C. Fan, F. J. Bachner, "Properties of Sn-Doped In_2O_3 Films Prepared by RF Sputtering"; J. Electrochem. Soc. 122, 1719-1725 (1975).

137. H. Knako, K. Miyake, "Physical Properties of Antimony-doped Tin Oxide Thick Films"; J. Appl. Phys. 53, 3629 (1982).

138. M. Mizuhashi, "Electrical properties of vacuum-deposited indium oxide and indium tin oxide films"; Thin Solid Films 70, 91-100 (1980).

139. E. Shanthi, A. Banerjee, V. Dutta, K. L. Chopra, "Electrical and optical properties of tin oxide films doped with F and (Sb+F)"; J. Appl. Phys. 53, 1615-1621 (1982).

140. A. M. E. Raj, G. Selvan, C. Ravidhas, M. Jayachandran, C. Sanjeeviraja, "Magnesiumindiumoxide ($MgIn_2O_4$) spinel thin films: Chemical spray pyrolysis (CSP) growth and materials characterizations"; J. of Colloid and Interface

Science. 328, 396–401 (2008).

141. S. E. Dali, V. V. S. S. Sai Sundar, M. Jayachandran and M. J. Chockalingam, "Synthesis and Characterization of AIn_2O_4 Indates, A= Mg, Ca, Sr, Ba"; Mat. Sci. Lett. 17, 619-623 (1998).

142. B. Li, L. Zeng, and F. Zhang, "Structure and electrical properties of $CdIn_2O_4$ thin films sputtered at elevated substrate temperatures," Phys. Stat. Sol. 201 (5), 960–966 (2004).

143. T. Minami, S. Takata, T. Kakumu, H. Sonohara, "New transparent conducting $MgIn_2O_4$–$Zn_2In_2O_5$ thin films prepared by magnetron sputtering"; Thin Solid Films. 270, 22-26 (1995). DOI: doi.org/10.1016/0040-6090(95)06852-X

144. E. T. Wherry, "Mineral determination by absorption spectra II"; *The American Mineralogist*, 14 (9), 323–328 (1929).

145. R. Pappalardo, D. L. Wood, R. C. Linares, "Optical absorption study of Co-doped oxide systems. II"; *The Journal of Chemical Physics*, 35, 6, 2041–2059 (1961).

146. E. S. Gaffney, "Spectra of tetrahedral Fe^{2+} in $MgA1_2O_4$"; *Physical Review B*. 8, 7, 3484–3486 (1973).

147. B. L. Dickson, G. Smith, "Low-temperature optical absorption and Mössbauer spectra of staurolite and spinel"; *Canadian Mineralogist*, 14, 206–215 (1976).

148. N. V. Kuleshov, V. P. Mikhailov, V. G. Sherbitsky, P. V. Prokoshin, K. V. Yumashev, "Absorption and luminescence of tetrahedral Co^{2+} ion in $MgAl_2O_4$"; *Journal of Luminescence*, 55, 265–269 (1993).

149. S. Muhlmeister, J. I. Koivula, R. C. Kammerling, C. P. Smith, E. Fritsch, J. E. Shigley, "Flux-grown synthetic red and blue spinels from Russia"; *G&G*, 29, 2, 81–98 (1993).

150. X. Duan, X. Wang, F. Yu, X. Liu, "Effects of Co content and annealing temperature on the structure and optical properties of $Co_xMg_{1-x}Al_2O_4$ nanoparticles"; *Materials Chemistry and Physics*, 137, 2, 652–659 (2012).

151. F. Bosi, U. Hålenius, V. D'Ippolito, G. B. Andreozzi, "Blue spinel crystals in the

$MgAl_2O_4$-$CoAl_2O_4$ series: Part II. Cation ordering over short-range and long-range scales"; *American Mineralogist*, 97 (11–12), 1834–1840 (2012).

152. V. D'Ippolito, G. B. Andreozzi, U. Hålenius, H. Skogby, K. Hametner, D. Günther, "Color mechanisms in spinels: cobalt and iron interplay for the blue color"; *Physics and Chemistry of Minerals*, 42(6), 431-439 (2015). DOI: dx.doi.org/10.1007/s00269-015-0734-0
153. Synthetic Gemstones: Spinel, *Gems: Their Sources, Descriptions and Identification*, edited by Michael O'Donoghue, Chapter 24, pages 495-502.
154. W. H. Bragg, "The Structrue of Magnetitie and the Spinels"; Nature 95, 561 (1915).
155. A. Miller, "Distribution of Cations in Spinels"; J. Appl. *Phys.* 30, (4), 24*S*-25*S* (1959).
156. H. S. C. O'Neill, A. Navrotsky, "Simple spinels: crystallographic parameters, cation radii, lattice energies, and cation distribution"; Am. Min. 68, 181-194 (1983).
157. H. S. C. O'Neill, A. Navrotsky, "Cation distributions and thermodynamic properties of binary spinel solid solutions"; Am. Min. 69, 733-753 (1984).
158. A. Bouhemeadou, R. Khenata, F. Zerarga "Ab Inition Study of the structural and elastic properties of spinels MgX_2O_4(X = Al, Ga, In) under Pressure"; Eur. Phys. J. B56, 1–5 (2007).
159. R. J. Hill, J. R. Graig, G.V. Gibbs, "Systematics of the Spinel Structure Type"; Phys. Chem. Miner. 4, 317 (1979).
160. A. F. Wells, Structural inorganic chemistry. Oxford University Press, 5th ed., Oxford, U.K. (1984).
161. J. B. Goodenough, A. L. Loeb, "Theory of ionic ordering, crystal distortion, and magnetic exchange due to covalent forces in spinels"; Physical Review. 98, 391-408 (1955).
162. J. D. Dunitz, L. E. Orgel, "Electronic properties of transition metal oxides II"; J. Phys. Chem. of Solids, 3, 318-323 (1957).

163. N. W. Grimes, A. J. Collett "Correlation of Infra-Red Spectra with Structural Distortions in the Spinel Series $Mg(Cr_xAl_{2-x})O_4$"; *J. Phys. Stat. Solidi.* 43, 591-599 (1971). DOI: 10.1002/pssb.2220430218

164. G. Pritosiwi, "Removal of Metal Ions from Synthetic and Galvanic Wastewater by Their Incorporation into Ferrites"; PhD Dessertation, Technical University Hamburg (2012).

165. W. H. Bragg, ''The Structure of the Spinel Group of Crystals,'' Philos. Mag. 30 , 305–315 (1915).

166. S. Nishikawa, ''Structure of Some Crystals of the Spinel Group,'' Proc. Math. Phys. Soc. Tokyo, 8, 199–209 (1915).

167. V. M. Goldschmidt, T. F. W. Barth, G. Lunde, "Geochemische Verteilungsgesetze der Elemente. V. lsomorphie und Polymorphie der Sesquioxyde, die Lanthaniden-Kontraktion und ihre Konsequenzen" Vidensk. – Akad. Skr. Mat.-Nat. Kl. 7, 1-59 (1025).

168 P. F. Kerr, "An artificial Gem-stone isomorphous with spinel": Journal of Minrol. Soc. Am., 14, 259-264 (1929).

169. E. Posnjak, "The Lattice Dimensions of Spinel ($MgAl_2O_4$)"; Am. Jour. Sci. 16, 528-530 (1928).

170. H. Sawada, "An electron density residual study of magnesium aluminium oxide spinel"; Materials Research Bulletin. 30, (3) 341-345 (1995).

171. K. E. Sickafus, J. M. Wills, N. W. Grimes, "Structure of Spinel", J. Am. Ceram. Soc., 82, 3279-92 (1999).

172. R. Smith, D. Bacorisen, B. P. Uberuaga, K. E. Sickafus, J. A. Ball and R. W. Grimes, "Dynamical simulations of radiation damage in magnesium aluminate spinel, $MgAl_2O_4$"; J. Phys. Condens. Matter 17, 875-891 (2005).

173. D. Bacorisen, R. Smith, J. A. Ball, R. W. Grimes, B. P. uberuaga, K. E. Sickafus, W. T. Rankin, "Molecular dynamics modeling of radiation damage in normal, partly inverse and inverse spinels"; Nuc. Inst. And Meth. Phys. Res. B 250, 36-45 (2006).

174. M. Lazzeri, P. Thibaudeau, "Ab *initio* Raman spectrum of the normal and disordered $MgAl_2O_4$ spinel"; Phys. Rev. B 74, 140301-4 (2006).

175. https://crystalsymmetry.wordpress.com/2014/08/08/227/

176. E. J. W. Verwey, E. L. Heilmann, "Physical Properties and Cation Arrangement of Oxides with Spinel Structures I. Cation Arrangement in Spinels"; Chem. Phys. 15, 174 (1947).

177. R. F. G. Gardner, F. Sweett and D. W. Tanner, "The electrical properties of alpha ferric oxide—II.: Ferric oxide of high purity," Phys. Chem. Sol. 24, 1183–1186, (1963).

178. S. Phanjoubam, C. Parkash, "Structural properties and d.c resistivity of Li-Zn-Ti ferrites"; Mod. Phys. Lett. B 16, (2002).

179. Irradiation induced structural transformations in normal spinels, potential materials for nuclear waste management, *Matériaux fonctionnels pour l'énergie SPMS, CNRS - École Centrale Paris & DEN/DMN/SRMA, CEA Saclay*.

180. http://www.physics.uwo.ca/~lgonchar/courses/p2800/Chapter10_Ceramics_Handouts.pdf (visit 23.09.2016, 01:28AM)

181. M. G. Brik, A. Suchocki, A. Kaminska, "Lattice parameters and stability of the spinel compounds in relation to the ionic radii and electronegativities of constituting chemical elements"; Inorg. Chem. 53, 5088-5099 (2014). DOI: 10.1021/ic500200a

182. Q. M. Wei, J. B. Li, Y. J. Chen, Y. S. Han, "X-ray study of cation distribution in $NiMn_{1-x}Fe_{2-x}O_4$ ferrites"; Mat. Char. 47, 247-252 (2001)

183. H. Jagodzinski, H. Saalfeld, "Kationenverteilung und Strukturbeziehungen in Mg-Al-Spinellen"; Z. Kristallogr. Bd. 110, 197-218 (1958).
DOI: https://doi.org/10.1524/zkri.1958.110.1-6.197

184. N. W. Grimes, "Structural distrortion in $MgCr_2O_4$"; *J. Phys. C: Solid State Phys.* 4, L342-L344 (1971). DOI: doi.org/10.1088/0022-3719/4/16/006

185. N. W. Grimes, "'Off-centre' ions in compounds with spinel structure"; *Phil. Mag.* 26(5), 1217-1226 (1972). DOI: 10.1080/14786437208227375

186. N. W. Grimes, "Antiferroelectricity among compounds with spinel structure?"; *J. Phys.* C. *Solid St. Phys.* 6, L78-L79 (1973).

187. N. W. Grimes, P. Thompson, "New symmetry and structure for spinels"; Proc. R. Lond. A 386, 333-345 (1983). DOI: 10.1098/rspa.1983.0039

188. International Tables for X-Ray Crystallography, Vol, 2. Kynoch Press, Birmingham, England, 1952.

189. A. H. Heuer, T. E. Mitchell, "Further discussion on the space group of spinel"; J. Phys. *C.* Solid. State. Phys. 8, L541-L543 (1975).

190. L. Hwang, A. H. Heuer, T. E. Mitchell, "On the space group of $MgAl_2O_4$ spinel"; Phil. Mag. 28, 241-243 (1973).

191. R. Stahl-Brada, W. Low, "Paramagnetic resonance spectra of Chromium and Manganese in the spinel structure"; *Phys. Rev.* 116, 561-564 (1959).

192. F. H. Lou, D. W. G. Ballentyne, "Visible and ultra-violet emission and absorption spectra of $MgAl_2O_4$:Cr"; *J. Phys.* C: *Solid St. Phys.* 1, 608-613 (1968).

193. N. W. Grimes, R. J. Hilleard, "X-ray diffraction studies of the spinel series $Mg(Cr_xAl_{2-x})O_4$ I: Lattice parameters and structure"; *J. Phys.* C: *Solid St. Phys.* 3, 866-71 (1970). DOI: doi.org/10.1088/0022-3719/3/4/015

194. K. D. Rouse, M. W. Thomas, B. T. M. Willis, "Space group of the spinel structure: A neutron diffraction study of $MgAl_2O_4$"; J. Phys. C. Solid. State. Phys. 9, L231-L233 (1976).

195. P. R. Staszak, J. E. Poetzinger, G. P. Wirtz, "$MgAl_2O_4$ ion positions calculated for the $F\bar{4}3m$ space group"; J. Phys, C: Solid State Phys., 17, 4751-4757 (1984).

196. R. F. Cooley, J. S. Reed, "Equilibrium Cation Distribution in $NiAl_2O_4$, $CuAl_2O_4$, and $ZnAl_2O_4$ Spinels"; J. Am. Ceram. Soc. 55(8), 395-398 (1972).

197. O. Muller, R. Roy, "The Major Ternary Structural Families"; *Springer-Verlag:* Berlin, Heidelberg, and New York. (1974).

198. H. Schmid, E. Ascher, "Are antiferroelectricity and other physical properties 'hidden' in spinel compounds"; J. Phys. C, Solid State Phys. 7, 2697-2705 (1974).

199. D. S. Walters, G. P. Wirtz, "Electron Diffraction Superlattice Lines in Magnesium Ferrite"; *J.* Am. *Ceram. Soc. 55,* 59 (1972).

200. E. J. Samuelsen, O. Steinsvoll, "On the space group of spinel"; J. Phys. C, Solid State Phys. 8, L427-L429 (1975).

201. P. Thompson, N. W. Grimes, "Madelung calculations for the spinel structure"; Philosophical Magazine, 36, 501-505 (1977).

202. R. K. Mishra, G. Thomas, "Structural phase transition in the spinel $MgAl_2O_4$"; Acta Cryst. A33, 678, 199-209 (1977).

203. M. E. Striefler, G. R. Barsch, "Lattice Dynamics of $MgAl_2O_4$ in Relation to the the Space Group of Spinel" Proc. Int. Conf. Lattice Dynamics (*Paris, September 5-9, 1977*), 75-76 (1978).

204. P. P. K. Smith, "Note on the space group of spinel minerals"; Phil. Mag. 38, 99-102 (1978).

205. O. Steinsvoll, E. J. Samuelsen, "The space group of spinel revisited"; J. Phys. Scr. 24, 57-58 (1981).

206. M. Tokonami, H. Horiuchi, "On the space group of spinel, $MgAl_2O_4$"; Acta Cryst. A36, 122-126 (1980).

207. D. M. Smyth, *The Defect Chemistry of Metal Oxides;* Oxford University Press: New York, 2000.

208. S. Ayyappan, S. Mahadevan, P. Chandramohan, M. P. Srinivasan, John Philip, and Baldev Raj, "Inflenence of Co^{2+} Ion Concentration on the Size, Magnetic Properties, and Purity of CoFe2O4 Spinel Ferrite Nanoparticles"; J. Phys. Chem. C. 114, 6334-6341 (2010).

209. T. F. W. Barth, E. Posnjak, "Spinels tructures, with and without variate atom equipoints"; Zeitschrift fi.ir Kristallographie, 82, 325-341 (1932).

210. A. Navrotksy, O. J. Kleppa, "The thermodynamics of cation distributions in simple spinels"; J. Inorg. Nucl. Chem. 29, 2701-2714 (1967).

211. Steven Dutch, Natural and Applied Sciences, University of Wisconsin-Green

Bay;
https://www.uwgb.edu/dutchs/Petrology/Spinel%20Structure.HTM.

212. F. de Boer, J. H. van Santen, E. J. W. Verwey, "Electrostatic Contribution to the Lattice Energy of Some Ordered Spinels"; J. Chem. Phys, 18 (8) 1032-1034 (1950).

213. G. D. Price, S. L. Price, J. K. Burdett, "The factors influencing cation site-preferences in spinels"; Phys. Chem. Miner. 8, 69-76 (1982).

214. R. Dekkers, C.F. Woensdregt, "Crystal structural control on surface topology and crystal morphology of normal spinel ($MgAl_2O_4$)"; J. Crystal Growth 236, 441–454 (2002).

215. E. H. Wallker Jr., J. W. Owens, M. Etinne and Don Walker, "Synthesis of $MgAl_2O_4$ spinel via "sol-gel""; Mater. Res. Bull. 37, 1041–1050 (2002).

216. N. Reeves, D. Pasero, A. R. West, "Order-disorder transition in the comples lithium spinel $Li_2CoTi_3O_8$"; J. Sol. St. Chem. 180, 1894-1901 (2007).

217. A. Feteira, "Negative Temperature Coefficient Resistance (NTCR) Ceramic Thermistors: An Industrial Perspective"; Am.Cerm. Soc. 92, 967-983 (2009).

218. F. P. Glasser, L. S. D. Glasser, "Crystal Chemistry of Some AB_2O_4 Compounds"; Ame. Ceram. Soc. 46, 377- 380 (1963).

219. A. R. Miedema, P. F. de Châtel, F. R. de Boer, "Cohesion in alloys — fundamentals of a semi-empirical model"; Physica B+C 100, 1-28, (1980).

220. H. Maekawa, S. Kato, K. Kawamura, T. Yokokawa, "Cation mixing in natural $MgAl_2O_4$ spinel: A high-temperture Al NMR study"; Am. Mine. 82, 1125-1132 (1997).

221. W. Y. Ching, M. Shang-Di, I. Tanaka and M. Yoshiya, "Prediction of spinel structure and properties of single and double nitrides"; Phys. Rev. B 63, 064102 (2001).

222. T. Mathew, "Synthesis and characterization of mixed oxides containing cobalt, copper and iron and study of their catalytic activity"; Ph.D. thesis, University of Pune, Indian (2002).

223. A. Navrotsky, B. A. Wechsler, K. Geisinger, F. Seifert, "Thermochemistry of $MgAl_2O_4$ -$Al_{8/3}O_4$ defect spinels"; J. Am. Ceram. Soc. 69, 418–422 (1986).

224. E. J. Verwey, F. de Boer, J. H. V. Santen,"Cation Arrangement in Spinels"; J. Chem.. Phys. 16, 1091-1092 (1948).

225. D. S. McClure, "The distribution of transition metal cations in spinels"; J. Phys. Chem. of Solids, 3, 311-317 (1957).

226. S. Hafner, F. Laves, "Ordnung/Unordnung und Ultrarotabsorption, III. Die Systeme $MgAl_2O_4$-Al_2O_3 und $MgAl_2O_4$-$LiAl_5O_8$"; Zeitscrift fur Kristallographie, 115, 321–330 (1961).

227. K. E. Sickafus, J. M. Wills, S. P. Chen, J. H. Terry Jr, T. Harmann, R. I. Sheldon"Development of a fundamental understanding of chemical bonding and electronic structure in spinel compounds"; Los Alamos National Laboratory, LA-UR-99-2227, (1999).

228. S. Wei, S. B. Zhang, "First-principles studyof cation distribution in eighteen closed-shell $A^{II}B_2^{III}O_4$ and $A^{IV}B_2^{II}O_4$ spinel oxides"; Phys. Rev. B 63, 045112-045118 (2002). DOI: doi.org/10.1103/PhysRevB.63.045112

229. L. N. Brewer, D. R. Kammler, T. O. Mason, V. P. Dravid, "Combined electron diffraction/microanalysis investigation of crystallography and cation distributions in the transparent conductive oxide $Cd_{1+x}In_{2-2x}Sn_xO_4$"; J. Appl. Phys. 89, 951 (2001). DOI: doi.org/10.1063/1.1340736

230. S. D. Mo, W. Y. Ching, "Electronic structure of normal, inverse, and partially inverse spinels in the $MgAl_2O_4$ system"; Phys. Rev. B54 (23), 16555-16561 (1996).

231. R. Khenata, M. Sahnoun, H. Baltache, M. R´erat, A. H. Reshak, Y. Al-Douri, B. Bouhafs, "Full-potential calculations of structural, elastic and electronic properties of $MgAl_2O_4$ and $ZnAl_2O_4$ compounds"; Phys. Lett. A344, 271-279 (2005).

232. A. Bouhemadou, R. Khenata, F. Zerarga, "Prediction study of structural and elastic properties under pressure effect of CdX_2O_2 (X=Al, Ga, In)"; Compt.

Mat.Sc. 39, 709-712 (2007).

233. M. L. Bortz, R. H. French, D. J. Jones, R.V. Kasowski, F. S. Ohuchi, "Temperature dependence of the electronic structure of oxides: MgO, $Mgal_2O_4$ and Al_2O_3"; Phys. Scr. 41, 537-541 (1990).

234. R. Caracas, E. J. Banigan, "Elasticity and Raman and infrared spectra of $MgAl_2O_4$ spinel from density functional perturbation theory"; Phys. Earth Planet. Inter. 174, 113-121 (2009). DOI: doi.org/10.1016/j.pepi.2009.01.001

235. P. Thibaudeau, F. Gervais, "*Ab initio* investigation of phonon modes in the $MgAl_2O_4$ spinel"; J. Phys.: Condens. Matter. 14, 3543-3552 (2002). DOI: doi.org/10.1088/0953-8984/14/13/312

236. A. K. Kushwaha, "Vibrational and elastic properties of aluminate spinel $MgAl_2O_4$"; Physica B 405, 2795-2798 (2010).

237. http://www.ruby-sapphire.com

238. J. F. Nye, Physical Properties of Crystals: Their Represnation by tensors and Matrices. Clarendon, Oxford University Press New York, ISBN 0198511655 (1985).

239. M. J. Mehl, J. E. Osburn, D. A. Papaconstantopoulos, and B. M. Klein, "Structural properties of ordered high-melting-temperature intermetallic alloys from first-principles total-energy calculations"; Phys Rev B, Condensed Matter, 41, 10313, (1990).

240. C. Kittel, Introduction to Solid State Physics, 6th Ed. Wiley, New York (1986).

241. M. B. Kanoun, A. E. Merad, H. Aourag, G. Merad, "Molecular-dynamics simulations of structural and thermodynamic perperties of ZnTe using a three-body potential"; Sol. St. Sci. 5, 1211-1216 (2003).

242. P. Ravindran, J. Wills, O. Eriksson, "Density functional theory for calculation of elastic properties of orthorhombic crystals: Application to $TiSi_2$": J. Appl. Phys. 84(9), 4891-4904 (1998).

243. H. Wang, G. Simmons, "Elasticity of some mantle crystal structures, 1, Pleonaste and hercynite spinel": J. Geophy. Res. 77, 4379 (1972).

244. R. K. Verma, "Elasticity of some high-density crystals"; J. Geophys. Res. 65, 757-766 (1960).

245. R. C. Liebermann, "Pressure and temperature dependence of the elastic properties of polycrystalline trevorite ($NiFe_2O_4$)"; Phys. Earth Planet, Interiors. 6, 360 (1972).

246. Z. P. Chang, G. R. Barsch, "Pressure dependence of single-crystal elastic constants and anharmonic properties of spinel"; J. Geophys. Res. 78, 2418 (1973).

247. Y. Syono, Y. Fukai, Y. Ishikawa, "Anomalous elastic properties of Fe_2TiO_4"; J. Phys. Soc. Jpn 31, 471-476 (1971).

248. J. Sakurai, "Ultrasonic propagation in Nickel and Mn-Ferrite at high magnetic fields"; J. Phys. Soc. Jpn 19, 311-317 (1964).

249. N. W. Grimes, "Elastic constants for Zinc Ferrite from the infrared spectrum"; Phys. Status solidi (b). 58, K129-K132 (1973). DOI: 10.1002/pssb.2220580255

250. Z. Ali, E. S. Fisher, J. Z. Liu, M. V. Nevitt, "Single-crystal elastic constants of Co-Al and CoFe spinels"; J. Mater. Sci. 26, 2621-2624 (1991).

251. M. Shafiq, I. Ahmad and S. Jalali Asadabadi, "Theorectical Studies of strongly correlated rare-earth intermetallics RIn_3 and RSn3 (R=Sm, Eu, and Gd)"; J. Appl. Phys. 116, 103905 (2014).

252. F. Changzeng, S. Liling, Z. Jun, J. Yuanzhi, Z. Lianyong, W. Zunjie, M. Mingzhen, L. Riping, Z. Songyan, W. Wenkui, "Valence electronic structure and cohesive property of a binary noble metal nitride"; Chinese Science Bulletin, 50, 1079-1082.S. (2005).

253. A. L. Ivanovskii, "Mechanical and electronic properties of diborides of transition *3d-5d* metals from first principles: Toward search of novel ultra-incompressible and superhard materials"; Pro. Mat. Sci. 57, 184-228 (2012).

254. O. L. Anderson, J. E. Nafe, "The bulk modulus-volume relationship for oxide compounds and related geophysical problems"; J. Geophys. Res. 70, 3951-3963 (1965).

255. N. W. Ashcroft, N. D. Mermin, *Solid State Physics*, Holt, Reinhart and Winston, New York (1976).

256. M. J. Mehl, B. M. Klein, D. A. Papaconstantopoulos, "First principles calculations of elastic properties of metals"; Intermetallic Compounds, J. H. West Brook & R. L. Fleischer , eds. John Wiley and Sons, London., 1, 195-210 (1994).

257. F. T. Docherty, A. J. Craven, D. W. McComb, J. Skakle, "ELNES investigations of the oxygen K-edge in spinels"; Ultramicroscopy, 86, 273-288 (2001).

258. M. Ustundag, M. Aslan, Battal G. Yalcin, "The first-principles study on physical properties and phase stability of Boron-V (BN, BP, Bas, BSb and BBI) compounds"; Compt. Mat. Sci. 81, 471-477 (2014).

259. E. Schreiber, O.L. Anderson, N. Soga, in: *Elastic Constants and Their Measurement,* (McGraw-Hill, pp.29-31, New York, 1973).

260. C. M. Fang, C. K. Loong, G. A. de Wijs, G. de With, "Phonon sectrum of ZnAl2O4 spinel from inelastic neutron scattering and first-principles calculations; Phys. Rev. B 66, 144301 (2002).

261. M. Ramisetty, S. Sastri, U. Kashalikar, L. M. goldman, N. Nag, "Transparent polycrystalline cubic spinels protect and defend"; Am. Ceram. Soc. Bull. 92 (2), 20-25 (2013).

262. J. A. Salem, "Transparent Armor Ceramics as spacecraft windows"; J. Am. Ceram. Soc. 96(1), 281-289 (2013).

263. O. Khasanov, E. Dvilis, A. Khasanov, E. Polisadova, A. Kachaev, "Optical and mechanical properties of transparent polycrystalline $MgAl_2O_4$ spinel depending on SPS conditions"; Phys. Status. Solidi C 10(6), 918-920 (2013).

264. A. K. Kushwaha, "Vibrational, elastic properties and sound velocities of zinc aluminate spinel"; Compt. Matt. Sci. 69, 505–509 (2013).

264A. A. Kloss, *History of Magnetism*, ISBN 978-3-8007-1878-8s, VDE-Verlag, Berlin (1994).

265. M. Blackman, "The lodestone: a survey of the history and the physics"; *Contemp.*

Phys., 24, 319 (1983).

266. J. M. Iwata, "Magnetism of complex oxide thin films and heterostructures"; Doctorate Thesis, University of California, Berkely (2012).

267. G. Shirane, D. E. Cox, S. J. Pickart, "Magnetic structures in $FeCr_2S_4$ and $FeCr_2O_4$"; Appl. Phys. 35, 954 (1964).

268. E. Schmidbauer, 'Magnetic properties of the synthetic cation deficient Fe_2TiO_4 and $FeCr_2O_4$ particles with size less than 1μm"; Phys. Chem. Min. 15, 201-207 (1987).

269. K. Ohgushi, Y. Okimoto, T. Ogasawara, S. Miyasaka, Y. Tokura, "Magnetic, optical, and magnetooptical properties of spinel-type ACr_2X_4 (A= Mn, Fe, Co, Cu, Zn, Cd; X= O, S, Se)"; Phys. Soc. Jpn. 77, 034713 (2008).

270. K. Tomiyasu, H. Hiraka, K. Ohoyama, K. Yamada, "Resonance-like magnetic excitations in spinel ferrimagnets $FeCr_2O_4$ and $NiCr_2O_4$ observed by neutron scattering"; Phys. Soc. Jpn. 77, 124703 (2008).

271. Q. Zhang, K. Singh, F. Guillou, C. Simon, Y. Breard, V. Caignaert and V. Hardy, "Ordering process and ferroelectricity in a spinel derived from FeV_2O_4"; *Physical Review B,* 85, 054405-1-10 (2012).

272. A. A. Bush, V. Ya.Shkuratov, K. E. Kamentsev, A. S. Prokhorov, E. S. Zhukova, B. P. Gorshunov and V. I. Torgashev, "Ferroelectricity in spinel solid solution $Co_{0.8}Ni_{0.2}Cr_2O_4$"; *Physical Review B,* 85, 214112-1-5 (2012).

273. A. Maignana, C. Martina, K. Singha, Ch. Simona, O.I. Lebedeva, S. Turnerb, "From spin induced ferroelectricity to dipolar galsses: Spinel chromites and mixed delafossites"; *Journal of Solid State Chemistry,* 195, 41-49 (2012).

274. D. J. Craik, *Magnetic Oxides*, John Wiley & Sons, Inc., New York (1975).

275. G. F. Dionne, *Magnetic Oxides*, Springer (2009).

276. J. M. D. Coey, *Magnetism and Magnetic Materials*, Cambridge University Press, Cambridge (2010).

277. J. M. D. Coey, M. Venkatesan, H. Xu, "Introduction to Magnetic Oxides" Chapt-1

in Functional Metal Oxides, Wiley-VCH (2013).

278. A. Petric, H. Ling, "Electrical Conductivity and Thermal Expansion of Spinels at Elevated Temperature"; *Journal of the American Ceramic Society, 90, 5, 1515-1520 (2007).*

279. Z. H. Huanga, X. Luob, S. Linb, Y. N. Huangb, L. Hub, L. Zhanga and Y.P. Suna, "Magnetic Phase diagram of Al-doped Spinel MnV_2O_4"; *Solid State Communications,* 159, 88-92 (2013).

280. W. L. Roth, "Magnetic Properties of Normal Spinels with only A-A Interactions"; *Le Journal De Physique*, 25, 507-515 (1964).

281. M. Hamedoun, M. Slimani, S. Sayouri, A. Benyoussef, "Magnetic Ordering in the Spinel compounds AB_2X_4"; Phys. Stat. Sol. (a) 144, 441-445 (1994).

282. H. Wang, Y. Yang, Y. Liang, G. Zheng, Y. Li, Y Cui, H. Dai,"Rechargeable Li-O_2 batteries with a covalently coupled $MnCo_2O_4$-graphene hybrid as an oxygen cathode catalyst"; *Energy and Environmental Science,* 5, 7, 7931-7935 (2012).

283. M. Y. Yoon, E. J. Lee, R. H. Song, H. Hwang, "Preparation and Properties of a $MnCo_2O_4$ for Ceramic interconnect of SOFC via Glycine Nitrate process"; *Metals and Materials International,* 17, 6, 1039-1043 (2011).

284. N. Padmanathan, S. Selladurai, "Mesoporous $MnCo_2O_4$ spinel oxide nanostructure synthesized by solvothermal technique for supercapacitor"; *Ionics*, 20, 4, 479 – 487 (2013).

285. S. G. Fritsch, C. Tenailleau, H. Bordeneuve, A. Rousset, "Magnetic properties of cobalt and manganese oxide spinel ceramics"; Adv. In Sc. And Technol. 67, 143-148 (2010).

286. V. Meriakri, M. Parckhomenko, S. V. Gratowski, R. N. Bhowmik, I. P. Muthuselvam, "Structural phase stability, magnetism and microwave properties of Co_2FeO_4 spinel oxide"; J. Phys. Conf. Series. 200, 082024 (2010).

287. I. P. Muthuselvam, R. N. Bhowmik, "Structural phase stability and magnetism in Co_2FeO_4 oxide"; Solid. Stat. Sc. 11, 719 (2009).

288. G. Blasse, "New Type of Superexchange in the Spinel Structure Some Magnetic Properties of Oxides $Me^{2+}Co_2O_4$ and $Me^{2+}Rh_2O_4$ with Spinel Structure"; *Philips Res. Repts., 18*, 383-392 (1963).

289. F. K. Lotgering, "On the Ferrimagnetism of Some Suphides and Oxides: 3. Oxygen and Sulphur Spinels Containing Cobalt (MCo_2O_4 and MCo_2S_4)"; *Phililps Res. Repts., 11*, 337-350 (1956).

290. J. S. McCloy, W. Jiang, W. Bennett, M. H. Engelhard, J. Lindemuth, N. S. Parmar, G. J. Exarhos, "Electrical and Magnetic Properties Modification in Heavy Ion Irradiated Nanograin $Ni_xCo_{(3-x)}O_4$ Films"; J. Phys. Chem. C. 119 (39). 22465-22476 (2015).

291. P. Silwal, L. Miao, I. Stern, X. Zhou, J.Hu, D. H. Kim, "Metal Insulator Transition with Ferrimagnetic Order in Epitaxial Thin Films of Spinel $NiCo_2O_4$"; *Appl. Phys. Lett., 100*, 032102 (2012).

292. Y. Zhang, H. X. Yang, C. Ma, H. F. Tian, J. Q. Li, "Charge-Stripe Order in the Electronic Ferroelectric $LuFe_2O_4$"; Phys. Rev. Lett. 98, 247602 (2007).

293. Y. Yamada, K. Kitsuda, S. Nohdo, N. Ikeda, 'Charge and spin ordering process in the mixed-valence system LuFe2O4: Charge ordering'; Phys. Rev. B 62, 12167 (2000).

294. Y. Yamada, S. Nohdo, N. Ikeda, 'Incommensurate Charge Ordering in Charge-Frustrated $LuFe_2O_4$ System"; Phys. Soc. Jpn. 66, 3733-3736 (1997).

295. H. J. Xiang, M. H. Whangbo, 'Charge Order and the Origin of Giant Magnetocapacitance in $LuFe_2O_4$"; Phys. Rev. Lett. 98, 246403 (2007).

296. Y. Yamasaki, S. Miyasaka, Y. Kaneko, J. P. He, T. Arima, Y. Tokura, "Magnetic Reversal of the Ferroelectric Polarization in a Multiferroic Spinel Oxide"; Phys. Rev. Lett. 96, 207204 (2006); Erratum Phys. Rev. Lett. 96, 249902 (2006).

297. B. B. V. Aken, T. T. M. Palstra, "Influence of magnetic on ferroelectric ordering in $LuMnO_3$" Phys. Rev. B 69, 134113 (2004).

298. R. J. Harrison, A. Putnis, "The magnetic properties and crystal chemistry of

oxide spinel solid solutions"; Surveys in Geophysics. 19, 461-520 (1999).

299. M. A. Carpenter, R.A. Powell, E. K. H. Salje, "Thermodynamics of nonconvergent cation ordering in minerals: I. An alternative approach"; *Amer. Miner.* 79, 1053–1067 (1994).

300. M. A. Carpenter, E. Salje, "Time-dependent Landau theory for order/disorder processes in minerals"; *Miner. Mag.* 53, 483–504 (1989).

301. R. J. Harrison, A. Putnis, "Magnetic properties of the magnetite-spinel solid solution: Saturation magnetization and cation distributions"; *Amer. Miner.* 80, 213–221 (1995).

302 R. J. Harrison, A. Putnis, "Magnetic properties of the magnetite-spinel solid solution: Curie temperatures, magnetic susceptibilities and cation ordering" *Amer. Miner.* 81, 375–384 (1996).

303. R. J. Harrison, A. Putnis, "The interaction between exsolution microstructures and magnetic properties of the magnetite-spinel solid solution"; *Amer. Miner.* 82, 131–142 (1997).

304. R. J. Harrison, A. Putnis, "The coupling between magnetic and cation ordering: A macroscopic approach"; *Europ. J. of Miner.* 9, 1115-1130 (1997).

305. M. A. Carpenter, E. K. H. Salje, "Thermodynamics of nonconvergent cation ordering in minerals: II. Spinels and the orthopyroxene solid solution', *Amer Miner.* 79, 1068–1083 (1994).

306. M. A. Carpenter, E. K. H. Salje, "Thermodynamics of nonconvergent cation ordering in minerals: III. Order parameter coupling in potassium feldspar"; *Amer. Miner.* 79, 1084–1098 (1994).

306. C. L. Muhich, B. W. Evanko, K. C. Weston, P. Lichty, X. Liang, J. Martinek, C. B. Musgrave, A. W. Weimer, "Efficient Generation of H_2 by Splitting Water with an Isothermal Redox Cycle"; *Science.* 341, 540-542 (2013).

307. L. Neel, "Magnetic Properties of ferrites: ferrimagnetism and antiferromagnetism"; Ann. Phys. Paris. 3, 137-98 (1948).

308. G. Blasse, "Crystal chemistry and some magnetic properties of mixed metal oxides with spinel structure"; *Philips Research Reports Supplements* 3, 1–139 (1964).

309. M. Kucab, *Magnetic Space Groups of Magnetic Structures Determined by Neutron Diffraction, Institute of Nuclear Technics (Cracow) Report* 25/PS, (1972).

310. C. A. Wert, R. M. Thomson, Physics of Solids, 2nd Ed. Materials Science and Engineering Series, McGraw-Hill New York (1970).

311. P. K. Blatzer, P. J. Wojtowicz, M. Robbins, E. Lopatin, "Exchange interactions in Ferromagnetic chromium chalcogenide spinels"; Phys. Rev. 151, 367-377 (1966).

312. T. Rudolf, C. Kant, F. Mayer, J. Hemberger, V. Tsurkan, A. Loidl, "Spin-phonon coupling in antiferromagnetic chromium spinels'; New J.Phys 9, 76 (2007).

313. B. C. Melot, J. E. Drewes, R. Seshadri, E. M. Stoudenmire, A. P. Ramirez, "Magnetic phase evolution in the spinel compounds $Zn_{1-x}Co_xCr_2O_4$"; J. Phys. Condesn. Matter, 21, 216007 (2009).

314. R. Moessner, A. P. Ramirez, "Geomeical Frustration"; Phys. Today. 59, 24 (2006).

315 B. G. Levin"New candidate emerges for a quantum spin liquid"; *Phys. Today*, 60, 16 (2007).

316. S. H. Lee, H. Takagi, D. Louca, M. Matsuda, S. Ji, H. Ueda, Y. Ueda, T. Katsufuji, J. H. Chung, S. Park, S. W. Cheong, C. Broholm "Frustrated magnetism and cooperative phase transitions in spinels"; *J. Phys. Soc. Jpn*, 79, 011004 (2010).

317. J. E. Mitchell, "Synthesis and Magnetic Properties of Spinel-based Transition Metal Oxides and related species"; Master Thesis, McMaster University Hamilton, Ontario (2009).

318. M. C. Kemei, P. T. Barton, S. L. Moffitt, M. W. Gaultois, J. A. Kurzman, R. Seshadri, M. R. Suchomel, Y. Kim, "Crystal structures of spin-Jahn-Teller-ordered $MgCr_2O_4$ and $ZnCr_2O_4$"; *J. Phys.: Condens. Matter*, 25(32), 326001 (2013).

319. K. Rabia, "Structural and optical properties of transition-metal compounds under pressure"; PhD Thesis, University of Augsburg Germany (2012).

320. A. P. Ramirez, "Strongly geometrically frustrated magnets"; Annu. Rev. Mater. Sci, 24, 453-480 (1994).

321. T. Kimura, "Spiral magnets as manetoelectrics"; Annu. Rev. Mater. Res. 37, 387-

413 (2007).

322. R. N. Bhowmik, R. Ranganathan, "Super-ferromagnetic" clusters in spinel oxide"; J. Mag. Mag. Mater. 247, 83-91 (2002).

323. G. M. Kalvius, A. Krimmel, O. Hartmann, F. J. Litterst, R. Wappling, V. Tsurkan, A. Loidl, "Magnetism of frustrated A-site spinels (Mn, Fe, Co)Al_2O_4"; Phys.Rev. B: Cond. Mater. 404, 660-662 (2009).

324. J. H. Park, L. H. Tjeng, J. W. Allen, P. Metcalf, C. T. Chen, "Single-particle gap above the Verwey transition in Fe_3O_4"; Phys. Rev. B 55, 12813-12817 (1997).

325. M. Schmidt, Z. Wang, C. Kant, F. Mayr, S. Toth, A. T. M. N. Islam, B. Lake, V. Tsurkan, A. Loidl, J. Disendhofer, "Exciton-magnon transitions in the grustrated chromium antiferromagnets CuCrO2, α-CaCr2O4, CdCr2O4, and ZnCr2O4"; Phys. Rev B. 87, 2244241-13 (2013).

326. T. A. Kaplan, "Classical spin-configuration stability in the presence of competing exchange forces"; Phys. Rev. 116, 888 (1959); Erratum Phys. Rev. B 79, 229901 (2009).

327. E. Prince, "Crystal and Magnetic structure of copper chromite"; Acta Crystallogr. 10, 554 (1957).

328. A. P. Ramirez, in Handbook of Magnetic Materials, edited by K. J. H. Busch (Elsevier Science, Amsterdam, 2001).

329. F. Nori, A. Tonomura, "Helical spin order on the move"; Science. 311, 344-345 (2006).

330. A. V. Ramos, M. J. Guittet, J. B. Moussy, R. Mattana, C. Deranlot, F. Petroff, C. Gatel, "Room temperature spin filtering in epitaxial cobalt-ferrite tunnel barriers"; Appl. Phys. Lett. 91, 122107 (2007).

331. N. Nishiguchi, M. Onoda, "A pseudotetramer in the geometrically frustrated spinel system CdV_2O_4"; Phys: Condens. Matter 14, L551–L557 (2002).

332. T. Rudolf, C. Kant, F. Mayr. J. Hemberger, V. Tsurkan, A. Loidl, "Spin-phonon coupling in antiferromagnetic chromium spinels"; New J. of Physics. 9, 76 (2007).

333. H. Ueda, H. A. Katori, H. Mitamura, T. Goto, H. Takagi, "Magnetic-field induced

transition to the 1/2 magnetization plateau state in the geometrically frustrated magnet $CdCr_2O_4$"; Phys. Rev. Lett. 94, 047202 (2005).

334. C. Kant, J. Deisenhofer, T. Rudolf, F. Mayer, F. Schrettle, A. Loidl, "Optical phonons, spin correlations, and spin-phonon coupling in the frustrated pyrochlore magnets $CdCr_2O_4$ and $ZnCr_2O_4$"; Phys. Rev B. 80, 214417 (2009).

335. V. Tsurkan, J. Hemberger, A. Krimmel, H.-A. K. von Nidda, P. Lunkenheimer, V. Z. S. Weber, A. Loidl, "Experimental evidence for competition between antiferromagnetic and ferromagnetic correlations in$HgCr_2S_4$"; Phys. Rev. B 73, 224442 (2006).

336. N. Menyuk, K. Dwight, R. J. Arnott, "Ferromagnetism in $CdCr_2S_4$ and $CdCr_2Se_4$"; Appl. Phys. 37, 1387 (1966).

337. P. K. Baltzer, P. J. Wojtowicz, M. Robbins, E. Lopatin, "Exchange interactions in ferromagnetic chromium chalcogenide spinels"; Phys. Rev. 151, 367 (1966).

338. Frederick Wooten, *Optical Properteis of Solids*. ACADEMIC PRESS, New York and London (1972).

339. A. Bouhemadou, S. Al-Essa, D. Allali, S. Binomran"Electronic and optical properties of $ZnSc_2S_4$ and $CdSc_2S_4$ cubic spinels by the modified Becke-Johnson density functional"; Sol. St. Sci. 20, 127-134 (2013).

340. D. Segev, S. H. Wei "Structure-derived electronic and optical properties of transparent conducting oxides"; Phys. Rev. B. 71, 125129 (2005)

341. K. L. Chopra, S. Major, D. K. Pandya, "transparent conductors"; Thin Solid Films 102, 1-46 (1983). DOI: doi.org/10.1016/0040-6090(83)90256-0

342. Y. Ayeb, T. Ouahrani, R. Khenata, Ali H. Reshak, D. Rached, A. Bouhemadou, R. Arrar, "FP-LAPW investigation of structural, electronic, linear and nonlinear optical properties of $ZnIn_2Te_4$ defect-chalcopyrite"; Comput. Mater. Sci, Vol 50(2), 651-655 (2010).

343. N. Chasserio, B. Durand, S. Guillemet, A. Rousset, "*Mixed manganese spinel oxides: optical properties in the infrared range*"; J. of Mat. Sci. 42 (n° 3). 794-800. ISSN 0022-

2461 (2007).

344. R. D. Shannon, R. C. Shannon, O. Medenbach, R. X. Fischer, "Refractive Index and Sispersion of Fluorides and Oxides" ; J. Phys. Chem. 31 (4), 931-970 (2002).

345. T. J. Mroz, T. M. Hartnett, J. M. Wahl, L. M. Goldman, J. Kirsch, W. R. Lindberg, "Recent Advances in Spinel Optical Ceramic"; *Proc. SPIE* 5786, Window and Dome Technologies and Materials IX, 64 (June 22, 2005); doi:10.1117/12.607593

346. E. Hanamura, Y. Kawabe, H. Takashima, T. Sato, A. Tomita, "Optical properties of transition metal doped spinels"; Nonlinear Optic. Phys. Mat. 12, 467 (2003).

347. K. A. Wickersheim, R. A. Lefever, "Optical Properteis of Synthetic Spinel"; J. of Opt. Soc. Of Am. 50 (8), 831-832 (1960).

348. C. C. Wang, P. J. Zanzucchi, "Dielectric and Optical properties of Stoichiometric Magnesium Aluminate Spinel Single Crystals"; J. of Elect. Chem. Soc. 118(4), 586-590 (1971).

349. A. F. Dericioglu, A. R. Boccaccini, I. Dlouhy, Y. kagawa, "Effect of Chemical Composition on the Optical Properties and Fracture Toughness of Transparent Magnesium Aluminate Spinel Ceramics"; Mat. Trans. 46, 5, 996-1003 (2005).

350. N. M. Ulmane, V. Skvortsova, A. Smirnovs, D. Riekstinya, "Optical properties of laser spinel"; SPIE. 2967, 24- 29 (1997).

351. S. Jiang, T. Lu, Y. Long, J. Chen, "Ab initio many-body study of the electronic and optical properties of $MgAl_2O_4$ spine"; J. of Applied Phys. 111, 043516 (2012).

352. V. Zviagin, P. Richter, T. Bontgen, M. Lorenz, M. Ziese, D. R. T. Zahn, G. Salvan M. Grundmann, R. S. Grund, "Comparative study of optical and magneto-optical properties of normal, disordered, and inverse spinel-type oxides";Phys. Status Solidi B. 253(3), 429-436 (2016).

353. A. Rahman, M. S. Charoo, R. Jayaganthan, "structural, optical and photocatalytic properties of zinc aluminate spinel nanoparticles"; Mat. Tech: Adv. Perform. Mater. 30, 168-176 (2015).

354. M. Arbi, N. Benramdane, Z. Kebbab, R. Miloua, F. Chiker, R. Khenata, “First principles calculations of structural, electronic and optical properties of zinc aluminum oxide”; Mat. Sc in semiconduct. Proc. 15, 301-307 (2012).

355. C. M. Fang, C. K. Loong, G. A. de Wijs, G. de With, “Phonon spectrum of $ZnAl_2O_4$ spinel from inelastic neutron scattering and first-principles calculations”; Phys. Rev. B 66, 144301 (2002).

356. D. Fabian, T. Psch, H. Mutschke, f. Kershbaum, J. dorschner, “A study of the carrier of the 13, 17 and 32 μm emission features observed in ISO-SWS spectra of oxygen-rich AGB stars”; Astonomy & Ast. Phys. 373, 1125-1138 (2001).

357. M. G. Brik, “First Principles calculations of electronic, optical and elastic properties of $ZnAl_2O_4$ and $ZnGa_2O_4$”; J. Phys. & Chem. of Solids. 71, 1435-1442 (2010).

358. S. Z. Karazhanov and P. Ravindran, "Ab Initio Study of double oxides ZnX_2O_4 (X=Al, Ga, In) having spinel structure," Am. Cerm. Soc. 93, 3335–3341, (2010).

359. K. M. Krishna, M. Nisha, R. Reshmi, R. Manoj, A. S. Asha, M. K. Jayaraj, "Electrical and optical properties of $ZnGa_2O_4$ thin films deposited by pulsed laser deposition," Mat. Foru. 29, 243 (2005).

360. S. E. Dali, M. Jayachandran, M. J. Chockalingam, “New transparent electronic conductor, $MgIn_2O_4$ spinel”; J. of Mater. Sci. Let. 18, 915-917 (1998).

361. A. Bouhemeadou, R. Khenata, D. Rached, F. Zerarga and M. Maamache, “Structural, electronic and optical properties of spinel oxides: cadmium Gallate and cadmium indate”; Eur. Phys. J. App. Phys. 38, 203-221 (2007).

362. N. Ichinose, “Elecronic ceramics for sensors”; Am. Ceram. Soc. Bull. 64, 1581-1585 (1985).

363. M. Alvaro, F. Nestola, N. Ross, M. C. Domeneghetti and L. Reznitsky, “High-pressure behavior of thiospinel $CuCr_2S_4$”; Ame. Min. Soc. 99, 908-913 (2014).

364. G. Baudin, R. Martinez, P. Pena, “High-temperature mechanical behavior of

stoichiometric magnesium spinel"; J. Am. Ceram. Soc., 8(7), 1857-1862 (1995).

365. R. D. Maschio, B. Fabbri, C. Fiori, "Industrial applications of refractories containing magnesium aluminate spinel"; Industrial Ceramics. 8 (2), 121–126 (1988).

366. M. A. Sainz, A. Mazzoni, E. Aglietti, A. Caballero, "Thermochemical formation and Stability of spinel under strongly reducing conditions"; Proc. UNITESR'97, pp. 387-392 (1995).

367. K. T. Jacob, K. P. Jayadevan, R. M. Mallya, Y. Waseda, "Nanocrystalline $MgAl_2O_4$: Measurement of Thermodynamic Properties Using a Solid State Cell"; Adv. Mater. 12, 440 (2000).

368. L. R. Ping, A. M. Azad, T. W. Dung, "Magnesium aluminate (MgAl2O4) spinel produced via self-heat-sustained (SHS) technique"; Mater. Res. Bullet. 36, 1417-1430 (2001).

369. C. Baudin, R. Martínez, and P. Pena, "High-Temperature Mechanical Behavior of Stiochiometric Magnesium Spinel"; J. Am. Ceram. Soc. 78, 1857-1862 (1995).

370. J. Wrzyszcz, M. Zawadzki, J. Trawczynski, H. Grabowska, W. Mista, ''Some Catalytic Properties of Hydrothermally Synthesised Zinc Aluminate Spinel''; Appl. Catal. A: Gen., 210, 263–9 (2001).

371. G. Aguilar-Ros, M. A. Valenzuela, H. Armendariz, P. Salas, J. M. Dominguez, D. R. Acosta, I. Schifter, "'Metal–Support Effects and Catalytic Properties of Platinum Supported on Zinc Aluminate"; Appl. Catal. A: Gen., 90, 25–34 (1992).

372. I. A. P. S. Murthy, C. S. Swamy, "Catalytic Behavior of Nickel Aluminate ($NiAl_2O_4$) Spinel upon Hydrogen Treatment"; J. Mater. Sci., 28, 1194 (1993).

373. L. Ji, S. Tang, H. C. Zeng, J. Lin, K. L. Tan, "CO_2 reforming of methane to synthesis gas over so-gel-made Co/γ-Al_2O_3 catalysts from organometallic precursors"; Appl. Catal. Gen. 207, 247-255 (2001).

374. R. I. Bel'skaya, E. V. Karpinchik, V. S. Komarov, M. D. Efros, "Catalytic Activity of Copper–Aluminum Spinel in Cyclohexanol Dehydrogenation"; Dokl. Akad.

Nauk BSSR, 19, 901-4 (1975).

375. W. S. Tzing, W. H. Tuan," The strength of duplex Al_2O_3-$ZnAl_2O_4$ composite "; J. Mater. Sci. Lett. 15, 1395-1396 (1996).

376. H. Grabowska, M. Zawadzki, J. Wrzyszcz, "Performance of CuO/Zn Al_2O_4–Al_2O_3 Catalysts in n-Hexanol Conversion"; Polish J. Chem., 77, 779–87 (2003).

377. T. K. Shioyama, "Alcohol Dehydration Employing a Zinc Aluminate Catalyst"; U.S. Patent 4, 260, 845, 1981.

378. L. R. Cobb, "Preparation of Polymethylbenzenes"; U.S. Patent 4, 568, 784, 1985.

379. M. B. Welch, "Zinc Aluminate Double Bond Isomerization Catalyst and Process for its Production"; U.S. Patent 4, 692, 430, 1986.

380. T. Numaguchi, H. Eida, K. Shoji, "Reduction of $NiAl_2O_4$ Containing Catalysts for Steam Methane Reforming Reaction"; Int. J. Hydrogen Energy, 22, 1111–1115 (1997).

381. F. Le Peltier, P. Chaumette, J. Saussey, M. M. Bettahar, J. C. Lavalley, "In-Situ FT-IR Spectroscopy and Kinetic Study of Methanol Synthesis from CO/ H_2 Over Zn Al_2O_4 and Cu–Zn Al_2O_4 Catalysts"; J. Mol. Catal. A: Chem., 122, 131–139 (1997).

382. R. Roesky, J. Weiguny, H. Bestgen, U. Dingerdissen, "An Improved Synthesis Method for Indenes and Styrenes by Use of a ZnO/ Al_2O_3 Spinel Catalyst"; Appl. Catal. A: Gen., 176, 213–20 (1999).

383. M. Zawadzki, J. Wrzyszcz, W. Strzek, D. Hreniak,"Preparation andoptical properties of nanocrystalline and nanoporous Tb doped alumina and zinc aluminate"; J. Alloys Compd. 323–324, 279-282 (2001).

384. P. F. Schubert, D. H. Kubicek, D. R. Kidd, "Preparation of Dehydrogenating Catalyst"; U.S. Patent 5, 151, 401, 1992.

385. G. Khare, R. A. Porter, "Platinum and Tin-Containing Catalyst and Use Thereof in Alkane Dehydrogenation"; U.S. Patent 5, 430, 220, 1995.

386. P. Lingyu, L. Yongdan, C. Jiuling, C. Liu, Y. S. Lin Jerry, "Methane Decomposition to Carbon Nanotubes and Hydrogen on an Alumina Supported

Nickel Aerogel Catalyst"; Catal. Today, 74, 145–55 (2002).

387. G. Baldi, D. Bonacchi, C. innocent, G. Lorenzi, C. J. Sangregorio, "Cobalr ferrite nanoparticles: The control of the particle size and surface state and their effects on magnetic properties"; J. Magn. Magn. Mater. 311, 10-16 (2007).

388. S. Bedanta, W. Kleemann, "Supermagnetism," Phys. D: Appl. Phys. 42, 013001 (2009).

389. R. Y. Hong, J. H. Li, S. Z. Zhang, G. Q. Di, H. Z. Li and D. G. Wei, "On the $Fe_3O_4/Mn_{1-x}Zn_xFe_2O_4$ core/shell magnetic nanoparticles," Alloy. Comp. 480, 947 (2009).

390. A. I. Kingon, J. Maria and S. K. Streiffer, "Review article Alternative dielectrics to silicon dioxide for memory and logic devices"; Nature 406, 1032-1038 (2000).

391. C. C. Wang, F. C. Dougherty, P. J. Zanzucchi and S. H. Mcfarlane, "Epitaxial Growth and Properties of GaAs on Magnesium Aluminate Spinel"; Electrochem. Soc. 121, 571-82 (1974).

392. Z. Branković, G. Branković, D. Poleti and J. A. Varela, "Structural and electrical properties of ZnO varistors containing different spinel phases," Ceram. Int. 27, 115-122 (2001).

393. B. Tan , E. Toman , Y. Li , and Y. Wu, "Zinc stannate (Zn_2SnO_4) dye-sensitized solar cells"; Am. Chem. Soc. *129*, 4162–4163 (2007).

394. A. Sutka, G. Mezinskis, G. Strikis and A. Siskin, "Gas sensitivity of stoichiometric and excess-iron Ni-Zn ferrite prepared by sol-gel auto-combustion"; Energetika 58, 166–172 (2012).

395. J. E. Pippin, "Frequency Doubling and mixing ferrites"; *Proc. IRE* 44, 1054-1055 (1956).

396. D. R. Brown, E. A. Schoenberg, "Ferrites Speed Digital Computers"; Electronics. 26(4), 146-149 (1953).

397. S. Yamamoto, K. Hirata, H. Krisu, M. Matsuura, T. Doi, K. Tamari, "Preparation and magnetic properties of ferrite thin-film media"; IEICE Trans. Elect. E84-C, 9,

f1142-1146 (2001).

398. R. Chandrasekhar, S. W. Charles, K. O'Grady, "Cobalt ferrite fluids and their application to magnetic in k-jet printing"; J. Imaging Tech. 13, 55-59 (1987).

399. G. S. Huff, C. N. Satterfield, "Intrinsic Kinetics of the Fischer-Tropsch Synthesis on a Reduced Fused-Magnetite Catalyst"; *Ind. Engin. Chem. Process Design and Development.* 23, 696-705 (1984).

400. M. Tinkle, J. Dumesic, "Isotopic Exchange Measurements of the Rates of Adsorption/Desorption and Interconversion of CO and CO_2 over Chromia-Promoted Magnetite: Implications for Water-Gas Shift"; *J. Cat.* 103, 65-78 (1987).

401. M. Kotani, T. Koike, J. Yamaguchi, N. Mizuno, "Ruthenium Hydroxide on Magnetite as a Magnetically Separable Heterogeneous Catalyst for Liquid-Phase Oxidation and Reduction"; *Green Chem.* 8, 735-741 (2006).

402. B. Jang, M. Park, O.B. Chae, S. Park, Y. Kim, S. M. Oh, Y. Piao, T. Hyeon, "Direct Synthesis of Self-Assembled Ferrite/Carbon Hybrid Nanosheets for High Performance LithiumIon Battery Anodes"; *JACS.* 134, 15010-15015 (2012).

403. E. A. Fletcher, R. L. Moen, "Hydrogen- and Oxygen from Water"; *Science.* 197, 1050-1056 (1977).

404. K. Svoboda, A. Siewiorek, D. Baxter, J. Rogut, M. Pohorely, "Thermodynamic Possibilities and Constraints for Pure Hydrogen Production by a Nickel and Cobalt-Based Chemical Looping Process at Lower Temperatures"; *Energy Conversion and Manag.* 49, 221-231 (2008).

405. M. D. Allendorf, R. B. Diver, N. P. Siegel, J. E. Miller, "Two-Step Water Splitting Using Mixed-Metal Ferrites: Thermodynamic Analysis and Characterization of Synthesized Materials"; *Energy & Fuels.* 22, 4115-4124 (2008).

407. Y. L. Kuo, W. M. Hsu, P. –C. Chiu, Y. –H. Tseng, Y. Ku, "Assessment of Redox Behavior of Nickel Ferrite as Oxygen Carriers for Chemical Looping Process"; *Ceramics Inter.* 39, 5459-5465 (2013).

408. C. L. Muhich, B. D. Ehrhart, V. A. Witte, S. L. Miller, E. N. Coker, C. B.

Musgrave, A. W. Weimer, "Predicting the Solar Thermochemical Water Splitting Ability and Reaction Mechanism of Metal Oxides: A Case Study of the Hercynite Family of Water Splitting Cycles"; *Energy & Environ. Science.* 8, 3687-3699 (2015).

409. C. L. Muhich, B. D. Ehrhart, I. Al-Shankiti, B. J. Ward, C. B.; Musgrave, A. W. Weimer, "A Review and Perspective of Efficient Hydrogen Generation Via Solar Thermal Water Splitting"; *Wiley Interdisciplinary Reviews: Energy & Environ. 5, 261-287 (2016). DOI: 10.1002/wene.174*
410. K. Maaz, M. Usman, S. Karim, A. Mumtaz, S. K. Hasanain and M. F. Bertino, "Magnetic response of core-shell cobalt ferrite nanoparticles at low temperature," Appl. Phys. 105, 113917 (2009).
411. E. E. Platero, C. O. Area´n CO, J. B. Parra, "Synthesis of high surface area $CoAl_2O_4$ and $NiAl_2O_4$ spinels by an Alkoxide route"; Res. Chem. Intermed 25, 187-194 (1999).
412. J. Merikhi, H. O. Jungk, C. Feldmann, "Sub-micrometer $CoAl_2O_4$ pigment particles Ð synthesis and preparation of coatings"; J. Mater. Chem. 10, 1311 (2000).
413. W. Schmidt, C. Weidenthaler, "Nanosized Transition Metal Spinels with High Surface Areas from Zeolite Precursors"; Chem. Mater. 13, 607 (2001).
414. M. Salavati-Niasari, F. Davar, M. Mazaheri, "Synthesis of Mn_3O_4 nanoparticles by thermal decomposition of a [bis(salicylidiminato)manganese(II)] complex"; Polyhedron 27, 3467-3471 (2008).
415. M. Salavati-Niasari, F. Davar, M. Mazaheri, M. Shaterian, "Preparation of cobalt nanoparticles from [bis(salicylidene)cobalt(II)]–oleylamine complex by thermal decomposition"; J. Magn. Magn. Mater. 320, 575-578 (2008).
416. M. Salavati-Niasari, F. Davar, M. Mazaheri, "Preparation of ZnO nanoparticles from [bis(acetylacetonato)zinc(II)]–oleylamine complex by thermal decomposition"; Mater. Lett. 62, 1890-1892 (2008).
417. M. Salavati-Niasari, F. Davar, Z. Fereshteh, "Synthesis and characterization of

ZnO nanocrystals from thermolysis of new precursor"; Chem. Eng. J. 146, 498-502 (2009).

418. M. Salavati-Niasari, F. Davar, "Synthesis of copper and copper(I) oxide nanoparticles by thermal decomposition of a new precursor"; Mater. Lett. 63, 441-443 (2009).

419. E. De Bie, P. Doyen, "Cobalt oxides and salts"; Cobalt. 15, 3-13 and 16, 3-15 (1962).

420. D. A. Fumo, M. R. Morelli, A. M. Segadaes, "Combusion synthesis of calcium aluminates"; Mater. Res. Bull. 31, 1243-1255 (1996).

421. D. Segev, S. H. Wei, "Structure-derived electronic and optical properties of transparent conducting oxides" Phys. Rev. B 71, 125129 (2005).

422. V. Ciupina, I. C. Popo, G. Prodan, "Characteristics of $ZnAl_2O_4$ Nanocrystals Prepared by Coprecipitation and Microemulsion"; Optoelectron. Adv. Mat. 6(4), 1317 (2004).

423. M. A. L. Marques, E. K. U. Gross, "Time Dependent Density Functional Theory"; Annu. Rev. Phys. Chem.. 55, 427-55 (2004).

424. A. J. Freeman, E. Wimmer, "Density Functional Theory as a major tool in computational material sciences"; Annu. Rev. Mater. Sci., 25, 7-25, (1995)

425. W. E. Pickett, "Density Functional in Solids: I. Ground State"; Comments on Solid State Phys. 12, 1 (1985).

426. D. R. Hartree, 'The wave mechanics of an atom with a non-Coulomb central field. Part II. Some results and discussion"; Proc. Cam. Phil. Soc. 24, 89 (1928).

427. F. Neese, "Efficient and accurate approximations to the molecular spin-orbit coupling operator and their use in molecular-tensor calculations"; Chem. Phys. 122, 034107 (2005).

427 A. S. Gurung, "Introduction to band structure calculations using the LAPW method"; Sci Vis. 12(3), 97-101 (2012).

428. P. Geerlings, F. D. Proft, W. Langenaeker, "Conceptual Density Functional

Theory"; Chem. Rev. 103, 1793-1873 (2003).

429. L. H. Thomas, "The calculation of atomic fields"; *Proc. Cambridge Phil. Soc.* 23, 542 (1927).

430. E. Z. Fermi, "Eine statistische Methode zur Bestimmung einiger Eigenschaften des Atoms und ihre Anwendung auf die Theorie des periodischen Systems der Elemente"; *Z. Phys. 48*, 73-79 (1928).

431. P. A. M. Dirac, "Note on Exchange Phenomena in the Thomas Atom"; *Proc. Cambridge Philos. Soc. 26*, 376-385 (1930).

432. C. F. Z. V. Weiszacker, "Zur Theorie der Kernmassen (On the theory of nuclear masses); Zeitschrift fur Physik ; (J. *Phys.) 96*, 431-458 (1935).

433. J. C. Slater, "A simplification of the Hartree-Fock method"; *Phys. Rev. 81*, 385-390 (1951).

434. J. C. Slater, "Statistical exchange-correlation in the selfconsistent field"; *Adv. Quantum Chem. 6*, 1-92 (1972).

435. J. C. Slater, *The Self-Consistent Field for Molecules and Solids*; Mc Graw Hill: New York, 1974.

436. E. J. Baerends, "Perspective on "Self-consistent equations including exchange and correlation effects"; *Theor. Chem. Acc. 103*, 265-269 (2000).

437. M. J. Frisch, G. W. Trucks, H. B. Schlegel, G. E. Scuseria, M. A. Robb, J. R. Cheeseman, V. G. Zakrzewski, J. A. Montgomery, R. E. Jr.; Stratmann, J. C. Burant, S. Dapprich, J. M. Millam, A. D. Daniels, K. N. Kudin, M. C. Strain, O. Farkas, J. Tomasi, V. Barone, M. Cossi, R. Cammi, B. Mennucci, C. Pomelli, C. Adamo, S. Clifford, J. Ochterski, G. A. Petersson, P. Y. Ayala, Q. Cui, K. Morokuma, D. K. Malick, A. D. Rabuck, K. Raghavachari, J. B. Foresman, J. Cioslowski, J. V. Ortiz, B. B. Stefanov, G. Liu, A. Liashenko, P. Piskorz, I. Komaromi, R. Gomperts, R. L. Martin, D. J. Fox, T. Keith, M. A. Al-Laham, C. Y. Peng, A. Nanayakkara, C. Gonzalez, M. Challacombe, P. M. W. Gill, B. G. Johnson, W. Chen, M. W. Wong, J. L. Andres, M. Head-Gordon, E. S. Replogle, J.

A. Pople, *Gaussian 98*; Gaussian Inc.: Pittsburgh PA, (1998).

438. C. C. J. Roothaan, "New Developments in Molecular Orbital Theory"; J. *Rev. Mod. Phys. 23*, 69 (1951).

439. C. Moller, M. S. Plesset, "Note on an Approximation Treatment for Many-Electron Systems"; *Phys. Rev. 46*, 618 (1934).

440. I. Shavitt, The Method of Configuration Interaction. In *Methods of Electronic Structure Theory*; Schaefer, H. F., III, Ed.; Modern Theoretical Chemistry 3; Plenum Press: New York and London, 1977;

441. R. J. J. Bartlett, "Coupled-cluster approach to molecular structure and spectra: a step toward predictive quantum chemistry"; *Phys. Chem. 93*, 1697-1708 (1989).

442. W. J. Hehre, L. Radom, P. V. R. Schleyer, J. A. Pople, *Ab Initio Molecular Orbital Theory*; Wiley: New York, 1986.

443. F. Jensen, *Introduction to Computational Chemistry*; Wiley: New York, 1999.

444. A. Szabo, N. S. Ostlund, "Modern quantum chemistry: Introduction to advanced electronic structure theory"; MacMillan Publishing Co., New York (1982).

445. T. Helgaker, P. Jørgenson, J. Olsen, J. *Molecular Electronic Structure Theory*; John Wiley: New York, 2000.

446. D. Baye, P. Capel, G. Goldstein, "Higher-order resolution of the time-dependent schordinger equation"; Proceedings of the International Symposium 19-22 Nov 2003, as appeared in '*A New Era of Nuclear Structure Physics*; World Scientific Publishing Co. Pte. Ltd. Singapore (2004).

447. A. B. Migadal, *Theory of Finite Fermi Systems and Applications to Atomic Nuclei (Interscinece, New York, 1967).*

448. J. W. Negele, "Structure of Finite Nuclei in the Local-Density Approximation"; Phys. Rev. C 1, 1260-1321 (1970).

449. J. W. Negele, "Density-Matrix Expansion for an Effective Nuclear Hamiltonian"; D. Vautherin, Phys. Rev. C 5, 1472-1493 (1972).

450. *M. Brack, R. K. Bhaduri,* Semicalssical Physics *(Addison Wesley, Reading (1997).*

451. E. Schrodinger, "Uber das Verhaltnis der Heisenberg-Born-Jordanschen Quantenmechanik zu der meinem, "Annalen der Physik 384, 734-756 (1926).
452. M. Born, R. Oppenheimer, “Zur Quantentheorie derMoleke ln”; Ann. Phys. (Leipzig) 84, 457-484 (1927).
453. K. Capelle, “A bird’s-eye view of Density-Funational Theory”; Braz. J. Phys. 36, 4A, 1318-1343 (2006).
454. W. Ritz, “Ueber eine neue Methode zur Lsung gewixxer Variations problem der mathematischen Physik”; J. Reine Angew. Math. 135, 161 (1908).
455. V. Fock, “Näherungsmethode zur Lösung des quantenmechanischen Mehrkörperproblems”; Z. Phys. 61, 126–148 (1930).
456. J. C. Slater, “Note on Hartree’s method”; Phys. Rev. 35, 210–211 (1930).
457. J. C. Slater, “The theory of complex spectra”; Phys. Rev. 34, 1293–1322 (1929).
458. F. Bloch, “Bemerkung zur Elektronentheorie des Ferromagnetismus und der elektrischen Leitfähigkeit”; Z. Phys. 57, 545–555 (1929).
459. Gombas, Die Statischtische Theorie des Atoms und lhre Anwendungen; Springer Verlag, Wien (1949).
460. R. O. Jones, “Denisty functional theory: Its origins, rise to prominence, and future”; Rev. Mod. Phys. 87, 897- 923 (2015).
461. U. V. Barth, “Basic Density-Functional Theory – an Overview”; Physica Script. Vol. T109, 9-39 (2004).
462. E. Fermi, “Un metodo statistico per la determinazione di alcune proprieta dell’atomo”; Rend. Accad. Lincei 6, 602-607 (1927).
463. J. Schwinger, “Thomas-Fermi model—the leading correction”; Phys. Rev. A 22, 1827–1832 (1980).
464. E. H. Lieb, “Thomas-Fermi and related theories of atoms and molecules”; Rev. Mod. Phys. 53, 603–641 (1981).
465. L. Spruch, “Pedagogic notes on Thomas-Fermi theory (and on some improvements)—atoms, stars, and the stability of bulk matter”; Rev. Mod. Phys.

63, 151–209 (1991).

466. R. O. Jones, "Density Functional Theory: A Personal View"; Springer Series in Sol. St. Sci. 171, 21830-9. Springer-Verlag Berlin Heidelberg, (2012).

467. M. Levy, "Electron densities in search of Hamiltonians"; Phys. Rev. A. 26, 1200 (1982).

468. S. Cottenier, *Density Funcational Theory and the family of (L)APW-methods: a step-by-step introduction;* (Instituut voor Kern- en Stralingsfysica, K. U. Leuven, Belgium) ISBN 90-807215-1-4 (2002)

469. T. L. Gilbert, "Hohenberg-Kohn theorem for nonlocal external potentials"; Phys. Rev. B 12, 2111-2120 (1975).

470. J. E. Harriman, "Orthonormal orbitals for the representation of an arbitrary density"; Phys. Rev. A 24, 680-682 (1981).

471. G. P. Robert, W. Yang, Density-Functional Theory of Atoms and Molecules. *Oxford University Press*, New York. *ISBN 978-0-19-509276-9*. (1994).

472. J. P. Perdew, R. G. Parr, M. Levy, J. L. Balduz, "Density-funcitonal theory for fractional particle number: Derivative discontinuities of the energy"; Phys. Rev. Lett. 49, 1691 (1982).

473. C. O. Almbladh, U. Von Barth, "Exact results for the charge and spin densities, exchange-correlation potentials, and density-funtional eigenvalues"; Phys. Rev. 31 3231 (1985).

474. A. Gorling, "Density-funtiojnal theory for excited states"; Phys. Rev. A54, 3912 (1996).

475. C. Filippi, C. J. Umrigar, X. Gonze, "Excitation energies from density functional perturbationtheory"; J. Chem. Phys. 107, 9994 (1997).

476. D. P. Chong, O. V. Gritsenko, E. J. Baerends, "Interpretation of the Kohn-Sham orbital energies as approximate vertical ionization potentials"; J. Chem. Phys. 116, 1760 (2002).

477. O. V. Gritsenko, E. J. Baerends, "The analog of Koopman's theorem in spin-density functional theory"; J. Chem. Phys. 117, 9154 (2002).

478. M. Levy, J. P. Perdew, V. Sahni, "Exact differential equation for the density and ionization energy of a many-particle system"; Phys. Rev. A 30, 2745–2748 (1984).

479. J. P. Perdew, M. Levy (1983), "Physical content of the exact Kohn-Sham orbital energies: Band gaps and derivative discontinuities"; Phys. Rev. Lett. 51, 1884 (1983).

480. L. J. Sham, M. Schluter, "density-functional theory of the energy gap"; Phys. Rev. Lett. 51, 1888 (1983).

481. R. M. Dreizler, E. K. U. Gross, *Density Functional theory: An Approach to the Many-Body Problem,* Springer, Berlin, 1990.

482. M. S. Hybertsen, S. G. Louie, "Ab initio static dielectric matrices from the density-funtional approach: Formulation and application to semiconductors and insulators"; Phys. Rev. B. 35, 5585 (1987).

483. R. G. Parr, W. Yang, "*Density Functional Theory of Atoms and Molecules*"; Oxford University Press, Oxford (1989).

484. O. V. Gritsenko, P. R. T. Schipper, E. J. Baerends, "Exchange and correlation energy in density functional theory: Comparison of accurate density functional theory quantitites with traditional Hartree-Forck based ones and generalized gradient approximations for the molecules Li2, N2, F2"; J. Chem. Phys. 107, 5007-5015 (2009).

485. W. Kohn, A. D. Becke, R. G. Parr, "Density Functional Theory of Electronic Structure"; J. Phys. Chem. 100, 12974-12980 (1996).

486. R. O. Jones, "Introduction to Density Functional Theory and Excgange-Coreelation Energy Functionals"; Compt. Nanosci. 31, 45-70 (2006).

487. S. Cottenier, Density Functional Theory and the family of (L)APW-methods: a step-by-step introduction (Instituut voor Kern- en Stralingsfysica, K.U.Leuven, Belgium), (2002). *ISBN 90-807215-1-4*

488. D. M. Ceperly, B. J. Alder, "Ground state of the electron gas by a stochastic method"; Phys. Rev. Lett. 45, 566 (1980).

489. S. J. Vosko, L. Wilk, M. Nusair, "Accurate spin-dependent electron liquid

correlation energies for local spin density calculations: A critical anyalysis"; Can. J. Phys. 58, 1200 (1980).

490. J. P. Perdew, A. Zunger, "Self-interaction correction to density-functional approximations for many-electron systems" Phys. Rev. B 23, 5048–5079 (1981).

491. J. P. Perdew, Y. Wang, "Accurate and simple analytic representation of the electron gas correlation energy"; Phys. Rev. B 45, 13244-13249 (1992).

492. U. V. Barth, L. Hedin, "Local exchange-correlation potential for spin-polarized case: I"; J. Phys. C 5, 1629–1642 (1972).

493. O. Gunnarsson, B. I. Lundqvist, "Exchange and correlation in atoms, molecules, and solids by spin-density functional formalism"; Phys. Rev. B 13, 4274–4298 (1976).

494. J. P. Perdew, "Density-funtional approximation for the correlation energy of the inhomogeneous electron gas"; Phys. Rev. B 33, 8822 (1986).

495. J. P. Perdew, K. Burke, M. Emzerhof, "Generalized Gradient Approximation Made Simple"; Phys. Rev. Lett. 77, 3865 (1996).

496. J. P. Perdew, K. Burke, M. Emzerhof, "Generalized Gradient Approximation made simple [*Phys. Rev. Lett. 77, 3865 (1996)*]" *ERRATA*; Phys. Rev. Lett. 78, 1396(E) (1997).

497. V. N. Staroverov, G. E. Gustavo, J. P. Perdew, E. R. Davidson, J. Katriel, "High-density limit of the Perdew-Burke-Ernzerhof generalized gradient approximation and related density functionals"; Phys. Rev. Lett. A 74, 044501-044503 (2006).

498. A. D. Becke, "Density-functional exchange-energy approximation with correct asymptotic behavior"; Phys. Rev. A. 38, 3098 (1988).

499. C. Lee, W. Yang, R. G. Part, "Development of the Colle-Salventti correlation-energy formula into a functional of the electron density" Phys. Rev. B 37, 785 (1988).

500. J. P. Perdew, W. Yue, "Accurate, simple density functional for the electronic

exchange energy: Generalized gradient approximation"; Phys. Rev. B 33, 8800 (1986).

501. O. K. Andersen, "Linear methods in band theory"; Phys. Rev. B 12, 3060 (1975).

502. D. D. Koelling and G. O. Arbman, "Use of energy derivative of the radial solution in an augmented plane wave method: application to copper"; Phys. F: Met. Phys. 5, 2041 (1975).

503. D. J. Singh, "Planewaves Pseudopotentials and the LAPW method"; Kluwer Academic Publishers, Boston, (1994).

504. J. C. Slater, "Wave Functions in a Periodic Potential"; Phys. Rev. 51, 846-851 (1937).

504. P. Blaha, K. Schwarz, P. Sorantin, S. B. Trickey, "Full-potential, linearized augmented plane wave programs for crystalline systems"; Comput. Phys.Comm. 59, 399 (1990).

505. M. Weinert, E. Wimmer, A. J. Freeman, "Total-energy all-electron density functional method for bulk solids and surfaces"; Phys. Rev. B 26, 4571 (1982).

506. T. Charpin, "A package or calculating elastic tensors of cubic phases using WIEN"; Lab. of. Geomaterials of IPGP 4, p1 Jussieu, F-75252 Paris, France (2001).

507. G. Gusmano, G. Montesperelli, E. Traversa, G. Mattogno, "Microstructure and Electrical Properties of $MgAl_2O_4$ Thin Film for Humidity Sensing"; J. Am. Ceram. Soc. 76, 743-50 (1993).

508. G. Gusmano, G. Montesperelli, P. Nunziante, E. Traversa, "Study of the conduction mechanism of $MgAl_2O_4$ at different environmental humidities"; Electrochim. Acta 38, 2617-2621 (1993).

509. S. H. Wei, S. B. Zhang, "First-principles study of cation distribution in eighteen closed-shell $A^{II}B_2^{III}O_4$ and $A^{IV}B_2^{II}O_4$ spinel oxides"; Phys. Rev. B 63 , 045112-18 (2001).

510. Y. N. Xu, W. Y. Ching, "Self-Consistent band structures, charge distributions, and optical-absorption spectra in Mgo, a-Alamo„and $MgAl_2O_4$"; Phys. Rev. B43

(5) , 4461-4472 (1991).

511. A. Wanner, E. H. Lutz, "Elastic anisotropy of plasma-sprayed, free-standing Ceramics," Am. Ceram. Soc. 81, 2706–2708 (1998).

512. A. M. Pandas, A. Costales, M. A. Blanco, J. M. Recio, V. Luana, "Local Compressibilities in Crystals"; Phys. Rev. B62, 13970-78 (2000).

513. C. Aksel, B. Rand, F. L. Riley, P. D. Warren, "Mechanical properties of magnesia-spinel composites," Euro. Ceram. Soc. 22, 745–754 (2002).

514. A. Yoneda, "Pressure Derivatives of Elastic Constants of Single Crystal MgO and $MgAl_2O_4$"; J. Phys. Earth 38, 19-55 (1990).

515. A. Chopelas, "The fluorescence sideband method for obtaining acoustic velocities at high compressions: application to MgO and $MgAl_2O_4$"; Phys. Chem. Minerals 23 (1), 25-37 (1996).

516. A. Ibarra, R. Vila, F. A. Garner, "Optical and Dielectric Properties of Neutron-Irradiated $MgAl_2O_4$ Spinels"; J. Nuclear Materials 233-237, 1336-1339 (1996).

517. I. V. A. Charkin, D. W. Cooke, V. T. Gritsyna, M. Ishimaru, K. .E. Sickafus, "Effects of He^+ ion implantation on optical and structural properties of $MgAl_2O_4$ "; Vacuum 58 (1), 2-9 (2000).

518. T. Suzuki, G. S. Murugan, Y. Ohishi, "Spectroscopic properties of a novel near-infrared tunable laser material Ni:$MgAg_2O_4$"; J. of Luminescence 113, 265-270 (2005).

519. R. Khenata, H. Baltache, M. Sahnoun, A. Bouhemadou, B. Bouhafs, M. Rerat, "Optical properties of spinel oxides: $MgAl_2O_4$ and $ZnAl_2O_4$ under hydrostatic pressure"; Algerian J. Adv. Mater. 3, 171 (2006).

520. J. M. Leger, J. Haines, M. Schmidt, J. P. Petitet, A. S. Pereira, J. A. H. Da Jordana, "Discovery of hardest known oxide"; Nature 383, 401 (1996).

521. W. Jones, L. J. Miles "Production of β-Al_2O_3 electrolyte"; Proc. Br. Ceram. Soc. 19, 161 (1971).

522. A. Govindaraj, E. Flahaut, Ch. Laurent, A. Peigney, A. Rousset, C. N. R. Rao, "An

Investigation of Carbon Nanotubes Obtained from the Decomposition of Methane Over Reduced $Mg_{1-x}M_xAl_2O_4$ Spinel Catalysts"; J. Mater. Res.14, 2567-76 (1999).

523. N. J. van der Laag, "Environnemental effects on the fracture of oxide ceramics"; Doctorat thesis, Technical University-Eindhoven (2002).

524. N. J. van der Laag, "Geometry of {001} Surfaces of Spinel ($MgAl_2O_4$): First-Principles Simulations and Experimental Measurements"; J. Am. Ceram. Soc., 88(6), 1544-1548 (2005).

525. T. Irifune, K. Fujino, E. Ohtani, "A new High-Pressure Form of $MgAl_2O_4$"; Nature 349, 409-11 (1991).

526. P. P. L. Regtien, ''Solid-State Humidity Sensors,'' Sensor Actuator, 2, 85–95 (1981/82).

527. A. Larbot, G. Philip, M. Persin, L. Cot, "$MgAl_2O_4$ Spinel as Material for Ultrafiltration embranes"; Key Eng. Mater.,132–136, 1719–22 (1997).

528. M. C. Warren, M. T. Dove, A. T. Redfern, "Ab Initio Simulations of Cation Ordering in Oxides: Application to Spinel"; J. Phys.: Condens. Matter, 12, L43–8 (2000).

529. G. A. de Wijs, C. M. Fang, G. Kresse, and G. de With, ''First-Principles Calculations of Phonon Spectra of Spinel $MgAl_2O_4$"; Phys. Rev. B, 65, 094305 (2002).

530. P. Blaha, K. Schwarz, G. K. H. Madsen, D. Kvanicka, J. Luitz, WIEN2K-An Augmented plane wave & Local Orbital Program for Calculating Crystal Properties (Techn. Universitat Wien, Austria, ISBN: 3-9501031-12 (2001).

530 P. Blaha, K. Schwarz, J. Luitz, A Full Potential Linearized Augmented Planewave

A. Package for Calcualting Crystal Properties, Technical university, Wien, Vienna, ISBN: 3-9501031-0-4 (2001).

531. M. Jamal, Cubic-elastic, http://www.wien2k.at/reg_user/unsupported/ (2012).

532. M. Jamal, S. J. Asadabadi, Iftikhar Ahmad, H. A. Rahnamaye Aliabad, "Elastic

constants of cubic crystals"; Compt. Mater. Sci. 95, 592-599 (2014).

533. R. Stadler, W. Wolf, R. Podloucky, G. Kresse, J. Furthmuller, J. Hafner, "*Ab Initio* calculations of the cohesive elastic, and dynamical properties of $CoSi_2$ by pseudopotential and all-electron techniques"; Phys. Rev. B 54, 1729 (1996). DOI: doi.org/10.1103/PhysRevB.54.1729

534. R. Yu, X.F. Zhang, L.C. de Jonghe, R.O. Ritchie, "Elastic constants and tensile properties of Al_2 OC by density functional calculations"; Phys. Rev. B 75, 104114 (2007).

535. S. P. Lepkowski, I. Gorczyca, "Ab initio study of elastic constants in In_xGa_{1-x} and $InxAl_{1-x}N$ wurtzite alloys"; Phys. Rev. B 83, 203201 (2011).

536. M. Y. Xie, F. Tasnadi, I. A. Abrikosov, L. Hultman, V. Darakchieva, "Elastic constants, composition, and piezolectric polarization in $In_xAl_{1-x}N$: From *ab initio* calculations to experimental implications for the applicability of Vegard's rule"; Phys. Rev. B 86, 155310 (2012).

537. M. H. Sadd, Elasticity: Theory, Applications, and Numerics, Elsevier Academic Press, 2005.

538. G. T. Mase, G. E. Mase, Elasticity: Theory, Applications, and Numerics, second ed., CRC Press LLC, 1999.

539. H. Yao, L. Ouyang, W. Chingw, "Ab initio Calculation of Elastic Constants of Ceramic Crystals"; J. Am. Ceram. Soc. 90, 3194 (2007).

540. W. B. Daniels, "Pressure Variation of the Elastic Constants of Sodium"; Phys. Rev. 119, 1246 (1960).

541. Y. He, V. Cvetkovic, C. M. Varma, "Elastic properties of a class of solids with negative thermal expansion"; Phys. Rev. B 82, 014111 (2010).

542. A. E. Petrova, V. N. Krasnorussky, A. A. Shikov, W. M. Yuhasz, T. A. Lograsso, J. C. Lashley, S. M. Stishov, "Elastic thermodynamic, and electronic properties of MnSi, Fesi, and CoSi"; Phys. Rev. B 82, 155124 (2010).

543. M. Sanati, R. C. Albers, T. Lookman, A. Saxena, "Elastic constants, phonon density of states, and thermal properties of UO_2 "; Phys. Rev. B 84, 014116 (2011).

544. S. L. Shang, Y. Wang, D. E. Kim, C.L. Zacherl, Y. Du, Z. K. Liu, "Structural, vibrational, and thermodynamic properties of ordered and disordered $Ni_{1-x}Pt_x$ alloys from first-principles calculations"; Phys. Rev. B 83, 144204 (2011).

545. V. Kanchana, G. Vaitheeswaran, Xinxin Zhang, Yanming Ma, A. Svane, O. Eriksson, "Lattice dynamics and elastic properties of the 4*f* electron system: CeN"; Phys. Rev. B 84, 205135 (2011).

546. A. Aguayo, G. Murrieta and R. de Coss, "Elastic stability and electronic structure of fcc Ti, Zr and Hf: A first-principles study"; Phys. Rev. B 65, 092106 (2002).

547. J. Callaway, Quantum Theory of the Solid State, second ed., Academic Press, New York, 1991.

548. M. Born, K. Huang, *Dynamical Theory of Crystal Lattices* (Clarendon, Oxford University Press, (1954).

549. B. B. Karki, G. J. Ackland, J. Crain "Elastic instabilities in crystals from *ab initio* stress-strain relations"; J. Phys. Condens. Matter. 9, 8579-8589 (1997)

550. J. Wang, S. Yip, S. R. Phillpot, Dieter Wolf, "Crystal instabilities at finite strain"; Phys. Rev. Lett. 71, 4182-4185 (1993). DOI https://doi.org/10.1103/PhysRevLett.71.4182

551. D. C. Wallace, Thermodynamics of Crystals, New York: John Wiley, (1972).

552. L. L. Boyer, "Theory of melting based on lattice instability"; Phase Transition 5, 1-47 (1985).

553. F. Milstein, B. Farber, "Theoretical ff→bcc Transition under [100] Tensile Loading"; Phys. Rev. Lett. 44, 277 (1980). DOI:https://doi.org/10.1103/PhysRevLett.44.277

554. J. S. Tse, D. D. Klug, "Mechanical instability of α–quartz: A molecular dynamics study"; Phys. Rev. Lett. 67, 3559 (1991).

555. G. Vaitheeswaran, V. Kanchana, S. Heathman, M. Idiri, T. Le Bihan, A. Svane, A.Delin, B. Johansson, "Elastic constants and high-pressure structural transitions in lanthanum monochalcogenides from experiment and theory"; Phys. Rev. 75, 184108 (2007).

556. Z. Charifi, H. Baaziz, Y. Saeed, A. H. Reshak, F. Soltani, "The effect of chalcogen

atom on the structural, elastic, and high-pressure properties of XY compounds (X = La, Ce, Eu, and Y = S, Se, and Te): An *ab initio* study"; Phys. Status Solidi B 249, 18-28 (2012).

557. R. Hill, "The Elastic Behaviour of a Crystalline Aggregate"; Proc. Phys. Soc. London A 65 349-354 (1952).

558. C. Zener, "Contributions to the Theory of Beta-Phase Alloys"; Phys Rev. 71, 846-851 (1947). DOI:https://doi.org/10.1103/PhysRev.71.846

559. A. Reuss, "Berechnung der Fließgrenze von Mischkristallen auf Grund der Plastizit¨atsbedingung f¨ur Einkristalle"; *Z. Angew. Math. Mech.* 9, 49, 49 (1929).

560. W. Voight, Lehrbuch der kristallphysik (mit ausschluss der kristalloptik), Springer-Verlag, Leipzig, (1928).

561. J. Haines, G. Bocquillon, "Synthesis and Design of Superhard Materials"; Ann. Rev. Mater. Res. 31, 1 (2001).

562. L. Max, A. Aguayo, G. Murrieta, "Elastic properties of 5d transition-metal carbides: An ab initio study"; Cond. Mater Phys. 18, 3, 33801-7 (2015).

563. D. G. Pettifor, "Theoretical predictions of structure and related properties of intermetallics"; Mater. Sci. Tech. 8, 345 (1992).

564. D. G. Sangiovanni, L Hultman, V. Chirita, "Supertoughening in B1 transition metal nitride alloys by increased valence electron concentration"; Acta Mater., 59, 2121 (2011).

565. S. F. Pugh, "XCII. Relations between the elastic moduli and the plastic properties of polycrystalline pure metals"; Philos. Mag. Ser. 7, 45, 823 (1954).

566. A. E. H. Love, A Treatise on the Mathematical Theory of Elasticity, fourth ed., Dover Publications, New York, 1927 re-issued 1944.

567. K Chen, L. R. Zhao, J. Rodgers, J. S. Tse, "Alloying effects on elastic properties of TiN-based nitrides"; J. Phys. D: Appl. Phys. 36, 2725-2729 (2003).

568. H. Fu, D. Li, F. Peng, T. Gao, X. Cheng, "Ab initio calculations of elastic constants and thermodynamic properties of NiAl under high pressures"; Comput. Mater.

Sci. 44, 774 (2008).

569. P. H. Mott, J. R. Dorgan, C. M. Roland, "The bulk modulus and Poisson's ratio of "incompressible" materils"; J. Sound Vib. 312, 572-575 (2008).

570. M. Shafiq, Suneela Arif, Iftikhar Ahmad, S. Jalali Asadabadi, M. Maqbool, H. A. Rahanamaye Aliabad, "Elastic and mechanical properties of lanthanide monoxides"; J. of Alloys & Comp. 618, 292-298 (2015).

571. L. Kleinman, "Deformation Potentials in Silicon. I. Uniaxial Strain"; Phys. Rev. 128, 2614 (1962).

572. W. A. Harrison, Electronic Structure and the Properties of Solids (Freeman San Francisco, San Francisco, 1980).

573. R. L. Stewart, R. C. Bradt, "Fracture of Single Crystal $MgAl_2O_4$"; J. Mater. Sci., 15, 67-72 (1980).

574. R. L. Stewart, R. C. Bradt, "The Brittle to Ductile Transformation in $MgAl_2O_4$ Spinel"; in Plastic Deformation of Ceramics, Edited by R. C. Bradt, C. A. Brookes and J. L. Routbort. Plenum Press, New York, pp.21-8 (1995).

576. J. M. Recio, R. Franco, A. M. Pandas, M.A. Blanco, L. Pueyo, R. Pandey, "Theoretical explanation of the uniform compressibility behavior observed in oxide spinels"; Phys. Rev. B 63, 184101 (2001).

577. P. D'Arco, B. Silvi, C. Roetti, R. Orlando, "Comparative study of spinel compounds: A pseudopotetial periodic Hartree-Fock calculation of Mg_2SiO_4, Mg_2GeO_4, Al_2MgO_4, and Ga_2MgO_4"; J. Geophys. Res. 96, B4, 6107-6112 (1991).

578. P. Fischer, "Neutron Diffraction Investigation of the Structure of $MgAl_2O_4$ and $ZnAl_2O_4$ Spinel as a Function of Previous History"; Z. Kristallogr. 124, 275 (1967).

579. G. V. Lewis, C. R. A. Catlow, "Potential models for ionic oxides"; J. Phys. C: Solid State Phys.18, 1149-1161 (1985).

580. E. Bruschini, S. Speziale, G. B. Andreozzi, F. Bosi and U. Halenius, "The elasticity of $MgAl_2O_4$-$MnAl_2O_4$ spinels by Brillouin scattering and an empirical approach for bulk modulus prediction"; Am. Miner. 100, 644-651 (2015).

581. H. J. Reichmann and S. D. Jacobsen, "Sound velocities and elstic constants of $ZnAl_2O_4$ spinel and implications for spine-elasticity sytematics"; American Mineralogist . 91, 1049-1054 (2006).

582. U. P. Wdowik, K. Parlinski, A. Siegel, "Elastic properties and high-pressure behavior of $MgAl_2O_4$ from ab initio calcualtions"; J. Phys. Chem.Solids 67, 1477-1483 (2006).

583. V. Askarpour, M. H. Manghnani, S. Fassbender, A. Yoneda, "Elasticity of Single-Crystal $MgAl_2O_2$ Spinel up to 1273 K by Brillouin Spectroscopy"; Phys. Chem. Miner. 19, 511-519 (1993).

584. F. Tielens, M. Calatayud, R. Franco, J. M. Recio, J. P. Ramirez and C. Monot, "Periodic DFT Study of the Structural and Electronic Properties of Bulk $CoAl_2O_4$ Spinel"; J. Phys. Chem. B 110, 988-995 (2006).

585. D. Errandonea, R. S. Kumar, F. J. Manjon, V. V. Ursaki, E. V. Rusu, "Post-spinel transformations and equation of state in $ZnGa_2O_4$: Determination at high pressure by *in situ* x-ray diffraction"; Phys. Rev. B 79, 024103 (2009).

586. Z. Wang, P. Lazor, S. K. Saxena, G. Artioli, "High-Pressure Raman Spectroscopic Study of Spinel $ZnCr_2O_4$"; J. Solid State Chem. 165, 165-170 (2002).

587. D. Levy, V. Diella, A. Pavese, M. Dapiaggi, A. Sani, "*P-V* equation of State, thermal expansion, and *P-T* stability of synthetic zincochromite ($ZnCr_2O_4$ spinel)"; Am. Mine., 90, 1157-1162 (2005).

588. F. Zerarga, A. Bouhemeadou and R. Khenata, "FP-LAPW study of the structural, elastic and thermodynamic properties of spinels ZnX_2O_4 (X=Al, Ga, In)"; Comp. Mat. Sc. 50, 2651-2657 (2011).

589. S. K. Sampath, D. G. Kanhere, R. Pandey, "Electronic structure of spinel oxides: zinc aluminate and zinc gallate"; J. Phys. Condes. Matt. 11, 3635-3644 (1999).

590. R. Pandey, J. D. Gale, S. K. Sampath, J. M. Recio, "Atomistic Simulation Study of Spinel Oxides: Zin Aluminate and Zinc Gallate"; J. Am. Ceram. Soc. 82, 3337-3341 (1999). DOI: doi/10.1111/j.1151-2916.1999.tb02248.x/full

591. D. Ko, K. R. Poeppelmeier, D. R. Kammler, G. B. Gonzalez, T. O. Mason, D. L. Williamson, D. L. Young, T. J. Coutts "Cation Distribution of the Transparent Conductor and Spinel Oxide Solution $Cd_{1+x}In_{2-x}Sn_xO_4$"; J. Solid State Chem. 163, 259-266 (2002).

592. C. O. Arean, E. G. Diaz, "Cation distribution and oxygen parameter in $CdGa_2O_4$ –$CoGa_2O_4$ solid solutions"; Mat. Chem. 7, 675 (1982).

593. R. D. Shannon, J. L. Gillson, R. J. Bouchard, "Single crystal synthesis and electrical properties of $CdSnO_3$, Cd_2SnO_4, In_2TeO_6 and $CdIn_2O_4$"; J. Phys. Chem. Solids 38, 877 (1977). DOI: doi.org/10.1016/0022-3697(77)90126-3

594. M. F. Lewis, "Elastic Constants of Magnesium Aluminate Spinel"; J. Acoust. Soc. Amer. 40, 728 (1966). *DOI:* doi.org/10.1121/1.1910143

595. K. M. Rabe, "First-principles calculations of complex metal-oxide materials," Cond. Mat. Phys. 1, 211-235 (2010).

596. A. Seko, K. Yuge, F. Oba, A. Kuwabara, I. Tanaka, "Prediction of ground-state structures and order-disorder phase trasitions II-III spinel oxides: A combined cluster-expansion method and first-principles study"; Phys. Rev. B. 73, 184117 (2006).]

597. D. Levy, A. Pavese, A. Sani, V. Pischedda, "Structure and compressibility of synthetic $ZnAl_2O_4$ (gahnite) under high-pressure conditions, from synchrotron X-ray powder diffraction": Phys. Chem. Minerals 28, 612-618 (2001) .

598. H. Lu, L. Yang, W. Huang, "Theoretical Investigations of the Electronic, Elastic, Thermodynamics Properties and the Superconducting Transition Temperature of MNiBN (M = La, Ca)"; Supercond. Magn. 27, 1671-1676 (2014).

599. M. Hachemaoui, F. Semari, R. Khenata, A. Bouhemadou, M. Rabah, "Structural, elastic and electronic properties of XAl2O4 (X=Mg, Zn) compounds"; Journal of Sc. Research No. 0 (1), 112-116 (2010).

600. F. Zerarga, A. Bouhemadou, R. Khenata and S. Bin-Omran, "Structural, electronic and optical properties of spinel oxides $ZnAl_2O_4$, $ZnGa_2O_4$ and $ZnIn_2O_4$," Sol. Stat.

Sci. 13, 1638 (2011).

601. N. Ueda, T. Omata, N. Hikuma, K. Ueda, H. Mizoguchi, T. Hashimoto, H. Kawazoe, "New oxide phase with wide band gap and high electroconductivity, $MgIn_2O_4$"; Appl. Phys. Lett. 61 1954-1955 (1992). DOI: dx.doi.org/10.1063/1.108374

602. A. Manzar, G. Murtaza, R. Khenata, S. Muhammad, Hayatullah, "Electronic band profile and optical response of spinel $MgIn_2O_4$ through modified Becke-Johnson potential"; Chin. Phys. Lett. 30, 067401 (2013).

603. A. Manzar, G. Murtaza, R. Khenata, S. Muhammad, Hayatullah, "Electronic and optic properties of cubic spinel CdX_2O_4 (X=In, Ga, Al) through modified Becke-Johnson potential"; Chin. Phys. Lett. 31, 067401 (2014).

604. D. L. Young, H. Moutinho, Y. Yan, T.J. Coutts, " Growth and characterization of radio frequency magnetron sputter-deposited zinc stannate, $ZnSn_2O_4$, thin films"; J. Appl. Phys. 92 (1), 310-319 (2002).

605. R. G. Gordon, "Criteria for Choosing Transparent Conductors"; MRS Bull. 25, 52 (2000).

606. Z. Yan, H. Takei, "Flux growth of single crystals of spinel $ZnGa_2O_4$ and $CdGa_2O_4$"; J. Cryst. Growth 71, 131-135 (1997).

607. A. Manzar, G. Murtaza, R. Khenata, S. Muhammad, Hayatullah, "Electronic band structure and optical response of spinel SnX_2O_4 (X=Mg, Zn) through modified Becke-Johnson potential"; Chin. Phys. Lett. 30, 047401 (2013).

608. A. Manzar, G. Murtaza, R. Khenata, S. Muhammad, Hayatullah, "Electronic and Optical Properties of Spinel $GeMg_2O_4$ and $GeCd_2O_4$"; Chin. Phys. Lett. 30, 127401 (2013).

609. R. T. Sharp, G. K. Horton, "A variational approach to the Unipotential Many-electron Problem"; Phys. Rev. 90, 317 (1953).

610. J. D. Talman, W. F. Shadwick, Optimized effective atomic central potential"; Phys. Rev. A 14, 36-40 (1976).

611. E. Engel, "Relevance of core-valence interaction for electronic structure

calculations with exact exchange"; Phys. Rev. B 80, 161205(R) (2009).

612. D. Koller, F. Tran, and P. Blaha, "Accurate band gaps of semiconductors and insulators with a semilocal exchange-correlation potential," Phys. Rev. B 83, 195134 (2011).

613. V. I. Anisimov, O. Gunnarsson, "Density-functional calculation of effective Coulomb interactions in metals"; Phys. Rev. B 43, 7570-5774 (1991).

614. B. N. Harmon, V. P. Antropov, A. I. Liechtenstein, I. V. Solovyev and V. V. I. Anisimov, "Calculation of magneto-optical properties for 4*f* systems: LSDA + Hubbard *U* results," Phys. Chem. Sol. 56, 1521–1524 (1995).

615. A. D. Becke, E. R. Johnson, "A simple effective potential for exchange"; Chem. Phys. 124, 221101 (2006).

616. F. Tran, P. Blaha, and K. Schwarz, "Accurate band gaps of semiconductors and insulators with a semilocal exchange-correlation potential"; Phys. Condens. Matt. 19, 196208 (2007).

617. Y. Kim, M. Marsman, G. Kresse, F. Tran, and P. Blaha, "Towards efficient band structure and effective mass calculations for III-V direct band-gap semiconductors" Phys. Rev. B 82, 205212 (2010).

618. W. Feng, D. Xiao, Y. Zhang and Y. Yao, "Half-Heusler topological insulators: A first-principles study with the Tran-Blaha modified Becke-Johnson density functional"; Phys. Rev. B 82, 235121 (2010).

619. Y. S. Kim, M. Marsman, G. Kresse, F. Tran and P. Blaha, "Towards efficient band structure and effective mass calculations for III-V direct band-gap semiconductors"; Phys. Rev. B 82, 205212 (2010).

620. Y. Wang, N. S. Rogado, R. J. Cava and N. P. Ong, "Spin entropy as the likely source of enhanced thermopower in $Na_xCo_2O_4$"; Nature 423, 425-428 (2003).

621. A. Walsh, S. H. Wei, Y. Yan, M. M. Al-Jassim, J. A. Turner, "Structural, magnetic, and electronic properties of the Co-Fe-Al oxide spinel system: Density-functional theory calculations"; Phys. Rev. B 76, 165119 (2007).

622. H. C. Choi, J. H. Shim, and B. I. Min, "Electronic structures and magnetic properties of spinel $ZnMn_2O_4$ under high pressure"; Phys. Rev. B 74, 172103 (2006).

623 Z. Wu, R. E. Cohen, "More accurate generalized gradient approximation for solids"; Phy. Rev. B 73, 235116 (2006).

624 J. Behler, M. Parrinello, "Generalized neural-network representation of high-dimensional potential-energy surfaces"; Phys. Rev. Lett. 98, 146401 (2007).

625 S. G. Ebbingaus, j. Hanss, m. Mlemm, S. Horn, "Crystal structure and magnetic properties of ZnV_2O_4"; J. of Alloys & Comp. 370, 75-79 (2005).